JAERI 1325

JAERI 1325
NEANDC (J)-163/U
INDC (JPN)-152/L

JENDL Dosimetry File

March 1992

日 本 原 子 力 研 究 所

Japan Atomic Energy Research Institute

JAERI レポートは，日本原子力研究所が研究成果編集委員会の審査を経て不定期に公刊している研究報告書です。

入手の問合わせは，日本原子力研究所技術情報部情報資料課（〒319－11 茨城県那珂郡東海村）あて，お申しこしください。なお，このほかに財団法人原子力弘済会資料センター（〒319－11 茨城県那珂郡東海村日本原子力研究所内）で複写による実費頒布をおこなっております。

JAERI reports are reviewed by the Board of Editors and issued irregularly.

Inquiries about availability of the reports should be addressed to Information Division Department of Technical Information, Japan Atomic Energy Research Institute, Tokai-mura, Naka-gun, Ibaraki-ken 319－11, Japan.

編集兼発行　日本原子力研究所
印　　刷　いばらき印刷㈱

JENDL Dosimetry File

Masaharu NAKAZAWA*, Katsuhei KOBAYASHI**, Shin IWASAKI***
Tetsuo IGUCHI*, Kiyoshi SAKURAI†, Yujiro IKEDA†† and Tsuneo NAKAGAWA

Department of Physics
Tokai Research Establishment
Japan Atomic Energy Research Institute
Tokai-mura, Naka-gun, Ibaraki-ken

(Received November 22, 1991)

Abstract

The JENDL Dosimetry File based on JENDL-3 was compiled and integral tests of cross section data were performed by the Dosimetry Integral Test Working Group of the Japanese Nuclear Data Committee. Data stored in the JENDL Dosimetry File are the cross sections and their covariance data for 61 reactions. The cross sections were mainly taken from JENDL-3 and the covariances from IRDF-85. For some reactions, data were adopted from other evaluated data files. The data are given in the neutron energy region below 20 MeV in both of point-wise and group-wise files in the ENDF-5 format. In order to confirm reliability of the data, several integral tests were carried out; comparison with the data in IRDF-85 and average cross sections measured in fission neutron fields, fast reactor spectra, DT neutron fields and Li(d, n) neutron fields. As a result, it has been found that the JENDL Dosimetry File gives better results than IRDF-85 but there are some problems to be improved in future. The contents of the JENDL Dosimetry File and the results of the integral tests are described in this report. All of the dosimetry cross sections are shown in a graphical form.

Keywords: Dosimetry, Cross Section, JENDL-3, IRDF, Covariance, ENDF-5 Format, Integral Test, Average Cross Section, Standard Neutron Field, Cf-252 Spontaneous Fission Spectrum, U-235 Fission Spectrum, DT Neutron, Li(d,n), ISNF, CFRMF, ΣΣ, YAYOI, Resonance Integral.

† Nuclear Safety Research Center
†† Department of Reactor Engineering
* Faculty of Engineering, University of Tokyo
** Research Reactor Institute, Kyoto University
*** Faculty of Engineering, Tohoku University

JENDL ドシメトリーファイル

日本原子力研究所東海研究所物理部

中沢　正治*，小林　捷平**，岩崎　　信***
井川　哲夫*，桜井　　淳†，池田裕二郎††，中川　庸雄

（1991 年 11 月 22 日受理）

要　　旨

シグマ研究委員会ドシメトリー積分テストワーキンググループの作業として，JENDL-3 の評価値を基にした JENDL ドシメトリーファイルの編集及び断面積データの積分テストを行った。JENDL ドシメトリーファイルに格納したデータは 61 反応の断面積と誤差データ（分散及び共分散）である。断面積データは主に JENDL-3 の評価値を，また，誤差データは IRDF-85 のデータを採用した。一部はそれ以外の評価値を採用している。データは，20 MeV 以下のエネルギー範囲で与え，ENDF-5 フォーマットで point-wise ファイルと group-wise ファイルの 2 種類を作成した。データの信頼性を確認するために，IRDF-85 の評価値との比較，核分裂中性子場，高速炉スペクトル場，DT 中性子場及び Li(d, n) 中性子場での平均断面積測定値との比較を行った。その結果，JENDL ドシメトリーファイルの断面積データは IRDF-85 に比較すると概ね良好な結果を与えるが，今後改善すべき問題点も見つかった。本報告では，JENDL ドシメトリーファイルの内容と積分テストの結果について述べる。また，付録として，全ドシメトリー断面積の図を載せる。

東海研究所：〒 319-11　茨城県那珂郡東海村白方字白根 2-4
† 安全性試験研究センター
†† 原子炉工学部
* 東京大学工学部
** 京都大学原子炉実験所
*** 東北大学工学部

Contents

目　　次

List of Tables

List of Figures

1. Introduction

A dosimetry file is a data set of neutron reaction cross sections which are basically used for determinations of nuetron flux/fluence and energy spectrum at specific neutron fields. While the IRDF -85 dosimetry file[1] mainly based on ENDF/B-V[2] has been so far used widely as the standard in various research fields, it has been a strong request to make a Japanese dosimetry file in the framework of the Japanese Evaluated Nuclear Data Library Version 3 (JENDL-3)[3]. Corresponding to this requirement, a working group was organized to endeavor to issue the first Japanese dosimetry file based on JENDL-3. Through this working, we expect to have a more consistent data set with JENDL-3 and some improvements in accuracy for the dosimetry applications to the current IRDF.

In general, higher accuracy and reliability are required for cross sections in the dosimetry file. Moreover, various applicaions need appropriate cross sections sensitive to the specific neutron energy spectra depending on the field characteristics. In this context, extensive efforts have been devoted to the integral test of the cross sections included in this dosimetry file by using available neutron fields, verifying adequacy of the data in term of reliability and consistency.

In Chapter 2, it is given the documentation of the JENDL Dosimetry File with the list of the reactions included, the data structure, the procedure how to use and figure outputs of each cross section with the IRDP curves in the Appendix. In Chapters 3 and 4, the present status of the integral test of the file is summarized in the various benchmark neutron fields relating to fission reactors and fusion reactors, respectively.

The 61 nuclear reactions have been included in the present JENDL Dosimetry File, and they are selected mainly for dosimetry applications to fission reactor fields, 14 MeV neutronic experiments and spallation neutron fields, as is the case of IRDF. This is a reason why many reactions are common to the JENDL Dosimetry File and IRDF. Precise comparisons between both files have been summarized in Chapter 5.

The covariance matrices of the cross sections, however, have not been evaluated in JENDL-3, so in the present JENDL Dosimetry File they are adopted mainly from IRDF-85 for the common reactions to both files, and for the other reactions their estimations have been made by this working group.

2. Compilation of JENDL Dosimetry File

2.1 Activities of Dosimetry File Integral Test Working Group

2.1.1 General Description of the Working Group

To compile and test the first Japanese Dosimetry File, a working group has been organized in 1987 in the framework of JENDL-3[3] nuclear data evaluation. At the moment to start the tasks of compilation of data, dosimetry files available, such as IRDF-85[1] and ENDF/B-V[2], were referred to get basic idea for the JENDL Dosimetry file. The first step was to identify and select the reactions to be included regarding the importance, availability and coverage for the energy of extending interest.

2.1.2 Selection of Dosimetry Reactions

The basic idea was to provide a dosimetry cross section set based on JENDL-3. Whatever the reactions of importance were in the JENDL-3 general purpose file, they were sited in the dosimetry file so that fully consistent data set could be provided. However, there should have been various reactions of useful but not included in the JENDL-3 general purpose file, because the reactions were highly specific on the dosimetry purpose. They are ^{64}Zn(n, p)^{64}Cu, ^{197}Au(n, γ)^{198}Au, ^{197}Au(n, 2n)^{196}Au, ^{93}Nb(n, n')^{93m}Nb, ^{93}Nb(n, 2n)^{92m}Nb, ^{199}Hg(n, n')^{199m}Hg, ^{115}In(n, n')^{115m}In, ^{115}In(n, γ)^{116m}In. In particular, the reactions of ^{93}Nb(n, n') and ^{199}Hg(n, n') seemed attractive due to considerably low threshold energies below 1 MeV. These two reaction cross sections were evaluated in the present framework of the JENDL Dosimetory File compilation. It has been considered of importance to include those reactions because the deficiency of such low threshold reactions has been so often quoted.

Three capture reactions of ^{151}Eu(n, γ)^{152m}Eu, ^{181}Ta(n, γ)^{182}Ta and ^{186}W(n, γ)^{187}W were included in view of the importance in the thermal reactor dosimetry although they were not included in IRDF-85.

Almost all of reactions stored in IRDF-85 were included in the JENDL Dosimetry File.

2.1.3 Scenario of the Integral Test

Comparison with IRDF

Preliminary consistency check on a prototype file was made through comparing with the dosimetry file of IRDF-85 by calculating Spectrum-averaged cross sections in 10 kinds of benchmark neutron spectra, numerical data of which were available in the IRDF-85 library. The results of comparison will be given in detail in section 3.1.

Neutron Fields

In order to assure the quality of the reaction cross sections in the JENDL Dosimetry File, integral tests have been performed.

We used four neutron fields for the test as follows;

(1) Cf-252 and U-235 fission neutron fields,

(2) ISNF/CFRMF/ΣΣ/YAYOI fast reactor neutron fields,

(3) D-T fusion neutron field,

(4) D-Li neutron field

These have been selected as the testing fields because many experimental data of dosimetry reaction rates were available with reasonable accuracy. The neutron spectra were assumed to be different from each other, covering wide sensitive energy range from thermal to the energy higher than 15 MeV.

Integral Test

Comparison between the experimental data and the calculations of spectrum averaged cross sections was carried out by considering uncertainties estimated from covariance matrices. In the calculations, a large part of covariance matrices for the dosimetry cross sections were tentatively taken from the IRDF -85 data library because there was no covariance data in JENDL Dosimetry File. The covariance between fluxes in different energies for the benchmark neutron spectrum was generated on the assumption that diagonal and off-diagonal elements were 5 and 2%, respectively. Details of the treatment of the error will be described in the corresponding section.

2.2 Contents of JENDL Dosimetry File

Table 1 shows the 61 reactions of which cross-section data are stored in the JENDL Dosimetry File. As described in the previous sections, most of the data were taken from the JENDL-3 General Purpose File[3] or JENDL-3 FP Data File[4] except covariance matrices. Since the JENDL-3 has no information on the covariance matrices, they were mainly adopted from IRDF-85 (International Reactor Dosimetry File)[1], IRDF-90[5] or ENDF/B-VI[6]. For the reactions whose covariance matrices were not given even in those files, only variance was estimated in the present work on the basis of available experimental data. **Table 2.2.1** lists the MAT numbers, reactions, threshold energies, half-lives of reaction products, and sources of cross-section data and covariance matrices. In addition to the data of the reactions listed in **Table 2.2.1**, the total cross section is given for the nuclides whose capture and/or fission cross sections are stored, in order to calculate self-shielding factors. No covariance matrix is given for the total cross section.

The data were compiled in the ENDF-5 format[7]. For convenience's sake, both of point-wise and group-wise data files were provided on separate tapes. The number of records is about 175,730 in the point-wise data file and about 17,260 in the group-wise data file.

1) Point-wise data file

In the point-wise data file, the fission and capture cross sections in the resolved and unresolved resonance regions were reconstructed from resonance parameters with RESENDD[8]. The number of energy points was reduced by using LINEAR[9]. The calculation from the resonance parameters was performed at 0 K with an accuracy of 1.0 %. For the nuclides with capture and/or fission cross sections, the total cross section was given in the point-wise form. The unresolved resonance parameters are also stored only for the purpose of self-shielding factor calculation.

2) Group-wise data file

The group-wise data file was obtained by averaging the cross sections in the SAND-II type energy intervals listed in **Table 2.2.2**. This structure is the same as that of IRDF. The calculation of average cross sections was simply carried out as follows by using CRECTJ5[10],

$$\sigma_i(E) = \int_{E_i^{min}}^{E_i^{max}} \sigma(E)\, dE/(E_i^{max} - E_i^{min}),$$

where E_i^{min} and E_i^{max} are boundary energies of the i-th energy interval. All cross sections except the total cross section thus obtained are given in Appendix in a graphical form.

Reference 3 gives brief descriptions of cross-section data taken from JENDL-3. Here, only short descriptions are given for selected reactions.

α and t producing cross sections of Li and B isotopes

Production cross sections were obtained by summing up the corresponding JENDL-3 data. For the covariance data, the same covariance matrix which was taken from IRDF-85 was adopted for the (n, α) reaction and the α production.

^{46}Sc, ^{47}Sc and ^{48}Sc productions from natural Ti

The cross sections were obtained from JENDL-3 data as follows:

$\sigma(^{46}\text{Sc production}) = \sigma(^{46}\text{Ti(n, p)}) \times 0.08 + \sigma(^{47}\text{Ti(n, np)}) \times 0.073,$

$\sigma(^{47}\text{Sc production}) = \sigma(^{47}\text{Ti(n, p)}) \times 0.073 + \sigma(^{48}\text{Ti(n,np)}) \times 0.738,$

$\sigma(^{48}\text{Sc production}) = \sigma(^{48}\text{Ti(n, p)}) \times 0.738 + \sigma(^{49}\text{Ti(n, np)}) \times 0.055,$

As is described later, MT numbers are not assigned for such reactions in the ENDF–5 format. Therefore, MT's of 210, 211 and 212 were tentatively used for ^{46}Sc, ^{47}Sc and ^{48}Sc productions, respectively. No covariance matrix was evaluated for these data.

^{49}Ti(n, np)^{48}Sc

This reaction is not considered in IRDF–85. Since this is important as a reaction which produces ^{48}Sc, data were stored in the JENDL Dosimetry File by taking the cross–section data from JENDL–3 and by estimating only variances on the basis of available experimental data.

^{64}Zn(n, p)^{64}Cu

The cross section was evaluated by Yamamuro[11] with the Simplified Input Nuclear Cross Section Calculation System version II (SINCROS–II)[12] whose main part consists of a modified version of GNASH[13]. The result agrees very well with the data measured by Weigold and Glover[14], and Santry and Butler[15]. The variance was adopted from IRDF–85.

^{93}Nb(n, n')^{93m}Nb

Evaluation was made by Sakurai mainly based on the new experimental data by Gayther et al.[16] in the energy range from 1 to 6 MeV, and that by Ryves and Kolkowski[17] at 14.68 MeV.

^{93}Nb(n, 2n)^{92m}Nb

The cross section calculated by Yamamuro[12] was adopted. The result reproduces very well the experimental data by Ikeda et al.[18] and Bormann et al.[19]

^{103}Rh(n, n')^{103m}Rh

The data were taken from IRDF–85, because the isomeric production cross section was not considered in the JENDL–3 FP Nuclear Data File.

^{115}In(n, n')^{115m}In

Since no evaluation was made for this reaction in JENDL–3, data were adopted from the evaluation performed by Smith et al.[20] They evaluated this reaction by applying the method least squares to available experimental data. The covariance data obtained by this evaluation which are compiled in IRDF–90[5] were adopted in the present work.

^{115}In(n, γ)^{116m}In

There are two isomeric states in ^{116}In. The first isomeric state at 0.127 MeV decays by emitting β^- with a half–life of 54.1 m, and the second one at 0.2897 MeV decays into the first isomeric state by emitting γ–rays with a half–life of 2.16 s. Therefore, the sum of capture cross sections to the both states is important for dosimetry.

In the resolved resonance region below 2 keV, the resolved resonance parameters were adopted from JENDL–3. This set of parameters gives the thermal capture cross section of 202 barns. Since the thermal cross section for the ^{115}In$(n, \gamma)^{116m}$In reaction is recommended by Mughabghab et al.[21] as 162.3 barns, the calculated cross section was multiplied by a factor of 0.803. Above 2 keV, the data of JENDL–3 reproduce existing experimental data for ^{116m1}In + ^{116m2}In production cross section. For the JENDL Dosimetry File, the capture cross section in this energy region was adopted from JENDL–3 without any modification. The covariance matrix was taken from IRDF–85.

^{197}Au(n, 2n)^{196}Au

The data were evaluated by Yamamuro[22] by using SINCROS–II. Covariance was taken from IRDF

–90 evaluated by Wagner et al.[23]

$^{197}Au(n, \gamma)^{198}Au$

Below 2.6126 keV, the cross section was calculated from the resolved resonance parameters on the basis of the recommendation by Mughabghab[21]. The parameters of negative resonances were slightly modified so as to get better agreement of the thermal cross section with the Mughabghab's recommendation. Above 2.6126 keV, the calculation made by Yamamuro[22] was adopted. The covariance matrix was taken from IRDF–85.

$^{199}Hg(n, n')^{199m}Hg$

The evaluation was made by Sakurai[24].

Table 2.2.1 List of Reactions in the JENDL Dosimetry File

Nuclide	MAT	Reaction	Threshold energy(MeV)	Half-life of product	Source σ	Source cov.
Li-6	331	(n, t) α	10^{-5}eV		J3	I
		α production	10^{-5}eV		J3	I
Li-7	332	t production	2.822		J3	I
B-10	531	(n, α) Li-7	10^{-5}eV		J3	I
		α production	10^{-5}eV		J3	I
F-19	931	(n, 2n) F-18	10.985	109.77 m	J3	I
Na-23	1131	(n, 2n) Na-22	12.958	2.602 y	J3	I
		(n, γ) Na-24	10^{-5}eV	15.02 h	J3	I
Mg-24	1231	(n, p) Na-24	4.9311	15.02 h	J3	I
Al-27	1331	(n, p) Mg-27	1.8964 (3.6)	9.462 m	J3	I
		(n, α) Na-24	3.2489	15.02 h	J3	I
P-31	1531	(n, p) Si-31	0.73233	2.62 h	J3	I
S-32	1631	(n, p) P-32	0.95690	14.26 h	J3	I
Sc-45	2131	(n, γ)Sc-46	10^{-5}eV	83.83 d	J3	I
Ti-nat	2230	(n, x) Sc-46	1.6197 (3.0)	83.83 d	J3	-
		(n, x) Sc-47	10^{-5}eV (0.7)	3.345 d	J3	-
		(n, x) Sc-48	3.2756 (4.65)	43.7 h	J3	-
Ti-46	2231	(n, p) Sc-46	1.6197 (3.0)	83.83 d	J3	I
Ti-47	2232	(n, np) Sc-46	10.685 (11.5)	83.83 d	J3	I
		(n, p) Sc-47	10^{-5}eV (0.7)	3.345 d	J3	I
Ti-48	2233	(n, np) Sc-47	11.687	3.345 d	J3	I
		(n, p) Sc-48	3.2756 (4.65)	43.7 h	J3	I
Ti-49	2234	(n, np) Sc-48	1.248 (5.45)	43.7 h	J3	A
Mn-55	2531	(n, 2n) Mn-54	10.415	312.5 d	J3	J3
		(n, γ) Mn-56	10^{-5}eV	2.5785 h	J3	J3
Fe-54	2631	(n, p) Mn-54	10^{-5}eV (1.0)	312.5 d	J3	I
Fe-56	2632	(n, p) Mn-56	2.9709 (3.5)	2.5785 h	J3	I
Fe-57	2633	(n, np) Mn-56	10.752	2.5785 h	J3	B6
Fe-58	2634	(n, γ) Fe-59	10^{-5}eV	44.496 h	J3	I
Co-59	2731	(n, 2n) Co-58	10.635 (10.8)	70.916 d	J3	I
		(n, γ) Co-60	10^{-5}eV	5.271 y	J3	I
		(n, α) Mn-56	10^{-5}eV (5.0)	2.5785 h	J3	I
Ni-58	2831	(n, 2n) Ni-57	12.415	36.08 h	J3	I
		(n, p) Co-58	10^{-5}eV (0.1)	70.916 d	J3	I
Ni-60	2832	(n, p) Co-60	2.0755 (3.5)	5.271 y	J3	I
Cu-63	2931	(n, 2n) Cu-62	11.028	9.74 m	J3	I
		(n, γ) Cu-64	10^{-5}eV	12.701 h	J3	I
		(n, α) Co-60	10^{-5}eV (1.5)	5.271 y	J3	I
Cu-65	2932	(n, 2n) Cu-64	10.058	12.701 h	J3	I
Zn-64	3031	(n, p) Cu-64	10^{-5}eV (0.1)	12.701 h	Y	I
Zr-90	4031	(n,2n)Zr-89	12.116	78.43 h	J3F	I

Table 2.2.1 (Continued)

Nuclide	MAT	Reaction	Threshold energy (MeV)	Half-life of product	Source ++ σ	Source ++ cov.
Nb-93	4131	(n, n') Nb-93m	0.03073 (0.1)	13.6 y	S	S
		(n, 2n) Nb-92m	9.0523	10.15 d	Y	A
Rh-103	4531	(n, n') Rh-103m	0.04	56.12 m	I	I
In-115	4931	(n, n') In-115m	0.32	4.486 h	C	C
		(n, γ) In-116m	10^{-5}eV	54.1 m	J3F	I
I-127	5331	(n, 2n) I-126	9.2178	13.02 d	J3F	I
Eu-151	6331	(n, γ) Eu-152	10^{-5}eV	13.33 y	J3F	A
Ta-181	7331	(n, γ) Ta-182	10^{-5}eV	114.5 d	J3	A
W-186	7431	(n, γ) W-187	10^{-5}eV	23.9 h	J3	A
Au-197	7931	(n, 2n) Au-196	8.1147	6.183 d	Y	I90
		(n, γ) Au-198	10^{-5}eV	2.696 d	Y	I
Hg-199	8031	(n, n') Hg-199m	0.5337	42.6 m	S	S
Th-232	9031	fission	10^{-5}eV (0.4)		J3	I
		(n, γ) Th-233	10^{-5}eV	22.3 m	J3	I
U-235	9231	fission	10^{-5}eV		J3	I
U-238	9232	fission	10^{-5}eV		J3	I
		(n, γ) U-239	10^{-5}eV	23.5 m	J3	I
Np-237	9331	fission	10^{-5}eV		J3	I
Pu-239	9431	fission	10^{-5}eV		J3	I
Am-241	9531	fission	10^{-5}eV		J3	B6

For the nuclides with capture and/or fission cross sections, total cross section is also given,

+: Values in ( ) are energies where the cross sections rise. The energy of 10^{-5}eV is the lowest energy of the data in the cases of reactions with a positive Q-value.

++: Data source

- J3 : JENDL-3 General Purpose File[1)]
- J3F : JENDL-3 Fission Product Nuclear Data File[2)]
- B6 : ENDF/B-VI[5)]
- I : IRDF-85[3)]
- I90 : IRDF-90[4)]
- A : estimated in the present work
- C : evaluated by A.B. Smith et al.[19)]
- S : evaluated by K. Sakurai
- Y : evaluated by N. Yamamuro[10,11,12)]

Table 2.2.2 SAND-II Type Energy Intervals

The lowest energy is 10^{5} eV. Upper boundaries of energy intervals are listed in this table.

No.	energy(eV)	No.	energy(eV)	No.	energy(eV)
1	1.0000-4	46	1.0000-3	91	1.0000-2
2	1.0500-4	47	1.0500-3	92	1.0500-2
3	1.1000-4	48	1.1000-3	93	1.1000-2
4	1.1500-4	49	1.1500-3	94	1.1500-2
5	1.2000-4	50	1.2000-3	95	1.2000-2
6	1.2750-4	51	1.2750-3	96	1.2750-2
7	1.3500-4	52	1.3500-3	97	1.3500-2
8	1.4250-4	53	1.4250-3	98	1.4250-2
9	1.5000-4	54	1.5000-3	99	1.5000-2
10	1.6000-4	55	1.6000-3	100	1.6000-2
11	1.7000-4	56	1.7000-3	101	1.7000-2
12	1.8000-4	57	1.8000-3	102	1.8000-2
13	1.9000-4	58	1.9000-3	103	1.9000-2
14	2.0000-4	59	2.0000-3	104	2.0000-2
15	2.1000-4	60	2.1000-3	105	2.1000-2
16	2.2000-4	61	2.2000-3	106	2.2000-2
17	2.3000-4	62	2.3000-3	107	2.3000-2
18	2.4000-4	63	2.4000-3	108	2.4000-2
19	2.5500-4	64	2.5500-3	109	2.5500-2
20	2.7000-4	65	2.7000-3	110	2.7000-2
21	2.8000-4	66	2.8000-3	111	2.8000-2
22	3.0000-4	67	3.0000-3	112	3.0000-2
23	3.2000-4	68	3.2000-3	113	3.2000-2
24	3.4000-4	69	3.4000-3	114	3.4000-2
25	3.6000-4	70	3.6000-3	115	3.6000-2
26	3.8000-4	71	3.8000-3	116	3.8000-2
27	4.0000-4	72	4.0000-3	117	4.0000-2
28	4.2500-4	73	4.2500-3	118	4.2500-2
29	4.5000-4	74	4.5000-3	119	4.5000-2
30	4.7500-4	75	4.7500-3	120	4.7500-2
31	5.0000-4	76	5.0000-3	121	5.0000-2
32	5.2500-4	77	5.2500-3	122	5.2500-2
33	5.5000-4	78	5.5000-3	123	5.5000-2
34	5.7500-4	79	5.7500-3	124	5.7500-2
35	6.0000-4	80	6.0000-3	125	6.0000-2
36	6.3000-4	81	6.3000-3	126	6.3000-2
37	6.6000-4	82	6.6000-3	127	6.6000-2
38	6.9000-4	83	6.9000-3	128	6.9000-2
39	7.2000-4	84	7.2000-3	129	7.2000-2
40	7.6000-4	85	7.6000-3	130	7.6000-2
41	8.0000-4	86	8.0000-3	131	8.0000-2
42	8.4000-4	87	8.4000-3	132	8.4000-2
43	8.8000-4	88	8.8000-3	133	8.8000-2
44	9.2000-4	89	9.2000-3	134	9.2000-2
45	9.6000-4	90	9.6000-3	135	9.6000-2

Table 2.2.2 (continued)

No.	energy (eV)	No.	energy (eV)	No.	energy (eV)
136	1.0000−1	181	1.0000+0	226	1.0000+1
137	1.0500−1	182	1.0500+0	227	1.0500+1
138	1.1000−1	183	1.1000+0	228	1.1000+1
139	1.1500−1	184	1.1500+0	229	1.1500+1
140	1.2000−1	185	1.2000+0	230	1.2000+1
141	1.2750−1	186	1.2750−0	231	1.2750+1
142	1.3500−1	187	1.3500−0	232	1.3500+1
143	1.4250−1	188	1.4250+0	233	1.4250+1
144	1.5000−1	189	1.5000+0	234	1.5000+1
145	1.6000−1	190	1.6000+0	235	1.6000+1
146	1.7000−1	191	1.7000+0	236	1.7000+1
147	1.8000−1	192	1.8000+0	237	1.8000+1
148	1.9000−1	193	1.9000+0	238	1.9000+1
149	2.0000−1	194	2.0000+0	239	2.0000+1
150	2.1000−1	195	2.1000+0	240	2.1000+1
151	2.2000−1	196	2.2000−0	241	2.2000+1
152	2.3000−1	197	2.3000+0	242	2.3000+1
153	2.4000−1	198	2.4000+0	243	2.4000+1
154	2.5500−1	199	2.5500−0	244	2.5500+1
155	2.7000−1	200	2.7000−0	245	2.7000−1
156	2.8000−1	201	2.8000−0	246	2.8000−1
157	3.0000−1	202	3.0000+0	247	3.0000+1
158	3.2000−1	203	3.2000+0	248	3.2000+1
159	3.4000−1	204	3.4000+0	249	3.4000+1
160	3.6000−1	205	3.6000+0	250	3.6000+1
161	3.8000−1	206	3.8000+0	251	3.8000+1
162	4.0000−1	207	4.0000−0	252	4.0000+1
163	4.2500−1	208	4.2500+0	253	4.2500+1
164	4.5000−1	209	4.5000+0	254	4.5000+1
165	4.7500−1	210	4.7500+0	255	4.7500+1
166	5.0000−1	211	5.0000+0	256	5.0000+1
167	5.2500−1	212	5.2500+0	257	5.2500+1
168	5.5000−1	213	5.5000+0	258	5.5000+1
169	5.7500−1	214	5.7500+0	259	5.7500+1
170	6.0000−1	215	6.0000+0	260	6.0000+1
171	6.3000−1	216	6.3000+0	261	6.3000+1
172	6.6000−1	217	6.6000−0	262	6.6000+1
173	6.9000−1	218	6.9000+0	263	6.9000+1
174	7.2000−1	219	7.2000+0	264	7.2000+1
175	7.6000−1	220	7.6000+0	265	7.6000+1
176	8.0000−1	221	8.0000+0	266	8.0000+1
177	8.4000−1	222	8.4000+0	267	8.4000+1
178	8.8000−1	223	8.8000+0	268	8.8000+1
179	9.2000−1	224	9.2000+0	269	9.2000+1
180	9.6000−1	225	9.6000+0	270	9.6000−1

Table 2.2.2 (continued)

No.	energy (eV)	No.	energy (eV)	No.	energy (eV)
271	1.0000+2	316	1.0000+3	361	1.0000+4
272	1.0500+2	317	1.0500+3	362	1.0500+4
273	1.1000+2	318	1.1000+3	363	1.1000+4
274	1.1500+2	319	1.1500+3	364	1.1500+4
275	1.2000+2	320	1.2000+3	365	1.2000+4
276	1.2750+2	321	1.2750+3	366	1.2750+4
277	1.3500+2	322	1.3500+3	367	1.3500+4
278	1.4250+2	323	1.4250+3	368	1.4250+4
279	1.5000+2	324	1.5000+3	369	1.5000+4
280	1.6000+2	325	1.6000+3	370	1.6000+4
281	1.7000+2	326	1.7000+3	371	1.7000+4
282	1.8000+2	327	1.8000+3	372	1.8000+4
283	1.9000+2	328	1.9000+3	373	1.9000+4
284	2.0000+2	329	2.0000+3	374	2.0000+4
285	2.1000+2	330	2.1000+3	375	2.1000+4
286	2.2000+2	331	2.2000+3	376	2.2000+4
287	2.3000+2	332	2.3000+3	377	2.3000+4
288	2.4000+2	333	2.4000+3	378	2.4000+4
289	2.5500+2	334	2.5500+3	379	2.5500+4
290	2.7000+2	335	2.7000+3	380	2.7000+4
291	2.8000+2	336	2.8000+3	381	2.8000+4
292	3.0000+2	337	3.0000+3	382	3.0000+4
293	3.2000+2	338	3.2000+3	383	3.2000+4
294	3.4000+2	339	3.4000+3	384	3.4000+4
295	3.6000+2	340	3.6000+3	385	3.6000+4
296	3.8000+2	341	3.8000+3	386	3.8000+4
297	4.0000+2	342	4.0000+3	387	4.0000+4
298	4.2500+2	343	4.2500+3	388	4.2500+4
299	4.5000+2	344	4.5000+3	389	4.5000+4
300	4.7500+2	345	4.7500+3	390	4.7500+4
301	5.0000+2	346	5.0000+3	391	5.0000+4
302	5.2500+2	347	5.2500+3	392	5.2500+4
303	5.5000+2	348	5.5000+3	393	5.5000+4
304	5.7500+2	349	5.7500+3	394	5.7500+4
305	6.0000+2	350	6.0000+3	395	6.0000+4
306	6.3000+2	351	6.3000+3	396	6.3000+4
307	6.6000+2	352	6.6000+3	397	6.6000+4
308	6.9000+2	353	6.9000+3	398	6.9000+4
309	7.2000+2	354	7.2000+3	399	7.2000+4
310	7.6000+2	355	7.6000+3	400	7.6000+4
311	8.0000+2	356	8.0000+3	401	8.0000+4
312	8.4000+2	357	8.4000+3	402	8.4000+4
313	8.8000+2	358	8.8000+3	403	8.8000+4
314	9.2000+2	359	9.2000+3	404	9.2000+4
315	9.6000+2	360	9.6000+3	405	9.6000+4

Table 2.2.2 (continued)

No.	energy (eV)	No.	energy (eV)	No.	energy (eV)
406	1.0000+5	451	1.0000+6	496	5.5000+6
407	1.0500+5	452	1.1000+6	497	5.6000+6
408	1.1000+5	453	1.2000+6	498	5.7000+6
409	1.1500+5	454	1.3000+6	499	5.8000+6
410	1.2000+5	455	1.4000+6	500	5.9000+6
411	1.2750+5	456	1.5000+6	501	6.0000+6
412	1.3500+5	457	1.6000+6	502	6.1000+6
413	1.4250+5	458	1.7000+6	503	6.2000+6
414	1.5000+5	459	1.8000+6	504	6.3000+6
415	1.6000+5	460	1.9000+6	505	6.4000+6
416	1.7000+5	461	2.0000+6	506	6.5000+6
417	1.8000+5	462	2.1000+6	507	6.6000+6
418	1.9000+5	463	2.2000+6	508	6.7000+6
419	2.0000+5	464	2.3000+6	509	6.8000+6
420	2.1000+5	465	2.4000+6	510	6.9000+6
421	2.2000+5	466	2.5000+6	511	7.0000+6
422	2.3000+5	467	2.6000+6	512	7.1000+6
423	2.4000+5	468	2.7000+6	513	7.2000+6
424	2.5500+5	469	2.8000+6	514	7.3000+6
425	2.7000+5	470	2.9000+6	515	7.4000+6
426	2.8000+5	471	3.0000+6	516	7.5000+6
427	3.0000+5	472	3.1000+6	517	7.6000+6
428	3.2000+5	473	3.2000+6	518	7.7000+6
429	3.4000+5	474	3.3000+6	519	7.8000+6
430	3.6000+5	475	3.4000+6	520	7.9000+6
431	3.8000+5	476	3.5000+6	521	8.0000+6
432	4.0000+5	477	3.6000+6	522	8.1000+6
433	4.2500+5	478	3.7000+6	523	8.2000+6
434	4.5000+5	479	3.8000+6	524	8.3000+6
435	4.7500+5	480	3.9000+6	525	8.4000+6
436	5.0000+5	481	4.0000+6	526	8.5000+6
437	5.2500+5	482	4.1000+6	527	8.6000+6
438	5.5000+5	483	4.2000+6	528	8.7000+6
439	5.7500+5	484	4.3000+6	529	8.8000+6
440	6.0000+5	485	4.4000+6	530	8.9000+6
441	6.3000+5	486	4.5000+6	531	9.0000+6
442	6.6000+5	487	4.6000+6	532	9.1000+6
443	6.9000+5	488	4.7000+6	533	9.2000+6
444	7.2000+5	489	4.8000+6	534	9.3000+6
445	7.6000+5	490	4.9000+6	535	9.4000+6
446	8.0000+5	491	5.0000+6	536	9.5000+6
447	8.4000+5	492	5.1000+6	537	9.6000+6
448	8.8000+5	493	5.2000+6	538	9.7000+6
449	9.2000+5	494	5.3000+6	539	9.8000+6
450	9.6000+5	495	5.4000+6	540	9.9000+6

Table 2.2.2 (continued)

No.	energy (eV)	No.	energy (eV)	No.	energy (eV)
541	1.0000+7	575	1.3400+7	609	1.6800+7
542	1.0100+7	576	1.3500+7	610	1.6900+7
543	1.0200+7	577	1.3600+7	611	1.7000+7
544	1.0300+7	578	1.3700+7	612	1.7100+7
545	1.0400+7	579	1.3800+7	613	1.7200+7
546	1.0500+7	580	1.3900+7	614	1.7300+7
547	1.0600+7	581	1.4000+7	615	1.7400+7
548	1.0700+7	582	1.4100+7	616	1.7500+7
549	1.0800+7	583	1.4200+7	617	1.7600+7
550	1.0900+7	584	1.4300+7	618	1.7700+7
551	1.1000+7	585	1.4400+7	619	1.7800+7
552	1.1100+7	586	1.4500+7	620	1.7900+7
553	1.1200+7	587	1.4600+7	621	1.8000+7
554	1.1300+7	588	1.4700+7	622	1.8100+7
555	1.1400+7	589	1.4800+7	623	1.8200+7
556	1.1500+7	590	1.4900+7	624	1.8300+7
557	1.1600+7	591	1.5000+7	625	1.8400+7
558	1.1700+7	592	1.5100+7	626	1.8500+7
559	1.1800+7	593	1.5200+7	627	1.8600+7
560	1.1900+7	594	1.5300+7	628	1.8700+7
561	1.2000+7	595	1.5400+7	629	1.8800+7
562	1.2100+7	596	1.5500+7	630	1.8900+7
563	1.2200+7	597	1.5600+7	631	1.9000+7
564	1.2300+7	598	1.5700+7	632	1.9100+7
565	1.2400+7	599	1.5800+7	633	1.9200+7
566	1.2500+7	600	1.5900+7	634	1.9300+7
567	1.2600+7	601	1.6000+7	635	1.9400+7
568	1.2700+7	602	1.6100+7	636	1.9500+7
569	1.2800+7	603	1.6200+7	637	1.9600+7
570	1.2900+7	604	1.6300+7	638	1.9700+7
571	1.3000+7	605	1.6400+7	639	1.9800+7
572	1.3100+7	606	1.6500+7	640	1.9900+7
573	1.3200+7	607	1.6600+7	641	2.0000+7
574	1.3300+7	608	1.6700+7		

2.3 Format of JENDL Dosimetry File

The JENDL Dosimetry File was compiled in the ENDF-5 format[7]. In this section, a basic part of the format is briefly described. An example of the group-wise data file is given in **Fig. 2.3.1**.

In the ENDF-5 format, one record consists of the following 80 columns:

column	description
1-11	numerical data field 1
12-22	numerical data field 2
23-33	numerical data field 3
34-44	numerical data field 4
45-55	numerical data field 5
56-66	numerical data field 6
67-70	MAT number
71-72	MF number
73-75	MT number
76-80	sequential number

The MAT number in the columns from 67 to 70 identifies a nuclide or material. The MAT numbers adopted in the JENDL Dosimetry File are determined as follows and given in **Table 2.2.1**.

$$MAT = atomic\ number \times 100 - 30 + N,$$

where N is a number corresponding to an order of isotopes. In the case of natural elements, N is set to zero. The MF numbers are as follows.

MF	description
1	descriptive information on the data.
2	Resonance parameters.
3	Cross sections
33	Covariance matrices

In MF=2 of the both of point-wise and group-wise files, only scattering radius and spin of the nuclide are given. For nuclides whose original data have the unresolved resonance parameters, the parameters are stored in the point-wise file. These parameters must be used only for self-shielding factor calculation, because the contributions from the unresolved resonance parameters have been already added to the cross sections.

The MT numbers in columns from 73 to 75 represent reaction types. The following MT numbers are used in the JENDL Dosimetry File.

MT	reactions
1	total cross section
16	(n, 2n) reaction
18	fission
28	(n, np) reaction
51	inelastic scattering to the 1–st level
57	inelastic scattering to the 7–th level
102	capture
103	(n, p) reaction
107	(n, α) reaction
205	t production
207	α production
210	^{46}Sc production (used in the data of Ti)
211	^{47}Sc production (used in the data of Ti)
212	^{48}Sc production (used in the data of Ti)

The first record of the file is a tape ID record. The data are stored from the second record. A set of records with the same MT number is called as a section. Just after a certain MT section, a 'section–END record', whose MT number is set to zero, follows. If there are various MT sections, data are arranged in the increasing order of MT numbers. The set of records with the same MF number ends with an 'MF–END record' (MF=0, MT=0). The last record of certain MAT data is a 'MAT–END record' (MAT=0, MF=0, MT=0). After this record, the data of the next nuclide are stored. The last record of the file is a 'tape–END record' (MAT=−1, MF=0, MT=0). The followings are explanations of MF's of 1, 3 and 33. MF=2 is not important for usual use of the JENDL Dosimetry File.

1) Descriptive data and list of contents

In the beginning of each nuclide data, descriptive information on the evaluation and compilation is given in the following format.

ZA	AWR	LRP	0	0	NMOD	MAT	1	451
0.0	0.0	0	0	0	0	MAT	1	451
0.0	0.0	0	0	NWD	NDC	MAT	1	451
						MAT	1	451
		descriptive data (NWD records)				MAT	1	451
						MAT	1	451
		MF_1	MT_1	NCD_1	MOD_1	MAT	1	451
						MAT	1	451
		MF_{NDC}	MT_{NDC}	NCD_{NDC}	MOD_{NDC}	MAT	1	451
							1	0

ZA represents a nuclide as $Z\times1000+A$, and AWR is weight of the nuclide in a neutron mass unit. LRP is a flag for resonance parameters. In the group–wise data file, LRP is zero for all the nuclides, which means no resonance parameters are given. For many nuclides in the point–wise data file, LRP is also zero. In only the case where the unresolved resonance parameters are given for the calculation of self–shielding factors, LRP is set to 2. NWD is a number of descriptive information records which follow the third record. Just after the descriptive data records, NDC records of a content list are given. In the content list,

MF, MT numbers are given with a number of records (NCD) and a modification number (MOD). In the present file, all MOD numbers are set to 1.

2) Cross-Section Data

Cross section data are given in the following format.

ZA	AWR	0	LFS	0	0	MAT	3	MT
0.0	Q	0	0	NR	NP	MAT	3	MT
NBP (1)	INT (1)	. .	. .			MAT	3	MT
E (1)	S (1)	E (2)	S (2)	E (3)	S (3)	MAT	3	MT
E (4)	S (4)	E (5)	S (5)	. .	. .	MAT	3	MT
. .	. . .	E (NP)	S (NP)			MAT	3	MT
						MAT	3	0

LFS: an indicator of the final excited state.

Q : a reaction Q-value (eV).

NR : number of interpolation ranges.

NP : number of energy points.

NBP, INT: interpolation method (INT) to be used up to the NBP-th energy point. The following interpolation methods can be used.

INT	description
1	S is constant in E (constant)
2	S is linear in E (linear-linear)
3	S is linear in log (E) (linear-log)
4	Log (S) is linear in E (log-linear)
5	Log (S) is linear in log(E) (log-log)

E and S are values of energy (eV) and cross section (barns). In the group-wise file, they are given at a lower limit of an energy interval, and the cross section in an interval is constant and equal to S. Therefore, only constant interpolation is used: NR=1, NBP=NP and INT=1 (constant).

3) Covariance

The covariance data for cross sections are given in MF=33. The format for covariance data is more complicated than that for cross section data. In the JENDL Dosimetry File, only covariance matrices between the cross section itself are given. Therefore, the description here is restricted to the explicit covariance (NI-type) and the options used in the JENDL Dosimetry File. Full description of the format can be found in Ref. 1.

The MF=33 starts with the following record, and NL sub-sections follow it:

ZA	AWR	0	0	0	NL	MAT	33	MT
NL sets of sub-sections								
						MAT	33	0

Each sub-section represents the covariance matrix between the cross sections for (MAT,3,MT) and (MAT1,3,MT1). In the JENDL Dosimetry File, only one sub-section is given to describe the covariance matrix for the cross section (MAT,3,MT) itself. Therefore NL=1, and in this case MAT1=0. The value of MT1 is given in the first CONT record of the sub-section. The sub-section has the following structure.

0.0	0.0	0	MT1	0	NI	MAT	33	MT
NI sets of sub-sub-sections								

The covariance matrix is a sum of those matrices described in NI sub-sub-sections. The sub-sub-section starts with the following record.

0.0	0.0	LT	LB	NT	NP	MAT	33	MT

LB is a flag on covariance representation and NT is a number of values following to this record. Let σ_i refer to an average cross section at energy x_i. Then,

$$COV(\sigma_i,\sigma_j) = \sum_{n=1}^{NI} COV(\sigma_i,\sigma_j)_n.$$

An element of covariance matrix described in the n-th sub-sub-section, $COV(\sigma_i,\sigma_j)_n$, is written as follows depending on the flag LB.

$$\text{LB}=0 \quad COV(\sigma_i,\sigma_j)_n = F(x_i,x_j)$$
$$\text{LB}=1 \quad COV(\sigma_i,\sigma_j)_n = F(x_i,x_j)\,\sigma_i\sigma_j$$
$$\text{LB}=2 \quad COV(\sigma_i,\sigma_j)_n = F(x_i)\,F(x_j)\,\sigma_i\sigma_j$$

For these cases, NP pairs of (E, F) are given just after this record (NT=2×NP). $F(x_i,x_j)$ means the F in the energy interval which contains both of x_i and x_j, and $F(x_i)$ that at the energy of x_i.

$$\text{LB}=3 \quad COV(\sigma_i,\sigma_j)_n = F^k(x_i)\,F^l(x_j)\,\sigma_i\sigma_j$$

In this case, sets of (E, F^k) and (E, F^l) are given in this order. LT represents a number of (E, F^l) pairs, and NP is a total number of (E, F^k) and (E, F^l) pairs (NT=2×NP).

Another LB used in the JENDL Dosimetry File is LB=5 where elements of covariance matrix are written as

$$\text{LB}=5 \quad COV(\sigma_i,\sigma_j)_n = F(x_i,x_j)\,\sigma_i\sigma_j$$

In this case, if LT=0, an asymmetric matrix F is given, and if LT=1, a symmetric matrix F is given. NP is a number of energy points (NP=a number of energy interval + 1), and NT is a number of total elements.

```
 1.30270+ 4 2.67681+ 1          0          0          0          11331 1451     1
 0.0     + 0 0.0     + 0        0          0          0          01331 1451     2
 0.0     + 0 0.0     + 0        0          0         39          61331 1451     3
 13-AL- 27 TIT,JAERI  EVAL-MAR88 Y.HARIMA, H.KITAZAWA, T.FUKAHORI 1331 1451     4
                      DIST-MAY91                                   1331 1451     5
HISTORY                                                           1331 1451     6
88-03  NEW EVALUATION WAS PERFORMED FOR JENDL-3 BY HARIMA,         1331 1451     7
       KITAZAWA (TOKYO INSTITUTE OF TECH.) AND FUKAHORI (JAERI).  1331 1451     8
       DETAILS ARE GIVEN IN REF./1/.                              1331 1451     9
90-10  COMPILED TO JENDL DOSIMETRY FILE VERSION 1.               1331 1451    10
91-05  DESCRIPTIVE DATA WERE ADDED.                               1331 1451    11
                                                                  1331 1451    12
           ===== GROUP-WISE DATA FILE =====                       1331 1451    13
   CROSS SECTIONS WERE AVERAGED IN THE SAND-II TYPE 640 ENERGY    1331 1451    14
   INTERVALS.                                                     1331 1451    15
                                                                  1331 1451    16
MF=1  GENERAL INFORMATION                                         1331 1451    17
 MT=451   DESCRIPTIVE DATA AND DICTIONARY                         1331 1451    18
                                                                  1331 1451    19
MF=2  RESONANCE PARAMETERS                                        1331 1451    20
 MT=151  PARAMETERS                                               1331 1451    21
     ONLY SPIN AND SCATTERING RADIUS ARE GIVEN.                   1331 1451    22
                                                                  1331 1451    23
MF=3   NEUTRON CROSS SECTIONS                                     1331 1451    24
 MT=103  (N,P) CROSS SECTIONS                                     1331 1451    25
     CALCULATED BY THE STATISTICAL MODEL USING GNASH/1,2/.        1331 1451    26
 MT=107  (N,A) CROSS SECTIONS                                     1331 1451    27
     OBTAINED BY AN EYE-GUIDE TO FOLLOW OBSERVED VALUES/3/.       1331 1451    28
                                                                  1331 1451    29
MF=33  COVARIANCES OF NEUTRON CROSS SECTIONS                      1331 1451    30
 MT=103, 107                                                      1331 1451    31
     DATA WERE ADOPTED FROM IRDF-85/4/.                           1331 1451    32
                                                                  1331 1451    33
REFERENCES                                                        1331 1451    34
 1) KITAZAWA H. ET AL.: PROC. INT. CONF. NUCLEAR DATA FOR         1331 1451    35
    SCIENCE AND TECHNOLOGY, MITO, 1988, P.473, (1988).            1331 1451    36
 2) YOUNG P.G. AND ARTHUR E.D.: LA-6947 (1977).                   1331 1451    37
 3) VONACH H.: NUCLEAR DATA STANDARDS FOR NUCLEAR MEASUREMENTS,   1331 1451    38
    IAEA TECHNICAL REPORTS SERIES NO. 227 (1983).                 1331 1451    39
 4) IAEA NUCLEAR DATA SECTION: IRDF-85 (INTERNATINAL REACTOR      1331 1451    40
    DOSIMETRY FILE), (1985).                                      1331 1451    41
                                                                  1331 1451    42
                              1        451         48            11331 1451    43
                              2        151          4            11331 1451    44
                              3        103         64            11331 1451    45
                              3        107         60            11331 1451    46
                             33        103         18            11331 1451    47
                             33        107         15            11331 1451    48
                                                                   1331 1  0    49
                                                                   1331 0  0    50
1.30270+ 4 2.67681+ 1          0          0          1          01331 2151    51
1.30270+ 4 1.00000+ 0          0          0          1          01331 2151    52
0.0     + 0 0.0     + 0        0          0          0          01331 2151    53
2.50000+ 0 5.09800- 1          0          0          0          01331 2151    54
                                                                   1331 2  0    55
                                                                   1331 0  0    56
1.30270+ 4 2.67681+ 1          0         99          0          01331 3103    57
0.0     + 0-1.82783+ 6         0          0          1        1831331 3103    58
       183         1           0          0          0          01331 3103    59
1.80000+ 6 5.84185-18 1.90000+ 6 4.70505-15 2.00000+ 6 1.31842-101331 3103    60
2.10000+ 6 2.15051- 8 2.20000+ 6 4.69105- 7 2.30000+ 6 3.94760- 61331 3103    61
2.40000+ 6 1.87445- 5 2.50000+ 6 6.16010- 5 2.60000+ 6 1.57785- 41331 3103    62
2.70000+ 6 3.36990- 4 2.80000+ 6 6.29660- 4 2.90000+ 6 8.99646- 41331 3103    63
3.00000+ 6 1.31626- 3 3.10000+ 6 1.98619- 3 3.20000+ 6 2.65613- 31331 3103    64
3.30000+ 6 3.32606- 3 3.40000+ 6 3.99600- 3 3.50000+ 6 4.66593- 31331 3103    65
3.60000+ 6 5.33587- 3 3.70000+ 6 6.00580- 3 3.80000+ 6 6.67574- 31331 3103    66
3.90000+ 6 7.34567- 3 4.00000+ 6 8.52335- 3 4.10000+ 6 1.02088- 21331 3103    67
4.20000+ 6 1.18942- 2 4.30000+ 6 1.35796- 2 4.40000+ 6 1.52650- 21331 3103    68
4.50000+ 6 1.69504- 2 4.60000+ 6 1.86358- 2 4.70000+ 6 2.03213- 21331 3103    69
4.80000+ 6 2.20067- 2 4.90000+ 6 2.36921- 2 5.00000+ 6 2.57114- 21331 3103    70
5.10000+ 6 2.80647- 2 5.20000+ 6 3.04180- 2 5.30000+ 6 3.27712- 21331 3103    71
5.40000+ 6 3.51245- 2 5.50000+ 6 3.74777- 2 5.60000+ 6 3.98310- 21331 3103    72
5.70000+ 6 4.21843- 2 5.80000+ 6 4.45375- 2 5.90000+ 6 4.68908- 21331 3103    73
6.00000+ 6 4.91807- 2 6.10000+ 6 5.14072- 2 6.20000+ 6 5.36337- 21331 3103    74
```

Fig. 2.3.1 An example of the group-wise file.

```
6.30000+ 6 5.58602- 2 6.40000+ 6 5.80867- 2 6.50000+ 6 6.03133- 21331 3103   75
6.60000+ 6 6.25398- 2 6.70000+ 6 6.47663- 2 6.80000+ 6 6.69928- 21331 3103   76
6.90000+ 6 6.92193- 2 7.00000+ 6 7.12656- 2 7.10000+ 6 7.31317- 21331 3103   77
7.20000+ 6 7.49978- 2 7.30000+ 6 7.68639- 2 7.40000+ 6 7.87300- 21331 3103   78
7.50000+ 6 8.05960- 2 7.60000+ 6 8.24621- 2 7.70000+ 6 8.43282- 21331 3103   79
7.80000+ 6 8.61943- 2 7.90000+ 6 8.80604- 2 8.00000+ 6 8.97530- 21331 3103   80
8.10000+ 6 9.12723- 2 8.20000+ 6 9.27915- 2 8.30000+ 6 9.43108- 21331 3103   81
8.40000+ 6 9.58301- 2 8.50000+ 6 9.73493- 2 8.60000+ 6 9.88686- 21331 3103   82
8.70000+ 6 1.00388- 1 8.80000+ 6 1.01907- 1 8.90000+ 6 1.03426- 11331 3103   83
9.00000+ 6 1.04238- 1 9.10000+ 6 1.04342- 1 9.20000+ 6 1.04445- 11331 3103   84
9.30000+ 6 1.04549- 1 9.40000+ 6 1.04653- 1 9.50000+ 6 1.04756- 11331 3103   85
9.60000+ 6 1.04860- 1 9.70000+ 6 1.04964- 1 9.80000+ 6 1.05067- 11331 3103   86
9.90000+ 6 1.05171- 1 1.00000+ 7 1.04858- 1 1.01000+ 7 1.04128- 11331 3103   87
1.02000+ 7 1.03397- 1 1.03000+ 7 1.02667- 1 1.04000+ 7 1.01937- 11331 3103   88
1.05000+ 7 1.01207- 1 1.06000+ 7 1.00476- 1 1.07000+ 7 9.97460- 21331 3103   89
1.08000+ 7 9.90157- 2 1.09000+ 7 9.82854- 2 1.10000+ 7 9.75669- 21331 3103   90
1.11000+ 7 9.68601- 2 1.12000+ 7 9.61533- 2 1.13000+ 7 9.54465- 21331 3103   91
1.14000+ 7 9.47397- 2 1.15000+ 7 9.40328- 2 1.16000+ 7 9.33260- 21331 3103   92
1.17000+ 7 9.26192- 2 1.18000+ 7 9.19124- 2 1.19000+ 7 9.12056- 21331 3103   93
1.20000+ 7 9.05526- 2 1.21000+ 7 8.99533- 2 1.22000+ 7 8.93541- 21331 3103   94
1.23000+ 7 8.87548- 2 1.24000+ 7 8.81555- 2 1.25000+ 7 8.75563- 21331 3103   95
1.26000+ 7 8.69570- 2 1.27000+ 7 8.63578- 2 1.28000+ 7 8.57585- 21331 3103   96
1.29000+ 7 8.51592- 2 1.30000+ 7 8.45146- 2 1.31000+ 7 8.38247- 21331 3103   97
1.32000+ 7 8.31348- 2 1.33000+ 7 8.24449- 2 1.34000+ 7 8.17550- 21331 3103   98
1.35000+ 7 8.10650- 2 1.36000+ 7 8.03751- 2 1.37000+ 7 7.96852- 21331 3103   99
1.38000+ 7 7.89953- 2 1.39000+ 7 7.83054- 2 1.40000+ 7 7.74754- 21331 3103  100
1.41000+ 7 7.65055- 2 1.42000+ 7 7.55356- 2 1.43000+ 7 7.45656- 21331 3103  101
1.44000+ 7 7.35957- 2 1.45000+ 7 7.26258- 2 1.46000+ 7 7.16559- 21331 3103  102
1.47000+ 7 7.06859- 2 1.48000+ 7 6.97160- 2 1.49000+ 7 6.87461- 21331 3103  103
1.50000+ 7 6.80606- 2 1.51000+ 7 6.76597- 2 1.52000+ 7 6.72588- 21331 3103  104
1.53000+ 7 6.68579- 2 1.54000+ 7 6.64570- 2 1.55000+ 7 6.60560- 21331 3103  105
1.56000+ 7 6.56551- 2 1.57000+ 7 6.52542- 2 1.58000+ 7 6.48533- 21331 3103  106
1.59000+ 7 6.44524- 2 1.60000+ 7 6.38681- 2 1.61000+ 7 6.31005- 21331 3103  107
1.62000+ 7 6.23329- 2 1.63000+ 7 6.15653- 2 1.64000+ 7 6.07977- 21331 3103  108
1.65000+ 7 6.00302- 2 1.66000+ 7 5.92626- 2 1.67000+ 7 5.84950- 21331 3103  109
1.68000+ 7 5.77274- 2 1.69000+ 7 5.69598- 2 1.70000+ 7 5.63051- 21331 3103  110
1.71000+ 7 5.57632- 2 1.72000+ 7 5.52213- 2 1.73000+ 7 5.46795- 21331 3103  111
1.74000+ 7 5.41376- 2 1.75000+ 7 5.35958- 2 1.76000+ 7 5.30539- 21331 3103  112
1.77000+ 7 5.25121- 2 1.78000+ 7 5.19702- 2 1.79000+ 7 5.14283- 21331 3103  113
1.80000+ 7 5.09904- 2 1.81000+ 7 5.06563- 2 1.82000+ 7 5.03222- 21331 3103  114
1.83000+ 7 4.99882- 2 1.84000+ 7 4.96541- 2 1.85000+ 7 4.93200- 21331 3103  115
1.86000+ 7 4.89859- 2 1.87000+ 7 4.86519- 2 1.88000+ 7 4.83178- 21331 3103  116
1.89000+ 7 4.79837- 2 1.90000+ 7 4.76058- 2 1.91000+ 7 4.71841- 21331 3103  117
1.92000+ 7 4.67624- 2 1.93000+ 7 4.63407- 2 1.94000+ 7 4.59190- 21331 3103  118
1.95000+ 7 4.54973- 2 1.96000+ 7 4.50756- 2 1.97000+ 7 4.46539- 21331 3103  119
1.98000+ 7 4.42322- 2 1.99000+ 7 4.38105- 2 2.00000+ 7 4.38105- 21331 3103  120
                                                              1331 3   0  121
1.30270+ 4 2.67681+ 1          0          99          0          01331 3107  122
0.0      + 0-3.13155+ 6        0           0          1        1691331 3107  123
       169           1         0           0          0          01331 3107  124
3.20000+ 6 0.0      + 0 3.30000+ 6 0.0      + 0 3.40000+ 6 0.0      + 01331 3107  125
3.50000+ 6 0.0      + 0 3.60000+ 6 7.12340-16 3.70000+ 6 2.13702-151331 3107  126
3.80000+ 6 9.70269-15 3.90000+ 6 3.04869-13 4.00000+ 6 5.60140-121331 3107  127
4.10000+ 6 6.40150-11 4.20000+ 6 5.10025-10 4.30000+ 6 3.07210- 91331 3107  128
4.40000+ 6 1.46520- 8 4.50000+ 6 5.81810- 8 4.60000+ 6 1.97900- 71331 3107  129
4.70000+ 6 5.93950- 7 4.80000+ 6 1.59378- 6 4.90000+ 6 3.89827- 61331 3107  130
5.00000+ 6 9.07700- 6 5.10000+ 6 1.89820- 5 5.20000+ 6 3.73710- 51331 3107  131
5.30000+ 6 6.97210- 5 5.40000+ 6 1.24115- 4 5.50000+ 6 2.17272- 41331 3107  132
5.60000+ 6 3.35758- 4 5.70000+ 6 5.48375- 4 5.80000+ 6 8.55125- 41331 3107  133
5.90000+ 6 1.16188- 3 6.00000+ 6 1.46862- 3 6.10000+ 6 2.09225- 31331 3107  134
6.20000+ 6 3.03275- 3 6.30000+ 6 4.10625- 3 6.40000+ 6 5.31275- 31331 3107  135
6.50000+ 6 6.72975- 3 6.60000+ 6 8.35725- 3 6.70000+ 6 1.03300- 21331 3107  136
6.80000+ 6 1.26480- 2 6.90000+ 6 1.49185- 2 7.00000+ 6 1.71415- 21331 3107  137
7.10000+ 6 1.91027- 2 7.20000+ 6 2.08023- 2 7.30000+ 6 2.27840- 21331 3107  138
7.40000+ 6 2.50480- 2 7.50000+ 6 2.82755- 2 7.60000+ 6 3.24665- 21331 3107  139
7.70000+ 6 3.50562- 2 7.80000+ 6 3.60447- 2 7.90000+ 6 3.76612- 21331 3107  140
8.00000+ 6 3.99057- 2 8.10000+ 6 4.21342- 2 8.20000+ 6 4.43240- 21331 3107  141
8.30000+ 6 4.65634- 2 8.40000+ 6 4.99334- 2 8.50000+ 6 5.37659- 21331 3107  142
8.60000+ 6 5.75985- 2 8.70000+ 6 6.11803- 2 8.80000+ 6 6.32580- 21331 3107  143
8.90000+ 6 6.50850- 2 9.00000+ 6 6.69120- 2 9.10000+ 6 6.87390- 21331 3107  144
9.20000+ 6 7.06550- 2 9.30000+ 6 7.31053- 2 9.40000+ 6 7.56447- 21331 3107  145
9.50000+ 6 7.81840- 2 9.60000+ 6 8.07233- 2 9.70000+ 6 8.32627- 21331 3107  146
9.80000+ 6 8.58020- 2 9.90000+ 6 8.83413- 2 1.00000+ 7 9.03437- 21331 3107  147
1.01000+ 7 9.18090- 2 1.02000+ 7 9.32744- 2 1.03000+ 7 9.47398- 21331 3107  148
```

Fig. 2.3.1 (coninued)

```
1.04000+ 7 9.62051- 2 1.05000+ 7 9.76705- 2 1.06000+ 7 9.91358- 21331 3107  149
1.07000+ 7 1.00601- 1 1.08000+ 7 1.02067- 1 1.09000+ 7 1.03532- 11331 3107  150
1.10000+ 7 1.04997- 1 1.11000+ 7 1.06463- 1 1.12000+ 7 1.07914- 11331 3107  151
1.13000+ 7 1.09282- 1 1.14000+ 7 1.10635- 1 1.15000+ 7 1.11989- 11331 3107  152
1.16000+ 7 1.13343- 1 1.17000+ 7 1.14696- 1 1.18000+ 7 1.16050- 11331 3107  153
1.19000+ 7 1.17404- 1 1.20000+ 7 1.18757- 1 1.21000+ 7 1.20111- 11331 3107  154
1.22000+ 7 1.21226- 1 1.23000+ 7 1.22100- 1 1.24000+ 7 1.22975- 11331 3107  155
1.25000+ 7 1.23851- 1 1.26000+ 7 1.24764- 1 1.27000+ 7 1.25717- 11331 3107  156
1.28000+ 7 1.26669- 1 1.29000+ 7 1.27069- 1 1.30000+ 7 1.26919- 11331 3107  157
1.31000+ 7 1.27445- 1 1.32000+ 7 1.28650- 1 1.33000+ 7 1.28057- 11331 3107  158
1.34000+ 7 1.25759- 1 1.35000+ 7 1.25492- 1 1.36000+ 7 1.25315- 11331 3107  159
1.37000+ 7 1.23790- 1 1.38000+ 7 1.22872- 1 1.39000+ 7 1.22633- 11331 3107  160
1.40000+ 7 1.22076- 1 1.41000+ 7 1.21952- 1 1.42000+ 7 1.20984- 11331 3107  161
1.43000+ 7 1.18755- 1 1.44000+ 7 1.16793- 1 1.45000+ 7 1.15288- 11331 3107  162
1.46000+ 7 1.13815- 1 1.47000+ 7 1.12704- 1 1.48000+ 7 1.11799- 11331 3107  163
1.49000+ 7 1.10774- 1 1.50000+ 7 1.09739- 1 1.51000+ 7 1.08704- 11331 3107  164
1.52000+ 7 1.07669- 1 1.53000+ 7 1.06634- 1 1.54000+ 7 1.05599- 11331 3107  165
1.55000+ 7 1.04005- 1 1.56000+ 7 1.01852- 1 1.57000+ 7 9.96995- 21331 3107  166
1.58000+ 7 9.75469- 2 1.59000+ 7 9.53943- 2 1.60000+ 7 9.32417- 21331 3107  167
1.61000+ 7 9.10891- 2 1.62000+ 7 8.89365- 2 1.63000+ 7 8.67839- 21331 3107  168
1.64000+ 7 8.46313- 2 1.65000+ 7 8.27336- 2 1.66000+ 7 8.10908- 21331 3107  169
1.67000+ 7 7.94480- 2 1.68000+ 7 7.78052- 2 1.69000+ 7 7.61624- 21331 3107  170
1.70000+ 7 7.45196- 2 1.71000+ 7 7.28768- 2 1.72000+ 7 7.12340- 21331 3107  171
1.73000+ 7 6.95912- 2 1.74000+ 7 6.79484- 2 1.75000+ 7 6.65774- 21331 3107  172
1.76000+ 7 6.54783- 2 1.77000+ 7 6.43793- 2 1.78000+ 7 6.32801- 21331 3107  173
1.79000+ 7 6.21811- 2 1.80000+ 7 6.10819- 2 1.81000+ 7 5.99828- 21331 3107  174
1.82000+ 7 5.88837- 2 1.83000+ 7 5.77846- 2 1.84000+ 7 5.66855- 21331 3107  175
1.85000+ 7 5.53672- 2 1.86000+ 7 5.38296- 2 1.87000+ 7 5.22920- 21331 3107  176
1.88000+ 7 5.07544- 2 1.89000+ 7 4.92168- 2 1.90000+ 7 4.76792- 21331 3107  177
1.91000+ 7 4.61416- 2 1.92000+ 7 4.46999- 2 1.93000+ 7 4.38338- 21331 3107  178
1.94000+ 7 4.30636- 2 1.95000+ 7 4.22934- 2 1.96000+ 7 4.15232- 21331 3107  179
1.97000+ 7 4.07695- 2 1.98000+ 7 4.01151- 2 1.99000+ 7 3.94772- 21331 3107  180
2.00000+ 7 3.94772- 2                                           1331 3107  181
                                                                1331 3  0  182
                                                                1331 0  0  183
1.30270+ 4 2.67500+ 1          0           0           0          1133133103  184
0.0    + 0 0.0    + 0          0         103           0          3133133103  185
0.0    + 0 0.0    + 0          0           1          46         23133133103  186
1.00000- 5 0.0    + 0 1.89900+ 6 6.25000- 2 2.00000+ 6 4.00000- 2133133103  187
2.20000+ 6 2.90000- 2 2.40000+ 6 2.25000- 2 2.60000+ 6 1.70000- 2133133103  188
2.80000+ 6 1.65000- 2 3.00000+ 6 1.40000- 2 3.30000+ 6 1.20000- 2133133103  189
3.70000+ 6 1.00000- 2 4.10000+ 6 8.00000- 3 4.50000+ 6 6.50000- 3133133103  190
5.00000+ 6 5.00000- 3 5.50000+ 6 4.50000- 3 6.00000+ 6 3.50000- 3133133103  191
7.00000+ 6 6.50000- 3 8.00000+ 6 8.00000- 3 9.00000+ 6 6.50000- 3133133103  192
1.10000+ 7 5.00000- 3 1.30000+ 7 4.50000- 3 1.50000+ 7 6.00000- 3133133103  193
1.70000+ 7 1.00000- 2 2.00000+ 7 0.0    + 0                      133133103  194
0.0    + 0 0.0    + 0          0           2          16          8133133103  195
1.00000- 5 0.0    + 0 1.89900+ 6 3.00000- 1 2.40000+ 6 2.00000- 1133133103  196
2.80000+ 6 1.50000- 1 3.30000+ 6 1.00000- 1 4.50000+ 6 8.00000- 2133133103  197
5.50000+ 6 0.0    + 0 2.00000+ 7 0.0    + 0                      133133103  198
0.0    + 0 0.0    + 0          0           1          12          6133133103  199
1.00000- 5 0.0    + 0 5.50000+ 6 5.00000- 3 8.00000+ 6 1.45000- 2133133103  200
1.30000+ 7 6.50000- 3 1.70000+ 7 1.00000- 2 2.00000+ 7 0.0    + 0133133103  201
                                                                133133  0  202
1.30270+ 4 2.67500+ 1          0           0           0          1133133107  203
0.0    + 0 0.0    + 0          0         107           0          3133133107  204
0.0    + 0 0.0    + 0          0           1          30         15133133107  205
1.00000- 5 0.0    + 0 3.24800+ 6 9.00000- 2 3.50000+ 6 4.00000- 2133133107  206
4.00000+ 6 2.00000- 2 4.50000+ 6 8.00000- 3 5.00000+ 6 6.50000- 3133133107  207
5.50000+ 6 3.50000- 3 6.00000+ 6 2.50000- 3 7.00000+ 6 1.60000- 3133133107  208
8.00000+ 6 9.00000- 4 9.00000+ 6 9.00000- 4 1.00000+ 7 6.00000- 4133133107  209
1.20000+ 7 9.00000- 4 1.50000+ 7 1.20000- 3 2.00000+ 7 0.0    + 0133133107  210
0.0    + 0 0.0    + 0          0           2          16          8133133107  211
1.00000- 5 0.0    + 0 3.24800+ 6 4.00000- 1 4.00000+ 6 2.00000- 1133133107  212
5.00000+ 6 8.00000- 2 6.00000+ 6 6.00000- 2 9.00000+ 6 5.00000- 2133133107  213
1.20000+ 7 0.0    + 0 2.00000+ 7 0.0    + 0                      133133107  214
0.0    + 0 0.0    + 0          0           1           8          4133133107  215
1.00000- 5 0.0    + 0 1.20000+ 7 1.60000- 3 1.50000+ 7 1.30000- 3133133107  216
2.00000+ 7 0.0    + 0                                           133133107  217
                                                                133133  0  218
                                                                1331 0  0  219
                                                                   0 0  0  220
                                                                  -1 0  0    0
```

Fig. 2.3.1 (continued)

3. Integral Tests for Fission Reactors

3.1 Comparison with IRDF-85

3.1.1 Resonance Integral

Resonance integrals calculated from the JENDL Dosimetry File are compared with recommended values by Mughabghab et al.[21], and those obtained from IRDF-85. The calculation was made above the cutoff energy of 0.5 eV. Results are given in **Table 3.1.1**.

The resonance integrals calculated from the JENDL Dosimetry File are in very good agreement with Mughabghab's recommendation except for the ^{55}Mn(n, γ) and ^{186}W(n, γ) cross sections. Small discrepancies are also found for the ^{58}Fe(n, γ) and ^{151}Eu(n, γ) cross sections. As a whole, the JENDL Dosimetry File reproduces better the recommended resonance integral values than IRDF-85.

Table 3.1.1 Comparison of resonance intergrals

reaction	Mughabghab (b)	JENDL(b) [%]	IRDF-85(b) [%]
^{6}Li(n, α)		425	
^{10}B(n, α)	1722±5	1720 [-0.1]	
^{23}Na(n, γ)	0.311±0.010	0.312 [0.3]	0.316 [1.6]
^{45}Sc(n, γ)	12.0±0.5	11.9 [-0.8]	12.1 [0.8]
^{55}Mn(n, γ)	14.0±0.3	11.8 [-16]	
^{58}Fe(n, γ)	1.7±0.1	1.57 [-7.6]	1.28 [-25]
^{59}Co(n, γ)	74±2	75.6 [2.2]	74.5 [0.7]
^{63}Cu(n, γ)	4.97±0.08	4.97 [0.0]	5.60 [13]
^{115}In(n, γ)^{116m}In	2650±100	2580 [-2.6]	3280 [24]
^{151}Eu(n, γ)	3300±300	3070 [-7.0]	
^{181}Ta(n, γ)	660±23	660 [0.0]	
^{186}W(n, γ)	485±15	347 [-28]	
^{197}Au(n, γ)	1550±28	1560 [0.6]	1570 [1.3]
^{232}Th(n, γ)	85±3	84.4 [-0.7]	85.9 [1.0]
^{235}U fission	275±5	275 [0.0]	282 [2.5]
^{238}U(n, γ)	277±3	279 [0.7]	279 [0.7]
^{239}Pu fission	301±10	299 [-0.7]	304 [1.0]
^{241}Am fission	14.4±1.0	13.9 [-3.5]	15.9 [10]

Values in [ ] are differences between calculated resonance integrals and the recommendations by Mughabghab[21].

3.1.2 Average Cross Sections in Neutron Fields given in IRDF-85

The JENDL Dosimetry File is compared with IRDF-85[1]. Graphical comparison is made in Appendix. In this section, both files are compared by calculating average cross sections using the ten standard group-wise spectra stored in IRDF-85, all of which are related to the fission neutron fields.

No.	spectra
1	^{252}Cf spontaneous fission spectrum (NBS evaluation)[25]
2	^{235}U thermal fission spectrum (NBS evaluation)[26]
3	^{235}U thermal fission spectrum (ENDF/B-V)[2]
4	Intermediate-Energy Standard Neutron Field (ISNF)[27]
5	Coupled Fast Reactivity Measurement Facility (CFRMF)[28]
6	10%-^{235}U-enriched uranium cylindrical critical assembly (BIG-TEN)[29]
7	Coupled thermal/fast uranium and boron carbide spherical assembly ($\Sigma\Sigma$)[30] (E < 15 MeV)
8	ORR[31] (E < 20 MeV)
9	YAYOI[32] (E < 20 MeV)
10	NEACRP benchmark spectrum[33] (E < 10.5 MeV)

These spectra are given in the energy range from 10^{-4} eV to 18 MeV, except that the $\Sigma\Sigma$, ORR, YAYOI and NEACRP benchmark spectra are defined below 15, 20, 20 and 10.5 MeV, respectively. **Figure 3.1.1** shows these 10 spectra. More detailed descriptions of ISNF, CFRMF, $\Sigma\Sigma$ and YAYOI are given in Section 3.3 together with comparison with experimental data.

The average cross sections were calculated from the group-wise data file in the energy range from 10^{4} eV to 18 MeV where the spectra are given.

$$\bar{\sigma} = \sum_i \bar{\sigma}\,(E_i)\ \phi\ (E_i)\ \Delta E_i, \tag{1}$$

where $\sigma\ (E_i)$ and $\phi\ (E_i)$ are group-wise cross section and spectrum in the i-th energy group, and ΔE_i is an energy width of the i-th energy interval. The spectrum is normalized as follows:

$$\sum_i \phi\ (E_i)\ \Delta E_i = 1. \tag{2}$$

Error of the average cross section was estimated as:

$$(\delta\bar{\sigma})^2 = \sum_i \sum_j \{COV\ (\sigma\ (E_i)\ \sigma\ (E_j))\ \phi\ (E_i)\ \phi\ (E_j)$$

$$+ \sigma\ (E_i)\ \sigma\ (E_j)\ COV\ (\phi\ (E_i)\ \phi\ (E_j))\}\ \Delta E_i \Delta E_j, \tag{3}$$

where $COV\ (\sigma\ (E_i)\ \sigma\ (E_j))$ and $COV\ (\phi\ (E_i)\ \phi\ (E_j))$ are components of covariance matrices for the cross section and the spectrum, respectively. Since covariance matrices of spectra are not given in the IRDF-85 spectrum file, the following covariance matrix was assumed for all the spectra.

diagonal parts : $COV\ (\phi\ (E_i)\ \phi\ (E_i)) = (0.05)^2\ \phi\ (E_i)^2$,
off-diagonal parts : $COV\ (\phi\ (E_i)\ \phi\ (E_j)) = (0.02)^2\ \phi\ (E_i)\ \phi\ (E_j)$.

Obtained average cross sections are compared with IRDF-85 in Tables 3.1.2 to 3.1.11. For each spectrum, the average cross sections calculated from the JENDL Dosimetry File and IRDF-85 are given

in the unit of mb. Calculated errors which include both contributions from cross-section and spectrum uncertainties are given only for JENDL. The contributions from spectrum uncertainties are about 2 or 3 %. The NEACRP benchmark spectrum is defined below 10.5 MeV. Therefore, the average cross sections are zero for the reactions with threshold energies larger than 10.5 MeV.

Differences between JENDL and IRDF-85 were obtained as:

$$Dif. = \frac{JENDL - IRDF\text{-}85}{IRDF\text{-}85} \times 100. \quad (4)$$

They are given in the last column of each table. Furthermore, an asterisk is written at the right end of each cross section in the case where the discrepancy is larger than 5 %, 2 asterisks in the cases discrepant more than 10 %, 3 asterisks in the cases discrepant more than 20 %, and 4 asterisks in the cases discrepant more than 40 %.

As the results of comparison of the average cross sections, large discrepancies are found for the following seven threshold reaction cross sections.

^{19}F(n, 2n)^{18}F, ^{31}P(n, p)^{31}Si, ^{47}Ti(n, np)^{46}Sc, ^{47}Ti(n, p)^{47}Sc, ^{48}Ti(n, np)^{47}Sc,
^{64}Zn(n, p)^{64}Cu, ^{127}I(n, 2n)^{126}I.

The following five capture cross sections are also discrepant.

^{23}Na(n, γ)^{24}Na, ^{45}Sc(n, γ)^{46}Sc, ^{58}Fe(n, γ)^{59}Fe, ^{63}Cu(n, γ)^{64}Cu, ^{115}In(n, γ)^{116m}In.

Other reaction cross sections are almost consistent with each other. Discrepancies among group-wise cross sections for these reactions can be seen in the figures in Appendix.

Contributions from each energy interval to the spectrum average cross sections are calculated. Examples of the contributions, $\sigma(E_i)\phi(E_i)\Delta E_i$, are shown in **Figs. 3.1.2** to **3.1.13** for the above mentioned discrepant reactions. **Figures 3.1.2** to **3.1.8** are those for the threshold reactions calculated with the ^{252}Cf spontaneous fission spectrum. It is seen from the figures that the discrepancies found in the spectrum average cross sections are due to the differences of cross sections in the energy range below 15 MeV for ^{19}F(n, 2n), below 5 MeV for ^{31}P(n, p), below 16 MeV for ^{47}Ti(n, np), below 6 MeV for ^{47}Ti(n, p), all energy range for ^{48}Ti(n, np), below 10 MeV for ^{64}Zn(n, p) and below about 13 MeV for ^{127}I(n, 2n) reactions. As will be also pointed out in Sec. 3.2, the ^{19}F(n, 2n)^{18}F cross section below 14 MeV and the ^{64}Zn(n, p)^{64}Cu cross section around 4 or 5 MeV of the JENDL Dosimetry File seem to be too large.

In the cases of the capture cross sections, contributions in the Big-Ten spectrum are shown in **Figs. 3.1.9** to **3.1.13.** In these figures, contributions in every 10 energy intervals of the SAND-II structure are bunched into one. In this spectrum, important discrepancies of cross sections are found at the energy around 100 keV for ^{23}Na(n, γ), from 100 keV to 1 MeV for ^{45}Sc(n, γ), from 30 keV to several 100 keV for ^{58}Fe(n, γ), from 50 keV to 100 keV for ^{63}Cu(n, γ) and from 30 keV to 2 MeV for ^{115}In(n, γ) reactions. In the case of ^{63}Cu, there seems to exist resonance missing around 100 keV in the JENDL evaluation.

Table 3.1.2 Average cross sections calculated with the ^{252}Cf spontaneous fission spectrum (NBS evaluation)

Reaction	JENDL(mb)	err(%)	IRDF-85(mb)	Dif.(%)	
Li- 6(n,t)a	3.295E+02	3.44			
Li- 6 a-production	4.780E+02	3.84	4.646E+02	2.9	
Li- 7 t-production	2.446E+01	4.55	2.574E+01	-5.0	
B - 10(n,a)Li-7	4.262E+02	6.44			
B - 10 a-production	5.405E+02	6.91	4.889E+02	10.5	**
F - 19(n,2n)F-18	2.001E-02	3.99	1.571E-02	27.4	***
Na- 23(n,2n)Na-22	6.827E-03	10.77	6.482E-03	5.3	*
Na- 23(n,g)Na-24	2.233E-01	12.97	2.712E-01	-17.6	**
Mg- 24(n,p)Na-24	2.333E+00	4.64	2.158E+00	8.2	*
Al- 27(n,p)Mg-27	5.190E+00	6.05	5.138E+00	1.0	
Al- 27(n,a)Na-24	1.014E+00	5.84	1.059E+00	-4.2	
P - 31(n,p)Si-31	3.918E+01	4.08	3.064E+01	27.9	***
S - 32(n,p)P-32	7.497E+01	8.13	7.600E+01	-1.4	
Sc- 45(n,g)Sc-46	6.883E+00	3.95	5.261E+00	30.8	***
Ti- 0(n,X)Sc-46	1.087E+00				
Ti- 0(n,X)Sc-47	1.515E+00				
Ti- 0(n,X)Sc-48	2.973E-01				
Ti- 46(n,p)Sc-46	1.358E+01	12.75	1.347E+01	0.8	
Ti- 47(n,np)Sc-46	1.528E-02	30.07	2.063E-02	-25.9	***
Ti- 47(n,p)Sc-47	2.071E+01	11.40	2.407E+01	-14.0	**
Ti- 48(n,np)Sc-47	5.136E-03	30.07	3.437E-03	49.4	****
Ti- 48(n,p)Sc-48	4.028E-01	10.52	4.091E-01	-1.5	
Ti- 49(n,np)Sc-48	1.069E-03	19.11			
Mn- 55(n,2n)Mn-54	4.574E-01	12.61	4.404E-01	3.9	
Mn- 55(n,g)Mn-56	2.812E+00	7.82			
Fe- 54(n,p)Mn-54	8.855E+01	4.03	8.828E+01	0.3	
Fe- 56(n,p)Mn-56	1.449E+00	4.90	1.415E+00	2.4	
Fe- 57(n,np)Mn-56	1.592E-03	16.70			
Fe- 58(n,g)Fe-59	1.769E+00	24.92	1.661E+00	6.5	*
Co- 59(n,2n)Co-58	3.977E-01	11.03	4.049E-01	-1.8	
Co- 59(n,g)Co-60	5.144E+00	4.70	6.028E+00	-14.7	**
Co- 59(n,a)Mn-56	2.360E-01	4.68	2.162E-01	9.2	*
Ni- 58(n,2n)Ni-57	7.757E-03	11.08	7.234E-03	7.2	*
Ni- 58(n,p)Co-58	1.159E+02	6.75	1.140E+02	1.6	
Ni- 60(n,p)Co-60	3.443E+00	7.79	3.444E+00	-0.0	
Cu- 63(n,2n)Cu-62	2.038E-01	2.76	1.928E-01	5.7	*
Cu- 63(n,g)Cu-64	8.567E+00	19.28	9.649E+00	-11.2	**
Cu- 63(n,a)Co-60	7.238E-01	5.81	7.581E-01	-4.5	
Cu- 65(n,2n)Cu-64	6.660E-01	7.56	6.491E-01	2.6	
Zn- 64(n,p)Cu-64	4.709E+01	7.76	3.923E+01	20.0	***
Zr- 90(n,2n)Zr-89	2.064E-01	3.15	1.977E-01	4.4	
Nb- 93(n,2n)Nb-92m	8.173E-01	4.31			
Nb- 93(n,n')Nb-93m	1.485E+02	6.82	1.616E+02	-8.1	*
Rh-103(n,n')Rh-103m	7.122E+02	3.72	7.122E+02	0.0	
In-115(n,n')In-115m	1.881E+02	3.02	1.819E+02	3.4	
In-115(n,g)In-116m	1.258E+02	4.60	1.535E+02	-18.0	**
I -127(n,2n)I-126	2.774E+00	17.34	2.311E+00	20.0	***
Eu-151(n,g)Eu-152	3.597E+02	3.37			
Ta-181(n,g)Ta-182	8.291E+01	5.90			
W -186(n,g)W-187	3.435E+01	5.13			
Au-197(n,2n)Au-196	5.868E+00	4.80			
Au-197(n,g)Au-198	7.492E+01	8.85	7.632E+01	-1.8	
Hg-199(n,n')Hg-199m	2.471E+02	8.07			
Th-232(n,f)	8.164E+01	5.49	7.807E+01	4.6	
Th-232(n,g)Th-233	8.340E+01	12.03	8.969E+01	-7.0	*
U -235(n,f)	1.235E+03	2.86	1.236E+03	-0.1	
U -238(n,f)	3.168E+02	2.91	3.136E+02	1.0	
U -238(n,g)U-239	6.460E+01	6.07	6.833E+01	-5.5	*
Np-237(n,f)	1.339E+03	9.43	1.352E+03	-1.0	
Pu-239(n,f)	1.801E+03	2.92	1.792E+03	0.5	
Am-241(n,f)	1.386E+03	3.50	1.426E+03	-2.8	

Table 3.1.3 Average cross sections claculated with the ^{235}U thermal fission spectrum (NBS evaluation)

Reaction	JENDL(mb)	err(%)	IRDF-85(mb)	Dif.(%)	
Li- 6(n,t)a	3.476E+02	3.39			
Li- 6 a-production	4.791E+02	3.68	4.650E+02	3.0	
Li- 7 t-production	1.951E+01	4.87	2.061E+01	-5.3	*
B - 10(n,a)Li-7	4.476E+02	6.15			
B - 10 a-production	5.530E+02	6.68	4.993E+02	10.7	**
F - 19(n,2n)F-18	8.663E-03	4.31	6.636E-03	30.6	***
Na- 23(n,2n)Na-22	2.614E-03	11.80	2.457E-03	6.4	*
Na- 23(n,g)Na-24	2.304E-01	12.73	2.817E-01	-18.2	**
Mg- 24(n,p)Na-24	1.584E+00	4.69	1.453E+00	9.0	*
Al- 27(n,p)Mg-27	4.148E+00	6.16	4.121E+00	0.7	
Al- 27(n,a)Na-24	6.636E-01	6.02	6.934E-01	-4.3	
P - 31(n,p)Si-31	3.544E+01	4.12	2.740E+01	29.4	***
S - 32(n,p)P-32	6.675E+01	8.42	6.761E+01	-1.3	
Sc- 45(n,g)Sc-46	7.347E+00	3.83	5.641E+00	30.2	***
Ti- 0(n,X)Sc-46	8.718E-01				
Ti- 0(n,X)Sc-47	1.356E+00				
Ti- 0(n,X)Sc-48	1.988E-01				
Ti- 46(n,p)Sc-46	1.089E+01	12.82	1.081E+01	0.7	
Ti- 47(n,np)Sc-46	6.014E-03	30.07	8.473E-03	-29.0	***
Ti- 47(n,p)Sc-47	1.856E+01	11.44	2.159E+01	-14.0	**
Ti- 48(n,np)Sc-47	2.101E-03	30.07	1.365E-03	54.0	****
Ti- 48(n,p)Sc-48	2.694E-01	10.67	2.726E-01	-1.2	
Ti- 49(n,np)Sc-48	3.786E-04	19.72			
Mn- 55(n,2n)Mn-54	2.109E-01	13.48	2.017E-01	4.6	
Mn- 55(n,g)Mn-56	2.968E+00	7.74			
Fe- 54(n,p)Mn-54	7.761E+01	4.08	7.784E+01	-0.3	
Fe- 56(n,p)Mn-56	1.026E+00	5.00	1.006E+00	2.0	
Fe- 57(n,np)Mn-56	5.846E-04	16.65			
Fe- 58(n,g)Fe-59	1.902E+00	24.01	1.712E+00	11.1	**
Co- 59(n,2n)Co-58	1.801E-01	11.97	1.829E-01	-1.6	
Co- 59(n,g)Co-60	5.363E+00	4.52	6.278E+00	-14.6	**
Co- 59(n,a)Mn-56	1.599E-01	4.78	1.448E-01	10.4	**
Ni- 58(n,2n)Ni-57	3.035E-03	11.10	2.859E-03	6.1	*
Ni- 58(n,p)Co-58	1.029E+02	6.87	1.011E+02	1.8	
Ni- 60(n,p)Co-60	2.542E+00	7.97	2.529E+00	0.5	
Cu- 63(n,2n)Cu-62	8.771E-02	2.85	8.246E-02	6.4	*
Cu- 63(n,g)Cu-64	9.023E+00	19.14	1.008E+01	-10.5	**
Cu- 63(n,a)Co-60	5.383E-01	5.97	5.402E-01	-0.4	
Cu- 65(n,2n)Cu-64	3.149E-01	8.07	3.057E-01	3.0	
Zn- 64(n,p)Cu-64	4.143E+01	7.71	3.466E+01	19.5	**
Zr- 90(n,2n)Zr-89	8.443E-02	3.26	8.008E-02	5.4	*
Nb- 93(n,2n)Nb-92m	4.287E-01	4.51			
Nb- 93(n,n')Nb-93m	1.420E+02	6.86	1.553E+02	-8.6	*
Rh-103(n,n')Rh-103m	6.890E+02	3.75	6.890E+02	0.0	
In-115(n,n')In-115m	1.793E+02	3.03	1.734E+02	3.4	
In-115(n,g)In-116m	1.321E+02	4.55	1.602E+02	-17.6	**
I -127(n,2n)I-126	1.431E+00	17.35	1.186E+00	20.7	***
Eu-151(n,g)Eu-152	3.854E+02	3.42			
Ta-181(n,g)Ta-182	8.817E+01	5.90			
W -186(n,g)W-187	3.604E+01	5.12			
Au-197(n,2n)Au-196	3.294E+00	4.98			
Au-197(n,g)Au-198	7.955E+01	8.46	8.094E+01	-1.7	
Hg-199(n,n')Hg-199m	2.312E+02	8.14			
Th-232(n,f)	7.575E+01	5.50	7.240E+01	4.6	
Th-232(n,g)Th-233	8.769E+01	11.84	9.424E+01	-6.9	*
U -235(n,f)	1.234E+03	2.86	1.236E+03	-0.1	
U -238(n,f)	2.978E+02	2.94	2.946E+02	1.1	
U -238(n,g)U-239	6.824E+01	5.97	7.206E+01	-5.3	*
Np-237(n,f)	1.309E+03	9.58	1.322E+03	-1.0	
Pu-239(n,f)	1.793E+03	2.92	1.786E+03	0.4	
Am-241(n,f)	1.344E+03	3.49	1.382E+03	-2.7	

Table 3.1.4 Average cross sections calculated with the ^{235}U thermal fission spectrum (ENDF/B-V)

Reaction	JENDL(mb)	err(%)	IRDF-85(mb)	Dif.(%)	
Li- 6(n,t)a	3.307E+02	3.46			
Li- 6 a-production	4.679E+02	3.78	4.545E+02	2.9	
Li- 7 t-production	2.006E+01	4.92	2.119E+01	-5.4	*
B - 10(n,a)Li-7	4.355E+02	6.44			
B - 10 a-production	5.437E+02	6.95	4.907E+02	10.8	**
F - 19(n,2n)F-18	8.502E-03	4.41	6.462E-03	31.6	***
Na- 23(n,2n)Na-22	2.459E-03	12.21	2.302E-03	6.8	*
Na- 23(n,g)Na-24	2.258E-01	13.03	2.750E-01	-17.9	**
Mg- 24(n,p)Na-24	1.641E+00	4.69	1.507E+00	8.9	*
Al- 27(n,p)Mg-27	4.288E+00	6.17	4.262E+00	0.6	
Al- 27(n,a)Na-24	6.885E-01	6.03	7.194E-01	-4.3	
P - 31(n,p)Si-31	3.700E+01	4.12	2.854E+01	29.6	***
S - 32(n,p)P-32	6.959E+01	8.46	7.049E+01	-1.3	
Sc- 45(n,g)Sc-46	7.080E+00	3.94	5.448E+00	30.0	***
Ti- 0(n,X)Sc-46	9.006E-01				
Ti- 0(n,X)Sc-47	1.409E+00				
Ti- 0(n,X)Sc-48	2.054E-01				
Ti- 46(n,p)Sc-46	1.125E+01	12.82	1.117E+01	0.7	
Ti- 47(n,np)Sc-46	5.714E-03	30.07	8.169E-03	-30.1	***
Ti- 47(n,p)Sc-47	1.928E+01	11.44	2.246E+01	-14.1	**
Ti- 48(n,np)Sc-47	2.024E-03	30.07	1.301E-03	55.6	****
Ti- 48(n,p)Sc-48	2.783E-01	10.68	2.817E-01	-1.2	
Ti- 49(n,np)Sc-48	3.448E-04	20.02			
Mn- 55(n,2n)Mn-54	2.107E-01	13.73	2.012E-01	4.7	
Mn- 55(n,g)Mn-56	2.897E+00	7.73			
Fe- 54(n,p)Mn-54	8.075E+01	4.08	8.104E+01	-0.4	
Fe- 56(n,p)Mn-56	1.058E+00	5.00	1.036E+00	2.1	
Fe- 57(n,np)Mn-56	5.407E-04	16.63			
Fe- 58(n,g)Fe-59	1.851E+00	24.17	1.688E+00	9.7	*
Co- 59(n,2n)Co-58	1.790E-01	12.24	1.818E-01	-1.5	
Co- 59(n,g)Co-60	5.255E+00	4.67	6.174E+00	-14.9	**
Co- 59(n,a)Mn-56	1.653E-01	4.77	1.497E-01	10.4	**
Ni- 58(n,2n)Ni-57	2.878E-03	11.11	2.722E-03	5.7	*
Ni- 58(n,p)Co-58	1.071E+02	6.89	1.052E+02	1.8	
Ni- 60(n,p)Co-60	2.623E+00	7.96	2.609E+00	0.5	
Cu- 63(n,2n)Cu-62	8.593E-02	2.88	8.063E-02	6.6	*
Cu- 63(n,g)Cu-64	8.777E+00	19.09	9.868E+00	-11.1	**
Cu- 63(n,a)Co-60	5.561E-01	5.96	5.582E-01	-0.4	
Cu- 65(n,2n)Cu-64	3.167E-01	8.20	3.071E-01	3.1	
Zn- 64(n,p)Cu-64	4.313E+01	7.71	3.613E+01	19.4	**
Zr- 90(n,2n)Zr-89	8.136E-02	3.30	7.691E-02	5.8	*
Nb- 93(n,2n)Nb-92m	4.402E-01	4.54			
Nb- 93(n,n')Nb-93m	1.464E+02	6.84	1.602E+02	-8.6	*
Rh-103(n,n')Rh-103m	7.051E+02	3.74	7.051E+02	0.0	
In-115(n,n')In-115m	1.854E+02	3.02	1.793E+02	3.4	
In-115(n,g)In-116m	1.292E+02	4.59	1.578E+02	-18.1	**
I -127(n,2n)I-126	1.466E+00	17.35	1.213E+00	20.8	***
Eu-151(n,g)Eu-152	3.703E+02	3.35			
Ta-181(n,g)Ta-182	8.562E+01	5.82			
W -186(n,g)W-187	3.531E+01	5.12			
Au-197(n,2n)Au-196	3.412E+00	5.00			
Au-197(n,g)Au-198	7.698E+01	8.84	7.826E+01	-1.6	
Hg-199(n,n')Hg-199m	2.395E+02	8.15			
Th-232(n,f)	7.850E+01	5.50	7.504E+01	4.6	
Th-232(n,g)Th-233	8.566E+01	12.03	9.197E+01	-6.9	*
U -235(n,f)	1.235E+03	2.87	1.236E+03	-0.1	
U -238(n,f)	3.084E+02	2.94	3.052E+02	1.1	
U -238(n,g)U-239	6.636E+01	6.06	7.025E+01	-5.5	*
Np-237(n,f)	1.334E+03	9.57	1.347E+03	-0.9	
Pu-239(n,f)	1.800E+03	2.92	1.791E+03	0.5	
Am-241(n,f)	1.378E+03	3.50	1.417E+03	-2.8	

Table 3.1.5 Average cross sections calculated with the ISNF spectrum

Reaction	JENDL(mb)	err(%)	IRDF-85(mb)	Dif.(%)	
Li- 6(n,t)a	7.736E+02	2.42			
Li- 6 a-production	8.183E+02	2.43	7.978E+02	2.6	
Li- 7 t-production	5.769E+00	5.16	6.101E+00	-5.4	*
B - 10(n,a)Li-7	1.698E+03	2.24			
B - 10 a-production	1.749E+03	2.34	1.706E+03	2.5	
F - 19(n,2n)F-18	2.374E-03	4.32	1.817E-03	30.7	***
Na- 23(n,2n)Na-22	7.116E-04	11.89	6.684E-04	6.5	*
Na- 23(n,g)Na-24	1.755E+00	9.67	1.918E+00	-8.5	*
Mg- 24(n,p)Na-24	4.445E-01	4.70	4.076E-01	9.1	*
Al- 27(n,p)Mg-27	1.247E+00	6.27	1.244E+00	0.2	
Al- 27(n,a)Na-24	1.856E-01	6.03	1.939E-01	-4.3	
P - 31(n,p)Si-31	1.319E+01	4.26	1.014E+01	30.1	***
S - 32(n,p)P-32	2.409E+01	8.92	2.426E+01	-0.7	
Sc- 45(n,g)Sc-46	2.935E+01	2.67	2.779E+01	5.6	*
Ti- 0(n,X)Sc-46	2.611E-01				
Ti- 0(n,X)Sc-47	5.333E-01				
Ti- 0(n,X)Sc-48	5.595E-02				
Ti- 46(n,p)Sc-46	3.262E+00	12.83	3.243E+00	0.6	
Ti- 47(n,np)Sc-46	1.639E-03	30.07	2.316E-03	-29.2	***
Ti- 47(n,p)Sc-47	7.300E+00	11.44	8.302E+00	-12.1	**
Ti- 48(n,np)Sc-47	5.728E-04	30.07	3.715E-04	54.2	****
Ti- 48(n,p)Sc-48	7.580E-02	10.69	7.662E-02	-1.1	
Ti- 49(n,np)Sc-48	1.017E-04	19.90			
Mn- 55(n,2n)Mn-54	5.791E-02	13.50	5.538E-02	4.6	
Mn- 55(n,g)Mn-56	3.271E+01	4.62			
Fe- 54(n,p)Mn-54	2.697E+01	4.15	2.739E+01	-1.5	
Fe- 56(n,p)Mn-56	2.913E-01	5.02	2.856E-01	2.0	
Fe- 57(n,np)Mn-56	1.579E-04	16.65			
Fe- 58(n,g)Fe-59	1.142E+01	8.78	7.203E+00	58.5	****
Co- 59(n,2n)Co-58	4.942E-02	11.99	5.021E-02	-1.6	
Co- 59(n,g)Co-60	4.197E+01	2.76	4.297E+01	-2.3	
Co- 59(n,a)Mn-56	4.506E-02	4.78	4.071E-02	10.7	**
Ni- 58(n,2n)Ni-57	8.280E-04	11.11	7.809E-04	6.0	*
Ni- 58(n,p)Co-58	3.764E+01	7.05	3.681E+01	2.3	
Ni- 60(n,p)Co-60	7.321E-01	7.94	7.260E-01	0.8	
Cu- 63(n,2n)Cu-62	2.404E-02	2.85	2.260E-02	6.4	*
Cu- 63(n,g)Cu-64	4.509E+01	5.01	5.271E+01	-14.4	**
Cu- 63(n,a)Co-60	1.569E-01	6.01	1.547E-01	1.5	
Cu- 65(n,2n)Cu-64	8.653E-02	8.08	8.398E-02	3.0	
Zn- 64(n,p)Cu-64	1.447E+01	7.77	1.214E+01	19.2	**
Zr- 90(n,2n)Zr-89	2.310E-02	3.26	2.190E-02	5.5	*
Nb- 93(n,2n)Nb-92m	1.178E-01	4.51			
Nb- 93(n,n')Nb-93m	7.135E+01	7.37	7.891E+01	-9.6	*
Rh-103(n,n')Rh-103m	3.876E+02	4.13	3.876E+02	0.0	
In-115(n,n')In-115m	8.724E+01	3.05	8.402E+01	3.8	
In-115(n,g)In-116m	3.383E+02	5.29	3.603E+02	-6.1	*
I -127(n,2n)I-126	3.934E-01	17.35	3.260E-01	20.7	***
Eu-151(n,g)Eu-152	2.054E+03	4.04			
Ta-181(n,g)Ta-182	4.928E+02	4.12			
W -186(n,g)W-187	1.163E+02	3.89			
Au-197(n,2n)Au-196	9.065E-01	4.99			
Au-197(n,g)Au-198	3.853E+02	5.29	4.028E+02	-4.3	
Hg-199(n,n')Hg-199m	1.047E+02	8.48			
Th-232(n,f)	3.419E+01	5.67	3.258E+01	4.9	
Th-232(n,g)Th-233	2.468E+02	10.68	2.639E+02	-6.5	*
U -235(n,f)	1.605E+03	2.82	1.614E+03	-0.6	
U -238(n,f)	1.387E+02	3.10	1.371E+02	1.2	
U -238(n,g)U-239	2.184E+02	4.28	2.270E+02	-3.8	
Np-237(n,f)	7.817E+02	9.86	7.928E+02	-1.4	
Pu-239(n,f)	1.820E+03	3.15	1.823E+03	-0.2	
Am-241(n,f)	7.416E+02	3.36	7.631E+02	-2.8	

Table 3.1.6 Average cross sections calculated with the CFRMF spectrum

Reaction	JENDL(mb)	err(%)	IRDF-85(mb)	Dif.(%)	
Li- 6(n,t)a	9.102E+02	2.50			
Li- 6 a-production	9.397E+02	2.49	9.154E+02	2.7	
Li- 7 t-production	4.449E+00	4.72	4.679E+00	-4.9	
B - 10(n,a)Li-7	1.681E+03	2.14			
B - 10 a-production	1.717E+03	2.18	1.676E+03	2.5	
F - 19(n,2n)F-18	2.584E-03	3.88	2.071E-03	24.8	***
Na- 23(n,2n)Na-22	1.031E-03	10.16	9.788E-04	5.3	*
Na- 23(n,g)Na-24	1.339E+00	9.48	1.509E+00	-11.3	**
Mg- 24(n,p)Na-24	3.971E-01	4.69	3.664E-01	8.4	*
Al- 27(n,p)Mg-27	9.486E-01	6.11	9.420E-01	0.7	
Al- 27(n,a)Na-24	1.688E-01	6.00	1.764E-01	-4.3	
P - 31(n,p)Si-31	8.188E+00	4.16	6.351E+00	28.9	***
S - 32(n,p)P-32	1.532E+01	8.45	1.548E+01	-1.0	
Sc- 45(n,g)Sc-46	2.661E+01	2.67	2.443E+01	8.9	*
Ti- 0(n,X)Sc-46	1.981E-01				
Ti- 0(n,X)Sc-47	3.303E-01				
Ti- 0(n,X)Sc-48	4.974E-02				
Ti- 46(n,p)Sc-46	2.474E+00	12.79	2.458E+00	0.7	
Ti- 47(n,np)Sc-46	2.210E-03	30.08	2.896E-03	-23.7	***
Ti- 47(n,p)Sc-47	4.517E+00	11.39	5.132E+00	-12.0	**
Ti- 48(n,np)Sc-47	7.195E-04	30.08	4.919E-04	46.3	****
Ti- 48(n,p)Sc-48	6.738E-02	10.62	6.827E-02	-1.3	
Ti- 49(n,np)Sc-48	1.826E-04	20.49			
Mn- 55(n,2n)Mn-54	5.893E-02	12.17	5.638E-02	4.5	
Mn- 55(n,g)Mn-56	3.201E+01	4.40			
Fe- 54(n,p)Mn-54	1.771E+01	4.07	1.781E+01	-0.5	
Fe- 56(n,p)Mn-56	2.499E-01	4.96	2.442E-01	2.3	
Fe- 57(n,np)Mn-56	2.574E-04	16.84			
Fe- 58(n,g)Fe-59	1.067E+01	8.17	6.646E+00	60.6	****
Co- 59(n,2n)Co-58	5.071E-02	11.28	5.161E-02	-1.7	
Co- 59(n,g)Co-60	8.788E+01	3.22	8.731E+01	0.7	
Co- 59(n,a)Mn-56	3.983E-02	4.74	3.628E-02	9.8	*
Ni- 58(n,2n)Ni-57	1.129E-03	11.12	1.052E-03	7.4	*
Ni- 58(n,p)Co-58	2.402E+01	6.82	2.374E+01	1.2	
Ni- 60(n,p)Co-60	6.055E-01	7.91	6.036E-01	0.3	
Cu- 63(n,2n)Cu-62	2.611E-02	2.68	2.469E-02	5.8	*
Cu- 63(n,g)Cu-64	3.871E+01	6.63	4.644E+01	-16.7	**
Cu- 63(n,a)Co-60	1.278E-01	5.90	1.310E-01	-2.5	
Cu- 65(n,2n)Cu-64	8.779E-02	8.19	8.531E-02	2.9	
Zn- 64(n,p)Cu-64	9.466E+00	7.77	7.902E+00	19.8	**
Zr- 90(n,2n)Zr-89	2.794E-02	3.01	2.750E-02	1.6	
Nb- 93(n,2n)Nb-92m	1.155E-01	4.46			
Nb- 93(n,n')Nb-93m	4.559E+01	8.41	4.938E+01	-7.7	*
Rh-103(n,n')Rh-103m	2.797E+02	4.61	2.797E+02	0.0	
In-115(n,n')In-115m	5.154E+01	3.02	4.959E+01	3.9	
In-115(n,g)In-116m	3.237E+02	4.49	3.489E+02	-7.2	*
I -127(n,2n)I-126	3.881E-01	17.22	3.216E-01	20.7	***
Eu-151(n,g)Eu-152	2.044E+03	3.80			
Ta-181(n,g)Ta-182	5.014E+02	4.35			
W -186(n,g)W-187	1.271E+02	3.95			
Au-197(n,2n)Au-196	8.802E-01	5.05			
Au-197(n,g)Au-198	3.882E+02	4.44	4.024E+02	-3.5	
Hg-199(n,n')Hg-199m	6.327E+01	8.34			
Th-232(n,f)	1.956E+01	5.52	1.862E+01	5.1	*
Th-232(n,g)Th-233	2.503E+02	10.91	2.696E+02	-7.1	*
U -235(n,f)	1.569E+03	2.82	1.581E+03	-0.8	
U -238(n,f)	7.805E+01	3.04	7.722E+01	1.1	
U -238(n,g)U-239	2.271E+02	4.13	2.341E+02	-3.0	
Np-237(n,f)	5.721E+02	9.82	5.857E+02	-2.3	
Pu-239(n,f)	1.768E+03	3.17	1.787E+03	-1.1	
Am-241(n,f)	4.791E+02	3.15	4.923E+02	-2.7	

Table 3.1.7 Average cross sections calculated with the BIG-TEN spectrum

Reaction	JENDL(mb)	err(%)	IRDF-85(mb)	Dif.(%)	
Li- 6(n,t)a	8.933E+02	2.68			
Li- 6 a-production	9.135E+02	2.67	8.878E+02	2.9	
Li- 7 t-production	3.033E+00	4.74	3.193E+00	-5.0	*
B - 10(n,a)Li-7	1.205E+03	2.24			
B - 10 a-production	1.233E+03	2.27	1.193E+03	3.4	
F - 19(n,2n)F-18	2.315E-03	4.07	1.811E-03	27.9	***
Na- 23(n,2n)Na-22	7.728E-04	11.20	7.305E-04	5.8	*
Na- 23(n,g)Na-24	5.190E-01	9.36	6.471E-01	-19.8	**
Mg- 24(n,p)Na-24	2.816E-01	4.65	2.602E-01	8.2	*
Al- 27(n,p)Mg-27	6.519E-01	6.10	6.478E-01	0.6	
Al- 27(n,a)Na-24	1.221E-01	5.86	1.275E-01	-4.2	
P - 31(n,p)Si-31	5.574E+00	4.16	4.312E+00	29.3	***
S - 32(n,p)P-32	1.044E+01	8.42	1.056E+01	-1.2	
Sc- 45(n,g)Sc-46	2.143E+01	2.99	1.885E+01	13.6	**
Ti- 0(n,X)Sc-46	1.363E-01				
Ti- 0(n,X)Sc-47	2.257E-01				
Ti- 0(n,X)Sc-48	3.585E-02				
Ti- 46(n,p)Sc-46	1.702E+00	12.76	1.691E+00	0.7	
Ti- 47(n,np)Sc-46	1.735E-03	30.07	2.359E-03	-26.5	***
Ti- 47(n,p)Sc-47	3.086E+00	11.36	3.497E+00	-11.7	**
Ti- 48(n,np)Sc-47	5.893E-04	30.07	3.915E-04	50.5	****
Ti- 48(n,p)Sc-48	4.857E-02	10.52	4.932E-02	-1.5	
Ti- 49(n,np)Sc-48	1.200E-04	19.20			
Mn- 55(n,2n)Mn-54	5.344E-02	12.69	5.141E-02	3.9	
Mn- 55(n,g)Mn-56	8.196E+00	7.20			
Fe- 54(n,p)Mn-54	1.209E+01	4.07	1.215E+01	-0.5	
Fe- 56(n,p)Mn-56	1.756E-01	4.91	1.714E-01	2.4	
Fe- 57(n,np)Mn-56	1.793E-04	16.68			
Fe- 58(n,g)Fe-59	7.083E+00	15.27	3.501E+00	102.3	****
Co- 59(n,2n)Co-58	4.632E-02	11.15	4.718E-02	-1.8	
Co- 59(n,g)Co-60	1.214E+01	2.85	1.250E+01	-2.9	
Co- 59(n,a)Mn-56	2.848E-02	4.68	2.606E-02	9.3	*
Ni- 58(n,2n)Ni-57	8.799E-04	11.08	8.237E-04	6.8	*
Ni- 58(n,p)Co-58	1.639E+01	6.80	1.631E+01	0.5	
Ni- 60(n,p)Co-60	4.206E-01	7.79	4.199E-01	0.2	
Cu- 63(n,2n)Cu-62	2.353E-02	2.78	2.226E-02	5.7	*
Cu- 63(n,g)Cu-64	1.746E+01	15.31	2.207E+01	-20.9	***
Cu- 63(n,a)Co-60	8.906E-02	5.83	9.234E-02	-3.6	
Cu- 65(n,2n)Cu-64	7.811E-02	7.64	7.606E-02	2.7	
Zn- 64(n,p)Cu-64	6.469E+00	7.76	5.397E+00	19.9	**
Zr- 90(n,2n)Zr-89	2.361E-02	3.18	2.262E-02	4.3	
Nb- 93(n,2n)Nb-92m	9.697E-02	4.33			
Nb- 93(n,n')Nb-93m	3.362E+01	9.35	3.611E+01	-6.9	*
Rh-103(n,n')Rh-103m	2.232E+02	5.24	2.232E+02	0.0	
In-115(n,n')In-115m	3.593E+01	3.02	3.454E+01	4.0	
In-115(n,g)In-116m	2.542E+02	4.71	2.768E+02	-8.2	*
I -127(n,2n)I-126	3.285E-01	17.35	2.734E-01	20.2	***
Eu-151(n,g)Eu-152	1.168E+03	5.25			
Ta-181(n,g)Ta-182	2.340E+02	6.43			
W -186(n,g)W-187	7.659E+01	6.15			
Au-197(n,2n)Au-196	6.999E-01	4.83			
Au-197(n,g)Au-198	2.129E+02	4.69	2.127E+02	0.1	
Hg-199(n,n')Hg-199m	4.395E+01	8.40			
Th-232(n,f)	1.330E+01	5.50	1.265E+01	5.1	*
Th-232(n,g)Th-233	1.697E+02	10.91	1.819E+02	-6.7	*
U -235(n,f)	1.353E+03	2.94	1.366E+03	-1.0	
U -238(n,f)	5.313E+01	3.04	5.257E+01	1.1	
U -238(n,g)U-239	1.449E+02	5.00	1.506E+02	-3.7	
Np-237(n,f)	4.539E+02	9.86	4.674E+02	-2.9	
Pu-239(n,f)	1.591E+03	3.33	1.620E+03	-1.8	
Am-241(n,f)	3.524E+02	3.05	3.594E+02	-1.9	

Table 3.1.8 Average cross sections calculated with the ΣΣ spectrum

Reaction	JENDL(mb)	err(%)	IRDF-85(mb)	Dif.(%)	
Li- 6(n,t)a	8.617E+02	2.54			
Li- 6 a-production	8.906E+02	2.53	8.662E+02	2.8	
Li- 7 t-production	4.095E+00	4.86	4.280E+00	-4.3	
B - 10(n,a)Li-7	1.488E+03	2.18			
B - 10 a-production	1.525E+03	2.23	1.482E+03	2.9	
F - 19(n,2n)F-18	1.526E-03	4.99	1.102E-03	38.4	***
Na- 23(n,2n)Na-22	2.696E-04	22.33	2.284E-04	18.0	**
Na- 23(n,g)Na-24	9.814E-01	9.31	1.120E+00	-12.4	**
Mg- 24(n,p)Na-24	3.507E-01	4.70	3.221E-01	8.9	*
Al- 27(n,p)Mg-27	8.708E-01	6.14	8.707E-01	0.0	
Al- 27(n,a)Na-24	1.471E-01	6.04	1.538E-01	-4.3	
P - 31(n,p)Si-31	8.239E+00	4.25	6.325E+00	30.3	***
S - 32(n,p)P-32	1.517E+01	8.70	1.523E+01	-0.4	
Sc- 45(n,g)Sc-46	2.497E+01	2.71	2.279E+01	9.6	*
Ti- 0(n,X)Sc-46	1.806E-01				
Ti- 0(n,X)Sc-47	3.336E-01				
Ti- 0(n,X)Sc-48	4.372E-02				
Ti- 46(n,p)Sc-46	2.256E+00	12.81	2.245E+00	0.5	
Ti- 47(n,np)Sc-46	7.288E-04	30.08	1.201E-03	-39.3	***
Ti- 47(n,p)Sc-47	4.567E+00	11.40	5.165E+00	-11.6	**
Ti- 48(n,np)Sc-47	2.990E-04	30.07	1.673E-04	78.7	****
Ti- 48(n,p)Sc-48	5.925E-02	10.69	5.999E-02	-1.2	
Ti- 49(n,np)Sc-48	1.394E-05	53.38			
Mn- 55(n,2n)Mn-54	4.165E-02	14.81	3.958E-02	5.2	*
Mn- 55(n,g)Mn-56	2.518E+01	4.45			
Fe- 54(n,p)Mn-54	1.729E+01	4.12	1.746E+01	-1.0	
Fe- 56(n,p)Mn-56	2.248E-01	5.00	2.201E-01	2.1	
Fe- 57(n,np)Mn-56	3.838E-05	17.24			
Fe- 58(n,g)Fe-59	1.001E+01	8.52	6.212E+00	61.1	****
Co- 59(n,2n)Co-58	3.474E-02	13.35	3.532E-02	-1.7	
Co- 59(n,g)Co-60	4.177E+01	2.81	4.212E+01	-0.8	
Co- 59(n,a)Mn-56	3.515E-02	4.81	3.203E-02	9.8	*
Ni- 58(n,2n)Ni-57	3.643E-04	11.87	3.752E-04	-2.9	
Ni- 58(n,p)Co-58	2.379E+01	6.99	2.347E+01	1.4	
Ni- 60(n,p)Co-60	5.456E-01	8.05	5.439E-01	0.3	
Cu- 63(n,2n)Cu-62	1.552E-02	3.11	1.425E-02	8.9	*
Cu- 63(n,g)Cu-64	3.113E+01	8.06	3.655E+01	-14.8	**
Cu- 63(n,a)Co-60	1.154E-01	5.96	1.169E-01	-1.3	
Cu- 65(n,2n)Cu-64	6.359E-02	8.49	6.147E-02	3.4	
Zn- 64(n,p)Cu-64	9.239E+00	7.93	7.760E+00	19.1	**
Zr- 90(n,2n)Zr-89	1.294E-02	3.83	1.185E-02	9.2	*
Nb- 93(n,2n)Nb-92m	9.245E-02	4.62			
Nb- 93(n,n')Nb-93m	4.794E+01	8.32	5.227E+01	-8.3	*
Rh-103(n,n')Rh-103m	2.923E+02	4.57	2.923E+02	0.0	
In-115(n,n')In-115m	5.466E+01	3.03	5.257E+01	4.0	
In-115(n,g)In-116m	3.014E+02	4.38	3.262E+02	-7.6	*
I -127(n,2n)I-126	3.068E-01	17.47	2.530E-01	21.3	***
Eu-151(n,g)Eu-152	1.731E+03	3.81			
Ta-181(n,g)Ta-182	4.092E+02	4.20			
W -186(n,g)W-187	1.068E+02	4.10			
Au-197(n,2n)Au-196	7.245E-01	5.06			
Au-197(n,g)Au-198	3.245E+02	4.19	3.351E+02	-3.2	
Hg-199(n,n')Hg-199m	6.608E+01	8.43			
Th-232(n,f)	2.060E+01	5.58	1.960E+01	5.1	*
Th-232(n,g)Th-233	2.238E+02	10.84	2.390E+02	-6.4	*
U -235(n,f)	1.493E+03	2.81	1.505E+03	-0.8	
U -238(n,f)	8.303E+01	3.07	8.213E+01	1.1	
U -238(n,g)U-239	2.029E+02	4.25	2.094E+02	-3.1	
Np-237(n,f)	6.003E+02	9.88	6.136E+02	-2.2	
Pu-239(n,f)	1.734E+03	3.14	1.752E+03	-1.1	
Am-241(n,f)	5.072E+02	3.16	5.199E+02	-2.5	

Table 3.1.9 Average cross sections calculated with the ORR spectrum

Reaction	JENDL(mb)	err(%)	IRDF-85(mb)	Dif.(%)	
Li- 6(n,t)a	2.123E+05	2.10			
Li- 6 a-production	2.123E+05	2.10	2.114E+05	0.4	
Li- 7 t-production	4.976E+00	4.80	5.229E+00	-4.8	
B - 10(n,a)Li-7	8.652E+05	2.08			
B - 10 a-production	8.652E+05	2.08	8.656E+05	-0.0	
F - 19(n,2n)F-18	4.891E-03	3.23	4.087E-03	19.7	**
Na- 23(n,2n)Na-22	2.324E-03	8.17	2.269E-03	2.4	
Na- 23(n,g)Na-24	1.215E+02	2.86	1.205E+02	0.8	
Mg- 24(n,p)Na-24	4.040E-01	4.63	3.704E-01	9.1	*
Al- 27(n,p)Mg-27	1.049E+00	6.15	1.042E+00	0.6	
Al- 27(n,a)Na-24	1.687E-01	5.86	1.761E-01	-4.2	
P - 31(n,p)Si-31	9.241E+00	4.19	7.136E+00	29.5	***
S - 32(n,p)P-32	1.727E+01	8.49	1.746E+01	-1.1	
Sc- 45(n,g)Sc-46	6.136E+03	2.22	6.143E+03	-0.1	
Ti- 0(n,X)Sc-46	2.204E-01				
Ti- 0(n,X)Sc-47	3.613E-01				
Ti- 0(n,X)Sc-48	5.186E-02				
Ti- 46(n,p)Sc-46	2.751E+00	12.80	2.729E+00	0.8	
Ti- 47(n,np)Sc-46	4.906E-03	30.07	5.991E-03	-18.1	**
Ti- 47(n,p)Sc-47	4.934E+00	11.43	5.695E+00	-13.4	**
Ti- 48(n,np)Sc-47	1.520E-03	30.07	1.099E-03	38.3	***
Ti- 48(n,p)Sc-48	7.024E-02	10.57	7.093E-02	-1.0	
Ti- 49(n,np)Sc-48	4.570E-04	18.16			
Mn- 55(n,2n)Mn-54	9.390E-02	10.28	9.170E-02	2.4	
Mn- 55(n,g)Mn-56	3.133E+03	4.62			
Fe- 54(n,p)Mn-54	1.998E+01	4.09	2.008E+01	-0.5	
Fe- 56(n,p)Mn-56	2.629E-01	4.96	2.583E-01	1.8	
Fe- 57(n,np)Mn-56	6.198E-04	16.97			
Fe- 58(n,g)Fe-59	3.069E+02	2.55	2.740E+02	12.0	**
Co- 59(n,2n)Co-58	8.523E-02	8.89	8.710E-02	-2.1	
Co- 59(n,g)Co-60	9.881E+03	2.20	9.866E+03	0.2	
Co- 59(n,a)Mn-56	4.134E-02	4.72	3.727E-02	10.9	**
Ni- 58(n,2n)Ni-57	2.480E-03	11.09	2.234E-03	11.1	**
Ni- 58(n,p)Co-58	2.679E+01	6.88	2.632E+01	1.8	
Ni- 60(n,p)Co-60	6.440E-01	7.95	6.408E-01	0.5	
Cu- 63(n,2n)Cu-62	5.000E-02	2.55	4.814E-02	3.8	
Cu- 63(n,g)Cu-64	1.067E+03	2.76	1.073E+03	-0.6	
Cu- 63(n,a)Co-60	1.367E-01	5.95	1.366E-01	0.1	
Cu- 65(n,2n)Cu-64	1.298E-01	6.82	1.274E-01	1.9	
Zn- 64(n,p)Cu-64	1.065E+01	7.67	8.936E+00	19.1	**
Zr- 90(n,2n)Zr-89	5.816E-02	2.98	5.712E-02	1.8	
Nb- 93(n,2n)Nb-92m	1.316E-01	3.97			
Nb- 93(n,n')Nb-93m	4.118E+01	7.05	4.511E+01	-8.7	*
Rh-103(n,n')Rh-103m	2.128E+02	4.09	2.128E+02	0.0	
In-115(n,n')In-115m	5.091E+01	3.03	4.915E+01	3.6	
In-115(n,g)In-116m	1.019E+05	6.49	1.308E+05	-22.1	***
I -127(n,2n)I-126	4.553E-01	17.23	3.854E-01	18.1	**
Eu-151(n,g)Eu-152	2.029E+06	2.83			
Ta-181(n,g)Ta-182	2.305E+04	4.97			
W -186(n,g)W-187	2.304E+04	4.77			
Au-197(n,2n)Au-196	8.985E-01	4.31			
Au-197(n,g)Au-198	6.345E+04	3.49	6.353E+04	-0.1	
Hg-199(n,n')Hg-199m	6.411E+01	8.20			
Th-232(n,f)	2.103E+01	5.53	2.008E+01	4.7	
Th-232(n,g)Th-233	4.101E+03	7.32	4.127E+03	-0.6	
U -235(n,f)	1.296E+05	2.09	1.304E+05	-0.6	
U -238(n,f)	8.341E+01	2.99	8.252E+01	1.1	
U -238(n,g)U-239	1.035E+04	4.40	1.038E+04	-0.3	
Np-237(n,f)	4.214E+02	9.47	4.293E+02	-1.8	
Pu-239(n,f)	2.089E+05	2.17	2.078E+05	0.5	
Am-241(n,f)	1.456E+03	2.61	1.528E+03	-4.7	

Table 3.1.10 Average cross sections calculated with the YAYOI spectrum

Reaction	JENDL(mb)	err(%)	IRDF-85(mb)	Dif.(%)	
Li- 6(n,t)a	5.441E+02	2.94			
Li- 6 a-production	6.190E+02	2.95	5.987E+02	3.4	
Li- 7 t-production	1.102E+01	4.76	1.162E+01	-5.1	*
B - 10(n,a)Li-7	6.554E+02	3.52			
B - 10 a-production	7.278E+02	3.97	6.721E+02	8.3	*
F - 19(n,2n)F-18	1.116E-02	3.50	9.079E-03	22.9	***
Na- 23(n,2n)Na-22	4.587E-03	9.61	4.427E-03	3.6	
Na- 23(n,g)Na-24	3.063E-01	9.97	3.869E-01	-20.8	***
Mg- 24(n,p)Na-24	1.053E+00	4.65	9.748E-01	8.0	*
Al- 27(n,p)Mg-27	2.394E+00	6.12	2.377E+00	0.7	
Al- 27(n,a)Na-24	4.627E-01	5.80	4.832E-01	-4.2	
P - 31(n,p)Si-31	2.065E+01	4.14	1.594E+01	29.5	***
S - 32(n,p)P-32	3.864E+01	8.48	3.913E+01	-1.2	
Sc- 45(n,g)Sc-46	1.147E+01	3.00	9.158E+00	25.2	***
Ti- 0(n,X)Sc-46	5.008E-01				
Ti- 0(n,X)Sc-47	8.160E-01				
Ti- 0(n,X)Sc-48	1.350E-01				
Ti- 46(n,p)Sc-46	6.251E+00	12.76	6.208E+00	0.7	
Ti- 47(n,np)Sc-46	9.918E-03	30.07	1.263E-02	-21.5	***
Ti- 47(n,p)Sc-47	1.115E+01	11.40	1.281E+01	-13.0	**
Ti- 48(n,np)Sc-47	3.156E-03	30.07	2.209E-03	42.8	****
Ti- 48(n,p)Sc-48	1.829E-01	10.52	1.859E-01	-1.6	
Ti- 49(n,np)Sc-48	8.084E-04	18.49			
Mn- 55(n,2n)Mn-54	2.323E-01	11.36	2.250E-01	3.2	
Mn- 55(n,g)Mn-56	4.311E+00	7.62			
Fe- 54(n,p)Mn-54	4.463E+01	4.07	4.486E+01	-0.5	
Fe- 56(n,p)Mn-56	6.497E-01	4.88	6.328E-01	2.7	
Fe- 57(n,np)Mn-56	1.145E-03	16.80			
Fe- 58(n,g)Fe-59	3.155E+00	19.52	2.184E+00	44.5	****
Co- 59(n,2n)Co-58	2.060E-01	9.83	2.105E-01	-2.1	
Co- 59(n,g)Co-60	7.198E+00	3.22	7.966E+00	-9.6	*
Co- 59(n,a)Mn-56	1.070E-01	4.69	9.807E-02	9.1	*
Ni- 58(n,2n)Ni-57	5.050E-03	11.07	4.633E-03	9.0	*
Ni- 58(n,p)Co-58	6.005E+01	6.86	5.900E+01	1.8	
Ni- 60(n,p)Co-60	1.551E+00	7.67	1.550E+00	0.0	
Cu- 63(n,2n)Cu-62	1.143E-01	2.62	1.088E-01	5.1	*
Cu- 63(n,g)Cu-64	1.194E+01	18.48	1.341E+01	-11.0	**
Cu- 63(n,a)Co-60	3.290E-01	5.78	3.439E-01	-4.3	
Cu- 65(n,2n)Cu-64	3.302E-01	7.52	3.224E-01	2.4	
Zn- 64(n,p)Cu-64	2.387E+01	7.70	1.999E+01	19.4	**
Zr- 90(n,2n)Zr-89	1.256E-01	3.01	1.223E-01	2.7	
Nb- 93(n,2n)Nb-92m	3.862E-01	4.27			
Nb- 93(n,n')Nb-93m	9.604E+01	7.23	1.051E+02	-8.6	*
Rh-103(n,n')Rh-103m	5.086E+02	3.97	5.086E+02	-0.0	
In-115(n,n')In-115m	1.174E+02	3.03	1.132E+02	3.7	
In-115(n,g)In-116m	1.714E+02	4.26	1.960E+02	-12.5	**
I -127(n,2n)I-126	1.308E+00	17.26	1.097E+00	19.2	**
Eu-151(n,g)Eu-152	6.161E+02	4.27			
Ta-181(n,g)Ta-182	1.295E+02	6.34			
W -186(n,g)W-187	4.785E+01	5.17			
Au-197(n,2n)Au-196	2.788E+00	4.46			
Au-197(n,g)Au-198	1.188E+02	5.27	1.203E+02	-1.2	
Hg-199(n,n')Hg-199m	1.469E+02	8.23			
Th-232(n,f)	4.771E+01	5.52	4.553E+01	4.8	
Th-232(n,g)Th-233	1.144E+02	10.54	1.234E+02	-7.3	*
U -235(n,f)	1.253E+03	2.83	1.260E+03	-0.6	
U -238(n,f)	1.891E+02	3.00	1.871E+02	1.1	
U -238(n,g)U-239	9.308E+01	5.25	9.681E+01	-3.8	
Np-237(n,f)	1.007E+03	9.73	1.021E+03	-1.4	
Pu-239(n,f)	1.716E+03	2.95	1.722E+03	-0.4	
Am-241(n,f)	9.615E+02	3.38	9.859E+02	-2.5	

Table 3.1.11 Average cross sections calculated with the NEACRP benckmark spectrum

Reaction	JENDL(mb)	err(%)	IRDF-85(mb)	Dif.(%)	
Li- 6(n,t)a	1.085E+03	2.31			
Li- 6 a-production	1.100E+03	2.31	1.078E+03	2.0	
Li- 7 t-production	1.917E+00	5.06	2.026E+00	-5.4	*
B - 10(n,a)Li-7	2.681E+03	2.08			
B - 10 a-production	2.700E+03	2.09	2.679E+03	0.8	
F - 19(n,2n)F-18	0.0	0.0			
Na- 23(n,2n)Na-22	0.0	0.0			
Na- 23(n,g)Na-24	1.451E+00	9.82	1.607E+00	-9.7	*
Mg- 24(n,p)Na-24	1.286E-01	4.80	1.169E-01	10.0	**
Al- 27(n,p)Mg-27	4.062E-01	6.32	4.036E-01	0.6	
Al- 27(n,a)Na-24	5.041E-02	6.41	5.286E-02	-4.6	
P - 31(n,p)Si-31	4.277E+00	4.23	3.307E+00	29.3	***
S - 32(n,p)P-32	7.828E+00	9.02	7.864E+00	-0.5	
Sc- 45(n,g)Sc-46	4.415E+01	2.91	4.332E+01	1.9	
Ti- 0(n,X)Sc-46	8.491E-02				
Ti- 0(n,X)Sc-47	1.715E-01				
Ti- 0(n,X)Sc-48	1.545E-02				
Ti- 46(n,p)Sc-46	1.061E+00	12.94	1.055E+00	0.6	
Ti- 47(n,np)Sc-46	0.0	0.0			
Ti- 47(n,p)Sc-47	2.350E+00	11.43	2.664E+00	-11.8	**
Ti- 48(n,np)Sc-47	0.0	0.0			
Ti- 48(n,p)Sc-48	2.093E-02	11.27	2.106E-02	-0.6	
Ti- 49(n,np)Sc-48	0.0	0.0			
Mn- 55(n,2n)Mn-54	2.090E-05	25.07	1.149E-05	82.0	****
Mn- 55(n,g)Mn-56	5.113E+01	5.07			
Fe- 54(n,p)Mn-54	8.776E+00	4.15	8.935E+00	-1.8	
Fe- 56(n,p)Mn-56	8.804E-02	5.20	8.658E-02	1.7	
Fe- 57(n,np)Mn-56	0.0	0.0			
Fe- 58(n,g)Fe-59	1.961E+01	10.98	1.150E+01	70.6	****
Co- 59(n,2n)Co-58	0.0	0.0			
Co- 59(n,g)Co-60	3.570E+01	2.53	3.697E+01	-3.4	
Co- 59(n,a)Mn-56	1.282E-02	5.09	1.141E-02	12.4	**
Ni- 58(n,2n)Ni-57	0.0	0.0			
Ni- 58(n,p)Co-58	1.222E+01	7.02	1.207E+01	1.2	
Ni- 60(n,p)Co-60	2.307E-01	8.29	2.293E-01	0.6	
Cu- 63(n,2n)Cu-62	0.0	0.0			
Cu- 63(n,g)Cu-64	5.941E+01	4.28	7.209E+01	-17.6	**
Cu- 63(n,a)Co-60	4.896E-02	6.21	4.663E-02	5.0	*
Cu- 65(n,2n)Cu-64	8.762E-04	3.12	4.399E-04	99.2	****
Zn- 64(n,p)Cu-64	4.709E+00	7.75	3.966E+00	18.7	**
Zr- 90(n,2n)Zr-89	0.0	0.0			
Nb- 93(n,2n)Nb-92m	1.161E-02	7.88			
Nb- 93(n,n')Nb-93m	2.541E+01	8.41	2.760E+01	-7.9	*
Rh-103(n,n')Rh-103m	1.594E+02	5.35	1.594E+02	0.0	
In-115(n,n')In-115m	2.869E+01	3.04	2.762E+01	3.9	
In-115(n,g)In-116m	4.820E+02	6.07	5.116E+02	-5.8	*
I -127(n,2n)I-126	2.978E-02	18.07	2.453E-02	21.4	***
Eu-151(n,g)Eu-152	3.235E+03	4.72			
Ta-181(n,g)Ta-182	7.524E+02	4.62			
W -186(n,g)W-187	1.628E+02	4.71			
Au-197(n,2n)Au-196	1.593E-01	5.71			
Au-197(n,g)Au-198	5.984E+02	5.93	6.232E+02	-4.0	
Hg-199(n,n')Hg-199m	3.449E+01	8.54			
Th-232(n,f)	1.078E+01	5.62	1.026E+01	5.1	*
Th-232(n,g)Th-233	3.571E+02	11.17	3.763E+02	-5.1	*
U -235(n,f)	1.881E+03	3.23	1.891E+03	-0.5	
U -238(n,f)	4.369E+01	3.09	4.321E+01	1.1	
U -238(n,g)U-239	3.220E+02	4.38	3.350E+02	-3.9	
Np-237(n,f)	3.227E+02	9.81	3.319E+02	-2.8	
Pu-239(n,f)	1.790E+03	3.77	1.799E+03	-0.5	
Am-241(n,f)	2.716E+02	3.11	2.837E+02	-4.3	

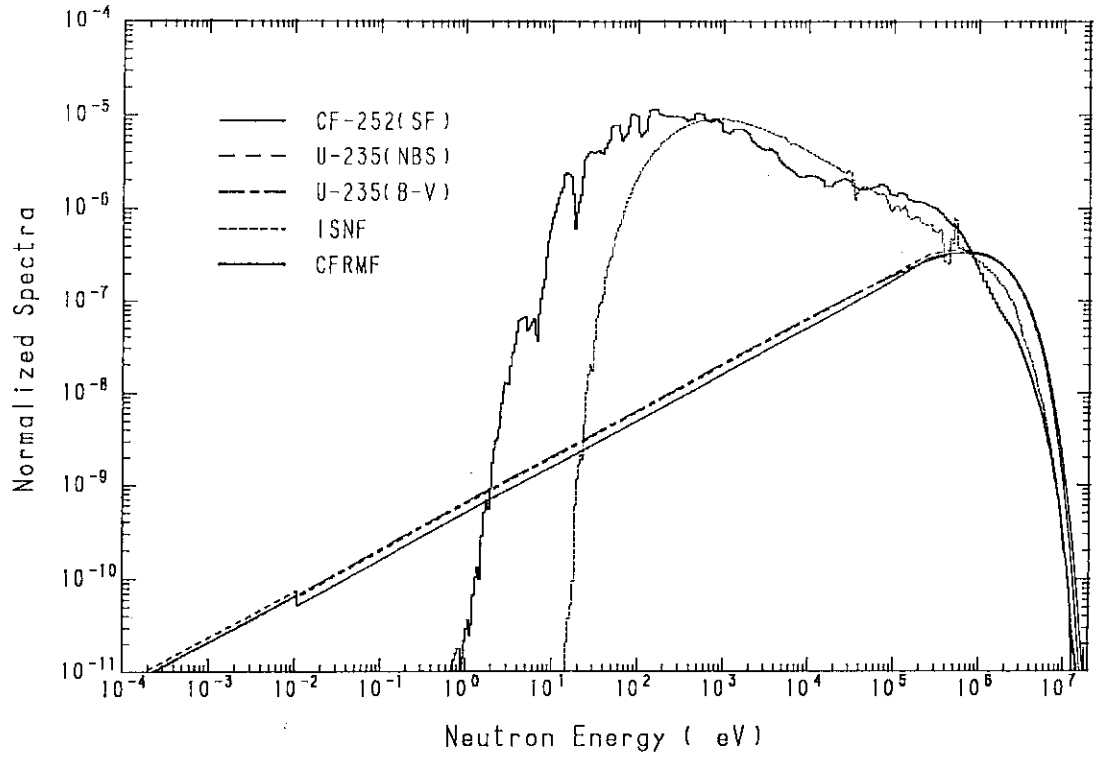

Fig. 3.1.1(a) Benchmark spectra stored in IRDF–85.

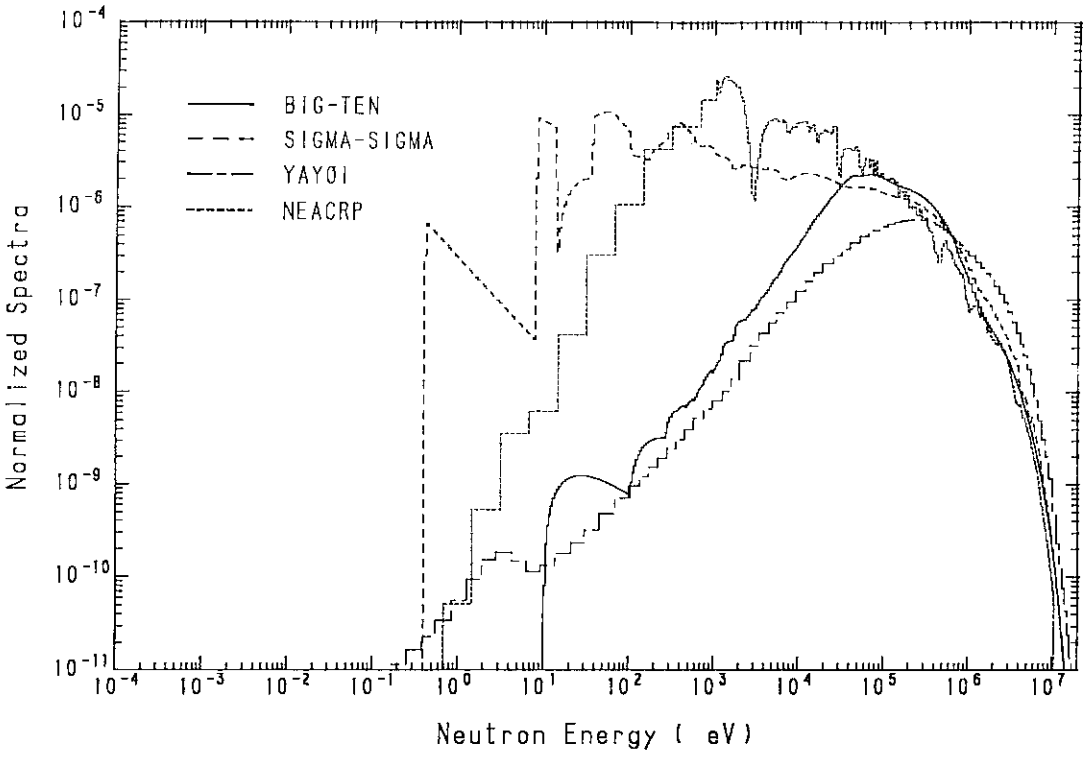

Fig. 3.1.1(b) Benchmark spectra stored in IRDF–85.

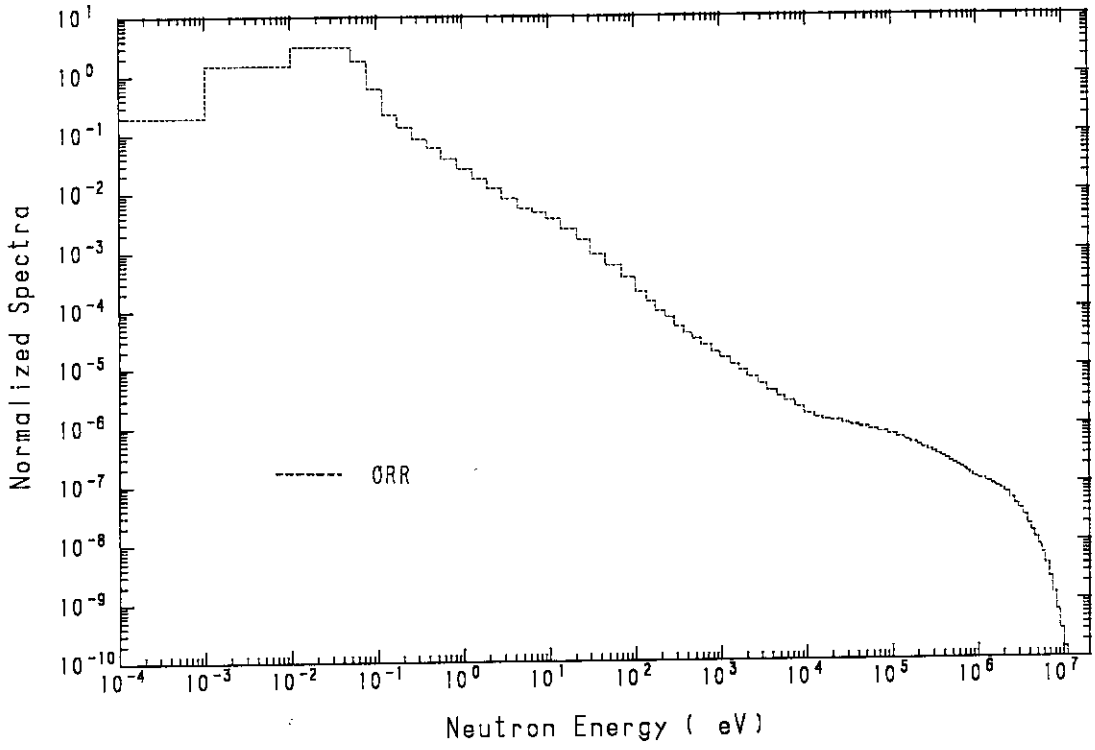

Fig. 3.1.1(c) Benchmark spectra stored in IRDF–85.

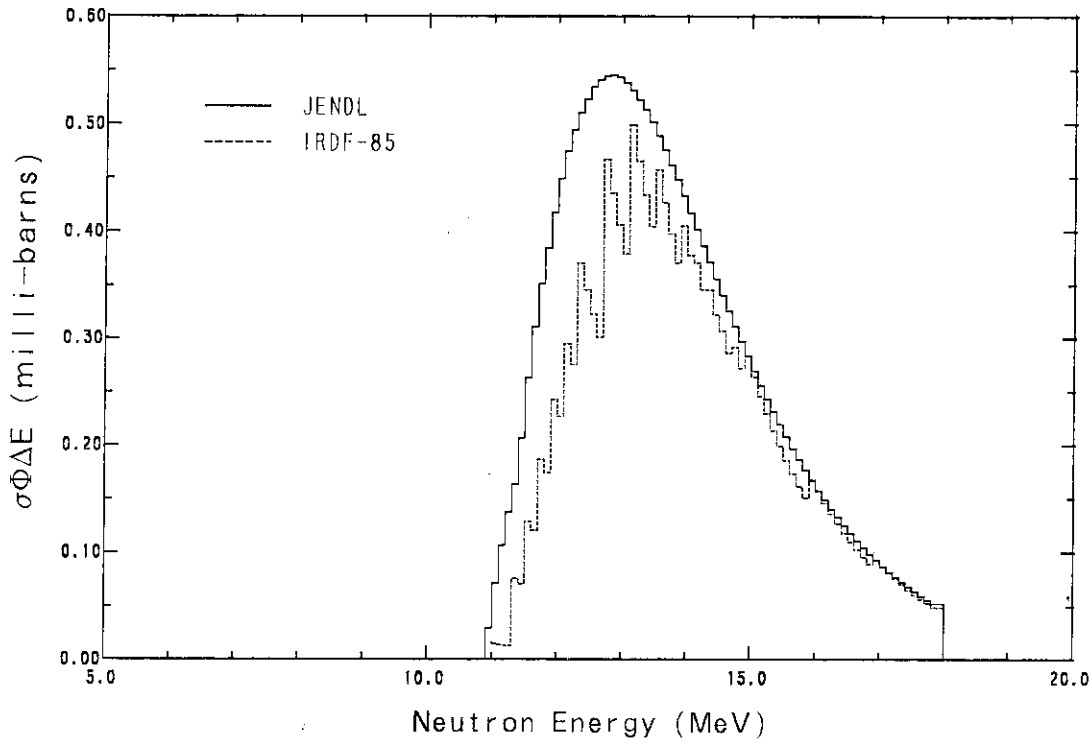

Fig. 3.1.2 Contributions to the ^{252}Cf spontaneous fission spectrum average values of ^{19}F(n, 2n)^{18}F reaction cross section.

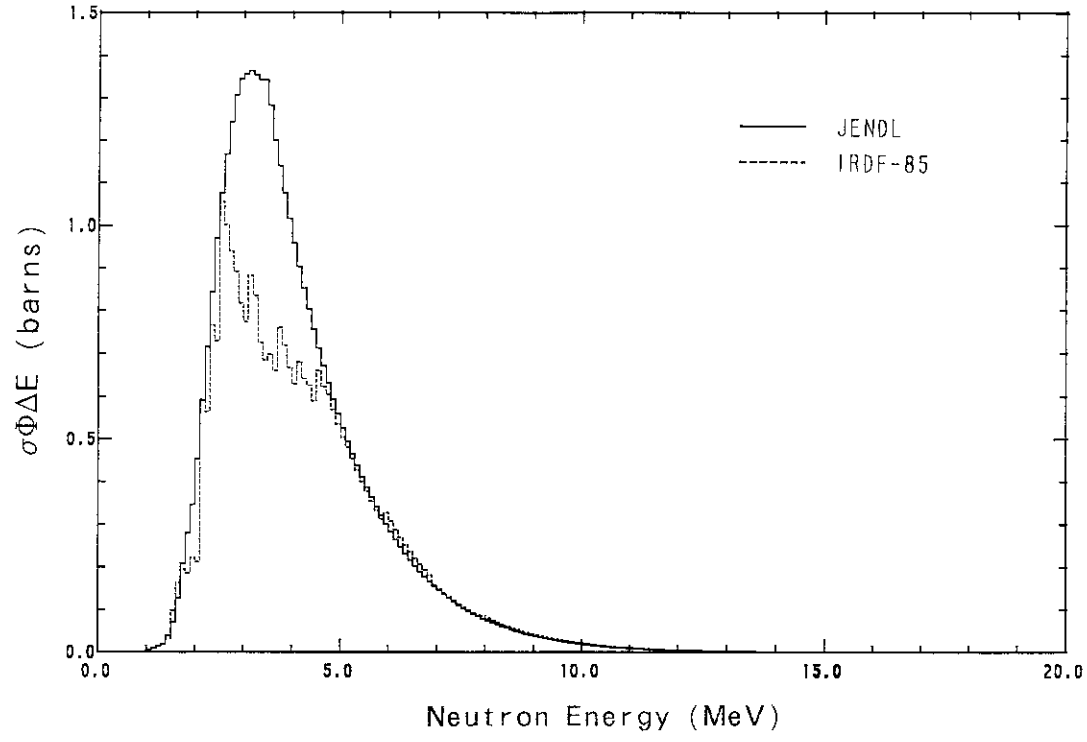

Fig. 3.1.3 Contributions to the ^{252}Cf spontaneous fission spectrum average values of ^{31}P(n, p)^{31}Si reaction cross section.

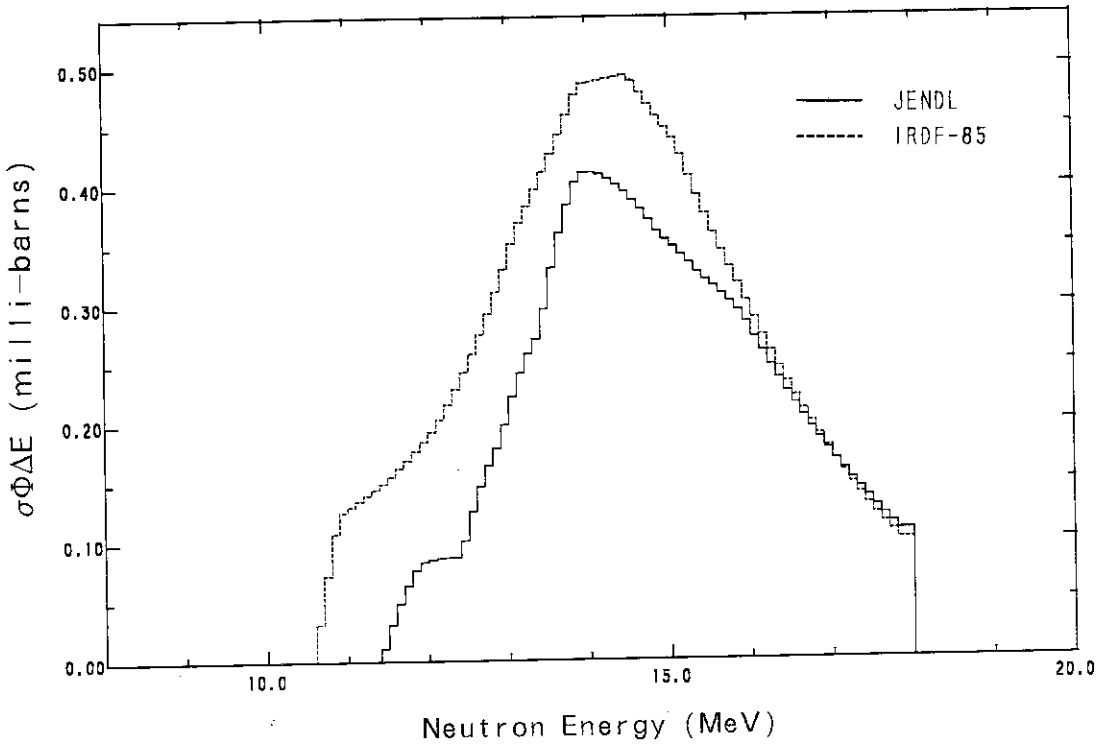

Fig. 3.1.4 Contributions to the ^{252}Cf spontaneous fission spectrum average values of $^{47}Ti(n, np)^{46}Sc$ reaction cross section.

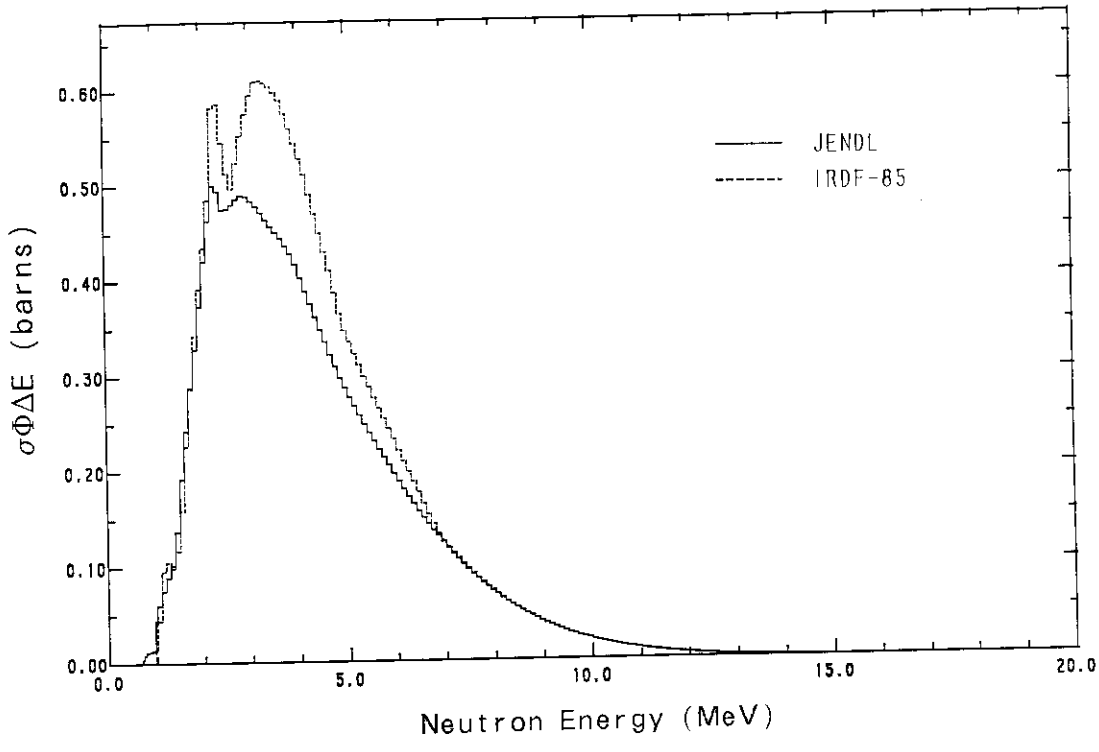

Fig. 3.1.5 Contributions to the ^{252}Cf spontaneous fission spectrum average values of $^{47}Ti(n, p)^{47}Sc$ reaction cross section.

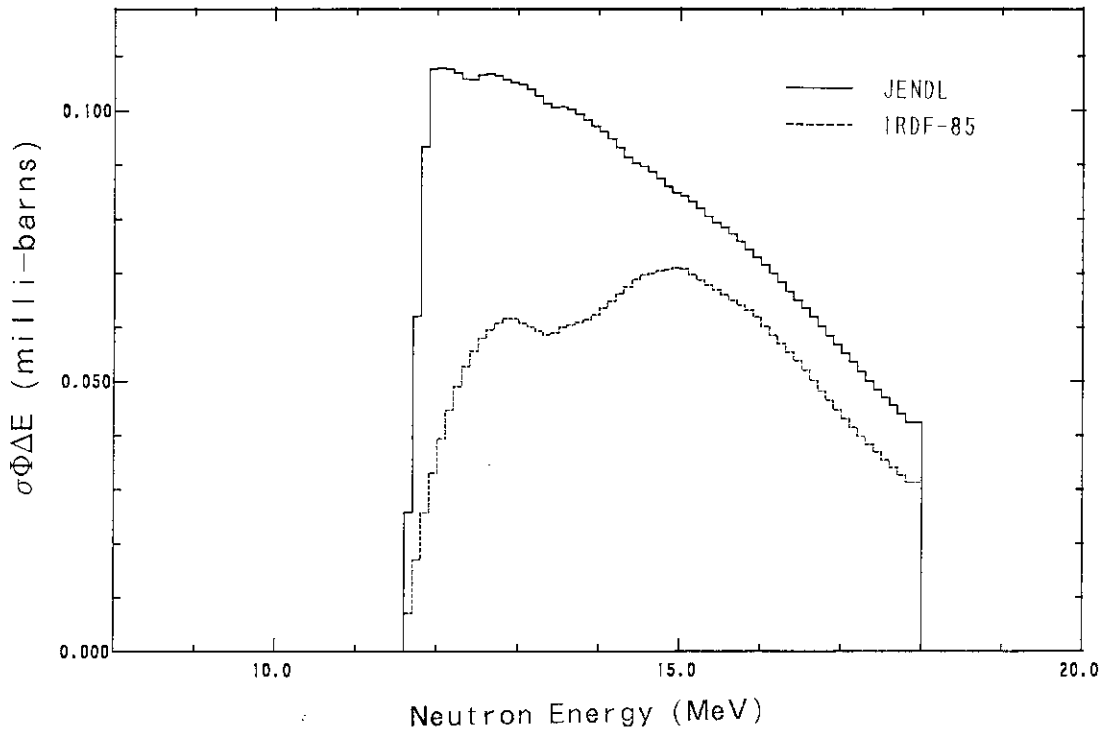

Fig. 3.1.6 Contributions to the ^{252}Cf spontaneous fission spectrum average values of ^{48}Ti(n, np)^{47}Sc reaction cross section.

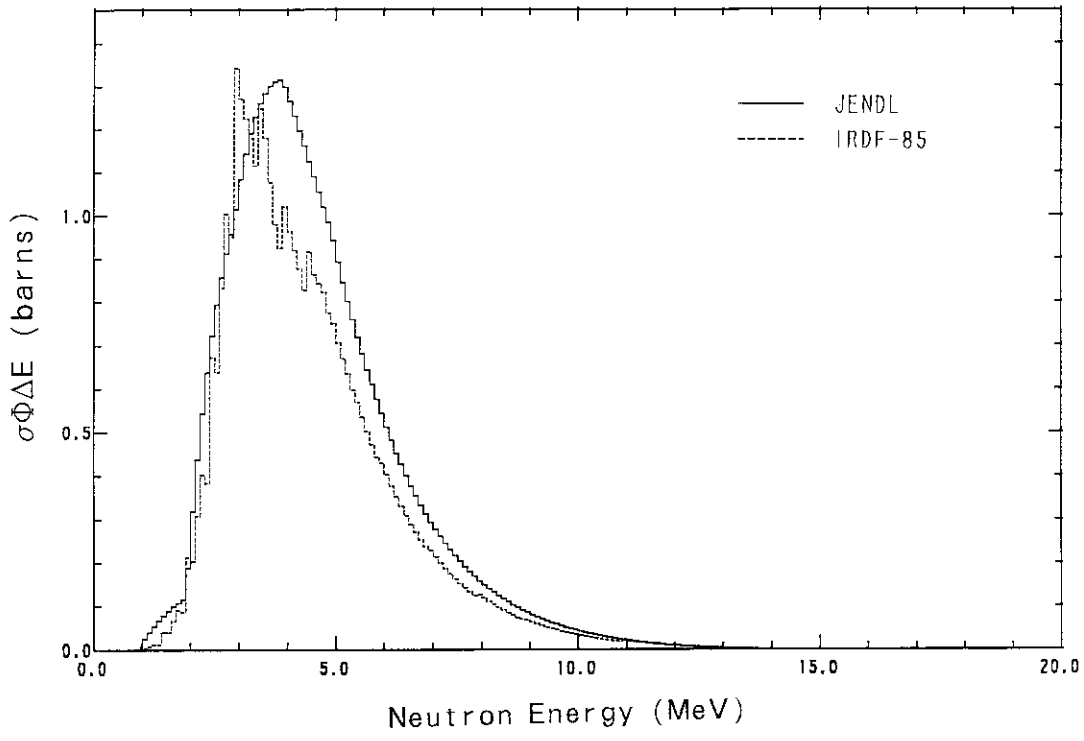

Fig. 3.1.7 Contributions to the ^{252}Cf spontaneous fission spectrum average values of ^{64}Zn(n, p)^{64}Cu reaction cross section.

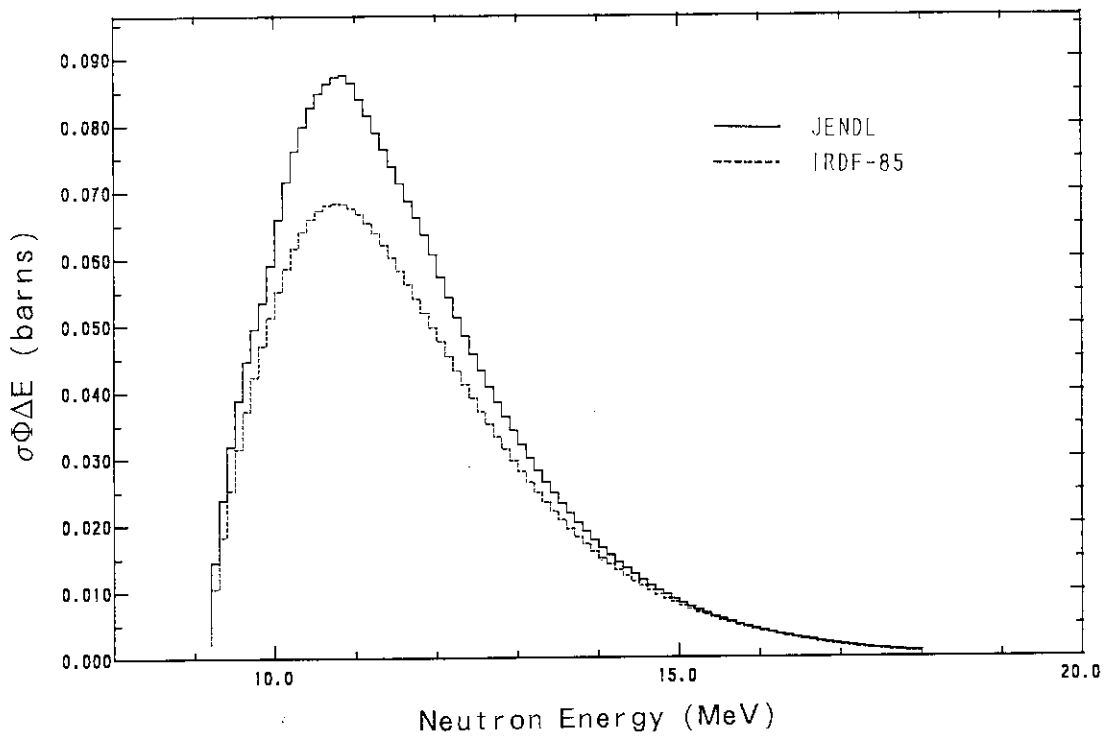

Fig. 3.1.8 Contributions to the ^{252}Cf spontaneous fission spectrum average values of $^{127}I(n, 2n)^{126}I$ reaction cross section.

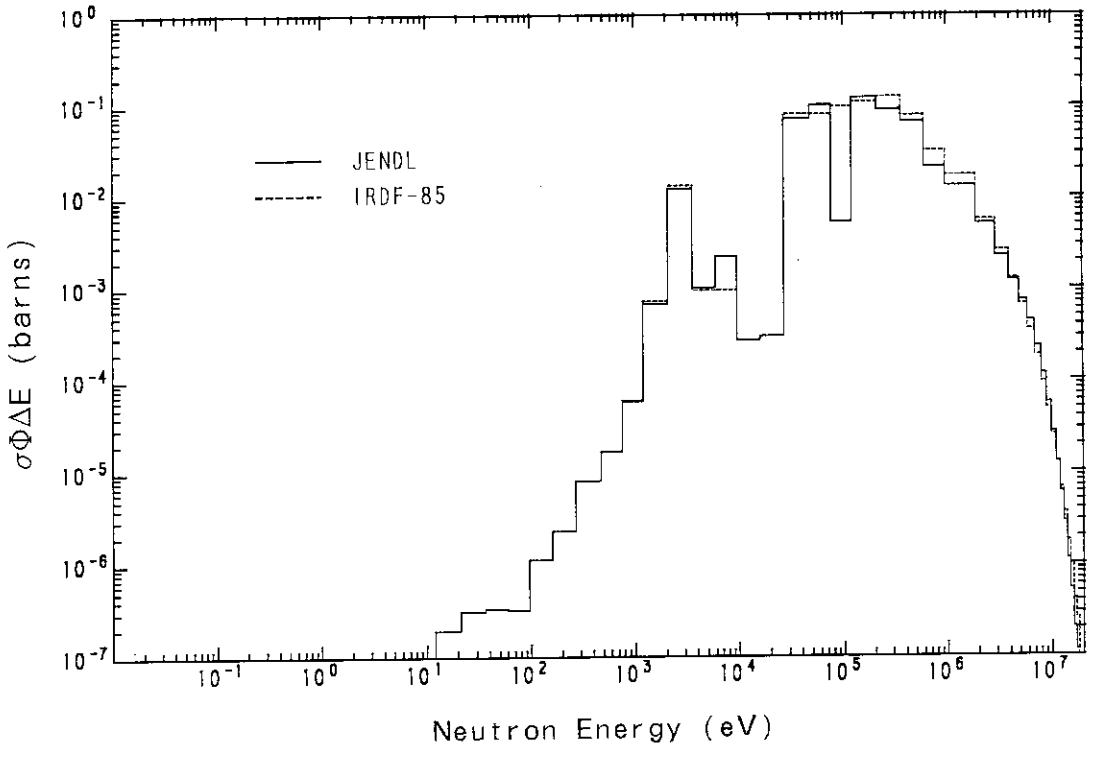

Fig. 3.1.9 Contributions to the BIG–TEN spectrum average values of $^{23}Na(n, \gamma)^{24}Na$ reaction cross section.

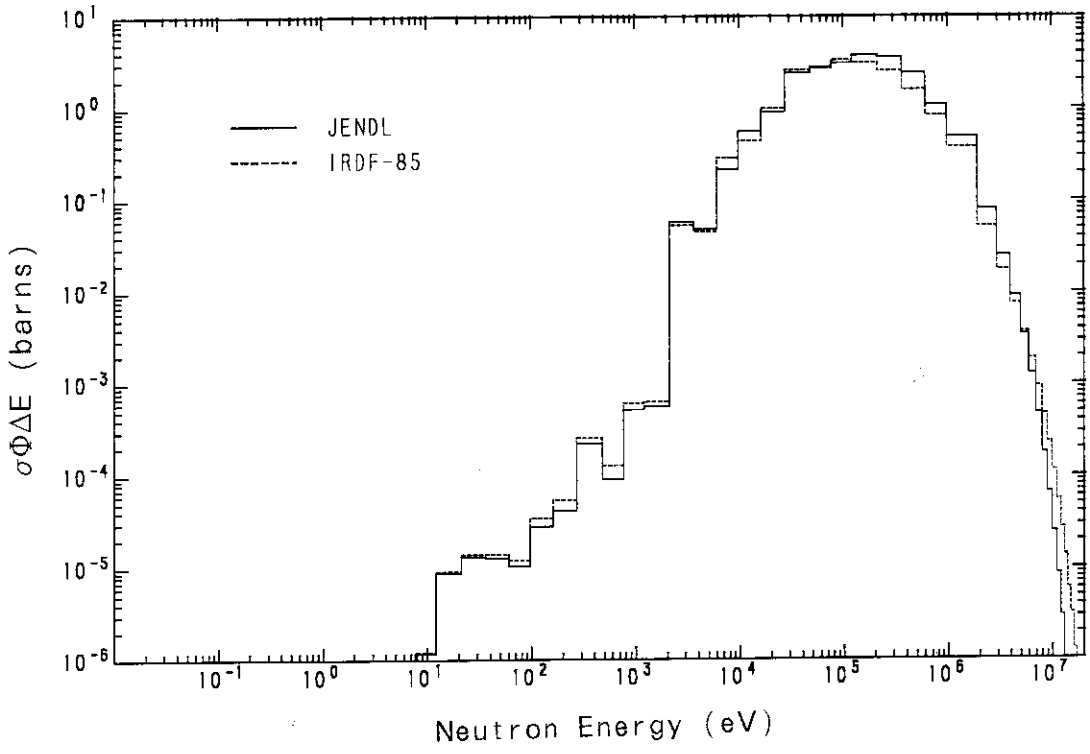

Fig. 3.1.10 Contributions to the BIG–TEN spectrum average values of ^{45}Sc (n, γ) ^{46}Sc reaction cross section.

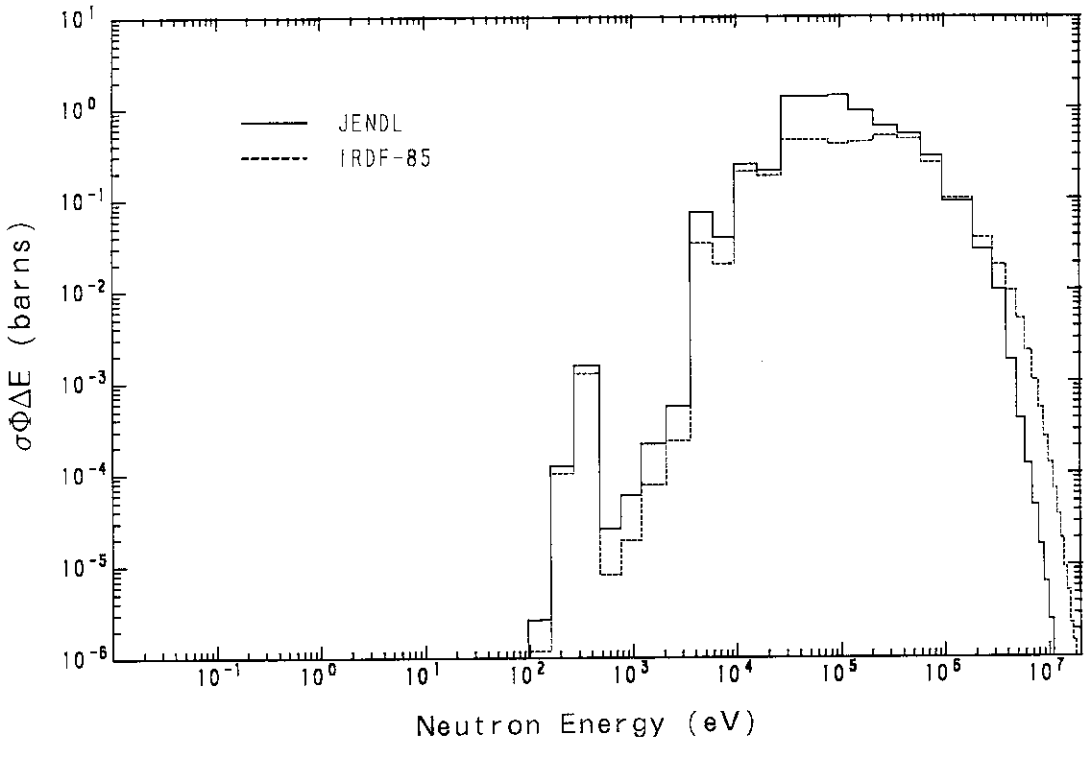

Fig. 3.1.11 Contributions to the BIG–TEN spectrum average values of ^{58}Fe (n, γ) ^{59}Fe reaction cross section.

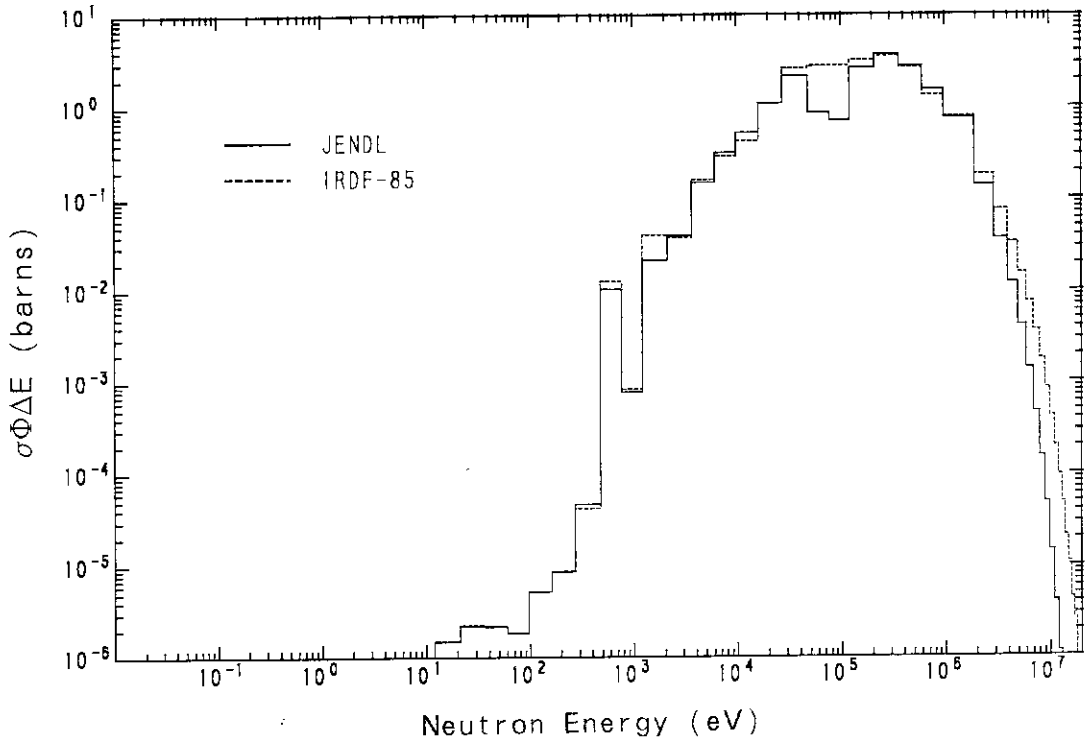

Fig. 3.1.12 Contributions to the BIG–TEN spectrum average values of ^{63}Cu (n, γ) ^{64}Cu reaction cross section.

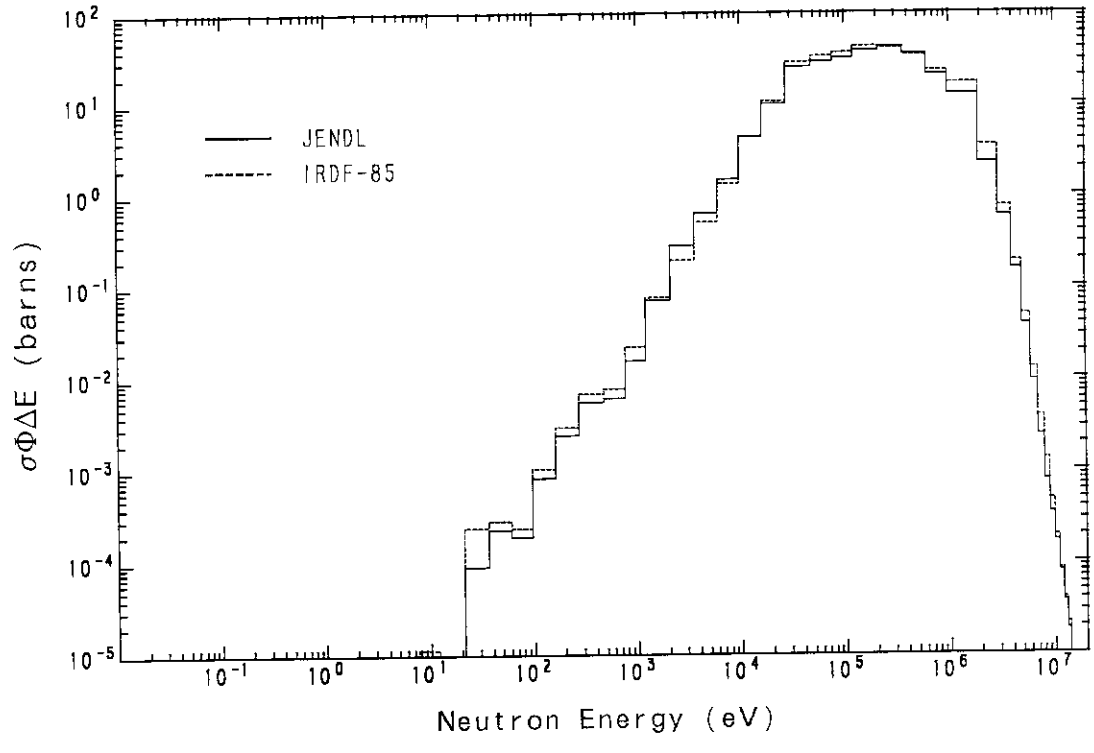

Fig. 3.1.13 Contributions to the BIG–TEN spectrum average values of ^{115}In (n, γ) ^{116m}In reaction cross section.

3.2 Integral Test with Fission Neutron Fields

3.2.1 Standard Neutron Fields

Standard neutron spectrum fields and neutron benchmark fields are important not only for the development of accurate and reliable reactor dosimetry techniques and surveillance programs but also for the application of dosimetry cross section measurements and neutron detector calibrations. The standard neutron field is required to fulfill the following conditions:

1) The neutron spectrum should be known as precisely as possible,
2) Its shape should be gently-sloping without resonant peaks and dips,
3) The spectrum is reproducible in inter-laboratories,
4) The neutron flux should be flat for position and angle,
5) The absolute value of the flux should be able to be obtained precisely,

A pure ^{235}U fission neutron field is apt to be hampered by perturbation effects arising from epithermal neutron background, wall returned and scattered neutrons. Due to these inherent disadvantages, the ^{235}U fission neutron field is superseded by the ^{252}Cf spontaneous fission neutron field. With a compact form of a ^{252}Cf source and a high specific neutron yield (2.3×10^9 n/mg/sec), the ^{252}Cf spontaneous fission neutron field can be realized to be almost free of spectrum distortion effects.

At the IAEA Consultants' Meeting in 1976, the classification of benchmark neutron fields was carried out[34]. In the fast neutron energy region, the spontaneous fission neutron spectrum of ^{252}Cf was classified as belonging to the standard neutron field in category I. The thermal neutron-induced fission spectrum of ^{235}U was identified as a reference neutron field. These standard and reference neutron fields make the spectrum-averaged data very useful for the validation of energy dependent cross section evaluations.

^{252}Cf Spontaneous Fission Neutron Field

In 1970s, it was regarded that most of the ^{252}Cf spontaneous fission neutron spectrum data between 250 keV and 8 MeV were in agreement with each other. The uncertainties of the spectrum in the lower and higher energy regions were, however, still considerably large. In recent years, much effort has been concentrated on new experiments and theoretical attempts in order to investigate and resolve the data discrepancies in the ^{252}Cf fission neutron spectrum[35,36].

Although a large number of measurements of the ^{252}Cf spontaneous fission neutron spectrum were made during the last 30 years, old experiments lack a detailed description which is needed for an estimate of corrections or re-analysis of the data. In order to evaluate the ^{252}Cf fission neutron spectrum precisely, Mannhart[37] confined to six recent differential experimental data between 25 keV and 19.8 MeV. Based on the documented uncertainties and additional information from the authors, he generated covariance matrix for each experiment, and used these values in the data fitting process performed with the least squares.

The ^{252}Cf spontaneous fission neutron spectrum evaluated by Mannhart[37] was illustrated relative to a Maxwellian distribution with T=1.42 MeV in **Fig. 3.2.1**. The uncertainties were obtained from the diagonal elements of the resulting covariance matrix. The relative uncertainty is 2 % between 0.25 and 8 MeV, more than 5 % in the lower energy range, and more than 10 % in the higher energy range.

^{235}U Thermal Fission Neutron Field

This fission spectrum was recommended as a reference neutron field[34]. A large number of experimental works have been carried out to obtain the ^{235}U fission neutron spectrum[38], and the results have been tried to fit with semi-empirical formulas such as a Maxwellian or a Watt-type spectrum[39,40]. Theoretical works have been also performed to predict the ^{235}U fission neutron spectrum[41-44]. Very recently, Kimura and Kobayashi presented the characteristics of the fission neutron spectrum with a large

fission plate, and measured some fission spectrum-averaged cross sections.[45,46] Kobayashi et al. also showed the results of the ^{235}U fission neutron spectrum unfolded by using multi-foil activation data.[46]

In recent years, much interest has been paid to the covariance matrix in the neutron spectrum which is required to give the uncertainties to the calculated spectrum-averaged cross sections. However, few papers report the neutron spectrum with the covariance matrix, except for the Kobayashi's and Petilli's works[47,48], while some of recent cross section libraries contain the covariance matrix.

In the ENDF/B-IV and JENDL-2, the Maxwellian distribution with $E_{av}=1.98$ MeV was adopted. A Watt-type spectrum was employed in ENDF/B-V. In the JENDL-3 General Purpose File[3], the Madland-Nix model description[41] was taken as the ^{235}U fission neutron spectrum. **Figure 3.2.2** shows these ratio to the Maxwellian distribution. Recent works by Johansson[39] and Kobayashi[47] support the Watt-type spectrum as the ^{235}U fission neutron spectrum, and show that the Maxwellian spectrum gives overestimation compared with the Watt spectrum, especially in the higher energy region above 10 MeV, as seen in **Fig. 3.2.2**.

3.2.2 Measured Average Cross Sections

^{252}Cf Spontaneous Fission Spectrum-Averaged Cross Sections

Spectrum-averaged cross sections measured with the ^{252}Cf neutron field are available for about 40 neutron reactions of importance in the reactor dosimetry[49]. There are two groups of experiments for the average cross sections: those with a complete uncertainty description and those to which the detailed information for uncertainty treatment is not always given. The former group of experiments is of particular importance, owing to their high accuracy and suitability for the evaluation of energy dependent cross sections.

In the present work, the data summarized by Mannhart[49] were practically used for the comparison with the calculated average cross sections. He included the experimental data with the covariance matrices measured by himself, Kobayashi and other seven groups, and he gave the covariance matrices to the summarized and evaluated 31 kinds of reactions. Additionally, the average cross section data[49], which were incomplete with experimental uncertainty and were not given in the best set of the above 31 least squares evaluation data, were also employed as supplemental data for the comparison with the calculated average cross sections.

^{235}U Fission Spectrum Averaged Cross Sections

Many groups have prepared and established the ^{235}U fission neutron field and measured spectrum-averaged cross sections which are often used for the integral assessment of energy dependent cross sections[45-48,50-53]. A review of all available data is given in an IAEA Handbook by Calamand[50]. Unfortunately, a detailed list of uncertainty contribution which makes it possible to generate covariance matrices is not given in Ref. 50. Then, it may be difficult to estimate the quality of these data, and this fact hampers trustworthy evaluation of the experimental data.

Recently, experimental data of the ^{235}U fission spectrum-averaged cross sections have been carefully measured with detailed experimental uncertainties. Mannhart measured the average cross sections of 17 reactions of importance in reactor dosimetry by making use of the ^{235}U fission neutron field of the BR1 at Mol.[52] A cylinder type of the ^{235}U fission neutron source and sample foils were set at the center of a spherical cavity of 1 m in diameter inside the vertical graphite thermal column. He gave a complete uncertainty covariance matrix to his results. The uncertainties in his experiment were 4 to 6 %. Gilliam et al. observed fission rates by means of NBS (now NIST) fission ionization chambers inserted into the central cavity of the Mol reactor BR1[51]. The experimental uncertainties obtained were about 2 to 3 %. Petilli and Gilliam analyzed these measured data and generated the covariance matrix.[48]

Very recently, Kobayashi et al. measured 12 kinds of threshold reactions for the ^{235}U fission neutron

spectrum-averaged cross sections[45-47]. They used a big fission plate of 31.3 cm in diameter and 1.1 cm thick, which was installed in an irradiation room ($2.4 \times 2.4 \times 2.4$ m^3) of the heavy water thermal neutron facility at the Kyoto University Reactor, KUR. They also gave a complete set of the correlation matrix to their results with the resultant uncertainties of several percent.

In this report, the experimental data obtained by Mannhart and Kobayashi et al. are practically employed for the comparison of the calculated average cross sections. The measured average cross sections for the (n, f) reactions of ^{235}U, ^{238}U, ^{237}Np and ^{239}Pu are adopted from the Gilliam's work[51].

3.2.3 Comparison of Average Cross Section Data

Spectrum-averaged cross sections and the error of calculated average cross sections have been derived by using Eqs. (1) and (2) given in the former Section 3.1.2. As standard neutron fields, two kinds of ^{252}Cf spontaneous fission neutron spectra and three kinds of ^{235}U fission neutron spectra were used. The calculated average cross sections were compared with experimental data. Since the covariance matrices were not always given in the neutron spectrum, the following covariance matrices were assumed for the present calculations, as seen in the former section: all of the diagonal elements have 5 % uncertainties, and all of the off-diagonal elements 2 %.

^{252}Cf Spontaneous Fission Spectrum-Averaged Cross Sections

For the comparison of the calculated and measured spectrum-averaged cross sections, the following ^{252}Cf spontaneous fission spectra were employed.

1) Maxwellian distribution:

$$X(E) \propto \sqrt{E} \exp(-1.5E/2.13)^{40},$$

where E is neutron energy in MeV.

2) The neutron spectrum evaluated by Mannhart[37].

The experimental data were taken from the Mannhart's recommended values and/or compilation data[49]. The measured and the calculated ^{252}Cf spectrum-averaged cross sections are given in **Table 3.2.1**.

It is found that the average cross sections calculated with the Maxwellian spectrum are larger than those with Mannhart spectrum in general for the reactions with higher threshold energies such as the (n, 2n) reactions. This could be estimated from the spectrum ratio, as seen in **Fig. 3.2.1**. Most of the data calculated by the Mannhart spectrum show, in general, good agreement with the measurements except for the some (n, 2n) and (n, γ) reactions.

From the comparison of the calculated data with the measured ones as shown in **Table 3.2.1**, it can be found that the JENDL dosimetry cross sections for the ^{19}F(n, 2n), ^{24}Mg(n, p), ^{55}Mn(n, 2n), ^{60}Ni(n, p), ^{63}Cu(n, 2n), ^{64}Zn(n, p) and ^{197}Au(n, 2n) reactions give larger average cross sections than the measured values. For the (n, γ) reaction data, the experimental data are higher in general than the calculated values. This may be due to the effects of the slow neutrons which disturb and soften the ideal spectrum shape of ^{252}Cf in the lower energy region. In addition, the (n, γ) reaction is more sensitive to the low energy neutrons.

^{235}U Fission Spectrum-Averaged Cross Sections

Neutron spectra used for the present calculation of the spectrum-averaged cross sections are as follows:

1) Maxwellian distribution:

$$X(E) \propto \sqrt{E} \exp(-1.5E/1.97)^{40},$$

where E is neutron energy in MeV.

2) Watt-type spectrum:

$$X(E) \propto \exp(-E/0.988) \sinh(\sqrt{2.249E})^{40}.$$

3) Neutron spectrum by the Madland–Nix model[41], which was adopted in JENDL–3.

The experimental data measured by three research groups, appearing in **Table 3.2.2**, were practically taken for the comparison of the calculated data. Comparison of the C/E ratios are also made for these three neutron spectra. The number of reactions which gives the difference more than 5 % is 15, 10 and 13 for the Maxwellian, Watt–type and Madland–Nix–type spectra, respectively. The number with difference more than 10 % is 7, 4 and 6, respectively. The spectrum–averaged (n, 2n) cross sections calculated with the Maxwellian distribution are generally larger than those calculated with other spectra. It can be pointed out that the Maxwellian distribution gives overestimation compared with the Watt–type and the Madland–Nix spectra, as seen in **Fig. 3.2.2**, in the higher energy region. The Watt–type spectrum gives closer results to most of the measurements, except for some high threshold energy reactions such as (n, 2n). The Madland–Nix spectrum shows a similar tendency to the Watt–type in the C/E ratio values.

Concerning the JENDL Dosimetry File, the calculated average cross sections for the ^{24}Mg(n, p) and ^{64}Zn(n, p) reactions are larger in general, and the ^{59}Co(n, 2n), ^{58}Ni(n, 2n), ^{90}Zr(n, 2n) and ^{93}Nb(n, 2n) are smaller than the measured ones. For the ^{90}Zr(n, 2n) reaction, Kobayashi et al. measured the value of 0.0860 ± 0.0065 mb[46], which was in good agreement with the calculation with the Watt–type spectrum.

The discrepancies observed in the calculated and measured average cross sections listed in **Tables 3.2.1** and **3.2.2** show the same tendency between the data for both ^{252}Cf and ^{235}U fission neutron spectra.

Table 3.2.1 Comparison of ^{252}Cf spontaneous fission spectrum-averaged cross sections. Values in parentheses are standard deviation in percent.

Reaction	Measurement[49] (mb)	Calculation and C/E ratio			
		Maxwellian spectrum		Mannhart spectrum	
		mb (%)	C/E ratio	mb (%)	C/E ratio
F-19 (n, 2n) F-18	.01628±.00054	.02529 (3.89)	1.553	.02094 (3.94)	1.286
Mg-24 (n, p) Na-24	2.005±0.048	2.517 (4.63)	1.255	2.270 (4.64)	1.132
Al-27 (n, p) Mg-27	4.892±0.106	5.330 (6.04)	1.090	5.073 (6.07)	1.037
Al-27 (n, α) Na-24	1.021±0.015	1.109 (5.77)	1.086	.9910 (5.81)	.9706
S-32 (n, p) P-32	72.74±2.54	75.42 (8.08)	1.037	74.89 (8.20)	1.030
Ti-46 (n, p) Sc-46	14.20±0.24	13.93 (12.7)	.9810	13.28 (12.7)	.9352
Ti-47 (n, p) Sc-47	19.43±0.31	20.87 (11.4)	1.074	20.70 (11.4)	1.065
Ti-48 (n,p) Sc-48	0.4275±0.0078	.4381 (10.5)	1.025	.3938 (10.5)	.9212
Mn-55 (n, 2n) Mn-54	0.4079±0.0092	.5651 (12.3)	1.385	.4731 (12.5)	1.160
Fe-54 (n, p) Mn-54	87.29±1.13	89.26 (4.02)	1.023	88.07 (4.04)	1.009
Fe-56 (n, p) Mn-56	1.471±0.025	1.543 (4.86)	1.049	1.408 (4.89)	.9572
Co-59 (n, 2n) Co-58	0.4058±0.0101	.4945 (10.7)	1.219	.4128 (10.9)	1.017
Co-59 (n, γ) Co-60	6.97±0.34	5.216 (4.65)	.7484	5.255 (4.66)	.7539
Co-59 (n, α) Mn-56	0.2221±0.0039	.2553 (4.65)	1.150	.2302 (4.67)	1.037
Ni-58 (n, 2n) Ni-57	(8.965±.279) $\times 10^{-3}$	1.015-2 (11.1)	1.132	8.295-3 (11.1)	.9212
Ni-58 (n, p) Co-58	117.6±1.5	116.6 (6.73)	.9915	115.5 (6.78)	.9821
Ni-60 (n, p) Co-60	2.39±0.13	3.617 (7.18)	1.513	3.346 (7.76)	1.400
Cu-63 (n,2n) Cu-62	0.1866±0.0071	.2579 (2.73)	1.382	.2135 (2.74)	1.144
Cu-63 (n, γ) Cu-64	10.55±0.32	8.617 (19.1)	.8168	8.565 (19.1)	.8118
Cu-63 (n, α) Co-60	0.6897±0.0130	.7603 (5.76)	1.102	.7054 (5.80)	1.023
Zn-64 (n, p) Cu-64	40.47±0.75	47.45 (7.78)	1.173	46.89 (7.75)	1.159
Zr-90 (n, 2n) Zr-89	0.2211±0.0061	.2659 (3.17)	1.203	.2182 (3.13)	.9869
Nb-93 (n, n') Nb-93m	149±10	148.5 (6.82)	.9966	149.5 (6.82)	1.003
Rh-103 (n, n') Rh-103m	757±53	712.7 (3.71)	.9415	716.1 (3.72)	.9460
In-115 (n, n') In-115m	198.1±2.6	188.2 (3.02)	.9500	189.7 (3.02)	.9576
Au-197 (n, 2n) Au-196	5.531±0.099	6.768 (4.73)	1.224	5.853 (4.77)	1.058
Au-197 (n, γ) Au-198	77.11±1.19	75.71 (8.76)	.9818	75.24 (8.91)	.9757
Th-232 fission	89.4±2.7	82.04 (5.50)	.9177	82.05 (5.50)	.9178
Th-232 (n, γ) Th-233	87.8±4.0	83.97 (12.0)	.9564	83.59 (12.1)	.9521
U-235 fission	1210±14	1237. (2.86)	1.022	1236. (2.87)	1.022
U-238 fission	323.4±5.6	317.7 (2.91)	.9824	319.1 (2.91)	.9867
Np-237 fission	1356±22	1340. (9.42)	.9882	1346. (9.46)	.9926
Pu-239 fission	1811±25	1802. (2.92)	.9950	1804. (2.92)	.9961

Table 3.2.2 Comparison of ^{235}U fission neutron spectrum-averaged cross sections. Values in parentheses are standard deviation in percent.

Reaction	Measurement (mb)	Ref.	Calculation and C/E ratio					
			Maxwellian spectrum		Watt-type spectrum		JENDL 3 (Madland-Nix)	
			mb (%)	C/E ratio	mb (%)	C/E ratio	mb (%)	C/E ratio
Mg-24 (n, p) Na-24	1.50±0.06	52	1.739 (4.66)	1.159	1.640 (4.69)	1.093	1.552 (4.70)	1.035
Al-27 (n, p) Mg-27	3.95±0.20	52	4.185 (6.12)	1.059	4.286 (6.17)	1.085	4.172 (6.20)	1.056
Al-27 (n, α) Na-24	0.706±0.028	52	.7469 (5.90)	1.058	.6880 (6.03)	.9745	.6482 (6.04)	.9181
Ti-46 (n,p) Sc-46	11.6±0.4	52	10.96 (12.8)	.9448	11.25 (12.8)	.9698	10.95 (12.8)	.9440
Ti-47 (n, p) Sc-47	17.7±0.6	52	18.43 (11.4)	1.041	19.28 (11.4)	1.089	19.31 (11.4)	1.091
Ti-48 (n, p) Sc-48	0.302±0.010	52	.2988 (10.6)	.9894	.2781 (10.7)	.9209	.2631 (10.7)	.8712
Fe-54 (n, p) Mn-54	80.5±2.3	52	76.74 (4.07)	.9533	80.73 (4.08)	1.003	80.39 (4.10)	.9990
Fe-56 (n, p) Mn-56	1.09±0.04	52	1.097 (4.94)	1.006	1.057 (5.00)	.9697	1.007 (5.01)	.9239
Co-59 (n, 2n) Co-58	0.202±0.006	52	.2604 (11.3)	1.289	.1788 (12.2)	.8851	.1639 (12.3)	.8114
Co-59 (n, α) Mn-56	0.161±0.007	52	.1758 (4.71)	1.092	.1652 (4.77)	1.026	.1564 (4.78)	.9714
Ni-58 (n, 2n) Ni-57	$(4.19\pm0.22)\times10^{-3}$	52	4.848-3 (11.1)	1.157	2.873-3 (11.1)	.6857	2.598-3 (11.1)	.6200
Ni-58 (n, p) Co-58	108.9±5.2	52	101.8 (6.86)	.9348	107.1 (6.90)	.9835	106.9 (6.94)	.9816
Zn-64 (n, p) Cu-64	31.68±1.82	46	40.95 (7.74)	1.293	43.12 (7.71)	1.361	42.98 (7.71)	1.357
Zr-90 (n, 2n) Zr-89	0.103±0.004	52	.1309 (3.18)	1.271	0.8123 (3.30)	.7886	.07378 (3.31)	.7163
Nb-93 (n, 2n) Nb-92m	0.4796±0.0293	46	.5609 (4.37)	1.170	.4397 (4.55)	.9168	.4076 (4.56)	.8499
Rh-103 (n, n') Rh-103m	673.5±52.2	46	686.7 (3.75)	1.020	705.0 (3.74)	1.047	710.6 (3.74)	1.055
In-115 (n, n') In-115m	190.3±7.3	52	178.1 (3.03)	.9359	185.4 (3.03)	.9743	187.6 (3.03)	.9858
Au-197 (n, 2n) Au-196	3.50±0.13	52	4.116 (4.86)	1.176	3.409 (5.00)	.9740	3.167 (5.04)	.9049
Th-232 fission	83±2.57	51	75.40 (5.51)	.9084	78.49 (5.50)	.9457	79.21 (5.51)	.9543
U-235 fission	1200±22.8	51	1236. (2.86)	1.030	1235. (2.87)	1.029	1235. (2.87)	1.029
U-238 fission	312±7.2	51	296.0 (2.94)	.9487	308.4 (2.94)	.9885	312.1 (2.94)	1.000
Np-237 fission	1359±28.5	51	1309. (9.57)	.9632	1334. (9.57)	.9816	1344. (9.60)	.9890
Pu-239 fission	1818±34.5	51	1794. (2.92)	.9868	1800. (2.92)	.9901	1804. (2.92)	.9923

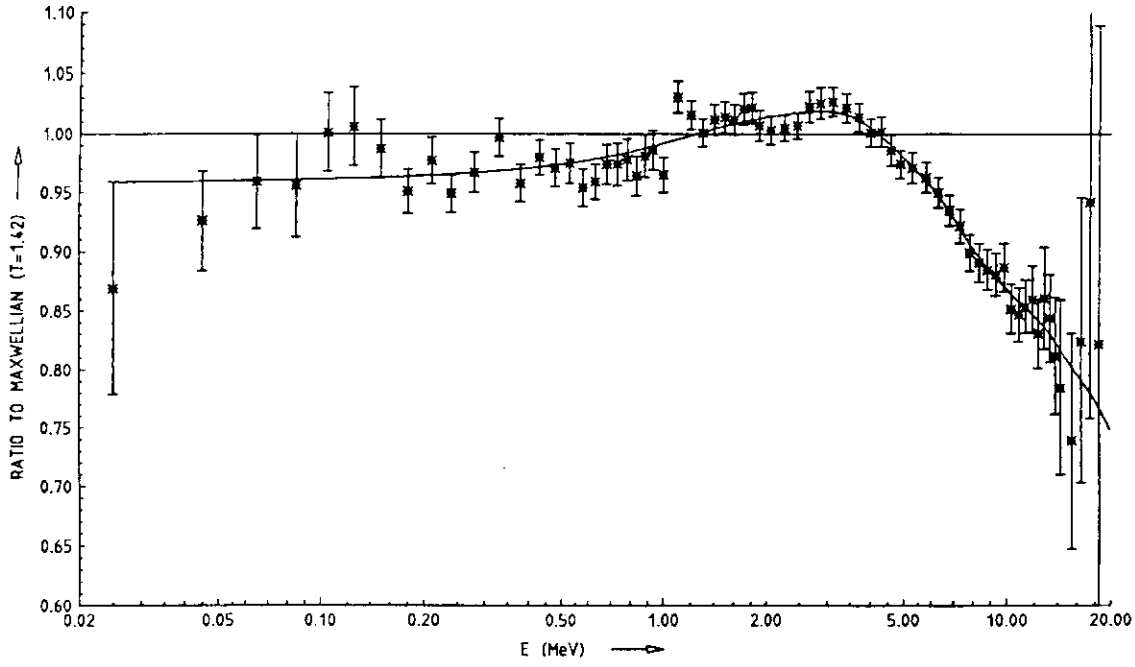

Fig. 3.2.1 Ratio of the evaluation of the spontaneous fission neutron spectrum of ^{252}Cf[37] to the Maxwellian spectrum (T=1.42). The data points represent the evaluation performed at discrete neutron energies. The solid curve is the continuous shape of the evaluated spectral distribution.

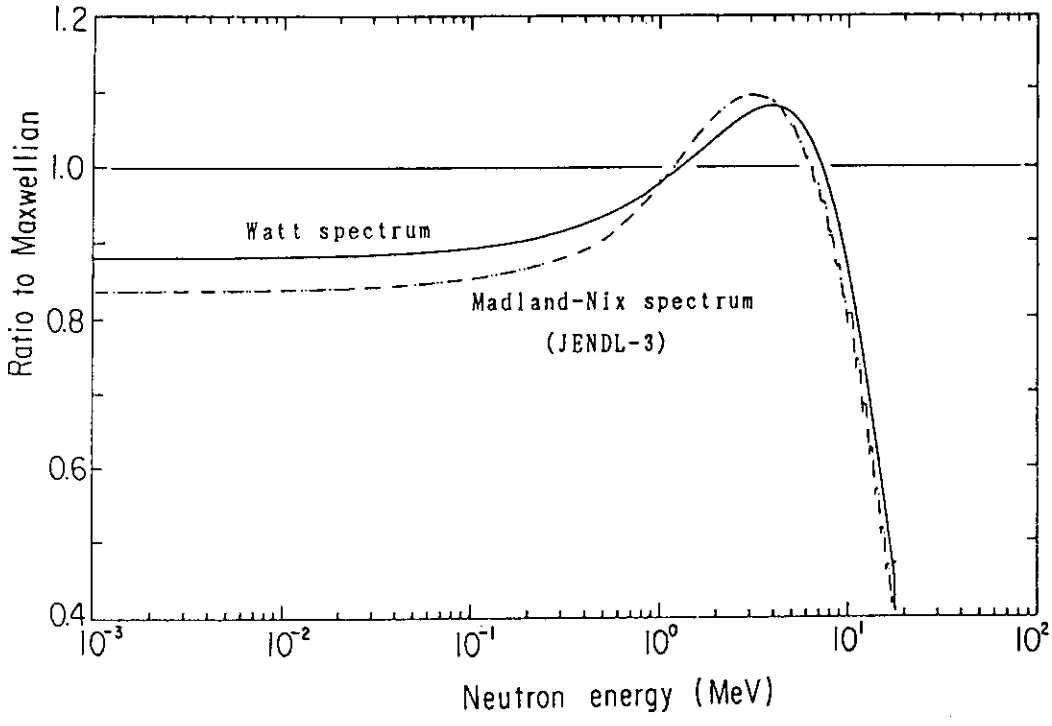

Fig. 3.2.2 Ratio of the Watt-type and the JENDL-3 spectra of ^{235}U to the Maxwellian spectrum (T=1.97).

3.3 Integral Test with Fast Reactor Neutron Fields

3.3.1 Fast Reactor Neutron Fields

Fast reactor neutron fields can be established in an assembly for irradiation attached with a research reactor. They are sometimes called the secondary standards or the reference neutron fields complementing the ^{252}Cf and ^{235}U fission neutron fields because the neutron spectra are similar to a fast reactor spectrum but have a much less complex structure due to the comparatively simple configuration of the assembly. These reference neutron fields have, in general, a suitable range, good stability and reproducibility of flux levels, in conjunction with their experimental amenabilities. Therefore, they are often used for high accuracy interlaboratory comparisons and standardizations of the dosimetry techniques.

For the integral test of the JENDL Dosimetry File, the following four kinds of fast reactor neutron fields were selected; ISNF, CFRMF, ΣΣ and YAYOI. These four neutron fields have been so far well characterized and have abundant experimental data available for integral test. The numerical data of their neutron spectra are also included in the IRDF–85 benchmark spectrum library as already shown in **Fig. 3.1.1**. The spectrum averaged cross sections calculated in Section 3.1 can be compared with the corresponding experimental data.

Here are presented the integral test results with brief descriptions of the outline of facilities, characteristics of the neutron spectrum fields and available data for testing the dosimetry reactions.

3.3.2 ISNF[27),54),55)]

The Intermediate–Energy Standard Neutron Field (ISNF) is an irradiation facility designed to produce a strong component of neutrons in the energy range of interest for fast reactors. The ISNF consists of eight ^{235}U disks symmetrically placed near the surface of a 30 cm diameter spherical cavity in the graphite thermal column of the 20 MW Research Reactor at the National Institute of Standards and Technology (NIST). The ^{235}U disks provide a neutron source with fission spectrum, and an inner spherical shell of ^{10}B (14.4 cm outside diameter and 1.29 cm thick) provides a 1/v absorber to remove the lower energy part of the moderated spectrum of neutrons. Samples to be irradiated are placed near the center of the ^{10}B shell. A scheme of the facility is shown in the upper view of **Fig. 3.3.1**.

The neutron spectrum shape in this system can be calculated with comparatively good accuracy because of the spherical symmetry of system and the use of materials whose nuclear cross sections are among the best known. The simplicity of one dimensional calculation permits detailed investigation of spectrum and cross–section sensitivity to uncertainties in physical and nuclear parameters of the system and spectrum perturbation due to extraneous material required for fabrication. The lower view of **Fig. 3.3.1** shows the ISNF spectrum together with the starting fission spectrum and the spectrum obtained without the ^{10}B shell. The median energy of the spectrum is about 0.58 MeV, with 98 % of the neutron fluence between 1.2 keV and 5.6 MeV. The low energy tail below 10 keV is calculable with an accuracy better than 5 %. The full flux covariance matrix as listed in **Table 3.3.1** is available, which was calculated through the ORNL FORSS sensitivity system along with cross section covariance matrices generated from ENDF/B–IV uncertainty files. The ISNF neutron spectrum uncertainty with respect to cross sections is dominated by uncertainties in the fission spectrum assuming a 2 % uncertainty in the effective neutron temperature of the Maxwell distribution.

For the present integral test of the JENDL Dosimtry File, the following spectrum–averaged cross sections measured in the ISNF were used; ^{23}Na(n, γ)^{24}Na, ^{45}Sc(n, γ)^{46}Sc, ^{59}Co(n, γ)^{60}Co, ^{197}Au(n, γ)^{198}Au and ^{115}In(n, n')^{115m}In. The uncertainties of these measured cross sections consist of two parts; one is from the measured fluence at the center of the ISNF and the other from the activation measurement. The total uncertainty of fluence measurement is 2.3 % common to all the data, which was determined by fluence transfer from a calibrated ^{252}Cf neutron source. The uncertainties of activation measurements are between 1.8 and 6.2 %. Since, except the ^{115}In(n, n')^{115m}In reaction, they are resonant

reactions, the dominant uncertainties are caused by some corrections of self-absorption effects and energy-dependent fluence gradient.

3.3.3 CFRMF[28),56),57),58),59)]

The Coupled Fast Reactivity Measurements Facility (CFRMF) located at the Idaho National Engineering Laboratory (INEL) is a zoned-core critical assembly with a fast neutron spectrum zone in the center. The central zone is a water-moderated thermal 'driver' using an enriched ^{235}U fuel. The core is contained in a large pool about 4.5 m beneath the surface. **Figure 3.3.2** shows a schematic view of the CFRMF. Fuel elements in the thermal driver zone are conventional plate type ones of enriched ($\sim$93 %) ^{235}U in aluminum clad. The fueled portion of the core is 60.96 cm long, and each element is 8.183 cm square. The central fast neutron zone is constructed of materials for keeping the zone water-free and filtering or tailoring the neutron energy spectrum. This filter consists primarily of a large depleted-uranium block clad externally with stainless steel and Boral. It also has a 5.295 cm diameter axial experimental hole lined with stainless steel clad coaxial cylinders of ^{10}B and ^{235}U, in which specimens are placed and positioned at the core midplane of the assembly.

The neutron spectrum of the central zone is spanned over the intermediate neutron energy range, where 95 % of the neutrons are between 4 keV and 4 MeV and the median neutron energy is about 370 keV. The characterization of the central spectrum shape is established by means of an extensive program of spectrum measurements and neutronics calculations using transport, Monte Carlo and resonance theory codes. The measurement by the proton-recoil spectrometry defined the differential spectrum to $\pm$ 5 % over the energy region from 10 keV to 1.0 MeV. The agreement among the calculated neutron spectra is reasonably good considering the difficulty of preparing a suitable calculational model for the complex assembly of CFRMF. **Figure 3.3.3** shows a typical example of the calculated central neutron spectrum of the CFRMF in a one-dimensional cylindrical model. For this central neutron spectrum, a flux covariance matrix related to uncertainties and correlations in the nuclear data is also available, which was obtained from the sensitivity analysis code systems, AMPX and FORSS, with the cross section covariance data file of ENDF/B-V and the fission spectrum covariances based on a Watt fission spectrum. **Table 3.3.2** lists the 26 grouped central relative flux per unit lethargy with the relative standard deviations and the 26 $\times$ 26 group correlation matrix.

The spectrum-averaged cross sections of 22 reactions in the CFRMF were taken from Ref. 59 for the present integral test of the JENDL Dosimetry File. These data had been also used for integral test of the ENDF/B-V dosimetry cross sections, and some of them were obtained from the intercomparison study on the reaction rate measurements among several U.S. laboratories, which demonstrated that reaction rates would be able to be determined with an accuracy of $\sim\pm$2 % (1σ).

3.3.4 $\Sigma\Sigma$[30),60)]

The $\Sigma\Sigma$ facility at MOL is a thermal-fast coupled spherical source assembly located within a conventional graphite thermal column, which features a one-dimensional geometry composed of homogeneous material zones of known size and composition with reasonably well known cross sections. **Figure 3.3.4** shows a cross-sectional in-pile view of the facility. The spherical source shell of natural uranium metal, 24.5 cm o.d. $\times$ 5 cm thick, is embedded at the center of a 50 cm diameter spherical cavity in graphite with a support of an aluminum holder ring. It contains a 15 mm thick aluminum-clad spherical shell of vibrocompacted natural boron carbide and in turn surrounds the central fast-flux exposure void of 11 cm in diameter. The natural uranium shell acts as a thermal-fast converter, that is, the bulk of fission neutrons is created within the first outer centimeter of this source and undergoes energy degradation through inelastic and elastic scattering collisions in the system components. This uranium shell also absorbs essentially all high-energy graphite capture γ rays. The inner boron carbide shell is aimed at shaping the neutron low-energy tail.

The recommended neutron spectrum in the center of ΣΣ was evaluated from the interlaboratory neutron spectrometry measurements combined with a discrete-ordinate transport calculation using the ENDF/B-Ⅲ nuclear data file. **Figure 3.3.5** summarizes the intercomparison results of all the neutron spectrometry measurements. A ±5 % agreement is generally found from 0.02 up to 4 MeV between the various experimental spectra. **Figure 3.3.6** presents a comparison of the evaluated spectrometry results with various discrete-ordinate calculations. The discrepancies between the spectrometry measurements and the ENDF/B-Ⅲ calculation never exceed ±15 % above 3 keV and are interpretable in terms of nuclear data inaccuracy of the ΣΣ structural materials, while the tremendous deviations between the various calculations below 3 keV can be explained due to differences in self-shielding prescriptions and to differences in the ^{238}U nuclear data.

The spectrum-averaged cross sections of 15 reactions were selected from the recommended ΣΣ central reaction rate data, which were measured relatively to a specific ΣΣ thermal neutron flux monitoring scheme essentially based on the activation reactions ^{115}In(n, n')^{115m}In and ^{197}Au(n, γ)^{198}Au. The spectrum-averaged cross sections were derived by dividing the corresponding experimental result by the total fast neutron flux at the ΣΣ center for a unit available thermal neutron flux, which was given by transport calculation. This possible systematic bias in normalization by the transport calculation is not considered in the uncertainty estimation of the experimental data.

3.3.5 YAYOI[32),61),62),63)]

The YAYOI at Nuclear Engineering Research Laboratory (NERL), the University of Tokyo, is a 2 kW air cooled fast neutron source reactor with about 28 kg core fuel of 93 % enriched uranium metal. It can provide a variety of standard neutron fields by moving the core assembly in different surroundings such as heavy-concrete shields, a lead octagonal pile and bare of shield. As shown in **Fig. 3.3.7**, the core assembly consists of the core fuel, 10 cm blanket of depleted uranium and about 10 cm thick reflector of lead, which have many experimental holes. In particular, the 'Glory-hole' penetrating through the core center region is often used for various irradiation experiments because the neutron flux and spectra in the YAYOI core-center field have been well characterized through the detector intercomparison studies.

The core-center neutron spectrum of YAYOI can be expressed by a linear combination of two fixed spectrum modes; ϕ (u) = a • ϕ_i (u) + b • χ (u), where ϕ_i (u) is a spectrum mode after inelastic scatterings, 11.73 • $E^{1.82}$exp (−3.74E), and χ (u) is a spectrum mode of fission neutron source, 0.770 • $E^{1.50}$exp (−0.776E) in E (MeV). Experimental values of a and b were determined from the four kinds of fission-chamber countings (i.e. enriched and natural Uranium, Thorium-232 and Neptunium-237) by using the least squares. They were a/(a+b) = 0.432 and the value of total flux was a+b = 7.5 ± 0.5 × 10^{11}n/cm^2 • sec at 2 kW. **Figure 3.3.8** summarizes the results of neutron spectrum in the core center field of YAYOI from the parameter representation, the adjustment of multi-foil activation rates, the spectrometry of a Li-6 sandwitch counter and the calculation by the ANISN transport code[64)]. The uncertainties of the neutron spectrum are roughly estimated as ±10 % (1σ) between 0.1 and 10.0 MeV, and ±30 % (1σ) outside of this energy region at present.

The spectrum-averaged cross sections of 21 reactions were used for the present integral test of the JENDL Dosimetry File, which were derived from the reaction-rate data or the reaction-rate ratio data relative to ^{58}Ni(n, p) reaction measured in the YAYOI core center field. Some of these data and their uncertainties were justified through intercomparison studies on reaction-rate measurements among the four dosimetry groups in Japan from NERL of University of Tokyo, KURRI of Kyoto University, Japan Material Test Reactor (JMTR) at JAERI and JOYO at Power Reactor and Nuclear Fuel Corporation.

3.3.6 Results and Discussion

Comparisons between the experimental data and the calculated results on the spectrum averaged cross sections in the above fast reactor neutron fields were made including uncertainty estimation of the

ratio of calculated to experimental values (C/E). In this comparison, the calculated results are quoted from those given in Section 3.1, and therefore the covariance matrix of the neutron spectra is assumed so that all of the diagonal elements were 5 % uncertainties and all of the off-diagonal elements 2 %.

Tables 3.3.3 to **3.3.6** summarize the comparison results of the spectrum averaged cross sections in the ISNF, CFRMF, ΣΣ and YAYOI fields, respectively. In the last column of each table, the degree of the discrepancy between the experimental and the calculational results is indicated by the number of asterisks corresponding to how many σ's of the predicted standard deviation the (C/E−1.0) exceeds.

In the ISNF results, the trend of C/E ratios for the JENDL dosimetry cross sections resembles that for the ENDF/B-V as given in Ref.53. The systematic C/E overestimation of non-threshold reactions, except the ^{197}Au(n, γ) reaction, might be due to insufficient correction of self-shielding effects for the experimental data.

In the CFRMF results, a large discrepancy is found on the C/E ratio of the ^{58}Fe(n, γ) reaction, for which some overestimation is pointed out on the off-resonance cross section values in the energy region from several tenth eV to a few hundred keV.

As for the ΣΣ and YAYOI results, there are two common trends on the C/E ratios; one is the systematic discrepancy for the high threshold energy reactions and the other is the large underestimation for the exothermic reactions. These trends are considered mainly due to larger uncertainties of the neutron spectrum data used here than those assumed in the higher energy region about several MeV and also in the thermal/epithermal energy region. There is also a problem of correction of the self-absorption effects for the exothermic reaction. It should be noted that the systematic error can be easily included in the experimental data through a normalization procedure from the relative reaction rate data to the absolute value of spectrum averaged cross sections. It is reasonable, therefore, to suspend critical judgement on the results of the C/E ratio showing larger deviation than 3 σs here because their cross sections are not sensitive in the well-characterized energy region of the ΣΣ and YAYOI neutron spectra.

Table 3.3.1 NBS-ISNF flux correlation matrix ($\times 10^{-3}$)

GROUP BOUNDARY (eV)	% REL. ST. DEV.														
0.1733D 08	4.9708	1000													
0.3679D 07	2.7889	998	1000												
0.2725D 07	0.8846	963	959	1000											
0.1353D 07	0.4448	−802	−803	−631	1000										
0.6721D 06	0.7631	−920	−920	−815	965	1000									
0.4979D 06	0.9410	−937	−936	−849	923	995	1000								
0.4076D 06	1.0862	−937	−936	−855	892	978	997	1000							
0.3020D 06	1.1805	−947	−946	−872	889	978	991	994	1000						
0.2237D 06	1.2182	−933	−932	−860	893	968	981	983	994	1000					
0.6738D 05	1.1844	−854	−854	−780	844	899	904	901	928	955	1000				
0.3183D 05	1.0941	−821	−820	−740	841	892	894	890	912	951	965	1000			
0.1503D 05	1.0046	−673	−672	−593	749	785	780	774	797	836	852	884	1000		
0.1234D 04	0.9156	−586	−585	−504	698	730	720	722	729	774	753	798	815	1000	
0.1670D 03	0.8426	−475	−474	−399	627	644	641	641	639	700	680	734	791	991	1000
0.1371D 02															
0.1000D−03															

Table 3.3.2 CFRMF central relative flux per unit lethargy with relative standard deviations and correlation matrix due to cross section uncerainties

Group Index	Upper Energy Boundary (eV)	Central Relative Flux	Relative Standard Deviation (%)
1	1.7330+07	0.6684−03	12.59
2	1.0000+07	0.1097 01	8.63
3	6.0633+06	0.5029−01	8.50
4	3.6788+06	0.1065+00	8.14
5	2.2313+06	0.1424+00	6.84
6	1.3534+06	0.2197+00	3.67
7	8.2085+05	0.3272+00	2.47
8	4.9787+05	0.3149+00	2.39
9	3.0197+05	0.2493+00	2.52
10	1.8316+05	0.1801+00	5.09
11	1.1109+05	0.1283+00	4.17
12	6.7380−04	0.8945 01	4.37
13	4.0868+04	0.5201 01	5.15
14	2.4788+04	0.3529 01	3.89
15	1.5034+04	0.2341 01	3.53
16	9.1188+03	0.1619 01	3.53
17	5.5308+03	0.1403 01	3.02
18	3.3546+03	0.1008 01	2.89
19	2.0347+03	0.8847 02	2.68
20	1.2341+03	0.8104 02	2.97
21	7.4852+02	0.5149−02	2.95
22	4.5400+02	0.3193−02	2.88
23	2.7536+02	0.2358−02	3.10
24	1.6702+02	0.5474−03	2.98
25	1.0130+02	0.8697−03	4.00
26	6.1442+01	0.1644−05	3.14

Lowest Energy Boundary
1.0000 3

Energy Group	1	2	3	4	5	6	7	8	9	10	11	12	13
1	1.00	0.56	0.29	0.14	0.08	0.06	−0.05	0.07	−0.10	−0.07	−0.10	−0.09	−0.10
2	0.56	1.00	0.91	0.83	0.79	0.73	−0.53	−0.72	0.79	−0.41	−0.48	0.42	0.35
3	0.29	0.91	1.00	0.98	0.97	0.90	−0.64	−0.88	−0.96	0.49	−0.56	−0.48	−0.39
4	0.14	0.83	0.98	1.00	1.00	0.94	0.66	−0.91	−0.98	−0.51	0.57	−0.48	−0.39
5	0.08	0.79	0.97	1.00	1.00	0.95	−0.66	0.91	−0.99	−0.51	−0.57	0.48	−0.38
6	0.06	0.73	0.90	0.94	0.95	1.00	−0.45	0.79	−0.93	−0.61	−0.73	0.54	−0.40
7	−0.05	−0.53	0.64	0.66	0.66	−0.45	1.00	0.88	0.68	0.05	−0.18	0.06	0.14
8	−0.07	−0.72	−0.88	−0.91	−0.91	0.79	0.88	1.00	0.93	0.25	0.23	0.33	0.32
9	−0.10	−0.79	−0.96	−0.98	−0.99	−0.93	0.68	0.93	1.00	0.44	0.51	0.50	0.41
10	−0.07	0.41	0.49	0.51	−0.51	−0.61	−0.05	0.25	0.44	1.00	0.90	−0.10	−0.34
11	−0.10	0.48	−0.56	0.57	−0.57	−0.73	−0.18	0.23	0.51	0.90	1.00	0.32	0.06
12	−0.09	−0.42	0.48	−0.48	0.48	−0.54	0.06	0.33	0.50	−0.10	0.32	1.00	0.94
13	−0.10	−0.35	−0.39	−0.39	−0.38	0.40	0.14	0.32	0.41	0.34	0.06	0.94	1.00
14	0.17	−0.42	−0.44	−0.43	−0.42	−0.43	0.20	0.36	0.44	−0.30	0.06	0.85	0.95
15	−0.21	0.46	−0.47	0.45	−0.43	−0.43	0.25	0.38	0.42	−0.11	0.10	0.55	0.66
16	−0.22	−0.46	−0.46	0.44	−0.43	−0.41	0.26	0.37	0.40	0.02	0.14	0.34	0.45
17	−0.27	0.54	0.54	0.51	−0.50	−0.48	0.31	0.43	0.46	0.13	0.21	0.31	0.38
18	−0.28	−0.57	−0.56	−0.53	0.51	−0.50	0.32	0.45	0.49	0.21	0.28	0.32	0.28
19	0.31	−0.61	−0.61	−0.57	−0.55	−0.54	0.35	0.48	0.53	0.23	0.30	0.33	0.29
20	−0.28	0.55	0.54	0.51	−0.50	−0.48	0.31	0.43	0.47	0.21	0.27	0.29	0.25
21	−0.28	0.66	−0.55	0.52	−0.50	−0.48	0.32	0.43	0.47	0.21	0.27	0.29	0.26
22	−0.29	−0.57	0.56	−0.53	−0.51	−0.50	0.32	0.44	0.48	0.22	0.28	0.30	0.26
23	0.27	−0.53	−0.52	−0.49	−0.48	0.46	0.30	0.41	0.45	0.20	0.26	0.28	0.24
24	−0.29	0.55	−0.54	0.51	−0.49	−0.48	0.31	0.43	0.46	0.21	0.27	0.29	0.25
25	−0.22	−0.41	−0.41	−0.38	−0.37	−0.36	0.22	0.31	0.34	0.15	0.19	0.21	0.19
26	0.28	−0.53	−0.52	−0.48	−0.47	0.45	0.29	0.40	0.44	0.20	0.25	0.27	0.24
	14	15	16	17	18	19	20	21	22	23	24	25	26
1	−0.17	−0.21	−0.22	−0.27	−0.28	−0.31	−0.28	−0.28	−0.29	−0.27	−0.29	−0.22	−0.28
2	0.42	−0.46	−0.46	−0.54	−0.57	0.61	−0.55	−0.56	−0.57	0.53	−0.55	−0.41	−0.53
3	−0.44	0.47	−0.46	−0.54	−0.56	−0.61	0.54	−0.55	−0.56	−0.52	−0.54	0.41	−0.52
4	−0.43	−0.45	−0.44	−0.51	0.53	−0.57	−0.51	−0.52	−0.53	−0.49	−0.51	−0.38	−0.48
5	−0.42	−0.43	−0.43	−0.50	−0.51	0.55	−0.50	−0.50	−0.51	0.48	−0.49	−0.37	−0.47
6	0.43	−0.43	−0.41	−0.48	−0.50	−0.54	−0.48	−0.48	0.50	−0.46	−0.48	−0.36	−0.45
7	0.20	0.25	0.26	0.31	0.32	0.35	0.31	0.32	0.32	0.30	0.31	0.22	0.29
8	0.36	0.38	0.37	0.43	0.45	0.48	0.43	0.43	0.44	0.41	0.43	0.31	0.40
9	0.44	0.42	0.40	0.46	0.49	0.53	0.47	0.47	0.48	0.45	0.46	0.34	0.44
10	−0.30	0.11	0.02	0.13	0.21	0.23	0.21	0.21	0.22	0.20	0.21	0.15	0.20
11	0.06	0.10	0.14	0.21	0.28	0.30	0.27	0.27	0.28	0.26	0.27	0.19	0.25
12	0.85	0.55	0.34	0.31	0.32	0.33	0.29	0.29	0.30	0.28	0.29	0.21	0.27
13	0.95	0.66	0.45	0.38	0.28	0.29	0.25	0.26	0.26	0.24	0.25	0.19	0.24
14	1.00	0.85	0.63	0.53	0.32	0.34	0.30	0.30	0.31	0.29	0.30	0.22	0.28
15	0.85	1.00	0.86	0.72	0.31	0.34	0.30	0.31	0.32	0.30	0.31	0.23	0.29
16	0.63	0.86	1.00	0.91	0.32	0.33	0.30	0.30	0.31	0.29	0.30	0.22	0.29
17	0.53	0.72	0.91	1.00	0.57	0.56	0.53	0.52	0.53	0.51	0.52	0.45	0.49
18	0.32	0.31	0.32	0.57	1.00	0.99	0.98	0.95	0.94	0.94	0.93	0.94	0.88
19	0.34	0.34	0.33	0.56	0.99	1.00	0.99	0.96	0.94	0.94	0.94	0.93	0.89
20	0.30	0.30	0.30	0.53	0.98	0.99	1.00	0.99	0.97	0.98	0.97	0.97	0.91
21	0.30	0.31	0.30	0.52	0.95	0.96	0.99	1.00	1.00	1.00	0.99	0.97	0.92
22	0.31	0.32	0.31	0.53	0.94	0.94	0.97	1.00	1.00	1.00	0.99	0.96	0.93
23	0.29	0.30	0.29	0.51	0.94	0.94	0.98	1.00	1.00	1.00	1.00	0.98	0.93
24	0.30	0.31	0.30	0.52	0.93	0.94	0.97	0.99	0.99	1.00	1.00	0.97	0.94
25	0.22	0.23	0.22	0.45	0.94	0.93	0.97	0.97	0.96	0.98	0.97	1.00	0.92
26	0.28	0.29	0.29	0.49	0.88	0.89	0.91	0.92	0.93	0.93	0.94	0.92	1.00

Table 3.3.3 Comparison results of the spectrum averaged cross sections in the ISNF.

Reaction	Exp. [mb] (err.%)	Cal. [mb] (err.%)	C/E (err.%)	Judge. of Deviation (#)
Na-23 (n, γ) Na-24	1.57 (6.4)	1.755 (9.67)	1.12 (11.6)	*
Sc-45 (n, γ) Sc-46	24.4 (3.3)	29.35 (2.67)	1.20 (4.2)	* * * *
Co-59 (n, γ) Co-60	36.3 (4.1)	41.97 (2.76)	1.16 (4.9)	* * *
In-115 (n, n') In-115m	97.0 (2.6)	87.24 (3.05)	0.90 (4.0)	* *
Au-197 (n, γ) Au-198	411. (2.7)	385.3 (5.29)	0.94 (5.9)	*

(#) The number of '*' shows how many σ's of the predicted standard deviation the (C/E-1.0) exceeds.

Table 3.3.4 Comparison results of the spectrum averaged cross sections in the CFRMF.

Reaction	Exp. [mb] (err.%)	Cal. [mb] (err.%)	C/E (err.%)	Judge. of Deviation (#)
Li-6 α-production	954.5 (2.7)	939.7 (2.49)	0.98 (3.7)	
B-10 α-production	1876. (2.8)	1717. (2.18)	0.92 (3.5)	* *
Al-27 (n, p) Mg-27	0.863 (3.4)	0.949 (6.11)	1.10 (7.0)	*
Al-27 (n, α) Na-24	0.1596 (3.0)	0.169 (6.00)	1.06 (6.7)	
Sc-45 (n, γ) Sc-46	23.2 (3.3)	26.61 (2.67)	1.15 (4.2)	* * *
Ti-46 (n, p) Sc-46	2.58 (3.4)	2.474 (12.8)	0.96 (13.2)	
Ti-47 (n, p) Sc-47	4.12 (4.8)	4.517 (11.4)	1.10 (12.4)	
Ti-48 (n, p) Sc-48	0.068 (4.1)	0.067 (10.6)	0.99 (11.4)	
Fe-54 (n, p) Mn-54	17.2 (2.9)	17.71 (4.07)	1.03 (5.0)	
Fe-58 (n, γ) Fe-59	6.04 (3.1)	10.67 (8.17)	1.77 (8.7)	* * * * * * * *
Co-59 (n, γ) Co-60	90.4 (3.6)	87.88 (3.22)	0.97 (4.8)	
Ni-58 (n, p) Co-58	25.6 (3.1)	24.02 (6.82)	0.94 (7.5)	
Cu-63 (n, γ) Cu-64	43.3 (6.2)	38.71 (6.63)	0.89 (9.1)	*
In-115 (n, n') In-115m	50.6 (3.9)	51.54 (3.02)	1.02 (4.9)	
Au-197 (n, γ) Au-198	419. (2.9)	388.2 (4.44)	0.93 (5.3)	*
Th-232 (n, f)	19.6 (5.2)	19.56 (5.52)	1.00 (7.6)	
Th-232 (n, γ) Th-233	290. (3.8)	250.3 (10.9)	0.86 (11.5)	*
U-235 (n, f)	1537. (3.1)	1569. (2.82)	1.02 (4.2)	
U-238 (n, f)	75.1 (3.3)	78.05 (3.04)	1.04 (4.5)	
U-238 (n, γ) U-239	217. (3.7)	227.1 (4.13)	1.05 (5.5)	
Np-237 (n, f)	548. (3.3)	572.1 (9.82)	1.04 (10.4)	
Pu-239 (n, f)	1792. (2.2)	1768. (3.17)	0.99 (3.9)	

(#) The number of '*' shows how many σ's of the predicted standard deviation the (C/E - 1.0) exceeds.

Table 3.3.5 Comparison results of the spectrum averaged cross sections in the ΣΣ.

Reaction	Exp. [mb] (err.%)	Cal. [mb] (err.%)	C/E (err.%)	Judge. of Deviation (#)
Al-27 (n, p) Mg-27	1.033(10.0)	0.871 (6.14)	0.84 (11.7)	*
Al-27 (n, α) Na-24	0.182 (3.0)	0.147 (6.04)	0.81 (6.7)	**
Mn-55 (n, γ) Mn-56	39.7 (3.0)	25.18 (4.45)	0.63 (5.4)	******
Fe-56 (n, p) Mn-56	0.273 (3.0)	0.225 (5.00)	0.82 (5.8)	***
Ni-58 (n, p) Co-58	28.8 (2.5)	23.79 (6.99)	0.83 (7.4)	**
Cu-63 (n, γ) Cu-64	40.0 (5.0)	31.13 (8.06)	0.78 (9.5)	**
In-115 (n, n') In-115m	58.6 (2.0)	54.66 (3.03)	0.93 (3.6)	*
In-115 (n, γ) In-116m	261. (3.5)	301.4 (4.38)	1.15 (5.6)	**
Au-197 (n, γ) Au-198	442. (2.0)	324.5 (4.19)	0.73 (4.6)	*****
Th-232 (n, f)	21.6 (6.0)	20.60 (5.58)	0.98 (8.2)	
U-235 (n, f)	1589. (3.5)	1493. (2.81)	0.94 (4.5)	*
U-238 (n, f)	87.4 (3.5)	83.03 (3.07)	0.95 (4.7)	*
U-238 (n, γ) U-239	194. (4.0)	202.9 (4.25)	1.05 (5.8)	
Np-237 (n, f)	634. (3.5)	600.3 (9.88)	0.95 (10.5)	
Pu-239 (n, f)	1875. (3.5)	1733. (3.14)	0.92 (4.7)	*

(#) The number of '*' shows how many σ's of the predicted standard deviation the (C/E − 1.0) exceeds.

Table 3.3.6 Comparison results of the spectrum averaged cross sections in the YAYOI.

Reaction	Exp. [mb] (err.%)	Cal. [mb] (err.%)	C/E (err.%)	Judge. of Deviation (#)
Li-7 t-production	10.54 (8.0)	11.02 (4.76)	1.05 (9.3)	
Na-23 (n, γ) Na-24	0.419 (7.8)	0.306 (9.97)	0.73 (12.7)	＊＊
Mg-24 (n, p) Na-24	0.802 (7.7)	1.053 (4.65)	1.31 (9.0)	＊＊＊
Al-27 (n, p) Mg-27	2.14 (11.0)	2.394 (6.12)	1.12 (12.6)	
Al-27 (n, α) Na-24	0.376 (7.7)	0.463 (5.80)	1.23 (9.6)	＊＊
Ti-46 (n, p) Sc-46	6.90 (9.7)	6.251 (12.76)	0.91 (16.0)	
Ti-47 (n, p) Sc-47	11.8 (13.5)	11.15 (11.40)	0.94 (17.7)	
Ti-48 (n, p) Sc-48	0.155 (8.1)	0.183 (10.52)	1.18 (13.3)	＊
Mn-55 (n, γ) Mn-56	4.61 (7.6)	4.311 (7.62)	0.94 (10.8)	
Fe-56 (n, p) Mn-56	0.579 (7.6)	0.650 (4.88)	1.12 (9.0)	＊
Co-59 (n, α) Mn-56	0.0813 (7.9)	0.107 (4.69)	1.32 (9.2)	＊＊＊
Ni-58 (n, 2n) Ni-57	0.00303 (4.7)	0.00505 (11.1)	1.67 (12.1)	＊＊＊＊＊
Ni-58 (n, p) Co-58	57.9 (7.1)	60.05 (6.86)	1.04 (9.9)	
Cu-63 (n, 2n) Cu-62	0.0658 (13.8)	0.114 (2.62)	1.73 (14.0)	＊＊＊＊＊
Cu-63 (n, α) Co-60	0.275 (7.0)	0.329 (5.78)	1.20 (9.1)	＊＊
Zr-90 (n, 2n) Zr-89	0.130 (6.6)	0.126 (3.01)	0.97 (7.3)	
Nb-93 (n, 2n) Nb-92m	0.244 (6.5)	0.386 (4.27)	1.58 (7.8)	＊＊＊＊＊＊＊
In-115 (n, n') In-115m	116.4 (8.1)	117.4 (3.03)	1.01 (8.6)	
W-186 (n, γ) W-187	62.8 (8.6)	47.85 (5.17)	0.76 (10.0)	＊＊
Au-197 (n, γ) Au-198	155.9 (8.1)	118.8 (5.27)	0.76 (9.7)	＊＊
Th-232 (n, f)	45.9 (5.0)	47.71 (5.52)	1.04 (7.4)	
U-238 (n, f)	172.7 (5.1)	189.1 (3.00)	1.09 (5.9)	＊

(#) The number of '＊' shows how many σ's of the predicted standard deviation the (C/E − 1.0) exceeds.

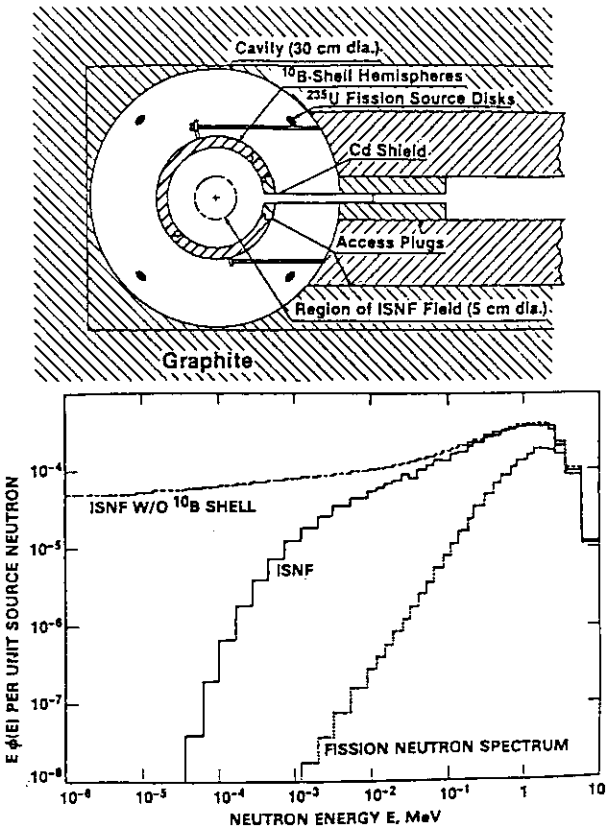

Fig. 3.3.1 Upper view: The ISNF located within a 30 cm diameter cavity in the thermal column of the NIST reactor.

Lower view: Comparison of ^{235}U fission spectrum to the ISNF spectra with and without the ^{10}B filter.

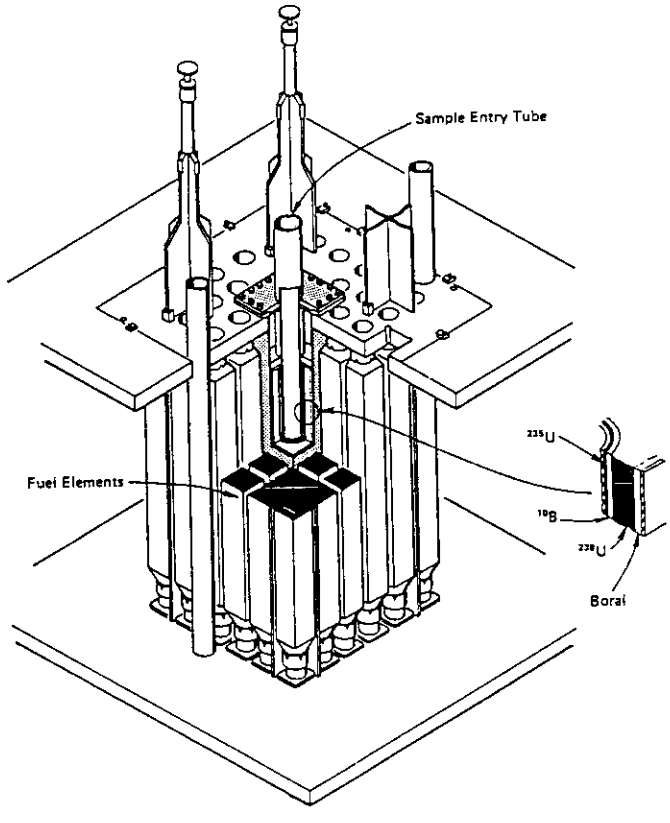

Fig. 3.3.2 Cutaway pictorial diagram showing the general assembly of the CFRMF.

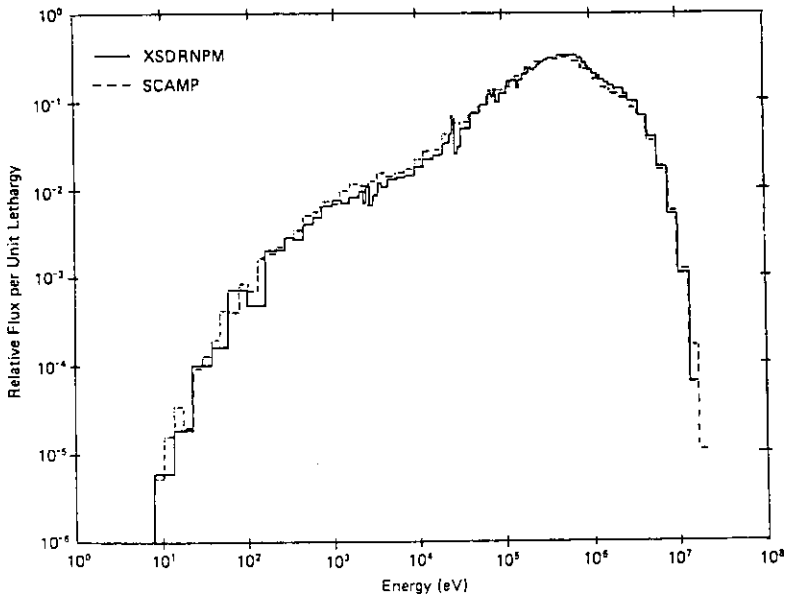

Fig. 3.3.3 Typical calculated CFRMF central flux spectra. Differences between two spectra show the uncertainty of CFRMF spectrum.

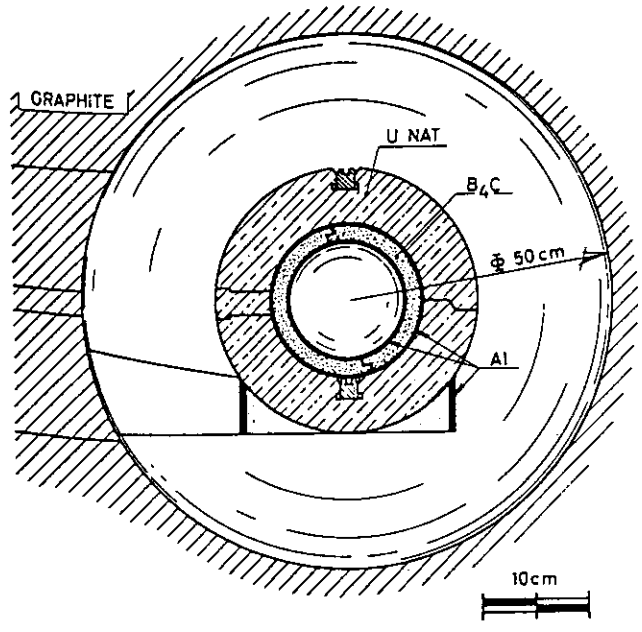

Fig. 3.3.4 Cross sectional in-pile view of the ΣΣ facility.

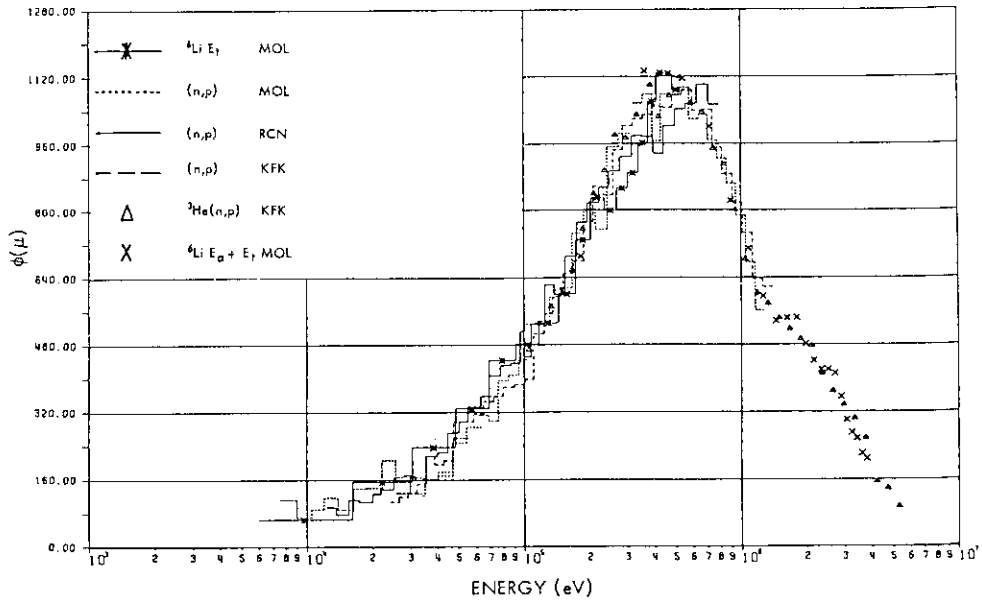

Fig. 3.3.5 ΣΣ central neutron spectral characterization by interlaboratory spectrometry measurements.

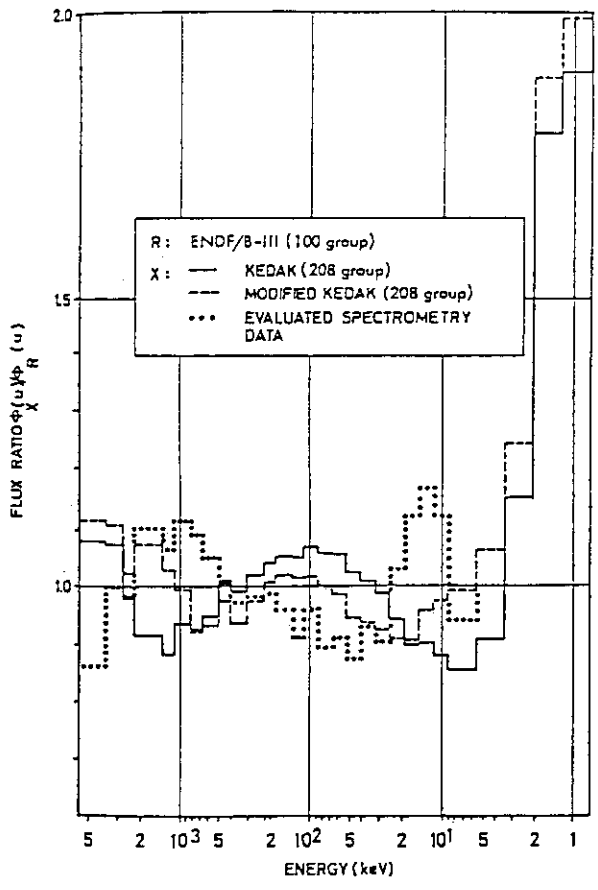

Fig. 3.3.6 Comparison of discrete-ordinate transport calculations and evaluated spectrometry measurements of the ΣΣ central neutron spectrum. (all data are collapsed in a similar multigroup structure and ratios are calculated relatively to the ENDF /B-Ⅲ, S_{16}-P_3, 100-group calculation)

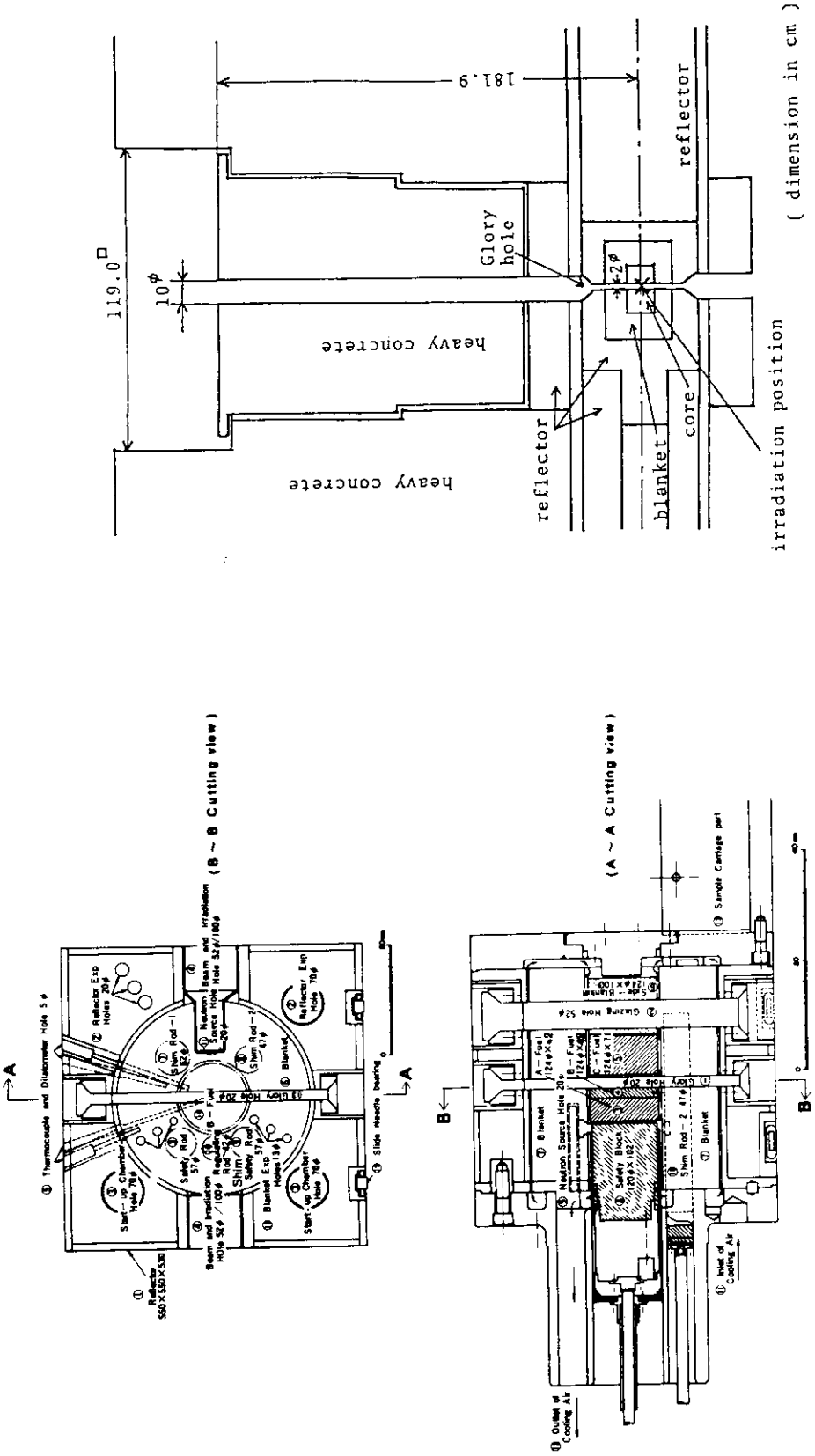

Fig. 3.3.7 Configuration of the YAYOI core assembly and Glory hole penetration.

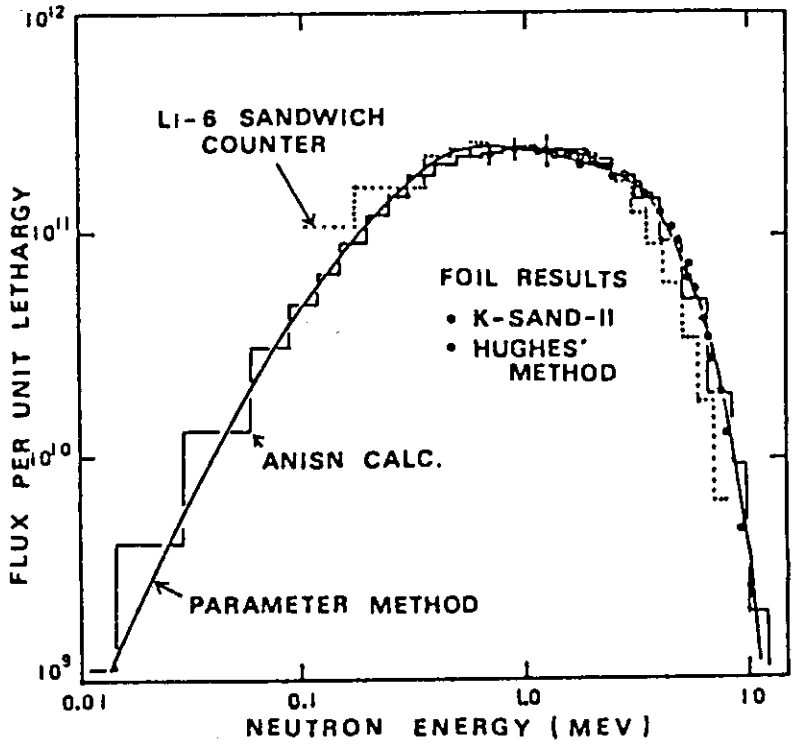

Fig. 3.3.8 Neutron spectrum in the core–center field of YAYOI.

4. Integral Tests for Fusion Reactors

4.1 Integral Test in DT Fusion Neutron Environment

Some important reaction cross sections in the JENDL Dosimetry File for the fusion dosimetry application have been tested by using experimental data of reaction rates of interest in D–T neutron fields which simulated D–T fusion environment. The test was carried out by comparing the reaction rates calculated from the neutron spectra and cross sections in the JENDL Dosimetry File with experimental values. Also the test using IRDF–85 was performed for comparison. In this section, results of the test are described in some details.

4.1.1 Neutron Fields Used in the Tests

Two neutron spectra at positions in the Phase–IIB experimental assembly of the JAERI/USDOE collaborative program on fusion neutronics[65,66] were chosen as the neutron fields for the present integral test. The experiment was carried out at FNS[67] at JAERI. The cross sectional view of the experimental configuration is given in **Fig. 4.1.1**. The D–T neutron source and a Li_2O region are enclosed with 200 mm thick Li_2CO_3 covered with 50 mm thick polyethylene insulator. The Li_2O zone is called as testing region, dimension of which is 850 mm × 850 mm × 600 mm. Additional 50 mm thick beryllium (Be) layer is lined inside the cavity of enclosure. This system was used for experiments investigating Be multiplication effects on the neutronics characteristics. As a part of the experiments, multiple reaction rates were measured at positions of #1 and #2, which are shown in the **Fig. 4.1.1**: the position #1 was located at the boundary between the Be and Li_2O regions, and the position #2 was at the 400 mm depth in the Li_2O region. Since almost all of the reactions measured were included in the JENDL Dosimetry File, these experimental data were employed in the present test.

Neutron spectra at the positions #1 and #2 used in the test were calculated by DOT3.5[68] with the JENDL–3PR2[69] nuclear data library. The spectra are shown in **Fig. 4.1.2**. In the spectrum at the position #1, the fractions of neutron flux integrated above 10 MeV to those above 1.0 MeV and 5.0 MeV were 36% and 77%, respectively. Thus, this spectrum was considered appropriate for the test of cross sections around 14 MeV for the reactions with threshold energies around 5 MeV. At the position #2, they were 22% and 58%, respectively. This indicated that the weight of low energy component below 10 MeV increased in comparison with that of the spectrum at the position #1. In particular, the spectrum at the position #2 had an important role in the test for the low threshold reactions because the contribution of 14 MeV flux to the total reaction rate was reasonably expected to be lower than 10%. The digital data of the spectra with a 125 neutron group structure are given in **Table 4.1.1**.

4.1.2 Criteria of the Test

Class A: For the cross sections, reaction rates of which agree with experiments within ±5% are assigned to be in Class A indicating the cross sections are good. This criterion is considered reasonable because almost all experimental errors are within ±5%.

Class B: If the discrepancy between the calculated and measured reaction rates is in the range from 5% to 10%, we assign the cross sections as Class B which indicates necessity of further examination of the cross sections.

Class C: When the difference of the calculated reaction rate from the experiment is larger than ± 10%, the cross sections are assinged to be Class C which clearly indicates unreasonable evaluation of the cross sections. The cross sections in Class C should be reevaluated with

high priority.

4.1.3 Results of the Integral Test

The results of the integral test are summarized in **Tables 4.1.2(a)** and **4.1.2(b)** for the Spectra #1 and #2, respectively. In the tables, the results for IRDF-85 are given for comparison. The tables show reactions, measured reaction rates and deviations of calculated reaction rates from measurements in percent. The integral test was carried out based on the deviations as the indices according to the criteria as specified before. **Figures 4.1.3(a)** and **4.1.3(b)** illustrate the deviations given in the tables.

1) *Comparison of JENDL Dosimetry File with IRDF-85*

In the following descriptions, the JENDL Dosimetry File and IRDF-85 are denoted as JENDL and IRDF for simplicity. As a whole, the standard deviations of the entire reaction rates in Spectrum #1 from the experiments for JENDL and IRDF are 7.9% and 9.1%, respectively, whereas in Spectrum #2 they are 5.6% and 7.2%, respectively. This result shows JENDL gives a better agreement than IRDF. **Figure 4.1.4** gives ratios of reaction rates calculated with JENDL to these with IRDF for both Spectra #1 and #2. The deviation between JENDL and IRDF for each reaction rate is clearly understood from this figure. Large differences of more than 10% are observed in the reactions of ^{58}Ni(n, 2n)^{57}Ni, ^{59}Co(n, α)^{56}Mn and Ti(n, x)^{47}Sc for Spectrum #1, reaction rates of which are higher in JENDL than those in IRDF. The ratios are decreased in Spectrum #2. This is mainly due to that the cross sections in JENDL are larger around 14 MeV than those in IRDF. On the other hand, JENDL in Spectrum #1 gives lower cross sections for the reactions of ^{64}Zn(n, p)^{64}Cu and ^{58}Ni(n, p)^{58}Co by 7 – 8% than IRDF does. This is due to the lower cross section values in JENDL than those in IRDF. A graphical comparison of the cross sections in JENDL and IRDF is given in Appendix.

2) *Discussion for Individual Reaction*

(1) ^{27}Al(n, α)^{24}Na

Both JENDL and IRDF underestimate the experiment by 6% (Class B) and about 3% (Class A) for Spectra #1 and #2, respectively. The range of the discrepancies seems reasonably small by taking both errors in the experiment and spectra used. As long as the present test is concerned, JENDL gives a satisfactory result by referring the criterion of the test. Though JENDL gives slightly lower values than IRDF, this difference could be negligibly small.

(2) ^{56}Fe(n, p)^{56}Mn

This reaction is also important as the standard. According to the criteria, JENDL belongs to Class A, giving reasonable agreement with the experiment within $\pm$4%.

(3) ^{54}Fe(n, p)^{54}Mn

JENDL and IRDF overestimate the experiment by 9% and 4%, respectively, in Spectrum #1. On the other hand, they underestimate it by 7% and 12%, respectively, in Spectrum #2. The experimental data for Spectrum #2 seems not to be appropriate for the test because of large experimental error of $\pm$10%. Considering that Spectrum #1 has much weight in the 14 MeV region, the rather large overestimation may be attributed to the overestimation in the cross section around 14 MeV. Nevertheless, verification of data over the whole energy range is recommended because this reaction has a low threshold energy around 1 MeV. In particular, it has been pointed out that large uncertainty exists in the cross section around several MeV region.

(4) ^{58}Ni(n, 2n)^{57}Ni

JENDL gives reasonably good agreements with the experiments belonging to Class A, whereas IRDF

largely underestimates the experiments by 17% and 5% in Spectra #1 and #2, respectively. Since the reaction has threshold energy at 12.4 MeV, the large discrepancies between JENDL and IRDF are definitely due to the difference in the cross section around 14 MeV in both libraries.

(5) ^{58}Ni(n, p)^{58}Co

The reaction rates derived by using JENDL agree well with the experiments in both Spectra, being assigned as Class A. Contrary to the case of the ^{58}Ni(n, 2n)^{57}Ni, IRDF–85 overestimates the experiments by 8% in Spectrum #1 and agrees well with the experiment in Spectrum #2. This difference in the deviations for IRDF between two Spectra is dominantly due to the overestimation in the cross section around 14 MeV.

(6) Ti(n, x)^{48}Sc

JENDL gives good results in Class A. This cross section is governed by the reaction cross section of ^{48}Ti(n, p)^{48}Sc because of small abundance of ^{49}Ti which contributes to the production rate of ^{48}Sc through the reaction of ^{49}Ti(n, np)^{48}Sc.

(7) Ti(n, x)^{47}Sc

A clear different tendency is found for the degree of discrepancy among JENDL and IRDF. For Spectrum #1, underestimation is found for JENDL by 4% (Class A) and for IRDF by 13% (Class C). On the other hand, for Spectrum #2, overestimation is found for JENDL by 12% (Class C) and for IRDF by 6% (Class B). The nuclide of ^{47}Sc is formed through two reactions of ^{47}Ti(n, p) and ^{48}Ti(n, np); the former reaction has the threshold energy of 0.7 MeV and cross sections gradually decrease around the 14 MeV energy region, and the latter reaction has the threshold energy of 11.7 MeV and very steep rise in the cross section around 14 MeV. Although the cross section at 14 MeV for ^{48}Ti(n, np) is one order of magnitude smaller than that for ^{47}Ti(n, p), it contributes very much to the ^{47}Sc production because of one order larger abundance of ^{48}Ti than that of ^{47}Ti in natural titanium. Thus, it is expected that the reaction rate is highly dependent on the neutron spectrum. In other words, if the spectrum has a peak around 14 MeV, the reaction cross section to produce ^{47}Sc is possibly influenced by the ^{48}Ti(n, np) reaction. Meanwhile, Mannhart[70] reported that the cross section for the ^{47}Ti(n, p)^{47}Sc reaction in several MeV energy region should be lower by around 20% than the value in ENDF/B–V, which is equivalent to that in IRDF–85. If this is true, the overestimation in Spectrum #2, where low energy neutrons largely contribute to the reaction rate, is reasonably understood. In the evaluation of JENDL, there still exists the same problem on this cross section. Reevaluation for the ^{47}Ti(n, p)^{47}Sc is highly recommended.

(8) Ti(n, x)^{46}Sc

JENDL overestimates the experiments by 7% and 3% for Spectra #1 and #2, respectively. The nuclide of ^{46}Sc is also formed through two different reactions of ^{46}Ti(n, p)^{46}Sc and ^{47}Ti(n, np)^{46}Sc with threshold energies of 3 MeV and 11.5 MeV, respectively. Abundances of ^{46}Ti and ^{47}Ti are 8.2 and 7.4%, respectively. The cross sections for these reactions at 14 MeV are 290 mb and 40 mb, respectively. Based on these data, the contribution of the ^{47}Ti(n, np) reaction to the total ^{46}Sc production is estimated to be less than 10%. Thus the problem of overestimation in JENDL, in particular in Spectrum #1, is attributable to the cross section of ^{46}Ti(n, p)^{46}Sc around 14 MeV. This reaction cross section should be reevaluated.

(9) ^{59}Co(n, 2n)^{58}Co

For this reaction with high threshold energy of 10.6 MeV, JENDL overestimates the experiments by 2% and 6% in Spectra #1 and #2, respectively, belonging to Class A and Class B. Although these are

considered fairly good results, the trend of the overestimation is contrary to the results of underestimation for the other high threshold energy reactions. Some further check on this cross section is recommended.

(10) $^{59}Co(n, \alpha)^{56}Mn$

For this reaction with an identical threshold energy around 3 MeV as $^{27}Al(n, \alpha)^{24}Na$ and $^{56}Fe(n, p)^{56}Mn$, JENDL gives very good results as Class A. However, IRDF underestimates the experiments by 9 and 5% in Spectra #1 and #2, respectively, being assigned to be Class B. It is considered that this cross section around 14 MeV is evaluated to be lower in IRDF.

4.1.4 Summary

In summary, as long as the reactions tested are concerned, the JENDL Dosimetry File gives reasonable results except for the $Ti(n, x)^{47}Sc$ and $Ti(n, x)^{46}Sc$ reactions. In particular, better agreements of calculations based on the JENDL Dosimetry File with the measurements are observed for the reactions of $^{58}Ni(n, 2n)^{57}Ni$, $^{58}Ni(n, p)^{58}Co$ and $^{59}Co(n, \alpha)^{56}Mn$ in comparison with those based on IRDF-85. These results assure the better reliability of the JENDL Dosimetry File in the D–T fusion dosimetry study.

Table 4.1.1 Neutron Flux Spectra at positions #1 and #2

No.	Energy boundary (MeV)	Flux(/Group)	
		Flux#1	Flux#2
1	1.00100E−11 − 3.22410E−07	7.19460E−06	3.22810E−18
2	3.22410E−07 − 5.31560E−07	1.54690E−06	1.19460E−16
3	5.31560E−07 − 8.76400E−07	1.76230E−06	1.93870E−15
4	8.76400E−07 − 1.44490E−06	1.98670E−06	2.62330E−14
5	1.44490E−06 − 2.38230E−06	2.22260E−06	2.84140E−13
6	2.38230E−06 − 3.92780E−06	2.46400E−06	2.52620E−12
7	3.92780E−06 − 6.47580E−06	2.71230E−06	1.80440E−11
8	6.47580E−06 − 1.06770E−05	2.96360E−06	1.04040E−10
9	1.06770E−05 − 1.76030E−05	3.21490E−06	4.86680E−10
10	1.76030E−05 − 2.90230E−05	3.46840E−06	1.88280E−09
11	2.90230E−05 − 4.78500E−05	3.71610E−06	6.11360E−09
12	4.78500E−05 − 7.88910E−05	3.96110E−06	1.65580E−08
13	7.88910E−05 − 1.30070E−04	4.19820E−06	3.84070E−08
14	1.30070E−04 − 2.14450E−04	4.42550E−06	7.77320E−08
15	2.14450E−04 − 3.53570E−04	4.63600E−06	1.39410E−07
16	3.53570E−04 − 5.82930E−04	4.85360E−06	2.24680E−07
17	5.82930E−04 − 9.61100E−04	5.06120E−06	3.31190E−07
18	9.61100E−04 − 1.23410E−03	2.58720E−06	2.20900E−07
19	1.23410E−03 − 1.58460E−03	2.74640E−06	2.56090E−07
20	1.58460E−03 − 2.03460E−03	2.79320E−06	2.89570E−07
21	2.03460E−03 − 2.61250E−03	2.88340E−06	3.23580E−07
22	2.61250E−03 − 3.35460E−03	2.97250E−06	3.56060E−07
23	3.35460E−03 − 4.30730E−03	3.01180E−06	3.85420E−07
24	4.30730E−03 − 5.53070E−03	3.00010E−06	4.12220E−07
25	5.53070E−03 − 7.10160E−03	2.97940E−06	4.35320E−07
26	7.10160E−03 − 9.11860E−03	2.90240E−06	4.56240E−07
27	9.11860E−03 − 1.17090E−02	3.13130E−06	4.86230E−07
28	1.17090E−02 − 1.50340E−02	3.28920E−06	5.06090E−07
29	1.50340E−02 − 1.93040E−02	2.97510E−06	5.09630E−07
30	1.93040E−02 − 2.18740E−02	1.56230E−06	2.66820E−07
31	2.18740E−02 − 2.47870E−02	1.67140E−06	2.68390E−07
32	2.47870E−02 − 2.80870E−02	2.26940E−06	2.85510E−07
33	2.80870E−02 − 3.18270E−02	1.16290E−06	2.39970E−07
34	3.18270E−02 − 3.60650E−02	1.61290E−06	2.68940E−07
35	3.60650E−02 − 4.08670E−02	1.67520E−06	2.71950E−07
36	4.08670E−02 − 4.63080E−02	1.75630E−06	2.73480E−07
37	4.63080E−02 − 5.24740E−02	1.83680E−06	2.73820E−07
38	5.24740E−02 − 5.94610E−02	1.77540E−06	2.70720E−07
39	5.94610E−02 − 6.73780E−02	1.83970E−06	2.71030E−07
40	6.73780E−02 − 7.63490E−02	1.84330E−06	2.68970E−07
41	7.63490E−02 − 8.65150E−02	1.97220E−06	2.67760E−07
42	8.65150E−02 − 9.80350E−02	1.93070E−06	2.63010E−07
43	9.80350E−02 − 1.11090E−01	1.83300E−06	2.57310E−07
44	1.11090E−01 − 1.25880E−01	1.98350E−06	2.54210E−07

Table 4.1.1 Continued

No.	Energy boundary (MeV)	Flux(/Group)	
		Flux#1	Flux#2
45	1.25880E−01 − 1.42640E−01	2.21530E−06	2.47400E−07
46	1.42640E−01 − 1.61630E−01	1.91380E−06	2.33080E−07
47	1.61630E−01 − 1.83150E−01	2.17750E−06	2.12580E−07
48	1.83150E−01 − 2.07540E−01	2.08510E−06	1.58900E−07
49	2.07540E−01 − 2.35170E−01	2.24440E−06	9.75540E−08
50	2.35170E−01 − 2.66490E−01	2.27550E−06	4.28480E−08
51	2.66490E−01 − 3.01970E−01	2.33880E−06	5.94520E−08
52	3.01970E−01 − 3.42170E−01	2.46760E−06	1.28500E−07
53	3.42170E−01 − 3.87740E−01	2.57050E−06	1.45650E−07
54	3.87740E−01 − 4.39360E−01	2.60880E−06	1.18210E−07
55	4.39360E−01 − 4.97860E−01	2.58070E−06	1.23830E−07
56	4.97860E−01 − 5.64150E−01	2.38840E−06	2.16890E−07
57	5.64150E−01 − 6.39270E−01	1.91510E−06	2.18110E−07
58	6.39270E−01 − 7.24380E−01	2.48450E−06	2.06510E−07
59	7.24380E−01 − 8.20840E−01	2.52060E−06	2.02150E−07
60	8.20840E−01 − 9.30130E−01	2.34690E−06	1.47310E−07
61	9.30130E−01 − 1.05400E+00	2.19070E−06	9.02450E−08
62	1.05400E+00 − 1.19430E+00	2.19480E−06	1.13160E−07
63	1.19430E+00 − 1.35330E+00	2.23870E−06	1.20420E−07
64	1.35330E+00 − 1.53350E+00	2.24540E−06	1.31440E−07
65	1.53350E+00 − 1.73770E+00	2.18460E−06	1.21370E−07
66	1.73770E+00 − 1.84980E+00	1.03490E−06	6.07020E−08
67	1.84980E+00 − 1.96910E+00	9.27680E−07	4.99850E−08
68	1.96910E+00 − 2.09610E+00	8.60080E−07	5.36270E−08
69	2.09610E+00 − 2.23130E+00	7.98680E−07	5.71740E−08
70	2.23130E+00 − 2.37520E+00	7.45510E−07	6.48950E−08
71	2.37520E+00 − 2.52840E+00	6.71060E−07	5.77250E−08
72	2.52840E+00 − 2.69140E+00	5.71320E−07	5.21270E−08
73	2.69140E+00 − 2.86500E+00	4.40750E−07	4.69680E−08
74	2.86500E+00 − 3.04980E+00	4.50560E−07	4.22020E−08
75	3.04980E+00 − 3.24650E+00	4.61650E−07	3.79810E−08
76	3.24650E+00 − 3.45590E+00	4.54360E−07	3.02560E−08
77	3.45590E+00 − 3.67870E+00	4.43270E−07	2.77870E−08
78	3.67870E+00 − 3.91600E+00	4.39380E−07	2.58620E−08
79	3.91600E+00 − 4.16860E+00	4.43480E−07	2.71280E−08
80	4.16860E+00 − 4.43740E+00	4.37830E−07	2.60200E−08
81	4.43740E+00 − 4.72360E+00	4.23830E−07	2.58580E−08
82	4.72360E+00 − 5.02820E+00	4.07910E−07	2.67830E−08
83	5.02820E+00 − 5.35250E+00	3.90960E−07	2.73140E−08
84	5.35250E+00 − 5.69780E+00	3.77290E−07	3.12150E−08
85	5.69780E+00 − 6.06520E+00	3.65330E−07	3.03060E−08
86	6.06520E+00 − 6.45640E+00	3.50550E−07	3.06620E−08
87	6.45640E+00 − 6.87280E+00	3.35560E−07	3.06120E−08
88	6.87280E+00 − 7.31610E+00	3.29990E−07	3.03150E−08

Table 4.1.1 Continued

No.	Energy boundary (MeV)	Flux(/Group)	
		Flux#1	Flux#2
89	7.31610E+00 – 7.78790E+00	3.20620E−07	2.94310E−08
90	7.78790E+00 – 8.29020E+00	3.43690E−07	3.00610E−08
91	8.29020E+00 – 8.82490E+00	4.20070E−07	2.94980E−08
92	8.82490E+00 – 9.39400E+00	4.89120E−07	2.88380E−08
93	9.39400E+00 – 9.99990E+00	4.71780E−07	2.82200E−08
94	9.99990E+00 – 1.01570E+01	1.00600E−07	6.90220E−09
95	1.01570E+01 – 1.03170E+01	9.71870E−08	6.95150E−09
96	1.03170E+01 – 1.04800E+01	9.77980E−08	7.29170E−09
97	1.04800E+01 – 1.06450E+01	1.02160E−07	7.67170E−09
98	1.06450E+01 – 1.08120E+01	1.09060E−07	8.14220E−09
99	1.08120E+01 – 1.09830E+01	1.18130E−07	8.46930E−09
100	1.09830E+01 – 1.11560E+01	1.25470E−07	8.38030E−09
101	1.11560E+01 – 1.13310E+01	1.29940E−07	8.63790E−09
102	1.13310E+01 – 1.15100E+01	1.29210E−07	9.29900E−09
103	1.15100E+01 – 1.16910E+01	1.18810E−07	9.75730E−09
104	1.16910E+01 – 1.18750E+01	1.01000E−07	1.05300E−08
105	1.18750E+01 – 1.20620E+01	8.05630E−08	1.15470E−08
106	1.20620E+01 – 1.22520E+01	6.85550E−08	1.29790E−08
107	1.22520E+01 – 1.24450E+01	6.03910E−08	1.41120E−08
108	1.24450E+01 – 1.26410E+01	5.56140E−08	1.55750E−08
109	1.26410E+01 – 1.28400E+01	4.80430E−08	1.73030E−08
110	1.28400E+01 – 1.30420E+01	3.99610E−08	1.89470E−08
111	1.30420E+01 – 1.32480E+01	3.64540E−08	2.14370E−08
112	1.32480E+01 – 1.34560E+01	5.02470E−08	2.34630E−08
113	1.34560E+01 – 1.36680E+01	6.99150E−08	2.55310E−08
114	1.36680E+01 – 1.38830E+01	9.44680E−08	2.72060E−08
115	1.38830E+01 – 1.41020E+01	6.85110E−08	2.97260E−08
116	1.41020E+01 – 1.43240E+01	7.36400E−08	3.22650E−08
117	1.43240E+01 – 1.45500E+01	3.60560E−07	3.56080E−08
118	1.45500E+01 – 1.47790E+01	2.79750E−06	3.74730E−08
119	1.47790E+01 – 1.50120E+01	4.86670E−06	2.92010E−08
120	1.50120E+01 – 1.52480E+01	2.67170E−06	1.39210E−08
121	1.52480E+01 – 1.54880E+01	1.70780E−06	6.02850E−09
122	1.54880E+01 – 1.57320E+01	0.00000E+00	0.00000E+00
123	1.57320E+01 – 1.59800E+01	0.00000E+00	0.00000E+00
124	1.59800E+01 – 1.62310E+01	0.00000E+00	0.00000E+00
125	1.62310E+01 – 1.64870E+01	0.00000E+00	0.00000E+00

Table 4.1.2(a) Results for test in Spctrum #1

Reaction	Expt.(Error)*	JENDL Dosimetry File			IRDF-85		
		Calc.	Deviation(%)	Status	Calc.	Deviation(%)	Status
^{27}Al (n, α) ^{24}Na	1.884e-30(3)	1.760e-31	-6.6	B	1.765e-30	-6.3	B
^{56}Fe (n, p) ^{56}Mn	1.641e-30(3)	1.625e-31	-1.0	A	6.878e-30	-4.9	A
^{54}Fe (n, p) ^{54}Mn	7.417e-30(4)	8.071e-30	8.8	B	7.698e-30	3.8	A
^{58}Ni (n, 2n) ^{57}Ni	5.540e-31(3)	5.303e-31	-4.3	A	4.617e-31	-16.7	C
^{58}Ni (n, p) ^{58}Co	8.693e-30(3)	8.735e-30	-0.5	A	9.367e-30	7.8	B
^{64}Zn (n, p) ^{64}Cu	3.582e-30(3)	3.531e-30	-1.4	A	3.843e-30	7.3	B
^{115}In (n, n') ^{115m}In	6.757e-30(3)	7.035e-30	4.1	A	6.878e-30	1.8	A
^{93}Nb (n, 2n) ^{92m}Nb	6.688e-30(3)	6.573e-30	-1.7	A	.....		
^{90}Zr (n, 2n) ^{89}Zr	1.117e-29(3)	1.122e-29	0.4	A	1.092e-29	-2.2	A
Ti (n, x) ^{48}Sc	9.003e-31(3)	8.873e-31	-1.4	A	8.513e-31	-5.4	B
Ti (n, x) ^{47}Sc	4.383e-31(4)	4.192e-31	-4.4	A	3.808e-31	-13.1	C
Ti (n, x) ^{46}Sc	2.781e-30(3)	2.971e-30	6.8	B	2.824e-30	1.5	A
^{59}Co (n, 2n) ^{58}Co	1.043e-29(3)	1.062e-29	1.8	A	1.064e-29	2.0	A
^{59}Co (n, α) ^{56}Mn	4.727e-31(3)	4.676e-31	-1.08	A	4.256e-31	-9.1	C

* Error in %.

Deviation (%) is given as [(Calc.-Expt.) /Expt.] .

Status follows the classifications presented in the text.

Table 4.1.2(b) Results for the test in Spectrum #2

Reaction	Expt.(Error)*	JENDL Dosimetry File			IRDF-85		
		Calc.	Deviation(%)	Status	Calc.	Deviation(%)	Status
^{27}Al (n, α) ^{24}Na	7.025e-32(4)	6.7893-32	-3.4	A	6.812e-32	-3.0	A
^{56}Fe (n, p) ^{56}Mn	6.531e-32(3)	6.270e-32	-4.0	A	6.096e-32	-6.7	B
^{54}Fe (n, p) ^{54}Mn	5.08e-31(10)	4.745e-31	-6.5	B	4.448e-31	-12.4	C
^{58}Ni (n, 2n) ^{57}Ni	8.00e-33 (5)	7.920e-33	-1.0	A	7.584e-33	-5.2	B
^{58}Ni (n, p) ^{58}Co	5.465e-31(3)	5.427e-31	-0.7	A	5.493e-31	0.5	A
^{64}Zn (n, p) ^{64}Cu	2.088e-31(4)	2.039e-31	-2.4	A	2.133e-31	2.1	A
^{115}In (n, n') ^{115m}In	4.942e-31(3)	4.851e-31	1.8	A	4.751e-31	-3.9	A
^{93}Nb (n, 2n) ^{92m}Nb	2.104e-31(3)	2.140e-31	1.7	A	.....		
^{90}Zr (n, 2n) ^{89}Zr	1.975e-31(4)	1.881e-31	-4.8	A	1.976e-31	0.0	A
Ti (n, x) ^{48}Sc	2.99e-32 (5)	2.980e-32	-0.3	A	2.930e-32	-1.9	A
Ti (n, x) ^{47}Sc	1.316e-32(4)	1.470e-32	11.7	C	1.398e-32	6.2	B
Ti (n, x) ^{46}Sc	1.12e-31(12)	1.156e-31	3.3	A	1.088e-31	-2.8	A
^{59}Co (n, 2n) ^{58}Co	2.454e-31(3)	2.591e-31	5.6	B	2.643e-31	7.7	B
^{59}Co (n, α) ^{56}Mn	1.550e-32(4)	1.597e-32	3.0	A	1.466e-32	-5.5	B

* Error in %.

Deviation (%) is given as [(Calc.-Expt.)/Expt.] .

Status follows the classifications presented in the text.

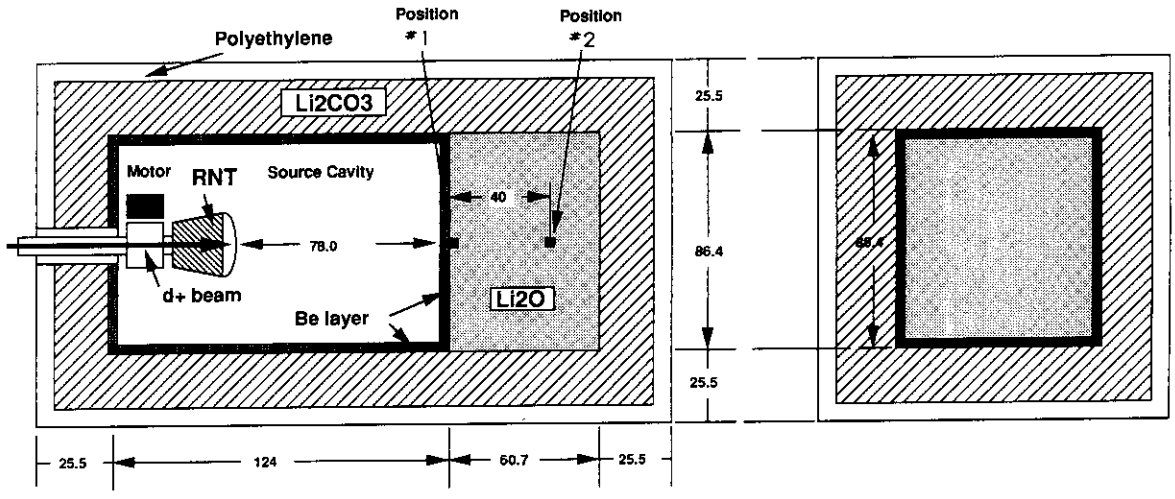

Fig. 4.1.1 Cross sectional view of the Phase-II B system. (unit of length is cm)

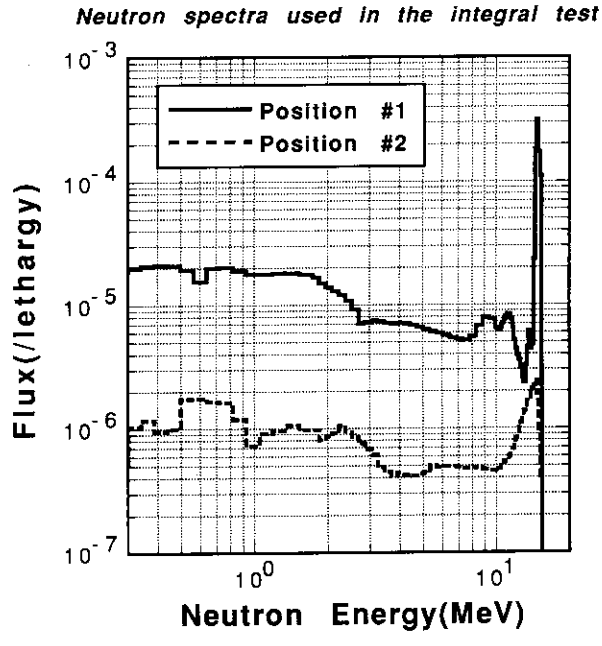

Fig. 4.1.2 Neutron spectra at Positions #1 and #2.

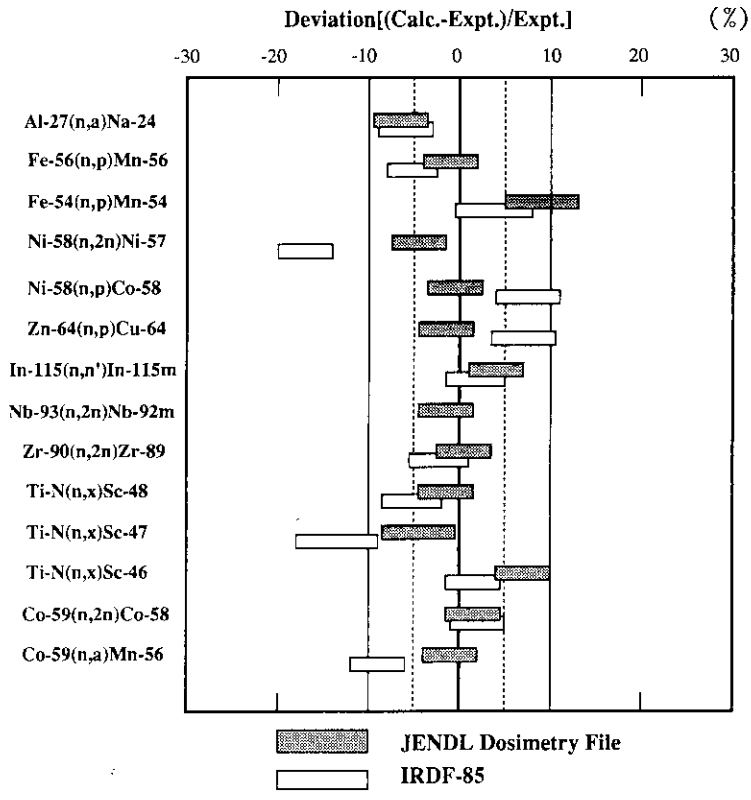

Fig. 4.1.3(a) Deviations of calculated reaction rates from measured ones for the spectrum #1.

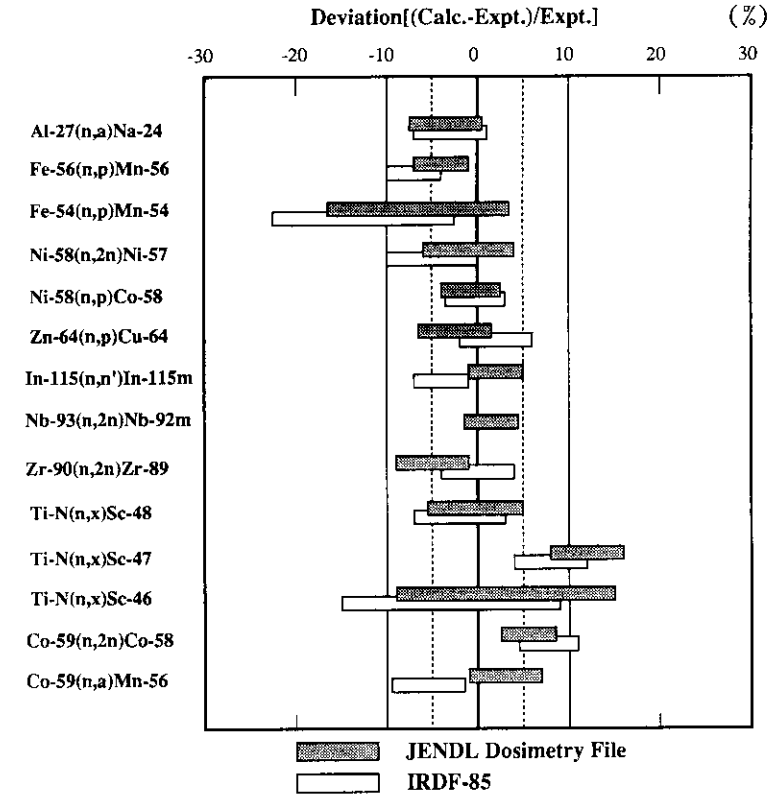

Fig. 4.1.3(b) Deviations of calculated reaction rates from measured ones for the spectrum #2.

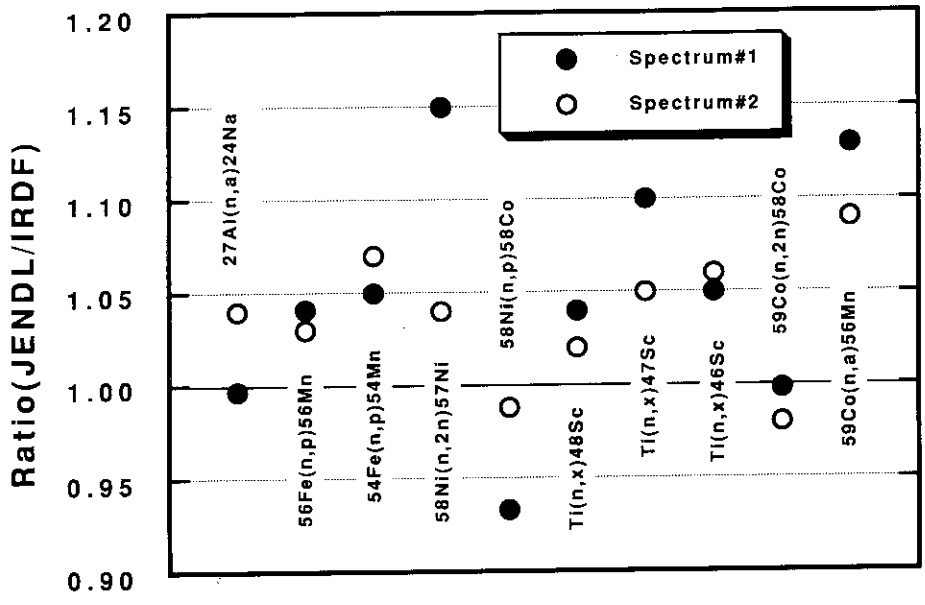

Fig. 4.1.4 Ratios of reaction rates derived from JENDL to those from IRDF.

4.2 Integral Test Using Thick Li (d, n) Neutron Field

The dosimetry cross sections are usually verified by the integral experiments using fission neutrons from reactors or ^{252}Cf sources. Because of the inherent characteristics of the fission spectrum, however, the neutron intensity rapidly decreases with the energy, and the average cross sections of threshold reactions are mostly determined by the cross-section data near the threshold energies[71]. Therefore such integral experiments are not so appropriate for the test of the cross sections in appreciably higher energy region above the threshold; this region is especially important for the 14-MeV fusion neutron dosimetry.

Another type of neutron fields which possess rather flat spectrum with relatively high intensity up to above 10 MeV can be obtained using accelerators[72,73]. Recently, utilization of a neutron field based on the Li(d, n) reaction on a thick target has been proposed and its feasibility for the integral test of the cross sections was demonstrated using a 4.5 MV Dynamitron accelerator at Fast Neutron Laboratory (FNL) of Tohoku University[74].

In the present work, the Li(d, n) neutron field was actually applied to validate the JENDL Dosimetry File as well as three files, the precedent dosimetry file IRDF-85[1] and the two recently released files, ENDF/B-VI[6] and IRDF-90[5]. In the validation, the experimental average cross sections in the field were compared with the calculated ones based on the above four files for selected fourteen dosimetry reaction cross sections.

4.2.1 Characteristics of Neutron Field

The neutron target was a metal lithium (natural element) disk of 8 mm in diameter and about 1 mm in thickness. The target was mounted in a low mass chamber made of copper with a forced air cooling system as shown in **Fig. 4.2.1**. During an irradiation, the target was bombarded by a DC deuteron beam of 10 μA with the energy of 2 MeV from the accelerator. Since the ^{7}Li(d, n) reaction has a high Q-value of 15.02 MeV, neutrons with energies up to about 17 MeV can be produced.

The angular spectra of the neutron source were measured by a time-of-flight(TOF) spectrometer with a goniometer in an angular range of 0° to 90° by 5° or 10° step. In this measurement, a 0.25-MHz pulsed beam with FWHM of 2-nsec was used. Emitted neutrons were detected by an NE213 scintillation counter (2"ϕ × 2" thick) which was placed at a distance of 5.3 m from the neutron target in a heavy shield collimator system on the goniometer as shown in **Fig. 4.2.2**.

Relative efficiency curve of the neutron detector in the energy range up to 6 MeV was obtained by the measurement of the ^{252}Cf spontaneous fission spectrum[75], and that above 6 MeV was given by a Monte Carlo calculation using the O5S code[76]. Both efficiency curves were combined together at 6 MeV.

The measured neutron spectrum (ϕ (E)) at 0° is shown in **Fig. 4.2.3**. Three arrows (A, B and C) in the figure indicate peaks correspond to the ground and the broad excited states of the residual nucleus of ^{8}Be, and the fourth peak (D) shows neutrons from the (d, n) reaction on the contaminated carbon at the target surface. Because of the degradation of the incident deuteron energy in the target, the shape of the peaks became further broadened.

In **Fig. 4.2.4**, the angular distributions of the outgoing neutrons in some energy intervals show rather flat shapes except for the group of the highest energy interval. **Figure 4.2.5** shows sensitivity functions (S (E) = ϕ (E) • σ (E)) of ^{58}Ni(n, p), ^{27}Al(n, α), ^{59}Co(n, 2n) and ^{58}Ni(n, 2n) reactions for both the ^{252}Cf spontaneous fission spectrum and the Li(d, n) neutron spectrum. In the case of the Li(d, n) spectrum, the peaks of the functions shifted appreciably to the higher energy region from the cases of the ^{252}Cf spontaneous fission spectrum and are large even for the ^{58}Ni(n, 2n) reaction, as expected.

From the above discussions and figures, the advantages of the Li(d, n) neutron source can be pointed out as follows: i) large response to the higher energy range of the cross sections especially for the reactions having high threshold energies; ii) availability of detailed spectrum data with less abmiguity by means of the TOF technique; iii) availability of the source only by a small accelerator.

On the other hand, the disadvantages of this neutron source are also pointed out: i) existence of the rather distinct structure and slight angular dependence in the spectrum; ii) less stability of the spectrum comparing with the fission-driven neutron sources. But these were not serious problems in the present experiment.

4.2.2 Benchmark Experiment

The spectrum-averaged cross sections of the fourteen reactions (listed in **Table 4.2.1**) have been measured in this neutron field relative to that of the standard reaction ^{27}Al(n, α)^{24}Na on the basis of the IRDF-85 file.

Two packets of the activation samples were prepared. Samples of each packet are arranged in a sandwich geometry as shown in **Table 4.2.2**. In the packets, several foils were placed between two or three monitor foils of aluminum. The #1 packet was hung by the tape in the hollow stainless steel plate at the position of 50 mm (P1) from the target in the 0° direction; the #2 was attached on the end surface of the chamber (see **Fig. 4.2.1**) at 7 mm (P2) from the target considering the small sensitivities of the tested reactions and the long half-lives of the induced activities. Both packets were simultaneously irradiated for 48 hours. Measurement of gamma rays from the activated samples was performed by a calibrated high purity germanium detector in order to obtain the reaction rates. The associated decay data with the tested dosimetry reactions are given in **Table 4.2.1**.

At the position P1, the anisotropic emission of the source neutrons was not appreciable. But, because of large angle spanning of the irradiated samples from 0° to 20° at the position P2, the anisotropy effect on the samples was not negligible and exactly corrected using the measured angular spectra.

4.2.3 Average Cross Sections

The measured cross section of the reaction i averaged over the spectrum E^i is obtained by the formula,

$$E^i = <\sigma^i>_E = R^i/(\Sigma_g \alpha^i \phi^{ir}{}_g \Delta E_g), \tag{1}$$

where R^i is the reaction rate for i, $\phi^{ir}{}_g$ relative group flux of the Li(d, n) neutrons, ΔE_g the energy bin width of the group g, and α^i the normalization factor for the relative flux. As mentioned before, E^i was actually measured relative to the average cross section $<\sigma^{Al}>_C$ of the ^{27}Al(n, α) reaction instead of directly obtaining the α^i's by other methods. Thus, the formula (1) becomes,

$$E^i = (R^i/R^{Al}) <\sigma^{Al}>_C F^i, \tag{2}$$

where, R^{Al} is the reaction rate of the ^{27}Al(n, α) and F^i the correction factor of the flux difference between the foil positions for reaction i and the ^{27}Al(n, α), which can be estimated from the reaction rates of the pair of aluminum foils.

The calculated average cross sections of the reaction i, C^i is given by the following formula,

$$C^i = <\sigma^i>_C = (\Sigma_g \phi^{ir}{}_g \sigma^i{}_g \Delta E_g)/(\Sigma_g \phi^{ir}{}_g \Delta E_g), \tag{3}$$

where $\sigma^i{}_g$ is the group cross section of the reaction i taken from each dosimetry file.

In the error estimation of both experimental and calculated average cross sections (E^i's and C^i's) and their ratios (C^i/E^i's), both covariances of the cross sections and of the neutron flux were taken into account. The former covariance data were taken from the files. The later ones were estimated from the analysis of the spectrum data. Main part of the flux covariances originated from the ^{252}Cf standard spectrum and the Monte Carlo calculations used for the estimation of the detector efficiency. Correlations between the R^i and R^{Al} were considered, while those between $\phi^{ir}{}_g$ and $\sigma^i{}_g$, and those between the $\sigma^i{}_g$ and $\sigma^{Al}{}_g$ were neglected. Major sources of the experimental error in the R^i were due to the gamma counting statistics, detector efficiency calibration, and flux correlations.

4.2.4 Results and Discussions

Numerical data of the results for the C^i and E^i for the four files are given in **Table 4.2.3** and their ratios (C^i/E^i) are given in Table 4.2.4. In **Fig. 4.2.6**, the C^i/E^i values with the ranges of the uncertainty are schematically compared.

In the JENDL Dosimetry File, the results for ^{54}Fe(n, p) and ^{55}Mn(n, 2n) reactions are beyond the respective uncertainties. As for ^{23}Na(n, 2n), ^{58}Ni(n, p) and ^{59}Co(n, 2n) reactions, the deviations are rather large (over 10 %), but within the uncertainties.

Remarkably large discrepancies are found for ^{23}Na(n, 2n) (50 %) in ENDF/B–VI and ^{63}Cu(n, α) (25 %) in IRDF–85 compared with those of other reactions. Furthermore, calculated cross sections are found systematically lower than experimental data for ^{54}Fe(n, p) reaction and larger for ^{55}Mn(n, 2n) reaction in all the libraries by more than 15%.

In summary of this section, the JENDL Dosimetry File shows generally good performance and owns better or similar quality compared with the other files as far as the tested cross sections are concerned. Further differential and integral studies for the several reactions mentioned above are strongly recommended.

Table 4.2.1 Dosimetry reactions tested in the thick Li (d, n) neutron field.

reaction			abundance (%)	half life		gamma ray energy (keV)	branching ratio (%)
Na-23	(n, 2n)	Na-22	100.	2.602	y	1274.5	99.94
Mg-24	(n, p)	Na-24	78.99	15.02	h	1368.6	99.994
Al-27	(n, α)	Na-24	100.	15.02	h	1368.6	99.994
Ti	(n, x)	Sc-46	-	83.8	d	889.28	99.984
Ti	(n, x)	Sc-48	-	43.67	h	983.5	100.
Mn-55	(n, 2n)	Mn-54	100.	312.2	d	834.84	99.975
Fe-54	(n, p)	Mn-54	5.8	312.2	d	834.84	99.975
Ni-58	(n, p)	Co-58	68.3	70.78	d	810.78	99.44
Ni-58	(n, 2n)	Ni-57	68.3	35.99	h	1377.59	77.6
Co-59	(n, 2n)	Co-58	100.	70.78	d	810.78	99.44
Ni-60	(n, p)	Co-60	26.1	5.2719	y	1173.24	99.89
						1332.5	99.987
Cu-63	(n, α)	Co-60	69.2	5.2719	y	1173.24	99.89
						1332.5	99.987
Nb-93	(n, 2n)	Nb-92m	100.	10.14	d	934.5	99.2
Au-197	(n, 2n)	Au-196	100.	6.183	d	355.7	87.6

Table 4.2.2 List of the samples contained in the foil packets used in the benchmark experiment.

Packet No.	Irradition position	Foils (ordered from the neutron source side)
#1	P1	Al, Nb, Ni, Ti, Zr, Fe, Mg, Al, Au, Nb, Al, Mn
#2	P2	Al, Nb, Cu, Ni, Fe, Nb, Al, NaCl

Note: NaCl and Mn (powder) : contained in thin plastic envelopes in a shape of about 15-mm dia. and 1.5-mm thickness; Cu: metal disks of 15 mm in dia. $\times$1 mm in thickness; the rest: all metal disks of 15 mm in dia. $\times$0.1-0.2 mm in thickness.

Table 4.2.3 The cross sections averaged over the thick Li(d,n) neutron spectrum obtained in the present experiment and calculated ones using the JENDL Dosimetry File, IRDF-85, IRDF-90 and ENDF/B-VI.

Reaction	Average Cross Section (mb)				
	Exp. (%error)	Cal. (%error)			
		JENDL	IRDF-85	IRDF-90	ENDF/B-VI
Na-23 (n, 2n)	6.96-0 (9.1)	6.12+0 (9.9)	5.99+0 (10.1)	.....	1.05+1 (12.2)
Mg-24 (n, p)	6.98+1[a] (9.7)	6.90+1 (3.5)	6.90+1 (3.5)	6.86+1 (3.1)	6.89+1 (3.1)
Al-27 (n, α)	4.30-1 (8.6)	4.22+1 (7.0)	4.30+1 (7.0)	4.23-1 (3.1)	4.30+1 (4.5)
Ti (n, x) Se-46	1.15-2 (9.1)	1.22+2 (13.3)	1.14+2 (13.2)	1.09-2 (13.2)	1.14+2 (13.2)
Ti (n, x) Sc-48	2.01+1 (8.8)	2.04+1 (13.0)	2.04+1 (13.0)	1.95+1 (6.1)	2.04+1 (13.0)
Mn-55 (n, 2n)	1.60-2 (8.5)	1.86-2 (9.0)	1.86+2 (8.9)	1.86+2 (9.0)	1.86+2 (9.0)
Fe-54 (n, p)	2.95-2 (8.6)	2.60+2 (1.6)	2.48+2 (2.0)	2.44+2 (1.3)	2.43+2 (1.3)
Ni-58 (n, p)	3.19+2 (8.4)	2.88-2 (6.7)	3.00+2 (6.9)	2.94+2 (1.0)	2.92+2 (1.0)
Ni-58 (n, 2n)	6.77+0 (9.8)	6.49-0 (11.6)	5.81+0 (11.6)	6.70+0 (3.2)	6.71+0 (3.3)
Co-59 (n, 2n)	1.62+2 (8.6)	1.79-2 (7.6)	1.83+2 (7.5)	1.77+2 (3.1)	.....
Ni-60 (n, p)	5.71+1 (8.9)	5.29-1 (7.2)	5.29+1 (7.2)	5.06+1 (7.6)	5.05+1 (9.2)
Cu-63 (n, α)	1.38+1 (8.7)	1.33+1 (3.6)	1.71+1 (3.6)	1.52+1 (3.3)	1.52+1 (3.3)
Nb-93 (n, 2n)	1.38+2 (8.5)	1.46+2 (4.3)	.....	1.45+2 (3.1)	.....
Au-197 (n, 2n)	6.68+2 (8.5)	6.73+2 (3.4)	.....	7.01-2 (3.4)	6.83+2 (3.1)

a) read as 6.98×10^{1}

Table 4.2.4 The ratio of the experimental cross sections averaged over the thick Li(d,n) neutron spectrum to the calculated ones using the JENDL Dosimetry File, IRDF-85, IRDF-90 and ENDF/B-VI.

Reaction			Ratio [Calc./Exp.] (%error)			
			JENDL	IRDF-85	IRDF-90	ENDF/B-VI
Na-23	(n, 2n)	Na-22	0.89 (11.0)	0.86 (11.2)	.....	1.51 (12.9)
Mg-24	(n, p)	Na-24	0.99 (6.5)	0.99 (6.5)	0.98 (6.4)	0.99 (6.3)
Al-27	(n, α)	Na-24	0.98 (7.0)	1.00 (-)	0.98 (3.0)	1.00 (4.5)
Ti	(n, x)	Sc-46	1.06 (13.9)	0.99 (13.9)	0.95 (13.8)	0.99 (13.8)
Ti	(n, x)	Sc-48	1.02 (13.5)	1.02 (13.5)	0.97 (7.1)	1.02 (13.5)
Mn-55	(n, 2n)	Mn-54	1.16 (9.4)	1.16 (9.4)	1.16 (9.4)	1.16 (9.4)
Fe-54	(n, p)	Mn-54	0.88 (3.7)	0.84 (3.7)	0.83 (3.6)	0.82 (1.1)
Ni-58	(n, p)	Co-58	0.90 (7.1)	0.94 (7.1)	0.92 (3.7)	0.99 (6.5)
Ni-58	(n, 2n)	Ni-57	0.96 (12.9)	0.86 (12.9)	0.99 (6.5)	0.96 (12.9)
Co-59	(n, 2n)	Co-58	1.10 (7.5)	1.13 (7.5)	1.10 (9.1)	.....
Ni-60	(n, p)	Co-60	0.93 (7.5)	0.93 (7.5)	0.89 (7.6)	0.88 (10.0)
Cu-63	(n, α)	Co-60	0.96 (6.0)	1.24 (6.0)	1.10 (6.0)	1.10 (6.0)
Nb-93	(n, 2n)	Nb-92m	1.06 (6.0)	.....	1.05 (6.1)	.....
Au-197	(n, 2n)	Au-196	1.01 (5.0)	.....	1.05 (6.0)	1.02 (6.1)

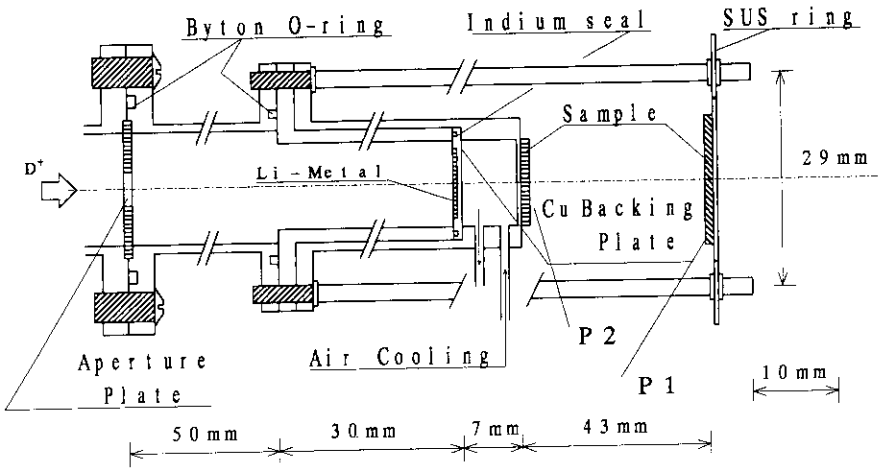

Fig. 4.2.1 The lithium metal target assembly.

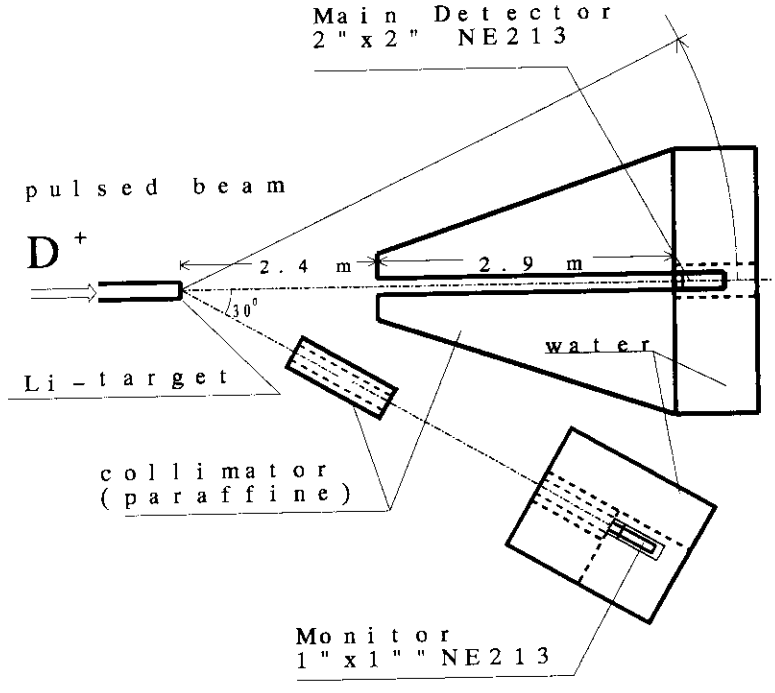

Fig. 4.2.2 Layout of the experiment for the neutron source characterization.

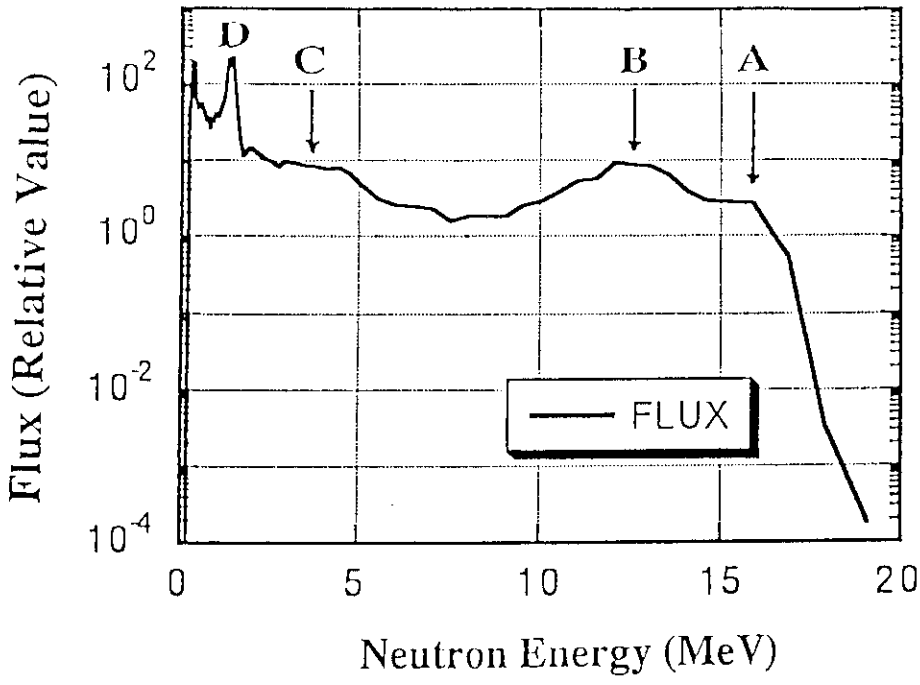

Fig. 4.2.3 Measured neutron spectra of the thick Li(d, n) neutron source at 0°. Arrows in the figure indicate peaks correspond to the ground state (A) and broad first (B) and fourth (C) excited states of residual nucleus of ^{8}Be, and a parasitic neutron group from ^{12}C(d, n) reactions (D).

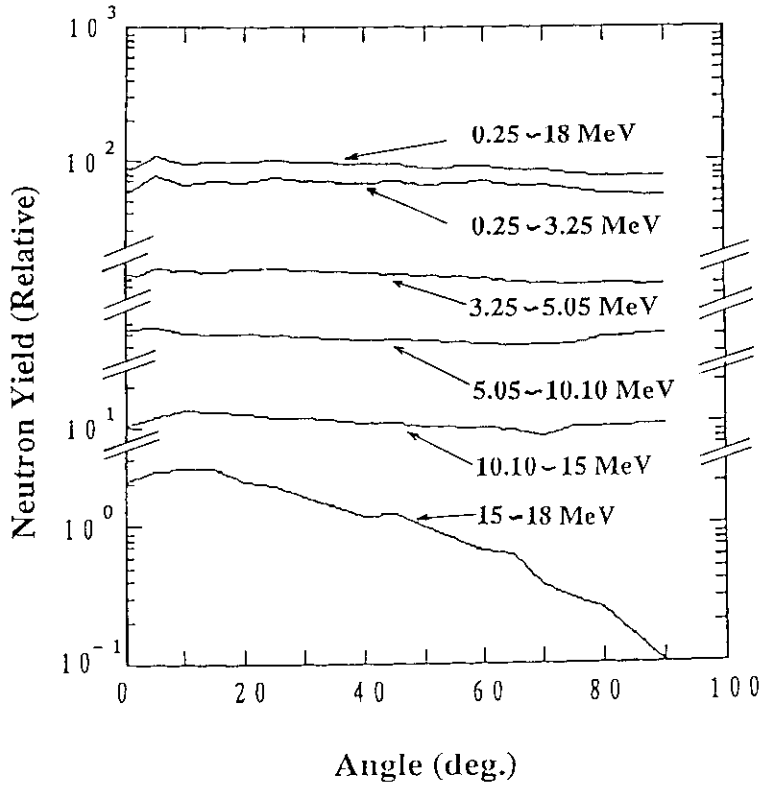

Fig. 4.2.4 Angular distributions of the thick Li(d, n) neutrons in some energy intervals.

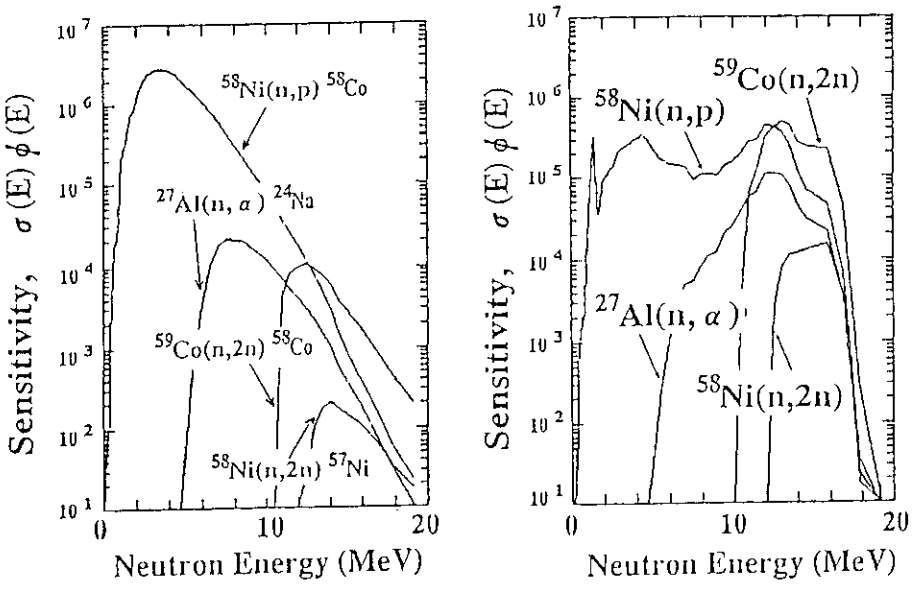

Fig. 4.2.5 Comparison of the responses of the ^{58}Ni(n, p), ^{27}Al(n, α), ^{59}Co(n, 2n) and ^{58}Ni(n, 2n) reactions to the spectra of the ^{252}Cf spontaneous fission neutrons (left) and thick Li(d, n) source (right), respectively.

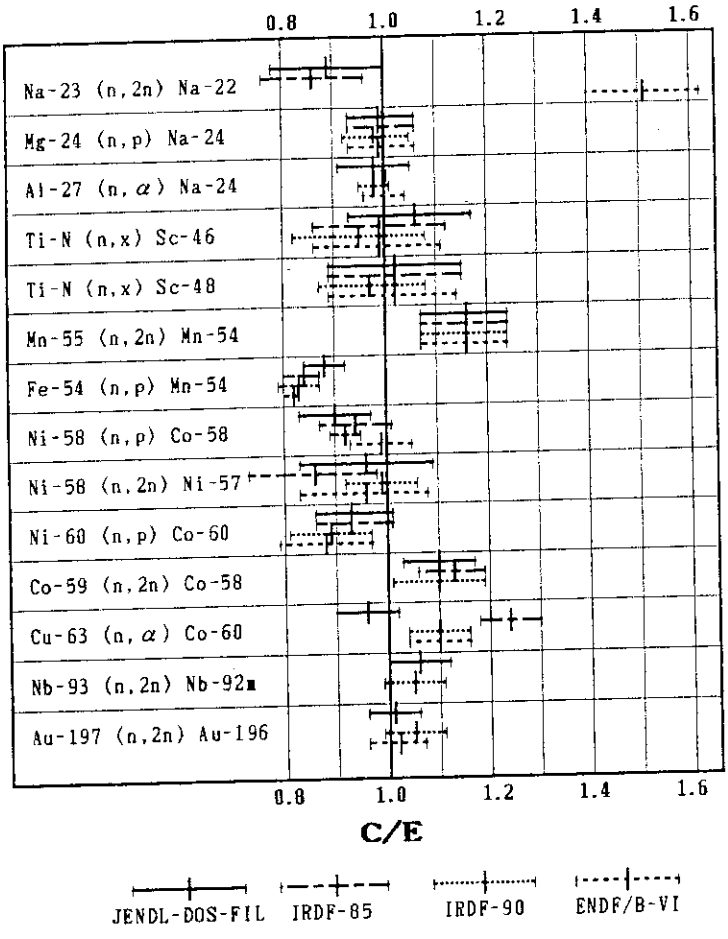

Fig. 4.2.6 Ratios of the average cross sections (C/E) in the thick Li(d, n) neutron spectrum with the ranges of their uncertainties of the tested dosimetry reactions for the files, the JENDL Dosimetry File, IRDF-85, IRDF-90 and ENDF/B-VI.

5. Summary Discussion of the Integral Tests

5.1 Integral Tests of the Dosimetry Cross Sections for Fission Reactors

Integral tests of group-wise cross sections of the JENDL Dosimetry File has been carried out by applying the standard, reference and controlled neurtron spectrum fields, as shown in **Fig. 3.1.1**, with respect to fission reactors such as light water reactors and fast breeder reactors. As described in the former Section 3.2, the calculated cross sections averaged with the ^{252}Cf spontaneous fission neutron spectrum evaluated by Mannhart[37] give better agreement with the measured ones[49] than those with the Maxwellian distribution spectrum of ^{252}Cf[40]. Concerning the ^{235}U fission neutron spectrum, in general, agreement between the measured average cross sections[46,51,52] and the calculated ones using the Watt-type spectrum[40] is also better than those obtained by using the Maxwellian and the Madland-Nix-type[41] (the latter is taken in the JENDL-3 General Purpose File) spectra. Average cross section by the Maxwellian spectrum gives larger values than those by the Watt and the Madland-Nix-type spectra, especially for higher energy threshold reactions, as seen in Section 3.2. Therefore, in this summary section of the integral tests, we selected the results with the Mannhart and the Watt-type spectra for the ^{252}Cf and the ^{235}U fission neutron spectra, respectively. The C/E ratio values, which show the criterion of data consistency between the calculated and the measured average cross sections, were taken from **Tables 3.2.1** and **3.2.2**. The following definition of discrepancy R between the calculation and the measurement was employed:

$$R = (C - E)/E ,$$

where, C is the calculated average cross section and E is the measured one. The quoted uncertainty comprises the uncertainties of measured and calculated cross sections which are uncorrelated each other.

The data used for the present comparison between the measured and calculated average cross sections are taken from **Tables 3.2.1**, **3.2.2**, **3.3.3**, **3.3.4**, **3.3.5** and **3.3.6**, and these results are summarized in **Table 5.1.1** and **Fig. 5.5.1** for the above defined R-values. In column 1, the neutron reactions under consideration are shown and the R-values for the respective reactions are listed in columns 2 to 7. The last column gives the criterion of consistency or status showing how good the agreement is between the calculated and the measured average cross sections.

In general, most of the average cross sections calculated by means of the JENDL Dosimetry File for each standard and reference neutron fields show good agreement with those measured, except for several reactions. Especially, the better agreement was obtained for the ^{252}Cf and the ^{235}U fission neutron spectra, except for the following 5 reactions of ^{19}F(n, 2n)^{18}F, ^{60}Ni(n, p)^{60}Co, ^{63}Cu(n, 2n)^{62}Cu, ^{63}Cu(n, γ)^{64}Cu and ^{64}Zn(n,p)^{64}Cu. For the ^{27}Al(n, α)^{24}Na reaction, relatively large deviations in the R-value exist in the $\Sigma\Sigma$ and YAYOI spectra. The calculated average cross sections are generally larger than the measured ones for the ^{19}F(n, 2n)^{18}F, ^{24}Mg(n, p)^{24}Na, ^{45}Sc(n, γ)^{46}Sc, ^{47}Ti(n, p)^{47}Sc, ^{55}Mn(n, 2n)^{54}Mn, ^{58}Fe(n, γ)^{59}Fe, ^{60}Ni(n, p)^{60}Co, ^{63}Cu(n, 2n)^{62}Cu and ^{64}Zn(n, p)^{64}Cu reactions. Large R-values can be seen for the ^{58}Ni(n, 2n)^{57}Ni and the ^{59}Co(n, γ)^{60}Co reactions. The ^{63}Cu(n, γ)^{64}Cu reaction cross section is obviously small. The average cross section for the ^{232}Th(n, γ)^{232}Th reaction seems to be too small. The JENDL dosimetry cross sections for the (n, fission) reactions give small R-values in general.

In this report, integral tests not only for the JENDL but also for the IRDF-85 dosimetry cross sections[3] have been examined. The calculated average cross sections for the both dosimetry files are given in **Tables 3.1.2** to **3.1.11** by using several standard and reference neutron fields. Concerning the measured average cross sections, the ^{252}Cf and the ^{235}U spectrum averaged cross section data are relatively

in good quality and are carefully measured to give a covariance matrix. In this summary discussion, we chose the ^{252}Cf spectrum evaluated by NIST group[40] and the Watt-type spectrum[40] appeared in ENDF /B-V for the ^{235}U spectrum. The calculated data for the ^{252}Cf spectrum using the IRDF-85 and the JENDL Dosimetry File are summarized in **Table 5.1.2** and **Fig. 5.1.2** and comparison of the calculated data from both files is made with the measured one for each dosimetry reaction. In **Table 5.1.3** and **Fig. 5.1.3** the results are shown for the ^{235}U spectrum. From these tables and figures, it is found that concerning the criterion of consistency between the measured and the calculated cross sections, the average cross sections calculated with the IRDF-85 data are close to those with JENDL, in general. There was, however, a big improvement for the three reactions of ^{47}Ti(n, p)^{47}Sc, ^{93}Nb(n, n')^{93m}Nb and ^{232}Th(n, f) in the JENDL Dosimetry File, whose evaluation was made basing on the recent measurements, while the deviations for the ^{19}F(n, 2n)^{18}F and ^{24}Mg(n, p)^{24}Na reactions in the JENDL Dosimetry File are larger than those in IRDF-85. Concerning the ^{55}Mn(n, 2n)^{54}Mn, ^{59}Co(n, γ)^{60}Co, ^{63}Cu(n, γ)^{64}Cu and ^{64}Zn(n, p)^{64}Cu reactions, the JENDL Dosimetry File data are not always in better agreement with the measured results than those in IRDF-85. A large deviation from the measurement is seen for the ^{60}Ni(n, p)^{60}Co reaction in both dosimetry files.

Table 5.1.1 Summary of R− (C−E) /E and its uncertainty (in %) Values.

Reaction	Cf-252	U-235	ISNF	CFRMF	ΣΣ	YAYOI	Status*
Li-6 (n, α) H-3				0.0155(3.67)			A
B-10 (n, α) Li-7				−0.0848(3.55)		0.0455(9.31)	B
F-19 (n, 2n) F-18	0.2862(5.15)						D
Na-23 (n, γ) Na-24			0.1178(11.6)			0.2697(12.7)	C
Mg-24 (n, p) Na-24	0.1322(5.22)	0.0933(6.16)				0.3130(8.99)	C
Al-27 (n, p) Mg-27	0.0370(6.45)	0.0851(7.98)		0.0997(6.99)	−0.1568(11.7)	0.1187(12.6)	B
Al-27 (n, α) Na-24	−0.0294(5.99)	−0.0255(7.22)		0.0589(6.71)	−0.1923(6.74)	0.2314(9.64)	A
S-32 (n, p) P-32	0.0296(8.91)						A
Sc-45 (n, γ) Sc-46			0.2029(4.24)	0.1470(4.24)			C
Ti-46 (n, p) Sc-46	−0.0648(12.8)	−0.0302(13.3)		−0.0411(13.2)		−0.0941(16.0)	B
Ti-47 (n, p) Sc-47	0.0654(11.5)	0.0893(11.9)		0.0964(12.4)		−0.0551(17.7)	B
Ti-48 (n, p) Sc-48	0.0788(10.6)	−0.0791(11.2)		0.0147(11.4)		0.1807(13.3)	B
Mn-55 (n, 2n) Mn-54	0.1598(12.7)						C
Mn-55 (n, γ) Mn-56					−0.3657(5.37)	−0.0649(10.8)	B
Fe-54 (n, p) Mn-54	0.0089(4.24)	0.0029(4.98)		0.0297(5.00)			A
Fe-56 (n, p) Mn-56	−0.0428(5.18)	−0.0303(6.20)			0.1758(5.83)	0.1226(9.03)	A
Fe-58 (n, γ) Fe-59				0.7666(8.74)			D
Co-59 (n, 2n) Co-58	0.0173(11.2)	−0.1149(12.6)					B
Co-59 (n, γ) Co-60	−0.2461(6.74)		0.1562(4.94)	−0.0279(4.83)			D
Co-59 (n, α) Mn-56	0.0365(4.99)	0.0261(6.45)				0.3161(9.18)	A
Ni-58 (n, 2n) Ni-57	−0.0788(11.5)	−0.3143(12.3)				0.6667(12.0)	P
Ni-58 (n, p) Co-58	0.0179(6.90)	−0.0165(8.44)			−0.1740(7.42)	0.0371(9.87)	A
Ni-60 (n, p) Co-60	0.4000(9.48)			−0.0617(7.49)			D
Cu-63 (n, 2n) Cu-62	0.1442(4.69)					0.7325(14.0)	C
Cu-63 (n, γ) Cu-64	−0.1882(19.3)			−0.1060(9.08)	−0.2218(9.48)		C
Cu-63 (n, α) Co-60	0.0228(6.10)					0.1964(9.08)	A

Zn-64 (n, p)	Cu-64	0.1586(7.97)	0.3611(9.62)					D
Zr-90 (n, 2n)	Zr-89	−0.0131(4.17)	−0.2114(5.10)				−0.0308(7.25)	P
Nb-93 (n, n')	Nb-93m	0.0034(9.57)						A
Nb-93 (n, 2n)	Nb-92m		−0.0832(7.62)				0.5820(7.78)	B
Rh-103 (n, n')	Rh-103m	−0.0540(7.93)	−0.0468(8.61)					B
In-115 (n, n')	In-115m	−0.0424(3.29)	−0.0257(4.89)	−0.1006(4.01)	0.0186(4.93)	−0.0672(3.63)	0.0086(8.65)	A
In-115 (n, γ)	In-116m					0.1548(5.61)		C
W-186 (n, γ)	W-187	−0.0424(3.29)	−0.0257(4.89)				−0.2381(10.0)	A
Au-197 (n, 2n)	Au-196	0.0582(5.09)	−0.0260(6.23)					B
Au-197 (n, γ)	Au-198	−0.0243(9.04)		−0.0625(5.94)	−0.0735(5.30)	−0.2658(4.64)	−0.2380(9.66)	B
Th-232 fission		−0.0822(6.27)	−0.0543(6.31)		0.0020(7.58)	−0.0190(8.19)	0.0394(7.45)	A
Th-232 (n, γ)	Th-233	−0.0480(12.9)			−0.1369(11.5)			B
U-235 fission		0.0215(3.09)	0.0292(3.44)		0.0208(4.19)	−0.0604(4.49)		A
U-238 fission		−0.0133(3.39)	−0.0115(3.73)		0.0393(4.49)	−0.0500(4.66)	0.0950(5.92)	A
U-238 (n, γ)	U-239				0.0465(5.55)	0.0459(5.84)		A
Np-237 fission		−0.0074(9.60)	−0.0184(9.80)		0.0447(10.4)	−0.0532(10.5)		A
Pu-239 fission		−0.0039(3.23)	−0.0099(3.48)		−0.0134(3.86)	−0.0757(4.70)		A

* The status is defined as the following 4 ranks (values are in %):

A : R < 5

B : 5 < R < 10

C : 10 < R < 20

D : 20 < R

P : pending.

Table 5.1.2 Comparison of R= (C–E)/E and its unceratinty (in %) for the evaluated dosimetry cross sections in the JENDL Dosimetry File and IRDF–85, by using the Cf–252 fission spectrum obtained by NIST group.

Reaction			Measurement* (mb)	R=(C–E)/E IRDF–85	R=(C–E)/E JENDL	Error(%)
F–19	(n, 2n)	F–18	.01628±.00054	−0.0350	0.2291	(5.19)
Mg–24	(n, p)	Na–24	2.005±0.048	0.0763	0.1636	(5.22)
Al–27	(n, p)	Mg–27	4.892±0.106	0.0503	0.0609	(6.42)
Al–27	(n, α)	Na–24	1.021±0.015	0.0372	−0.0069	(6.02)
S–32	(n, p)	P–32	72.74±2.54	0.0448	0.0307	(8.85)
Ti–46	(n, p)	Sc–46	14.20±0.24	−0.0514	−0.0437	(12.9)
Ti–47	(n, p)	Sc–47	19.43±0.31	0.2388	0.0659	(11.5)
Ti–48	(n, p)	Sc–48	0.4275±0.0078	−0.0430	−0.0578	(10.7)
Mn–55	(n, 2n)	Mn–54	0.4079±0.0092	0.0797	0.1214	(12.8)
Fe–54	(n, p)	Mn–54	87.29±1.13	0.0113	0.0144	(4.23)
Fe–56	(n, p)	Mn–56	1.471±0.025	−0.0381	−0.0150	(5.18)
Co–59	(n, 2n)	Co–58	0.4058±0.0101	−0.0022	−0.0200	(11.3)
Co–59	(n, γ)	Co–60	6.97±0.34	−0.1352	−0.2620	(6.77)
Co–59	(n, α)	Mn–56	0.2221±0.0039	−0.0266	0.0626	(5.00)
Ni–58	(n, 2n)	Ni–57	$(8.965\pm.279)\times10^{-3}$	−0.1931	−0.1347	(11.5)
Ni–58	(n, p)	Co–58	117.6±1.5	−0.0306	−0.0145	(6.87)
Ni–60	(n, p)	Co–60	2.39±0.13	0.4410	0.4406	(9.50)
Cu–63	(n, 2n)	Cu–62	0.1866±0.0071	0.0332	0.0922	(4.70)
Cu–63	(n, γ)	Cu–64	10.55±0.32	−0.0854	−0.1880	(19.5)
Cu–63	(n, α)	Co–60	0.6897±0.0130	0.0992	0.0494	(6.11)
Zn–64	(n, p)	Cu–64	40.47±0.75	−0.0306	0.1636	(7.98)
Zr–90	(n, 2n)	Zr–89	0.2211±0.0061	−0.1058	−0.0665	(4.19)
Nb–93	(n, n')	Nb–93m	149±10	0.0846	−0.0034	(9.57)
Rh–103	(n, n')	Rh–103m	757±53	−0.0592	−0.0592	(7.93)
In–115	(n, n')	In–115m	198.1±2.6	−0.0818	−0.0505	(3.29)
Au–197	(n, 2n)	Au–196	5.531±0.099		0.0609	(5.12)
Au–197	(n, γ)	Au–198	77.11±1.19	−0.0102	−0.0284	(8.98)
Th–232	fission		89.4±2.7	−0.1267	−0.0868	(6.27)
Th–232	(n, γ)	Th–233	87.8±4.0	0.0215	−0.0501	(12.9)
U–235	fission		1210±14	0.0215	0.0207	(3.09)
U–238	fission		323.4±5.6	−0.0303	−0.0204	(3.39)
Np–237	fission		1356±22	−0.0029	−0.0125	(9.57)
Pu–239	fission		1811±25	−0.0105	−0.0055	(3.23)

*Referred to Ref.49).

Table 5.1.3 Comparison of R = (C–E)/E and its uncerainty (in %) values for the evaluated dosimetry cross sections in the JENDL Dosimetry File and IRDF–85, by using the U–235 fission spectrum in ENDF/B–V (Watt–type spectrum).

Reaction			Measurement (mb)	Ref.	R=(C–E)/E		
					IRDF–85	JENDL	Error(%)
Mg–24	(n, p)	Na–24	1.50±0.06	52	0.0047	0.0940	(6.16)
Al–27	(n, p)	Mg–27	3.95±0.20	52	0.0790	0.0856	(7.98)
Al–27	(n, α)	Na–24	0.706±0.028	52	0.0190	−0.0248	(7.22)
Ti–46	(n, p)	Sc–46	11.6±0.4	52	−0.0371	−0.0302	(13.3)
Ti–47	(n, p)	Sc–47	17.7±0.6	52	0.2689	0.0893	(11.9)
Ti–48	(n, p)	Sc–48	0.302±0.010	52	−0.0672	−0.0785	(11.2)
Fe–54	(n, p)	Mn–54	80.5±2.3	52	0.0067	0.0031	(4.98)
Fe–56	(n, p)	Mn–56	1.09±0.04	52	−0.0495	−0.0294	(6.20)
Co–59	(n, 2n)	Co–58	0.202±0.006	52	−0.1000	−0.1139	(12.6)
Co–59	(n, α)	Mn–56	0.161±0.007	52	−0.0702	0.0267	(6.45)
Ni–58	(n, 2n)	Ni–57	$(4.19\pm0.22)\times10^{-3}$	52	−0.3504	−0.3131	(12.3)
Ni–58	(n, p)	Co–58	108.9±5.3	52	−0.0340	−0.0165	(8.44)
Zn–64	(n, p)	Cu–64	31.68±1.82	46	0.1405	0.3614	(9.62)
Zr–90	(n, 2n)	Zr–89	0.103±0.004	52	−0.2533	−0.2101	(5.10)
Nb–93	(n, 2n)	Nb–92m	0.4796±0.0293	46		−0.0822	(7.61)
Rh–103	(n, n')	Rh–103m	673.5±52.2	46	0.0469	0.0469	(8.61)
In–115	(n, n')	In–115m	190.3±7.3	52	−0.0587	−0.0257	(4.88)
Au–197	(n, 2n)	Au–196	3.50±0.13	52		−0.0251	(6.23)
Th–232	fission		83±2.57	51	−0.0959	−0.0543	(6.31)
U–235	fission		1200±22.8	51	0.0300	0.0292	(3.44)
U–238	fission		312±7.2	51	−0.0218	−0.0115	(3.74)
Np–237	fission		1359±28.5	51	−0.0088	−0.0184	(9.80)
Pu–239	fission		1818±34.5	51	−0.0149	−0.0099	(3.48)

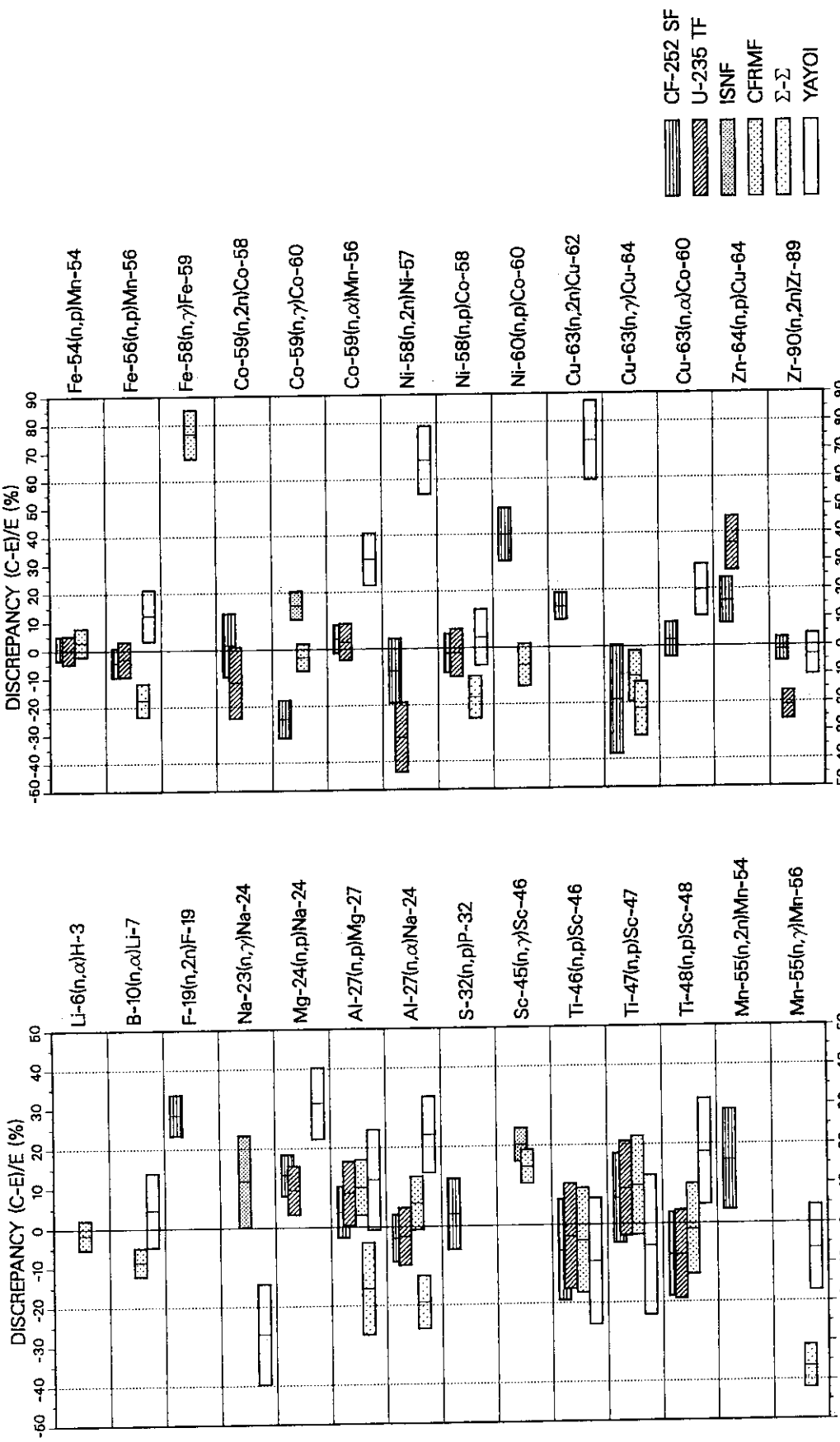

Fig. 5.1.1 Discrepancies of average cross sections from measured data in various neutron fields. Center and width of each rectangle show (C–E)/E and uncertainty, respectively.

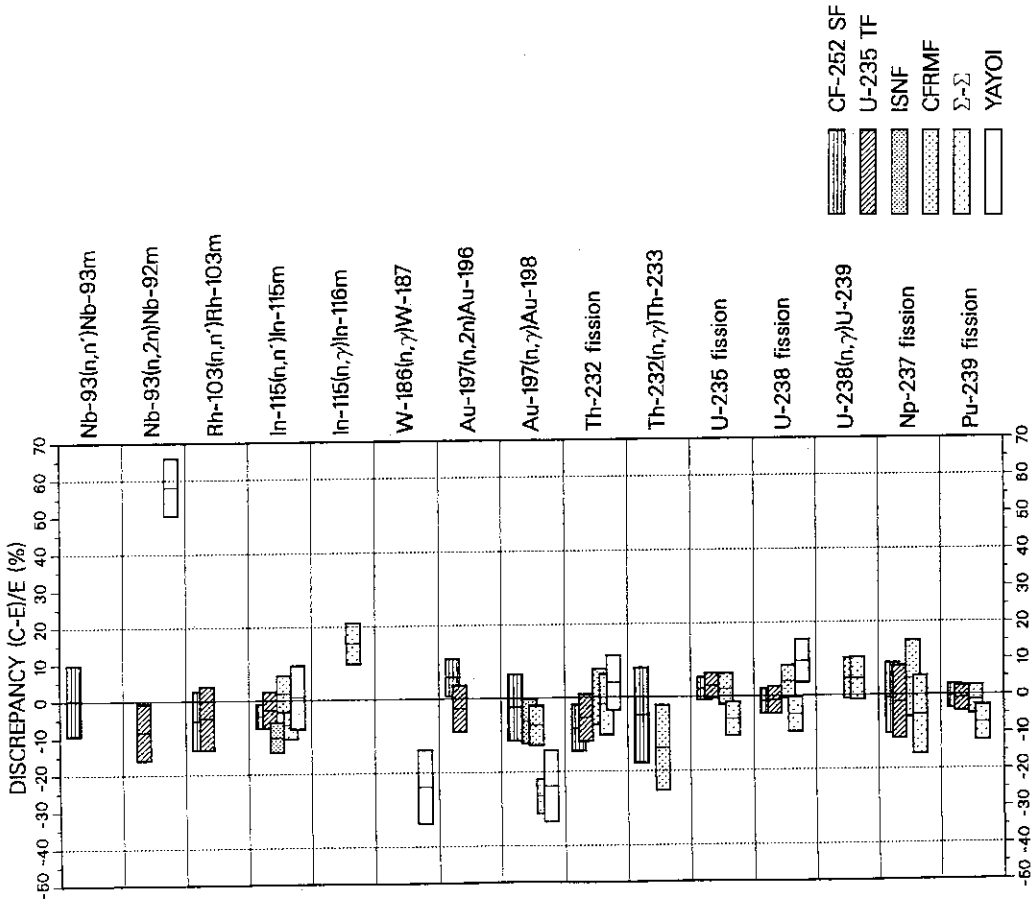

Fig. 5.1.1 (continued)

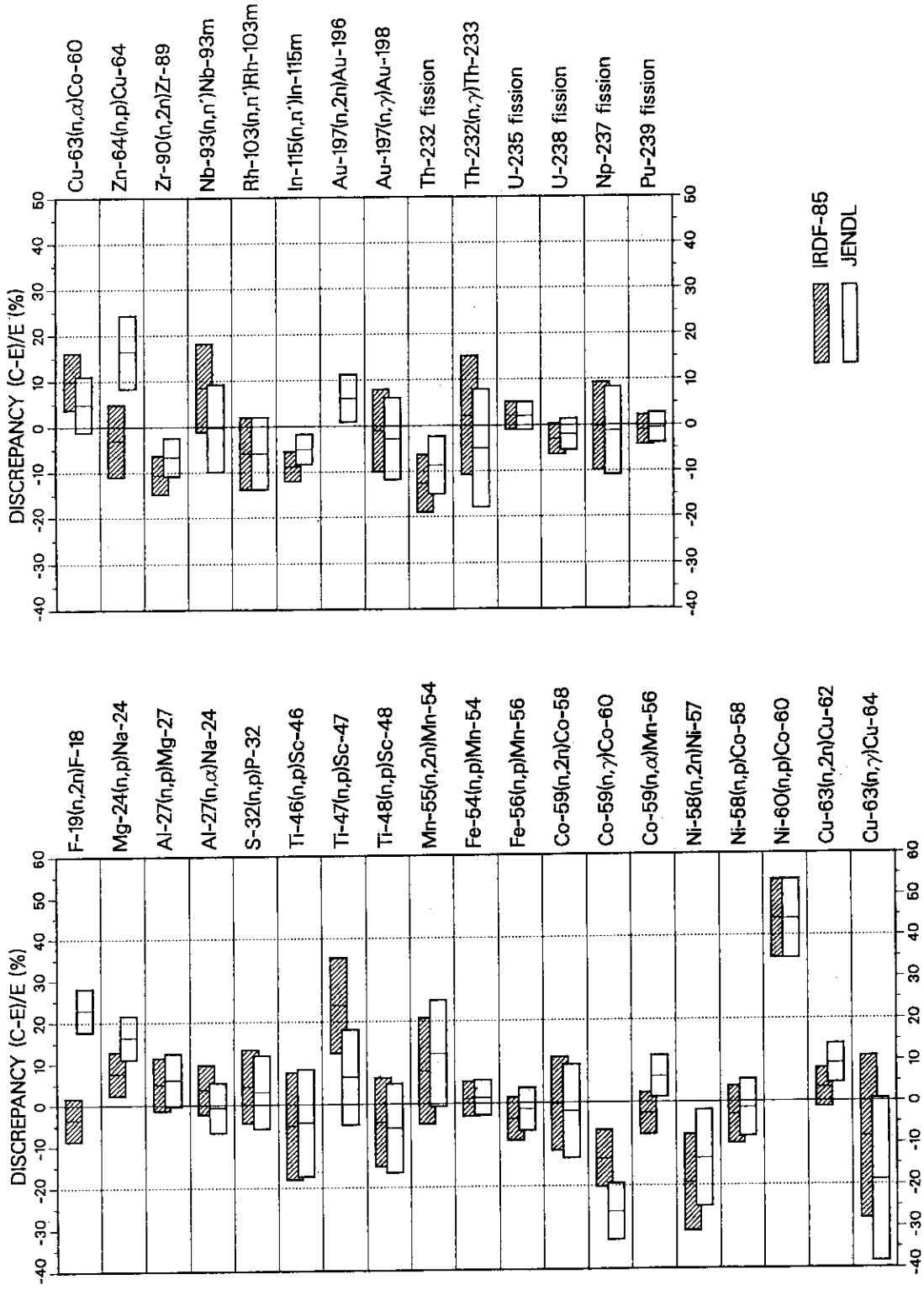

Fig. 5.1.2 Comparison of (C–E)/E values calculated from the JENDL Dosimetry File and IRDF-85 by using the ^{252}Cf spontaneous fission spectrum evaluated by NIST group.

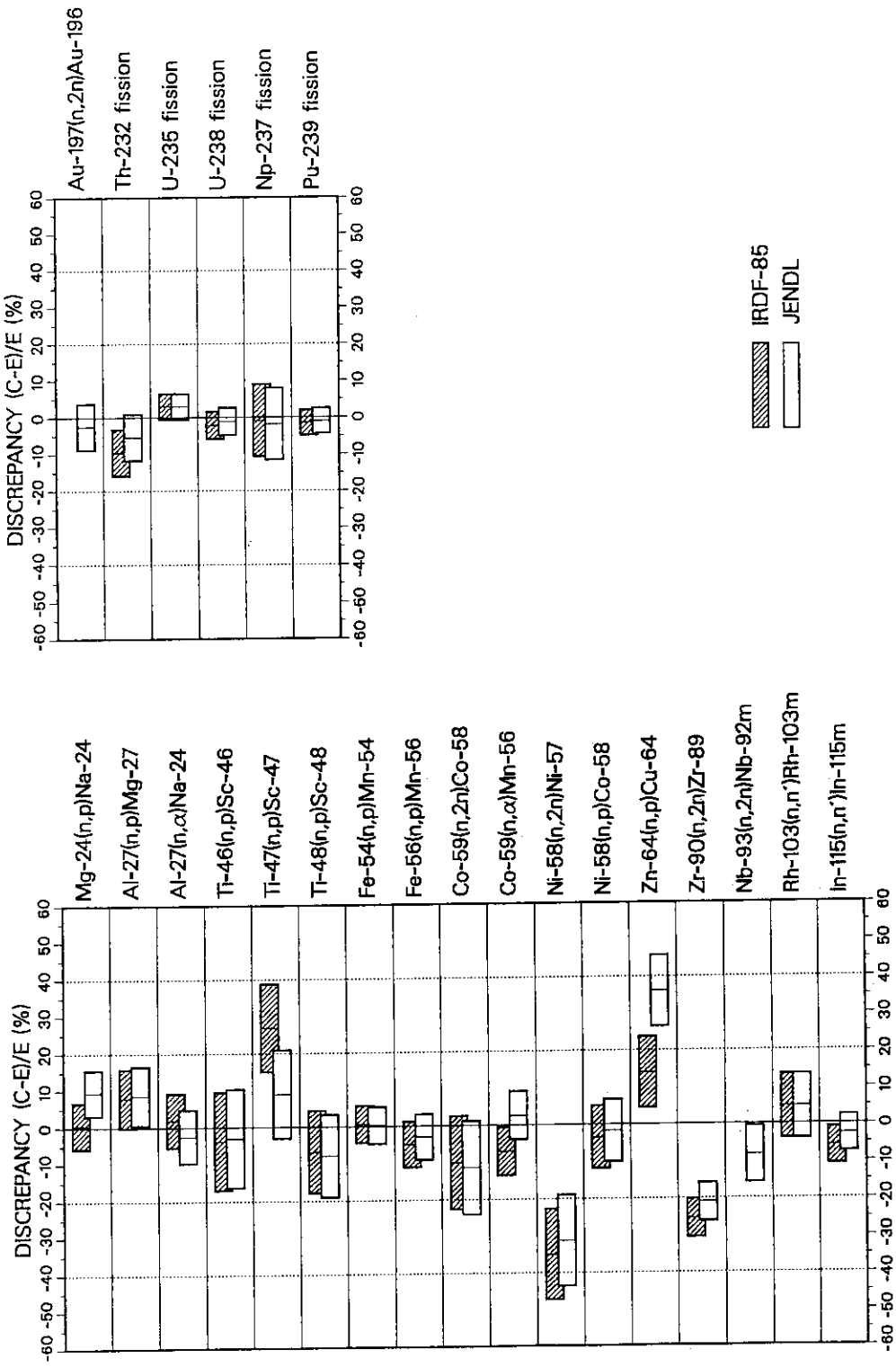

Fig. 5.1.3 Comparison of (C–E)/E values calculated from the JENDL Dosimetry File and IRDF–85 by using the ^{235}U thermal fission spectrum in ENDF/B–V.

5.2 Integral Tests of the Threshold Reaction Cross Sections for Fusion Rectors

The validation experiments for the JENDL Dosimetry File have been conducted in the two accelerator-based neutron fields. The cross sections for twenty threshold reactions in total were tested, i. e., the fourteen reactions in the d+T fusion simulated field at FNS, JAERI, and the common eight and the other six reactions in the Li+d neutron source at FNL, Tohoku University, as described in Sections 4.1 and 4.2, respectively.

In order to clarify the trend of agreement between the calculation and both integral experiments, we have rearranged the *C/E* values of **Tables 4.1.2(b)** (T+d spectrum #2) and **4.2.4** (Li+d) into **Tables 5.2.1** and **5.2.2** for the JENDL Dosimetry File and IRDF-85, respectively, because both fields have broad spectra and similar responses to the reactions investigated. In these tables, we adopted the same assignment of the criterion for the latter results with that of the Section 4.1, i.e., A: with discrepancy less than 5 %, B: between 5 and 10 %, C: between 10 and 20 %, and D: more than 20 %. These results are also given in **Figs. 5.2.1** and **5.2.2**.

First, we check the consistency of the two tests for the JENDL Dosimetry File. Among the eight commonly tested reactions, both tests assigned class A to five reactions ^{27}Al(n, α)^{24}Na, Ti(n, x)^{46}Sc, Ti(n, x)^{48}Sc, ^{93}Nb(n, 2n)^{92m}Nb and ^{58}Ni(n, 2n)^{57}Ni, and class B to two reactions ^{54}Fe(n, p)^{54}Mn and ^{59}Co(n, 2n)^{58}Co, respectively. A little large difference of $(C-E)/E$ value is found only for one reaction of ^{58}Ni(n, p)^{58}Co, the reason of which is discussed later. As for the sign of the deviation, almost all reactions showed the same direction of deviation. Similar tendency can be seen also in the case of the IRDF-85 file (**Table 5.2.2**). Thus, the consistency between the two tests can be verified.

The ^{58}Ni(n, p)^{58}Co reaction has relatively low threshold energy among the reactions. One of the possible reasons of the difference between the two tests for ^{58}Ni(n, p)^{58}Co reaction is due to ambiguity of the spectrum in the low energy region in the Li(d, n) field, where the parasitic component of the ^{12}C(d, n) neutrons around 1 MeV could contribute to this reaction.

In the sixth column of both tables, we give the overall degree of performance (status) of each reaction considering the error bands of the results and characteristic of both fields. If both assignments were different, the results of the T+d field were in general more weighted than that in the Li+d field because the former experimental uncertainties were smaller than the latter; e.g., for the ^{93}Nb(n, 2n) reaction in **Table 5.2.1**, the status A in the former field and B the latter resulted in A as the overall status. We can also find reversed cases for the ^{58}Fe(n, p) reaction in both tables where the results of the Li+d field were more weighted. Almost two-thirds of the tested cross sections of the JENDL Dosimetry File are classified as A, and 85 % of the tested cross sections are considered to be good or marginal (A or B). This situation is considerably better than that of the IRDF-85 file.

It is recommended, however, that further differential and integral measurements, and evaluation should be performed for the following reactions assigned as classes B, C and D; three reactions assigned as classes B and C from the test in the T+d field: ^{54}Fe(n, p)^{54}Mn, Ti(n, x)^{47}Sc and ^{59}Co(n, 2n)^{58}Co; five reactions assigned as B, C and D from the test in the Li+d: ^{54}Fe(n, p)^{54}Mn, ^{58}Ni(n, p)^{58}Co, ^{55}Mn(n, 2n)^{54}Mn, ^{23}Na(n, 2n)^{22}Na and ^{59}Co(n, 2n)^{58}Co. It is worth to note that the ^{54}Fe(n, p)^{54}Mn reaction is commonly recommended for further examination because this reaction is very important not only for the dosimetry of fusion reactors but also for the fission reactor pressure vessel surveillance because of its low threshold energy and long half-life.

Table 5.2.1 (Cal. −Exp.) /Exp. values in % and status of the respective spectrum averaged cross sections of the T+d fusion simulated field #2 and of the thich Li (d, n) neutron field for the JENDL Dosimetry File taken from Tables 4.1.2 (b) and 4.2.4, respectively.

Reaction[a]			(C-E)/E (%) and status[b]				overall status[c]
			T+d field #2		Li(d, n)		
In-115	(n, n')	In-115m	−1.8	A	−[d]		A
Fe-54	(n, p)	Mn-54	−6.5	B	−12.0	C	C
Ni-58	(n, p)	Co-58	−0.7	A	−10.0	B	A
Zn-64	(n, p)	Cu-64	−2.4	A	−		A
Ti	(n, x)	Sc-47	11.7	C	−		C
Ti	(n, x)	Sc-46	3.3	A	6.0	B	A
Ni-60	(n, p)	Co-60	−		−7.0	B	B
Mg-24	(n, p)	Na-24	−		−1.0	A	A
Au-197	(n, 2n)	Au-196	−		1.0	A	A
Al-27	(n, α)	Na-24	−3.4	A	−2.0	A	A
Fe-56	(n, p)	Mn-56	−4.0	A	−		A
Co-59	(n, α)	Mn-56	3.0	A	−		A
Cu-63	(n, α)	Co-60	−		−4.0	A	A
Ti	(n, x)	Sc-48	−0.3	A	2.0	A	A
Nb-93	(n, 2n)	Nb-92m	1.7	A	6.0	B	A
Zr-90	(n, 2n)	Zr-89	−4.8	A	−		A
Mn-55	(n, 2n)	Mn-54	−		16.0	C	C
Na-23	(n, 2n)	Na-22	−		−11.0	C	C
Co-59	(n, 2n)	Co-58	5.6	B	10.0	B	B
Ni-58	(n, 2n)	Ni-57	−1.0	A	−4.0	A	A

a) ordered by threshold energy.

b) A: discrepancy less than 5 %, B: between 5 and 10 %,
C: between 10 and 20 %, D: over 20 %.

c) see text.

d) −: not measured.

Table 5.2.2 (Cal. −Exp.) /Exp. values in % and status of the respective spectrum averaged cross sections of the T+d fusion simulated field #2 and of the thich Li (d, n) neutron field for IRDF-85 taken from Tables 4.1.2 (b) and 4.2.4, respectively.

Reaction[a]			(C−E)/E (%) and status[b]				overall status[c]
			T+d field #2		Li(d, n)		
In-115	(n, n')	In-115m	−3.9	A	−[d]		A
Fe-54	(n, p)	Mn-54	−12.4	C	−16.0	C	C
Ni-58	(n, p)	Co-58	0.5	A	−7.0	B	A
Zn-64	(n, p)	Cu-64	2.1	A	−		A
Ti	(n, x)	Sc-47	6.2	B	−		B
Ti	(n, x)	Sc-46	−2.8	A	−1.0	A	A
Ni-60	(n, p)	Co-60	−		−7.0	B	B
Mg-24	(n, p)	Na-24	−		−1.0	A	A
Au-197	(n, 2n)	Au-196	−		−		−
Al-27	(n, α)	Na-24	−3.0	A	(0.0)[e]		A
Fe-56	(n, p)	Mn-56	−6.7	B	−		B
Co-59	(n, α)	Mn-56	−5.5	B	−		B
Cu-63	(n, α)	Co-60	−		24.0	D	D
Ti	(n, x)	Sc-48	−1.9	A	2.0	A	A
Nb-93	(n, 2n)	Nb-92m	−		−		−
Zr-90	(n, 2n)	Zr-89	−0.0	A	−		A
Mn-55	(n, 2n)	Mn-54	−		16.0	C	C
Na-23	(n, 2n)	Na-22	−		−14.0	C	C
Co-59	(n, 2n)	Co-58	7.7	B	13.0	C	B
Ni-58	(n, 2n)	Ni-57	−5.2	B	−14.0	C	B

a) ordered by threshold energy.

b) A: discrepancy less than 5 %, B: between 5 and 10 %, C: between 10 and 20 %, D: over 20 %.

c) see text.

d) −: not measured or not given in the file.

e) reference cross section for Li(d, n) field.

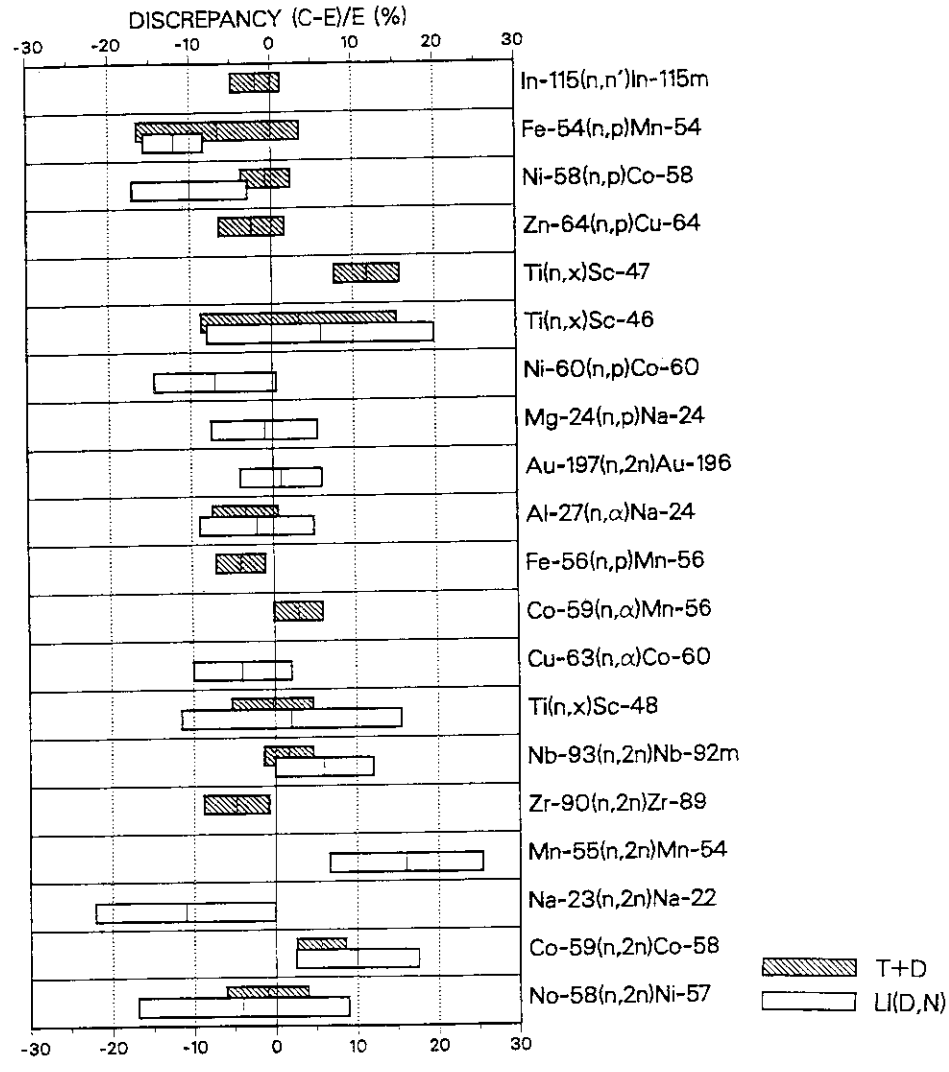

Fig. 5.2.1 (C–E)/E values of the average cross sections of tested 14 reactions for the JENDL Dosimetry File in the T+d fusion simulated field and the thick Li (d, n) neutron field.

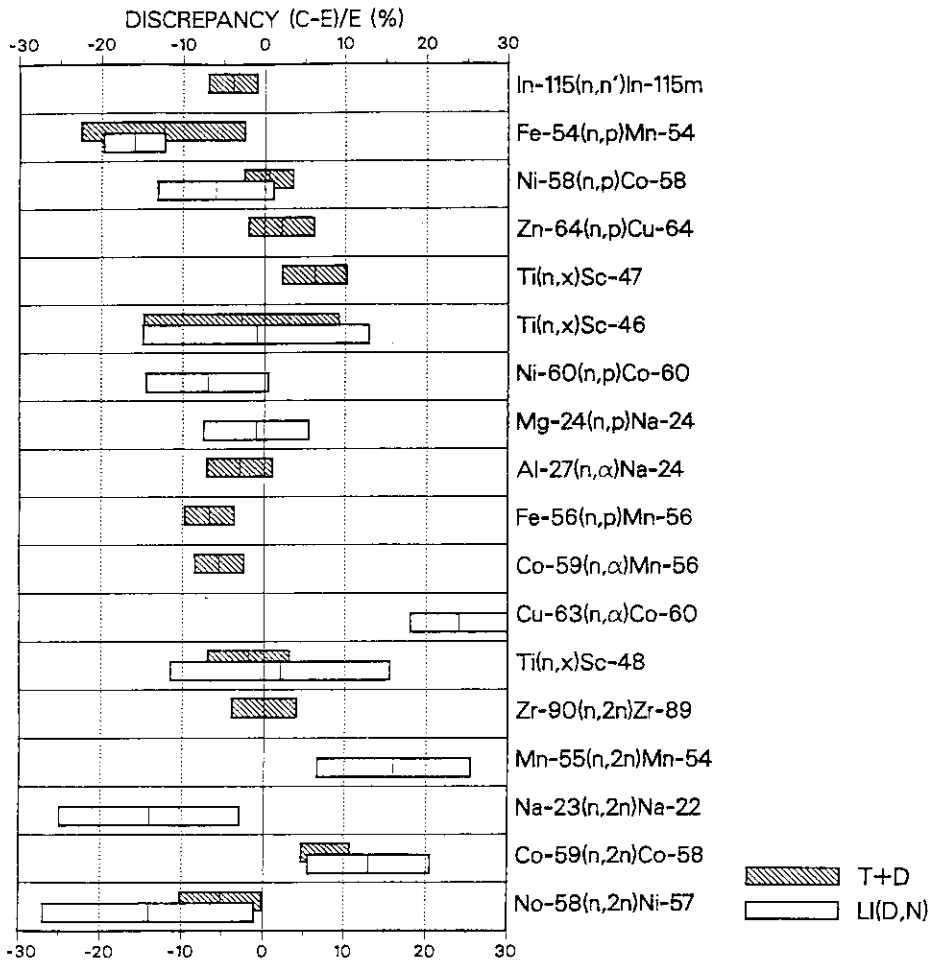

Fig. 5.2.2 (C–E)/E values of the average cross sections of tested 14 reactions for IRDF–85 in the T+d fusion simulated field and the thick Li (d, n) neutron field.

6. Conclusion

A new dosimetry file has been completed on the basis of Japanese Evaluated Nuclear Data Library Version 3 (JENDL–3), and here are summarized all the documentations of this JENDL Dosimetry File including both results of the comparison study with IRDF–85 and several integral tests in the benchmark neutron fields.

Generally good agreement has been obtained in those comparison studies with IRDF–85 and/or experimental data, and a little improvement has been observed especially in the benchmark test of the 14 MeV neutron field.

As is sometimes mentioned in this report, many covariance matrices of the cross sections in this dosimetry file are much indebted to IRDF–85 data. Through the work to produce the dosimetry file from JENDL–3, necessity of covariance matrices has been felt many times. They are expected to be included in the next version of JENDL.

Finally, we welcome any comments, questions and suggestions to this dosimetry file, on which we would like to improve in the next version of the JENDL Dosimetry File.

Acknowledgments

The authors sincerely appreciate all the persons concerning to complete the JENDL–3, the present result is perfectly indebted to their faithful and continuous efforts in the evaluation for long years. They would like to appreciate Drs. Y. Kikuchi and Y. Nakajima for a careful reading of this manuscript and for many helpful suggestions and comments. They hope to write here the name of late Dr. Shungo Iijima. He was basically a pioneer in the Japanese nuclear data evaluation study, and he was also a very important member in our dosimetry integral test working group. They are truly glad to have had an opportunity to dedicate the JENDL Dosimetry File to him.

6. Conclusion

A new dosimetry file has been completed on the basis of Japanese Evaluated Nuclear Data Library Version 3 (JENDL–3), and here are summarized all the documentations of this JENDL Dosimetry File including both results of the comparison study with IRDF–85 and several integral tests in the benchmark neutron fields.

Generally good agreement has been obtained in those comparison studies with IRDF–85 and/or experimental data, and a little improvement has been observed especially in the benchmark test of the 14 MeV neutron field.

As is sometimes mentioned in this report, many covariance matrices of the cross sections in this dosimetry file are much indebted to IRDF–85 data. Through the work to produce the dosimetry file from JENDL–3, necessity of covariance matrices has been felt many times. They are expected to be included in the next version of JENDL.

Finally, we welcome any comments, questions and suggestions to this dosimetry file, on which we would like to improve in the next version of the JENDL Dosimetry File.

Acknowledgments

The authors sincerely appreciate all the persons concerning to complete the JENDL–3, the present result is perfectly indebted to their faithful and continuous efforts in the evaluation for long years. They would like to appreciate Drs. Y. Kikuchi and Y. Nakajima for a careful reading of this manuscript and for many helpful suggestions and comments. They hope to write here the name of late Dr. Shungo Iijima. He was basically a pioneer in the Japanese nuclear data evaluation study, and he was also a very important member in our dosimetry integral test working group. They are truly glad to have had an opportunity to dedicate the JENDL Dosimetry File to him.

References

1) Cullen D.E., Kocherov N., and McLaughlin P.M.: "The International Reactor Dosimetry File (IRDF-82)", IAEA-NDS-41/R, rev.0 (1982). IRDF-85 is a modified version with additional cross section data.
2) BNL/National Nuclear Data Center: ENDF/B-V.
3) Shibata K., Nakagawa T., Asami T., Fukahori T., Narita T., Chiba S., Mizumoto M., Hasegawa A., Kikuchi Y., Nakajima Y., and Igarasi S.: "Japanese Evaluated Nuclear Data Library, version-3", JAERI 1319 (1990).
4) Kawai M., Iijima S., Nakagawa T., Nakajima Y., Sugi T., Watanabe T., Matsunobu H., Sasaki M., and Zukeran A.: J. Nucl. Sci. Technol., **29**, 195 (1992).
5) Kocherov N., and Vonach H.K.: Proc. 7-th ASTM-EURATOM Symposium on Reactor Dosimetry, Strasbourg, France, Aug. 27-31, 1990 (to be published).
6) BNL/National Nuclear Data Center: ENDF/B-VI (1990).
7) (Revised by) Kinsey R.: "Data Formats and Procedures for the Evaluated Nuclear Data File, ENDF", BNL-NCS-50496 (ENDF 102), 2nd edition (1979).
8) Nakagawa T.: "Program RESENDD (version 84-07): A Program for Reconstruction of Resonance Cross Sections from Evaluated Nuclear Data in the ENDF/B Format", JAERI-M 84-192 (1984).
9) Cullen D.E.: "Summary of ENDF/B Pre-processing Codes", IAEA-NDS 39, Rev.(1983).
10) Nakagawa T.: "Program CRECTJ5", to be published.
11) Yamamuro N., Iijima S., and Asami T.: "Activation Cross Section Data File (II)", JAERI-M 91-006 (1991).
12) Yamamuro N.: "A Nuclear Cross Section Calculation System with Simplified Input Format version II (SINCROS-II)", JAERI-M 90-006 (1990).
13) Young P.G., and Arthur E.D.: "GNASH: A Preequilibrium, Statistical Nuclear-Model Code for Calculation of Cross Sections and Emission Spectra", LA-6947 (1977).
14) Weigold E., and Glover R.N.: Nucl. Phys., **32**, 106 (1962).
15) Santry D.C., and Butler J.P.: Can, J. Phys., **50**, 2536 (1972).
16) Gayther D.B., Uttey C.A., Murphy M.F., Taylor W.H., and Randle K.: Proc. Int. Conf. on Nuclear Data for Science and Technol., Mito, Japan, May 30 - June 3, 1988, p. 1057 (1988).
17) Ryves T.B., and Kolkowski P.: J. Phys., **G7**, 529 (1981).
18) Ikeda Y., Konno C., Oishi K., Nakamura T., Miyade H., Kawade H., Yamamoto H., and Katoh T.: "Activation Cross Section Measurements for Fusion Reactor Structural Materials at Neutron Energy from 13.3 to 15.0 MeV using FNS Facility", JAERI 1312 (1988).
19) Bormann M., Bissem H.H., Magiera E., and Warnemuende R.: Nucl. Phys., **A157**, 481 (1970).
20) Smith A.B., Chiba S., Smith D.L., Meadows J.W., Guenther P.T., Lawson R.D., and Howerton R. J.: "Evaluated Neutronic File for Indium", ANL/NDM-115 (1990).
21) Mughabghab S.F., Divadeenam M., and Holden N.E.: "Neutron Cross Sections, vol. 1, Part A", Academic Press (1981), and Mughabghab S.F.: "Neutron Cross Sections, vol.1, Part B", Academic Press (1984).
22) Yamamuro N.: private communication (1990).
23) Wagner M., Vonach H., Pavlik A., Strohmaier B., Tagesen S., and Martinez-Rico J.: "Evaluation of Cross Sections for 14 Important Neutron-Dosimetry Reactions", Physics Data 13-5 (1990).
24) Sakurai K.: J. Nucl. Sci. Technol., **19**, 775 (1982).
25) Heaton H.T.II, Gilliam D.M., Spiegel V., Eisenhauer C., and Grundl J.A.: Proc. NEANDC/

NEACRP Specialists Meeting on Fast Neutron Fission Cross Sections of U-233, U-235, U-238, and Pu-239, Argonne, USA, Jun. 28 - 30, 1976, ANL-76-90, p. 333 (1976).
26) Grundl J.A., and Eisenhauer C.M.: Proc. Conf. on Nuclear Cross Sections and Technology, Washington, USA, Mar. 3-7, 1975, Vol. I, p. 250 (1975).
27) Eisenhauer C.M., Grundl J.A., and Fabry A.: Proc. Int. Specialists Symposium on Neutron Standards and Applications, Gaithersburg, USA, Mar. 28-31, 1977, p. 329 (1977).
28) Rogers J.W., Harker Y.D., and Millsap D.A.: Proc. Consultants' Meeting on Integral Cross-section Measurements in Standard Neutron Fields for Reactor Dosimetry, IAEA Vienna, Austria, Nov. 15 -19, 1976, IAEA-208, vol. II, p. 117 (1978).
29) Dowdy E.J., Lozito E.J., and Plassman E.A.: Nucl. Tech., **25**, 381 (1975).
30) Grundl J., and Eisenhauer C.: Proc. Consultants' Meeting on Integral Cross-section Measurements in Standard Neutron Fields for Reactor Dosimetry, IAEA Vienna, Austria, Nov. 15-19, 1976, IAEA -208, vol.I, p. 53 (1978).
31) Greenwood L.: Oak Ridge Research Reactor (ORR), private communication to IAEA(1981).
32) Kobayashi K., Kimura I., Nakazawa M., and Akiyama M.: J. Nucl. Sci. Technol., **13**, 531 (1976), and Greenwood L.: private communication to IAEA.
33) Goel B.: private communication to IAEA (1981).
34) Vlasov M.F.(Ed.): "IAEA Consultants' Meeting on Integral Cross-section Measurements in Standard Fields", IAEA Vienna, Nov. 15-19, 1976, INDC (NDS)-81/L+M (1977).
35) Okamoto K.(Ed.): Proc. IAEA Advisory Group Meeting on Properties of Neutron Source, Leningrad, USSR, Jun. 9-13, 1986, IAEA-TECDOC-410 (1987).
36) Lemmel H.D.(Ed.): Proc. IAEA Consultants' Meeting on Physics of Neutron Emission in Fission, Mito, Japan, May 24-27, 1988, INDC (NDS)-220/L (1989).
37) Mannhart W.: Proc. 6-th ASTM-EURATOM Symposium on Reactor Dosimetry, Jackson Hole, USA, May 31 - Jun. 5, 1987, p.340 (1989) and IAEA Consultants' Meeting on Physics of Neutron Emission in Fission, Mito, May 24-27, 1988, INDC(NDS)-220/L, p. 305 (1989).
38) Armitage B.H., and Sowerby M.G.(Ed.): Proc. Specialist Meeting on Inelastic Scattering and Fission Neutron Spectra, Harwell, UK, Apr. 14-16, 1975, AERE-R 8636 (1977).
39) Johansson P.I., and Holmqvist B.: Nucl. Sci. Eng., **62**, 695 (1977).
40) Baard J.H., Zijp W.L., Nolthenius H.J.: "Nuclear Data Guide for Reactor Neutron Metrology", Kluwer Academic Publishers (1989).
41) Madland D.G., and Nix J.R.: Nucl. Sci. Eng., **81**, 213 (1982).
42) Maerten H., and Seeliger D.: Proc. Advisory Group Meeting on Nuclear Standards Reference Data, Geel, Belgium, Nov. 12-16, 1984, IAEA-TECDOC-335, p. 255 (1985).
43) Browne J.C., and Dietrich F.S.: Phys. Rev., **C10**, 2545 (1974).
44) Ohsawa T.: to be published as a KURRI-TR Technical Report, and "Two-Temperature Madland-Nix Model for Fission Neutron Spectrum Calculation", 1990 Fall Meeting of the Atomic Energy Society of Japan, Bll (p. 69), Oct. 1990.
45) Kimura I., and Kobayashi K.: Nucl. Sci. Eng., **106**, 332 (1990).
46) Kobayashi K., and Kobayashi T.: NEANDC(J)-155/U, p. 52 (1990).
47) Kobayashi K., Kimura I., Li ZhaoHuan and Wang YongQing: Proc. 7-th ASTM-EURATOM Symp. on Reactor Dosimetry, Strasbourg, France, Aug. 27-31, 1990 (to be published).
48) Petilli M., and Gilliam D.M.: Proc. 5-th ASTM-EURATOM Symp. on Reactor Dosimetry, Geesthacht, Germany, Sep. 24-28, 1984, p.657 (1984).
49) Mannhart W.: "Handbook on Nuclear Activation Data", IAEA Technical Report Series No.273, IAEA, p. 413 (1987).
50) Calamand A.: "Handbook on Nuclear Activation Cross Sections", IAEA Technical Reports series No.156, IAEA, p. 273 (1974).

51) Gilliam D.M., Grundl J.A., Lamaze G.P., McGarry E.D., and Fabry A.: Proc. 5-th ASTM-EURATOM Symposium on Reactor Dosimetry, Geesthacht, Germany, Sep. 24-28, 1984, Vol. 2, p. 867 (1984).
52) Mannhart W.: ibid., Vol. 2, p. 813 (1985).
53) Cullen D.E., Kocherov N.P., and McLaughlin P.M.: Nucl. Sci. Eng., **83**, 497 (1983).
54) Lamaze G.P., Eisenhauer C.M., Grundl J.A., McGarry E.D., Schima F.J., and Spiegel V.: Proc. Int. Conf. on Nuclear Data for Sci. Technol., Mito, Japan, May 30 - Jun. 3, 1988, p. 1033 (1988).
55) Broadhead B.L., et al.: Trans. Am. Nucl. Soc., **30**, 590 (1978).
56) Greenwood R.G., Helmer R.G., Rogers J.W., Dudey N.D., Popek R.J., Kellogg L.S., and Zimmer W. H.: Nucl. Technol., **25**, 274 (1975).
57) Rogers J.W., Millsap D.A., and Harker Y.D.: Nucl. Technol., **25**, 330 (1975).
58) Ryskamp J.M., Andrel R.A., Broadhead B.L., Ford W.E., Lucius J.L., Marable J.H., and Wagschal J.J.: Nucl. Technol., **57**, 20 (1982).
59) Anderl R.A., Millsap D.A., Rogers J.W., and Harker Y.D.: "INEL Integral Data Testing Report for ENDF/B-V Dosimetry Cross Sections", USDOE Report EGG-PHYS-5608 (1981).
60) Fabry A., De Leeuw G., and De Leeuw S.: Nucl. Technol., **25**, 349 (1975).
61) Nakazawa M., and Sekiguchi A.: "Dosimetry Data Collection in the Fast Neutron Source Reactor YAYOI", UTNL-R 0037 (1976).
62) Nakazawa M., Taniguchi T., Kato M., Sekiguchi A., Kobayashi K., Sakurai K., and Suzuki S.: "The YAYOI Blind Intercomparison on Multi-Foil Reaction Rate Measurements", UTNL-R 0099 (1981).
63) Zijp W.L., Nolthenius H.J., Zsolnay E.M., Szondi E.J., Verhaag G.C.H.M., Cullen D.E., and Ertek C.: "Interim Report on the REAL-80 Exercise", ECN-82-65 (1982).
64) Engl W.W.Jr.: "A User's Manual for ANISN, A One-Dimensional Discrete Ordinates Transport Code with Anisotropic Scattering", K-1693 (1967).
65) Nakamura T., and Abdou M.A.: Proc. First Int. Symposium on Fusion Nucl. Technol., Tokyo, Japan, Apr. 11-15, 1988, Fusion Eng. Design, **9**, 303 (1989).
66) Oyama Y.: ibid., **9**, 309 (1989).
67) Nakamura T., Maekawa H., Kusano J., Oyama Y., Ikeda Y., Kutsukake C., Tanaka S., and Tanaka Shu.: Proc. 4th Symp. on Accelerator Sci. Technol., RIKEN, Saitama, Japan, Nov. 24-26, 1982, p. 155 (1982).
68) Rhoades W.A., and Mymatt F.R.: "The DOT III Two-Dimensional Discrete Ordinates Transport Code", ORNL/TM-4280 (1979).
69) Shibata K., and Kikuchi Y.: Proc. Int. Conf. on Nuclear Data for Basic and Applied Science, Santa Fe, USA, May 13-17, 1985 Vol .2, p. 1585 (1986).
70) Mannhart W., Smith D.L., and Meadows J.W.: Proc. of a Specialists' Meeting on Neutron Activation Cross Section for Fission and Fusion Energy Applications, Argonne, USA, Sep. 13-15, 1989, p. 121 (1989).
71) Smith D.L.: Proc. Int. Conf. on Nuclear Cross Sections for Technology, Knoxville, USA, Oct. 22-26, 1979, NBS Special Publication 594, p. 285 (1980).
72) Greenwood L.R., Heinrich R.R., Kennerly R.J., and Medrzychowsky R.: Nucl. Technol., **41**, 109 (1978).
73) Smith D.L., Meadows J.W., and Greenwood L.R.: Proc. of 7-th ASTM-EURATOM Symposium on Reactor Dosimetry, Strasbourg, France, Aug. 27-31, 1990 (to be published).
74) Dumais J.R., Iwasaki S., Tanaka S., Odano N., and Sugiyama K.: ibid. (to be published).
75) Mannhart W.: Proc. IAEA Advisory Group Meeting on Properties of Neutron Source, Leningrad, USSR, Jun. 9-13, 1986, IAEA-TECDOC-410, p. 158 (1987).
76) Textor R.E., and Verbinski V.V.: "O5S Monte Carlo Code", ORNL-4160 (1968).

Appendix Graphs of Dosimetry Cross Sections

In this Appendix, the cross sections stored in the JENDL Dosimetry File are shown in a graphical form. As described in 2.3, there are two kinds of files; point-wise file and group-wise file. Here, only the group-wise data are shown together with their one standard deviation and data in IRDF-85. In the graphs, *thick solid lines* represent the JENDL dosimetry file, *thin solid lines* their standard deviations and *dashed lines* IRDF-85.

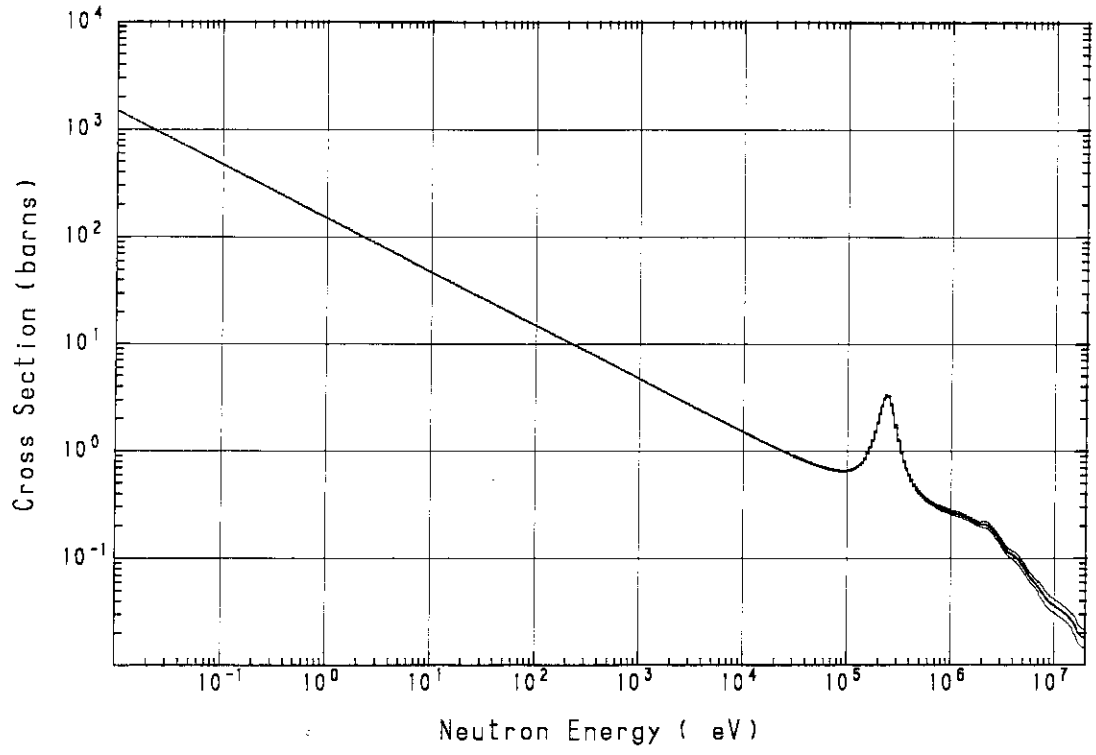

Fig. A.1 ^{6}Li (n, t) α cross section

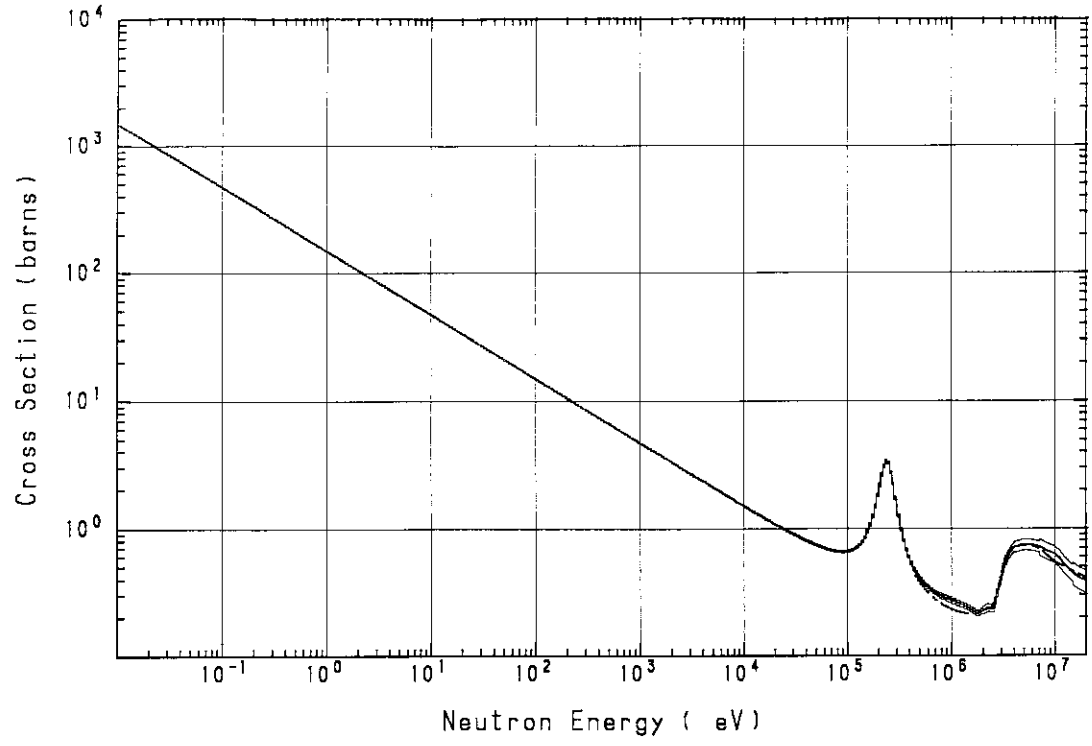

Fig. A.2 ^{6}Li α production cross section

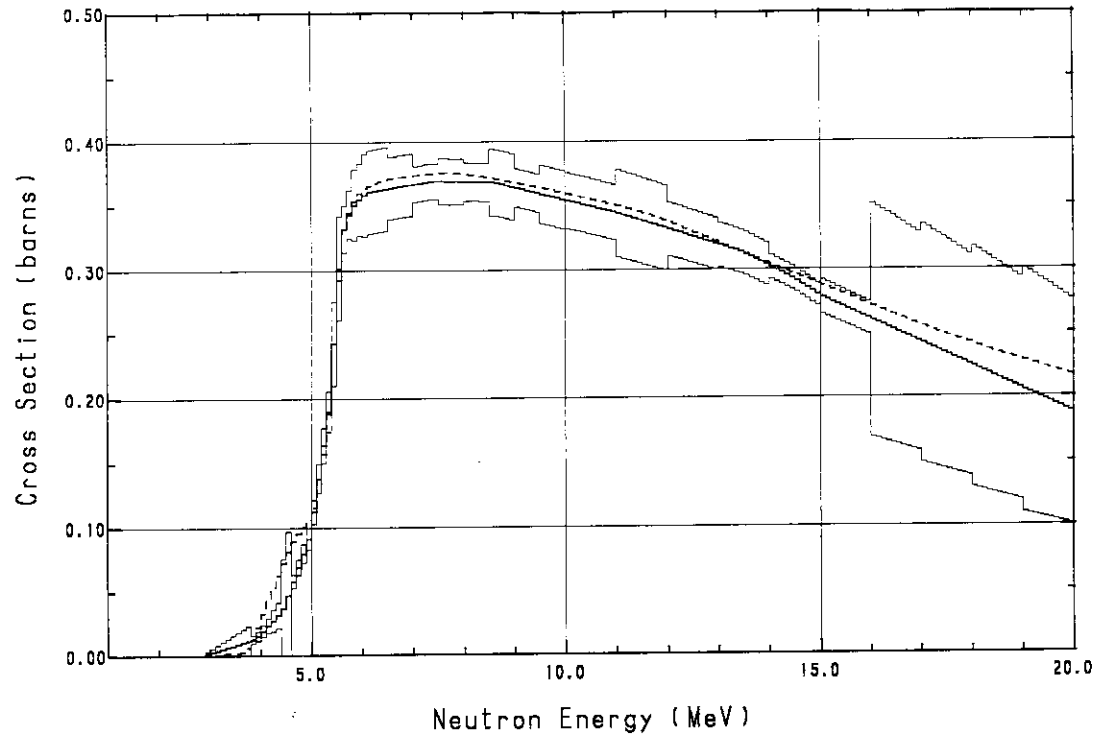

Fig. A.3 ^{7}Li t production cross section

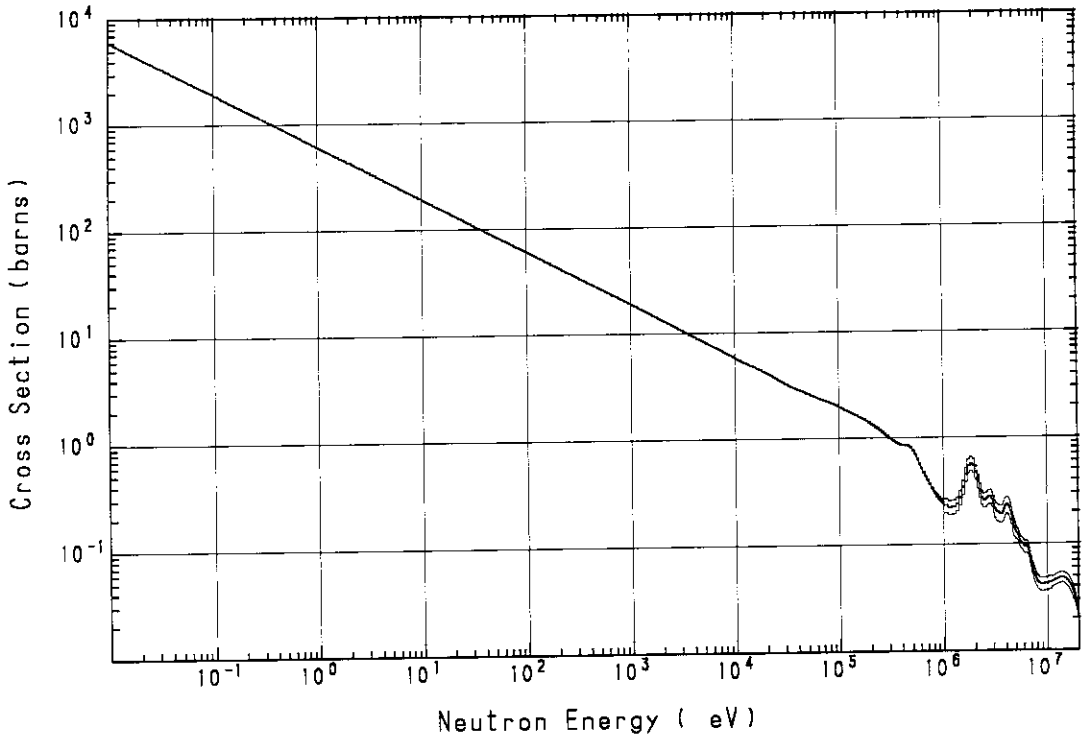

Fig. A.4 ^{10}B (n, α) ^{7}Li cross section

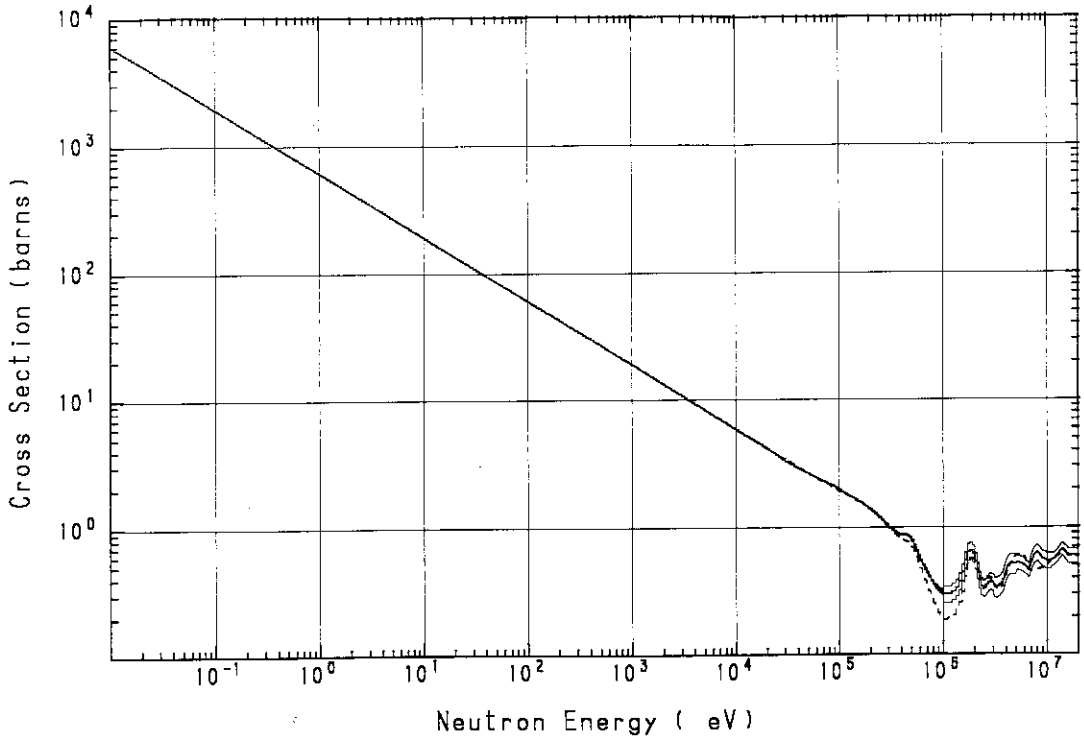

Fig. A.5 ^{10}B α production cross section

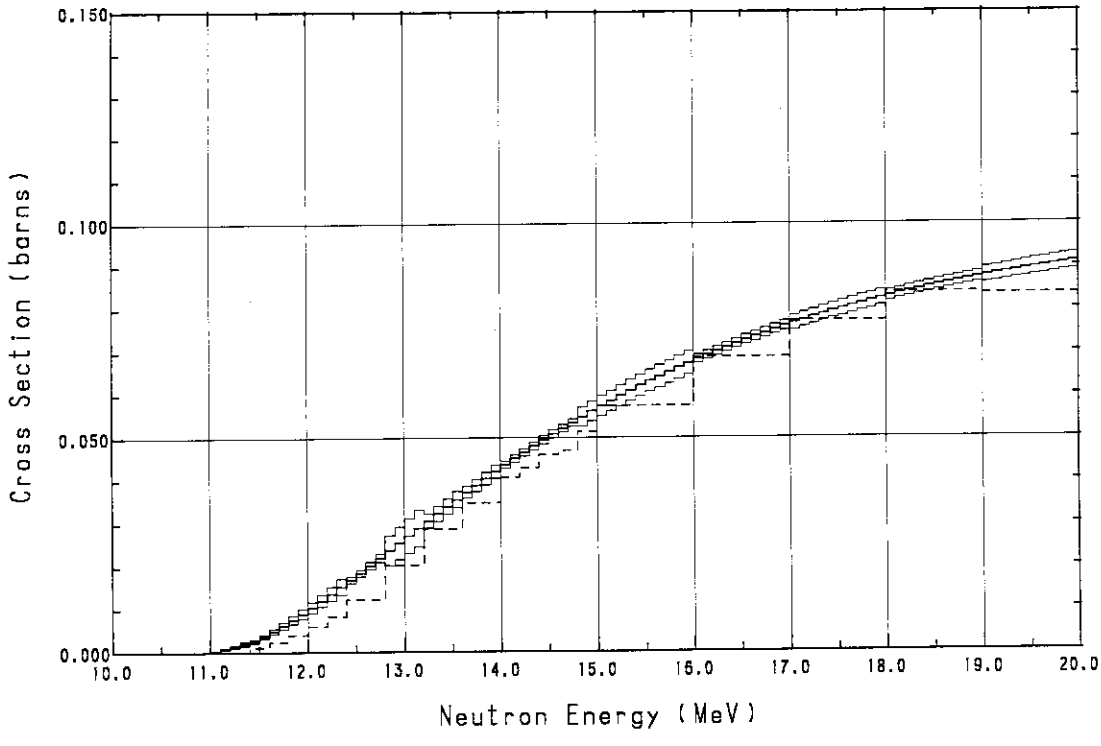

Fig. A.6 ^{19}F (n, 2n) ^{18}F cross section

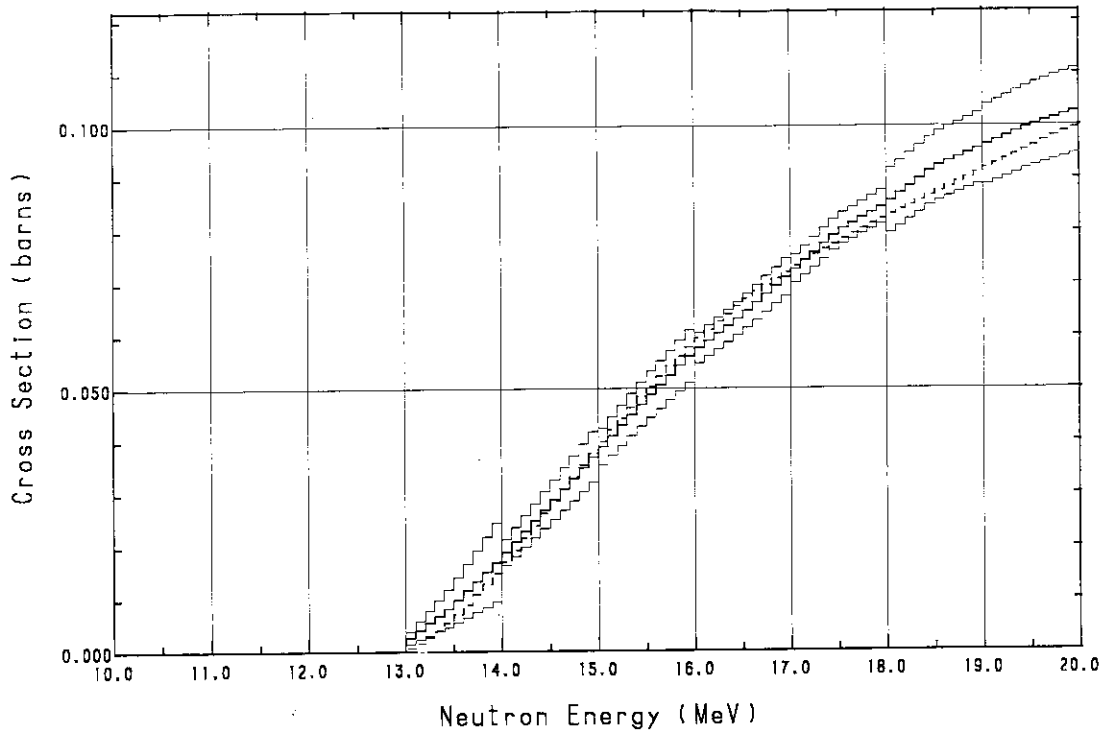

Fig. A.7 ^{23}Na (n, 2n) ^{23}Na cross section

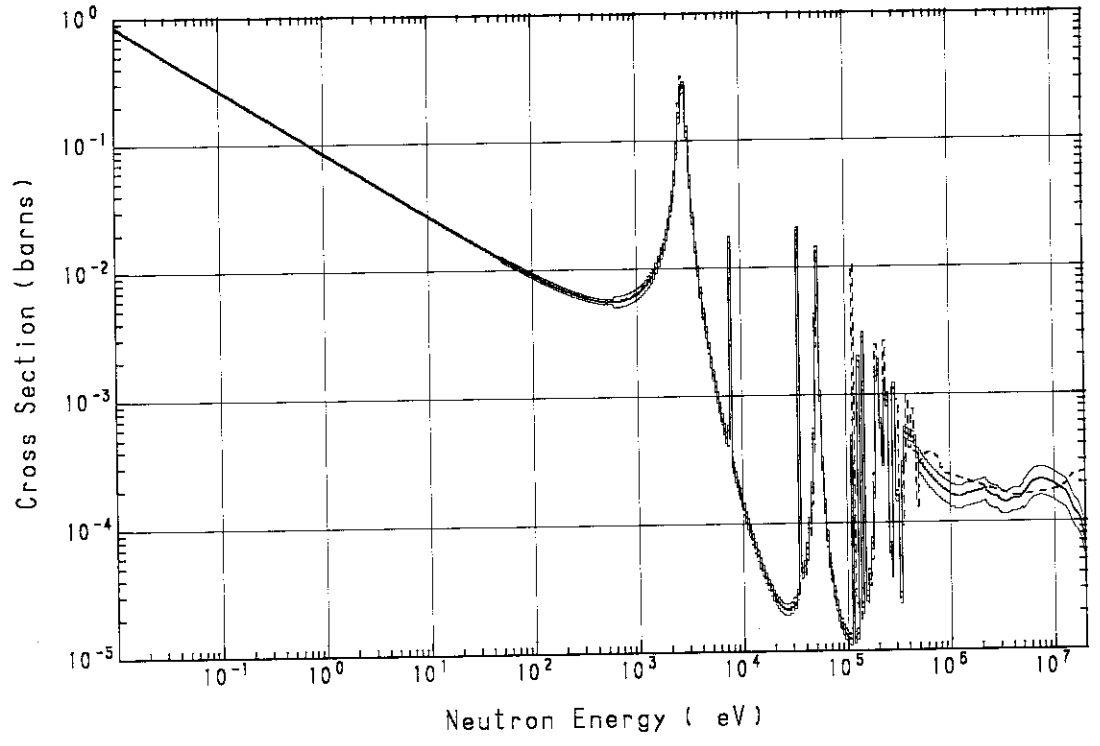

Fig. A.8 ^{23}Na (n, γ) ^{24}Na cross section

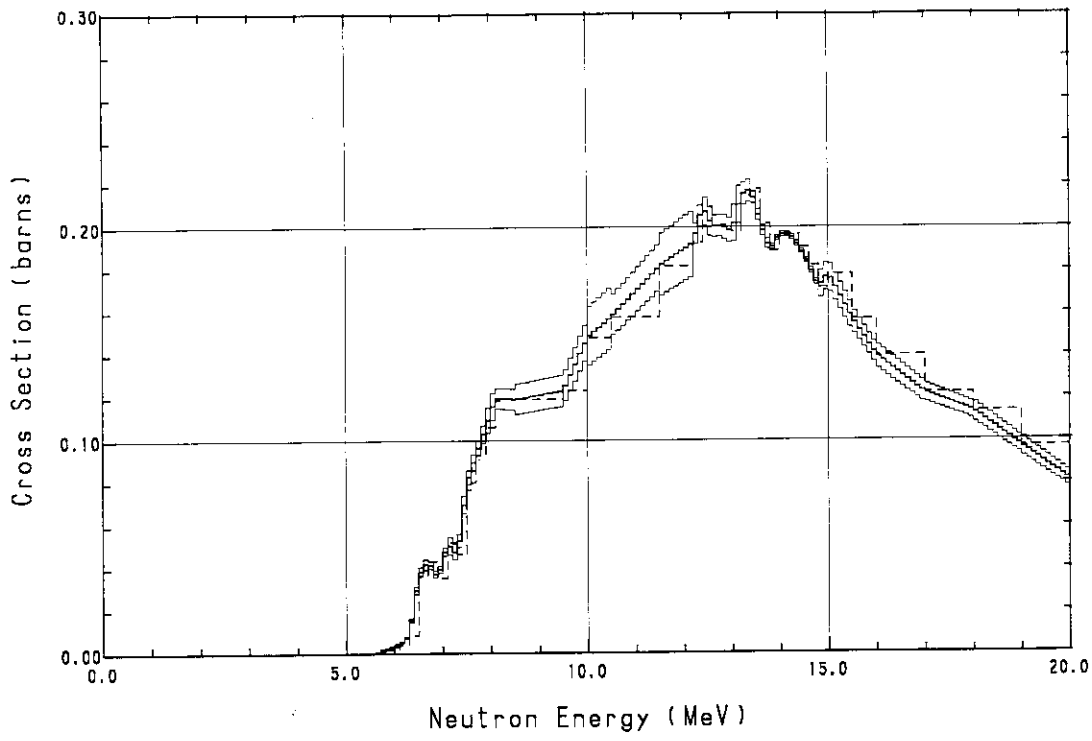

Fig. A.9 ^{24}Mg (n, p) ^{24}Na cross section

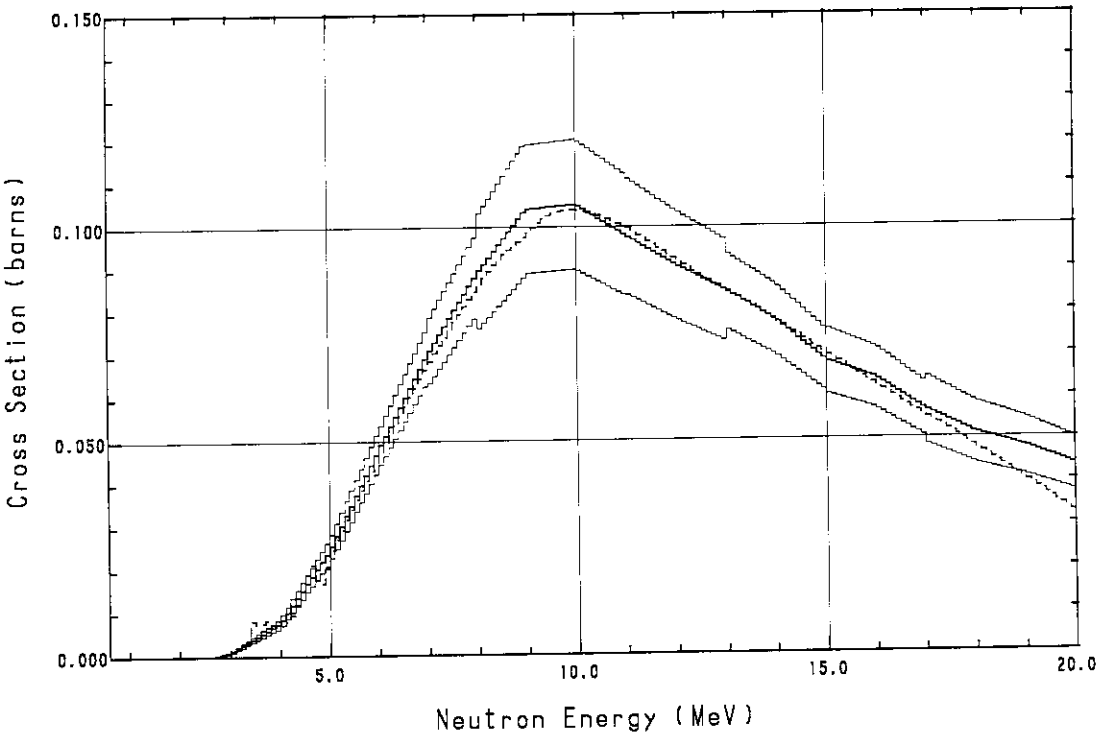

Fig. A.10 ^{27}Al (n, p) ^{27}Mg cross section

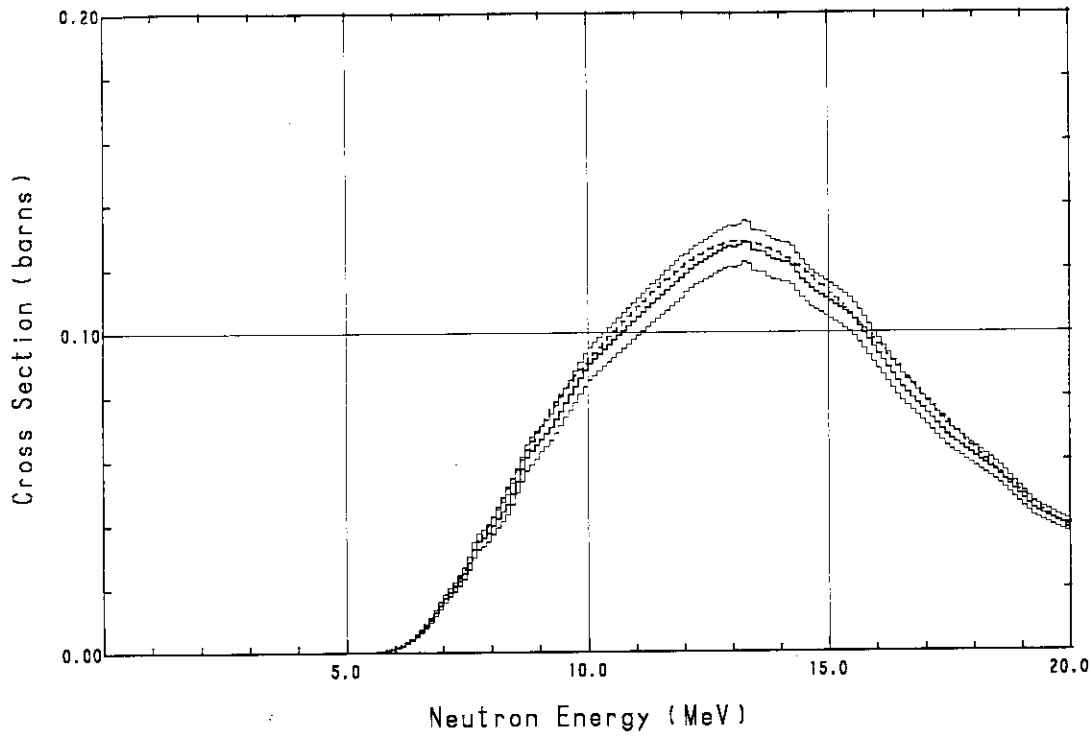

Fig. A.11 ^{27}Al (n, α) ^{24}Na cross section

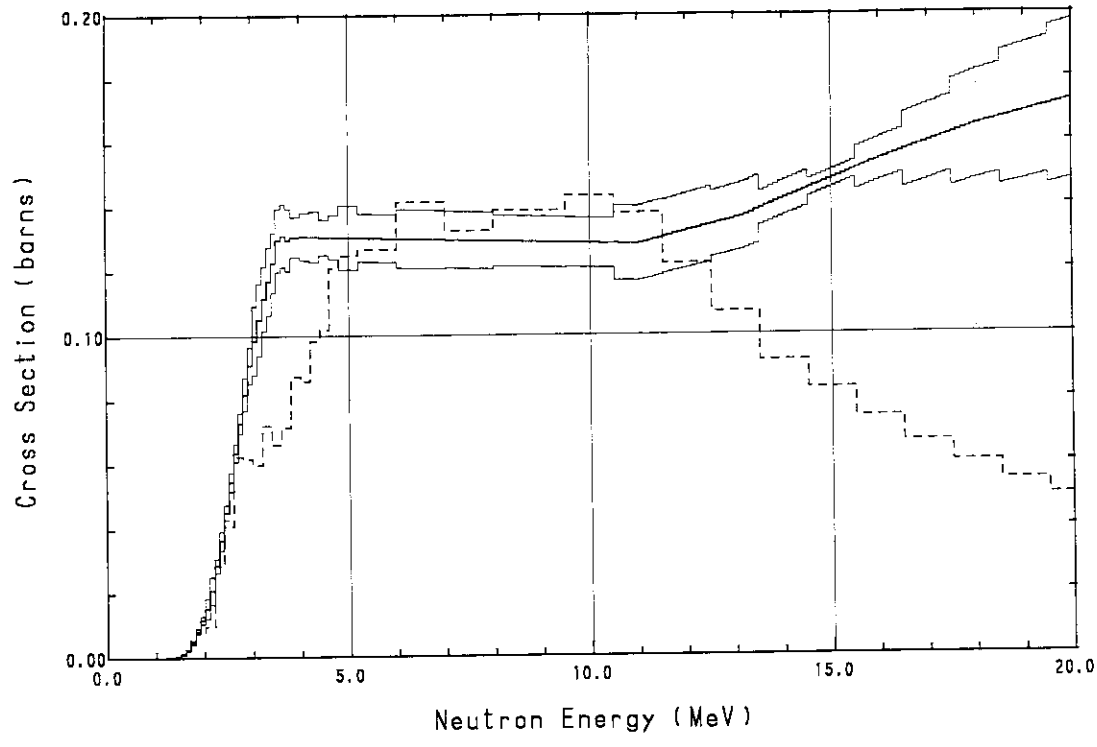

Fig. A.12 ^{31}P (n, p) ^{31}Si cross section

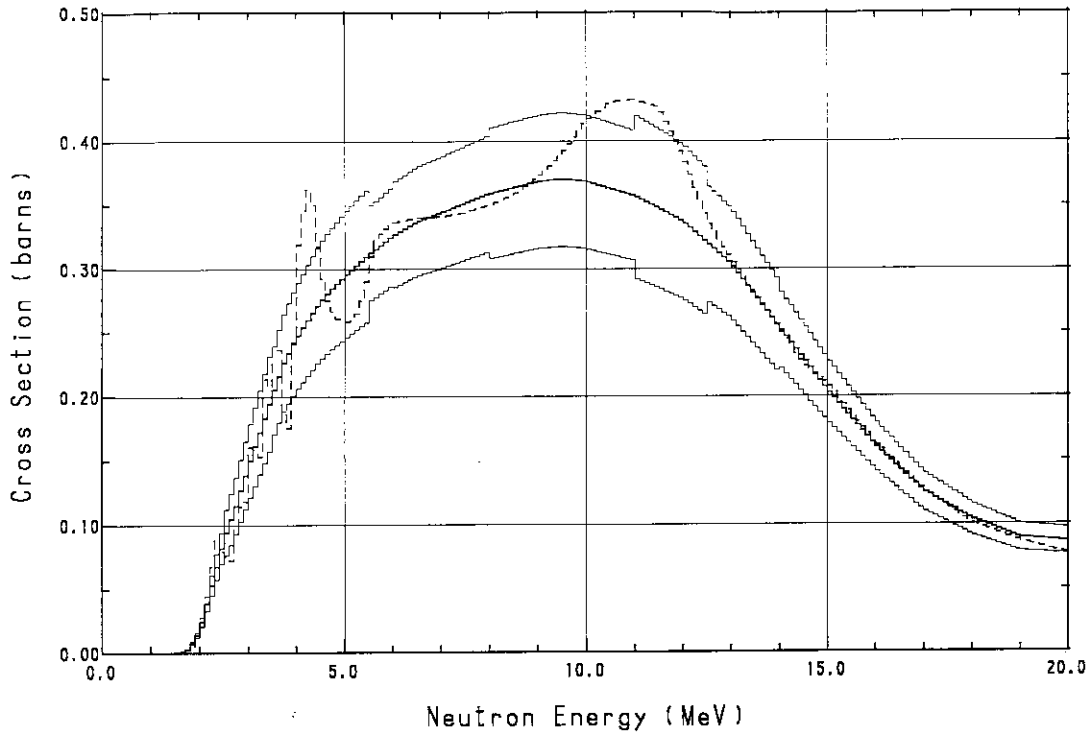

Fig. A.13 ^{32}S (n, p) ^{32}P cross section

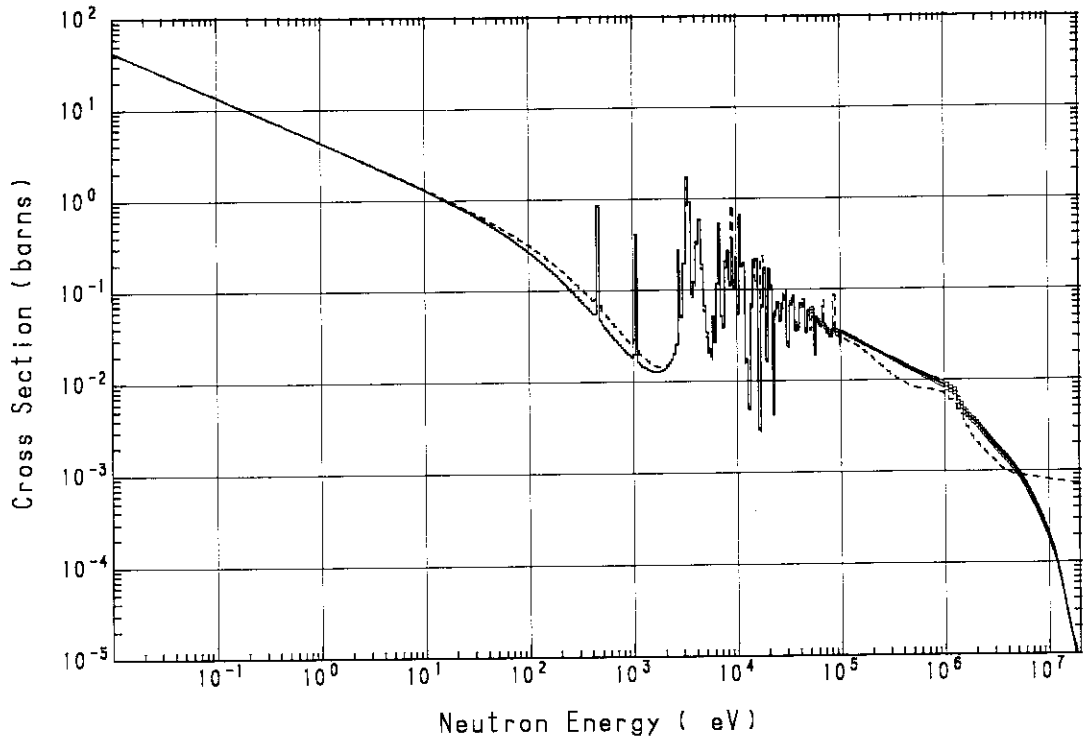

Fig. A.14 ^{45}Sc (n, γ) ^{46}Sc cross section

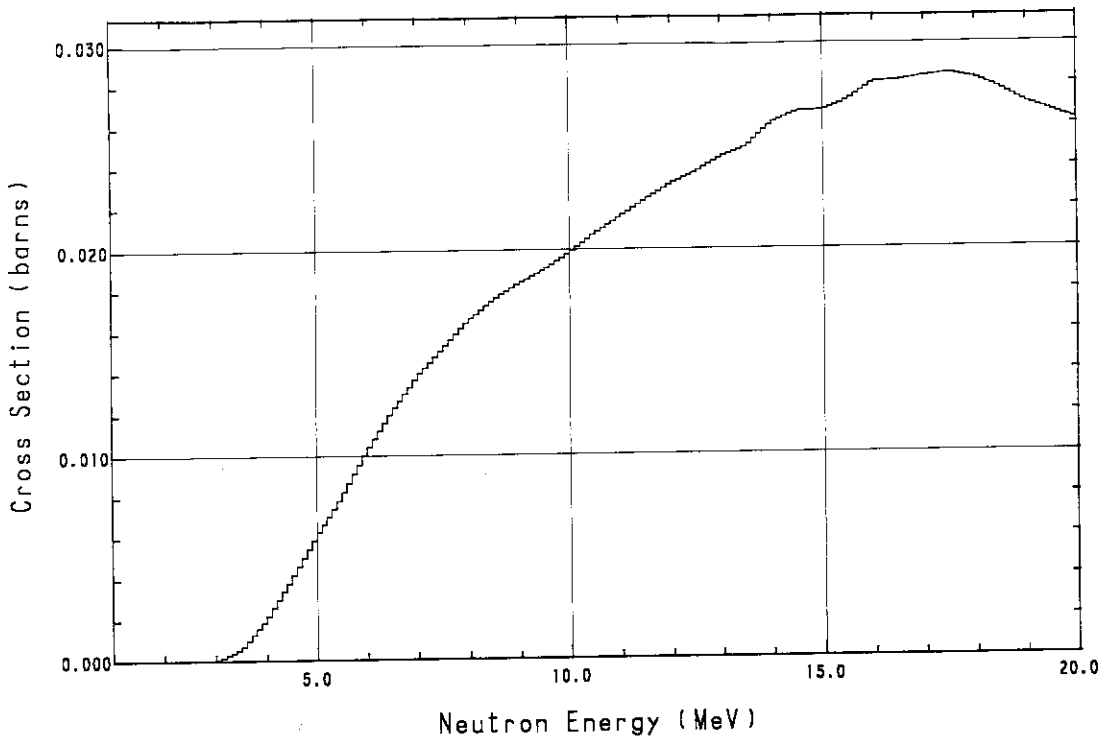

Fig. A.15 Ti (n, x) ^{46}Sc cross section

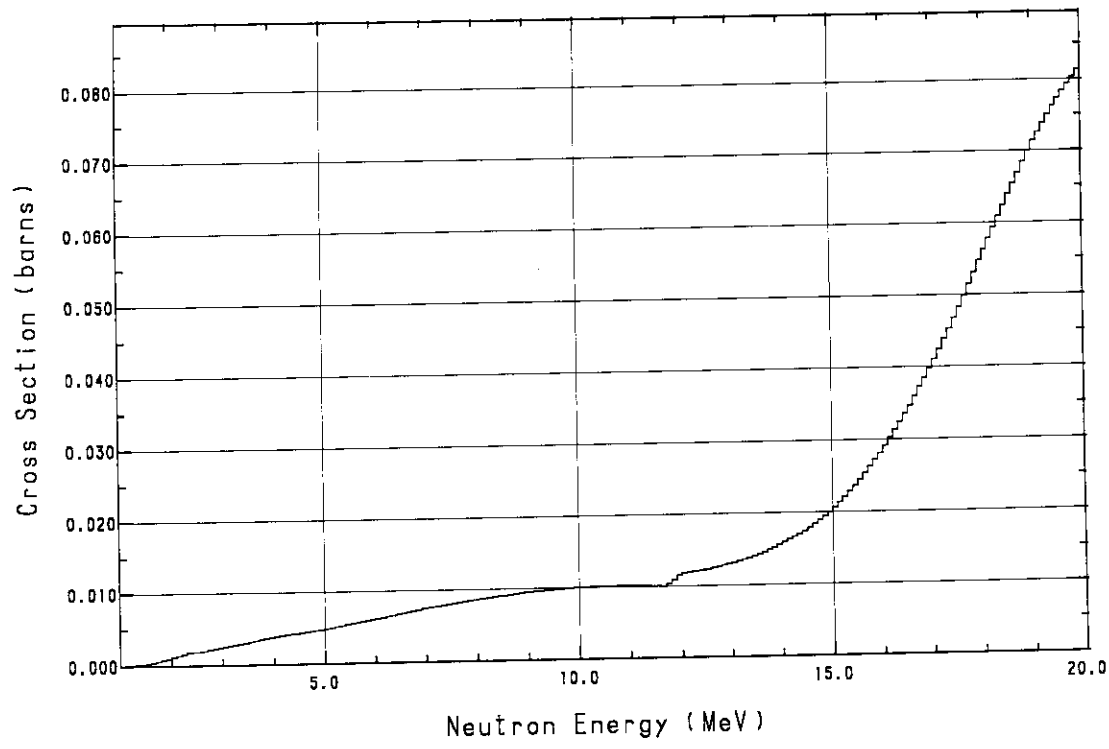

Fig. A.16 Ti (n, x) ^{47}Sc cross section

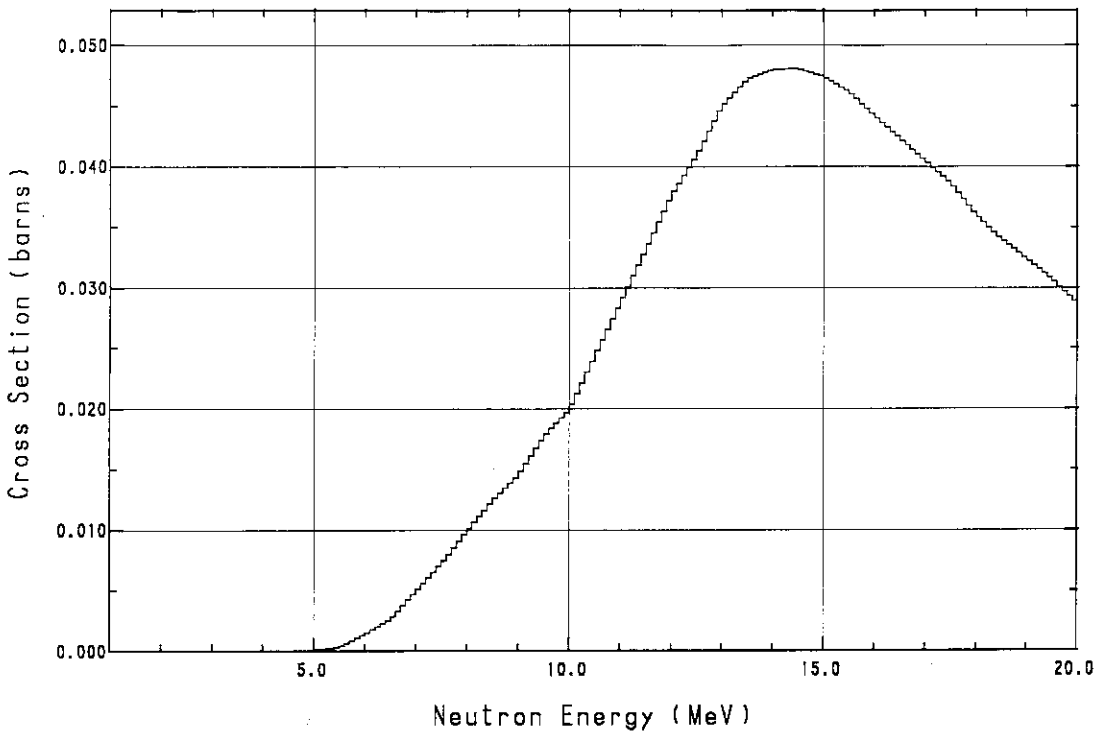

Fig. A.17 Ti (n, x) ^{48}Sc cross section

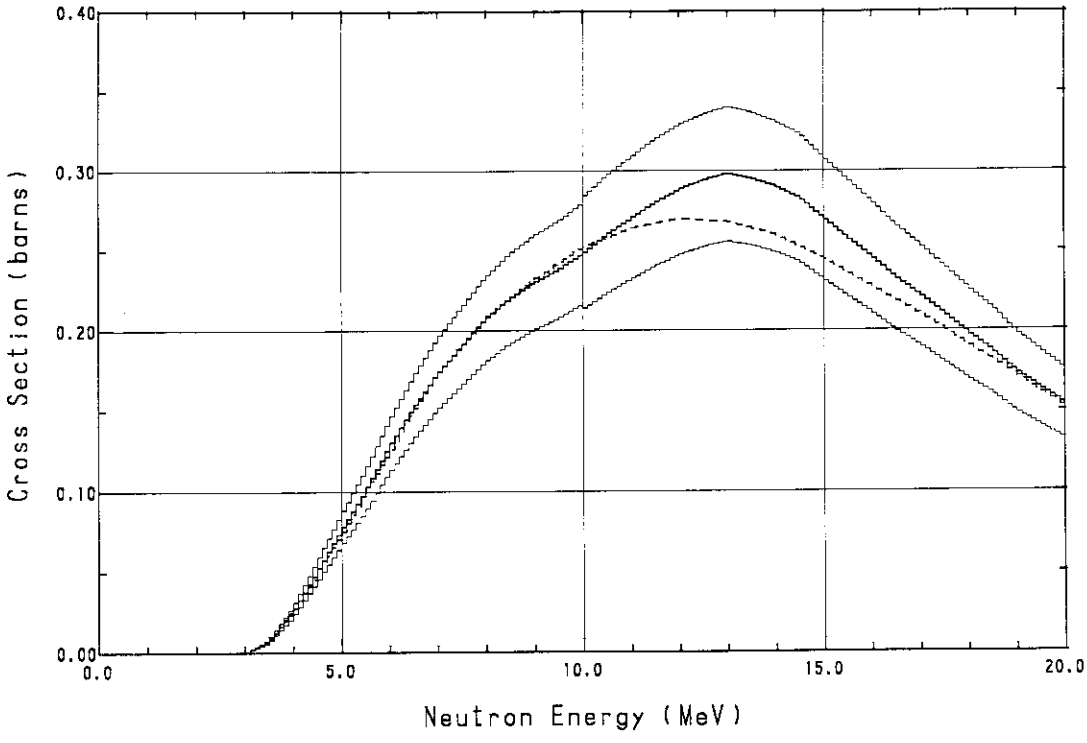

Fig. A.18 ^{46}Ti (n, p) ^{46}Sc cross section

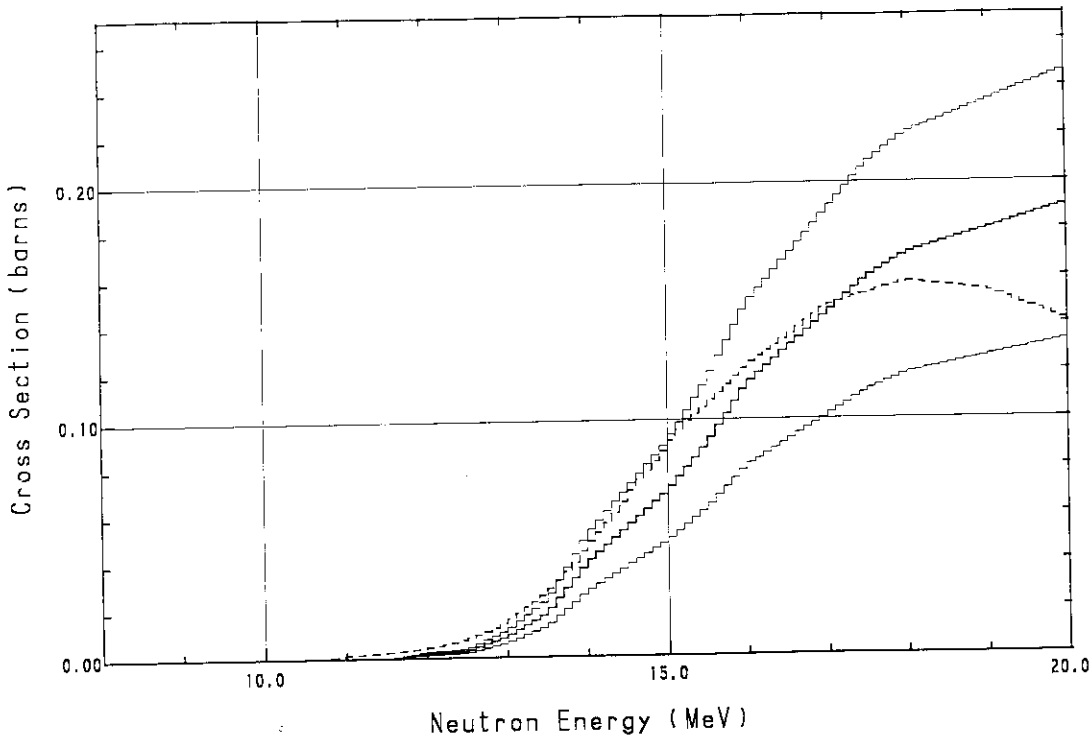

Fig. A.19 ^{47}Ti (n, np) ^{46}Sc cross section

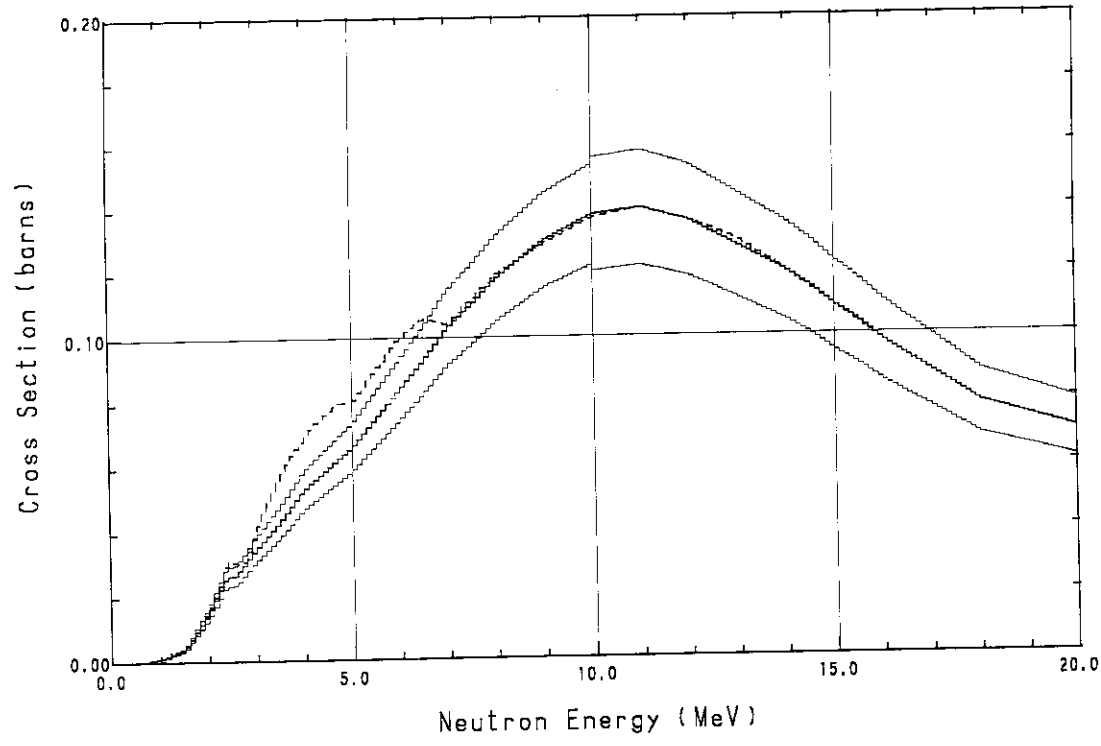

Fig. A.20 ^{47}Ti (n, p) ^{47}Sc cross section

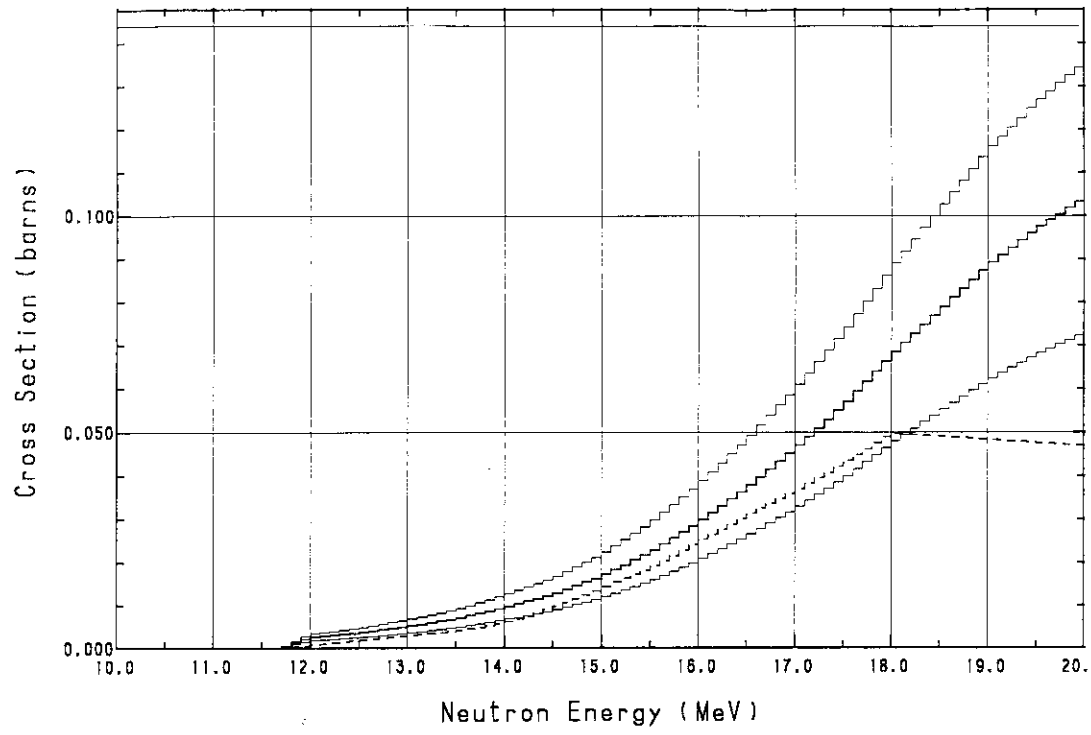

Fig. A.21 ^{48}Ti (n, np) ^{47}Sc cross section

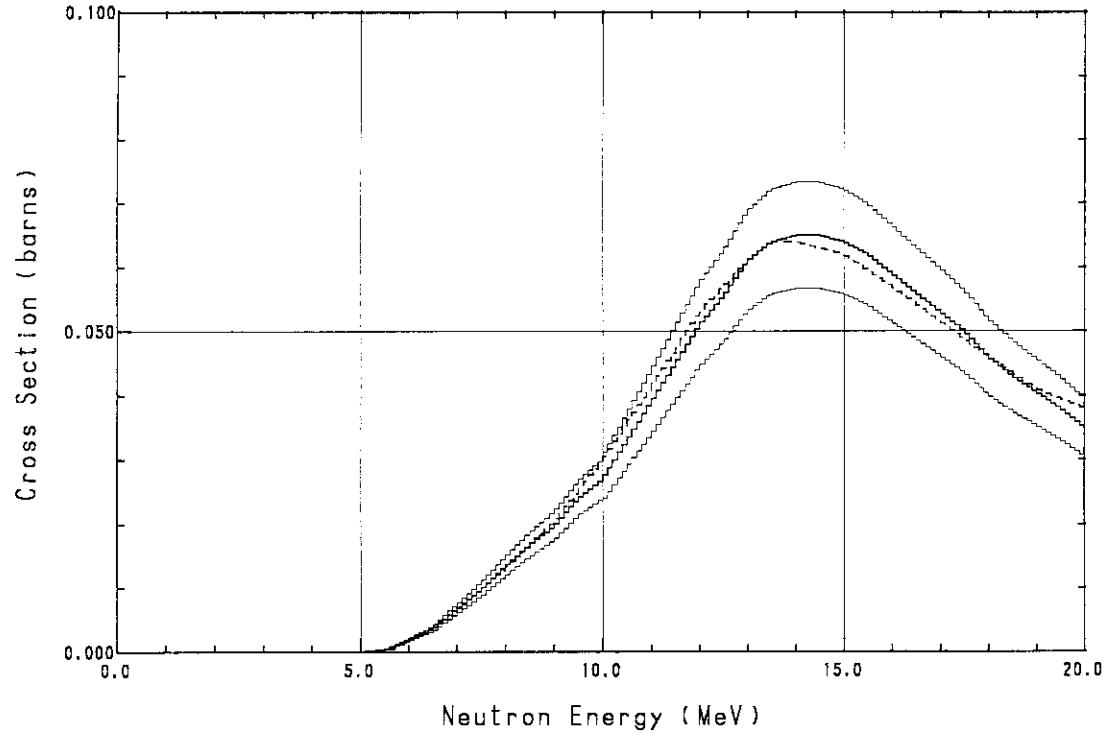

Fig. A.22 ^{48}Ti (n, p) ^{48}Sc cross section

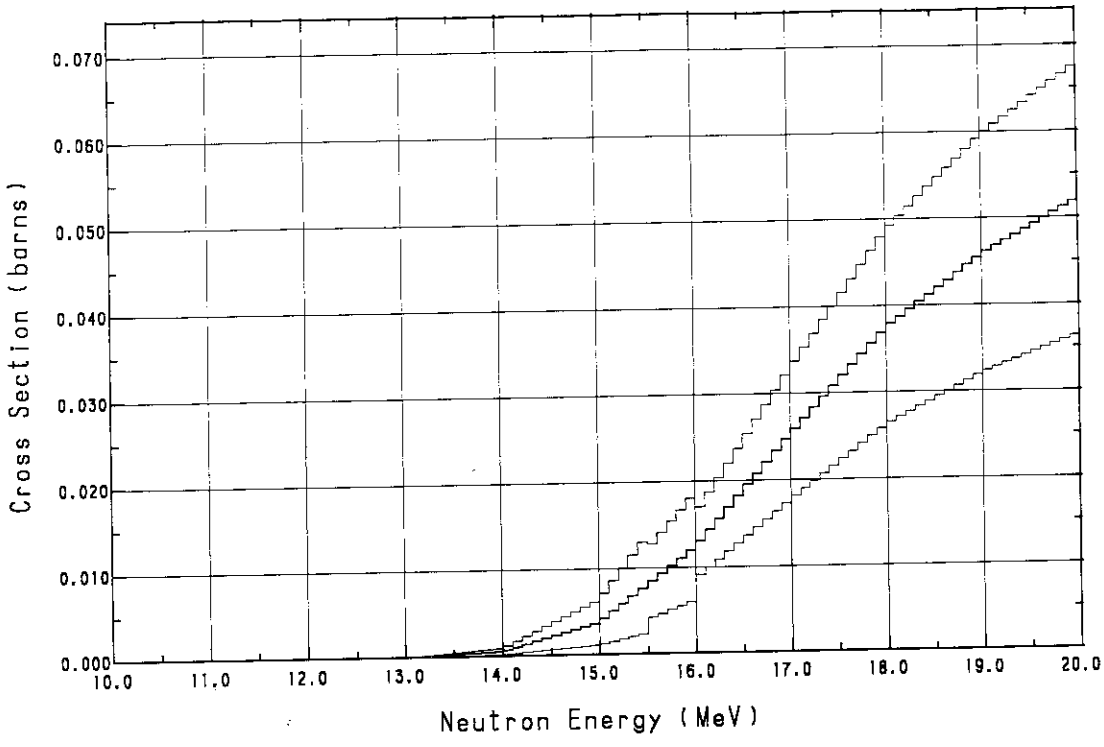

Fig. A.23 ^{49}Ti (n, np) ^{48}Sc cross section

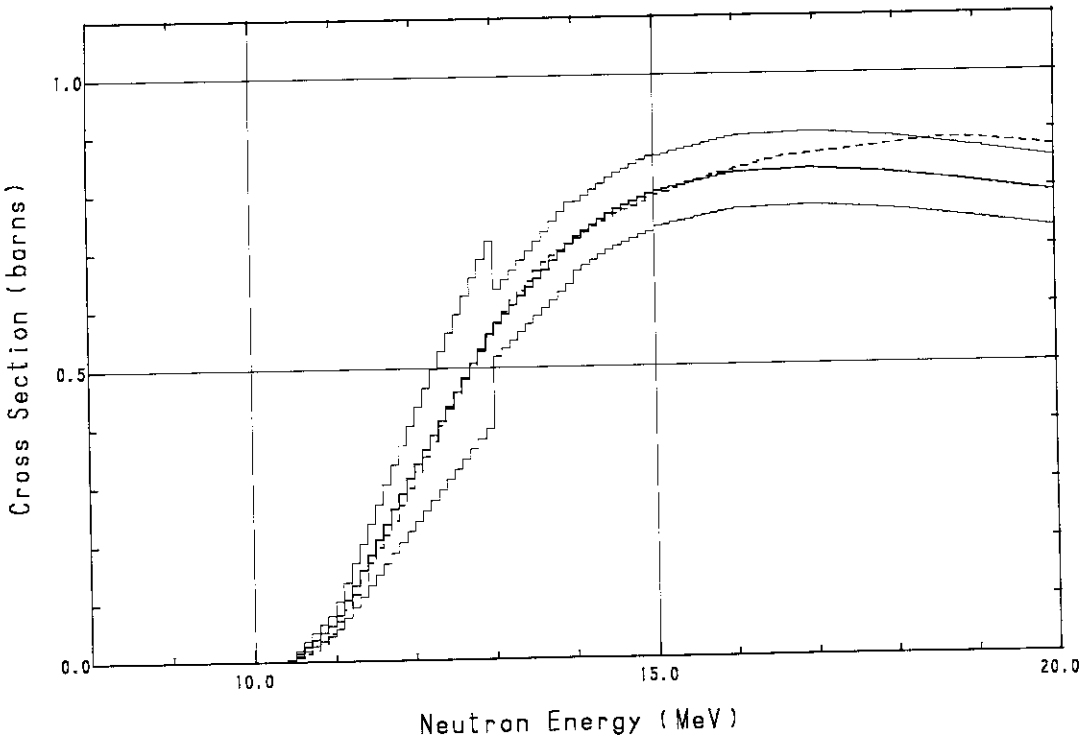

Fig. A.24 ^{55}Mn (n, 2n) ^{54}Mn cross section

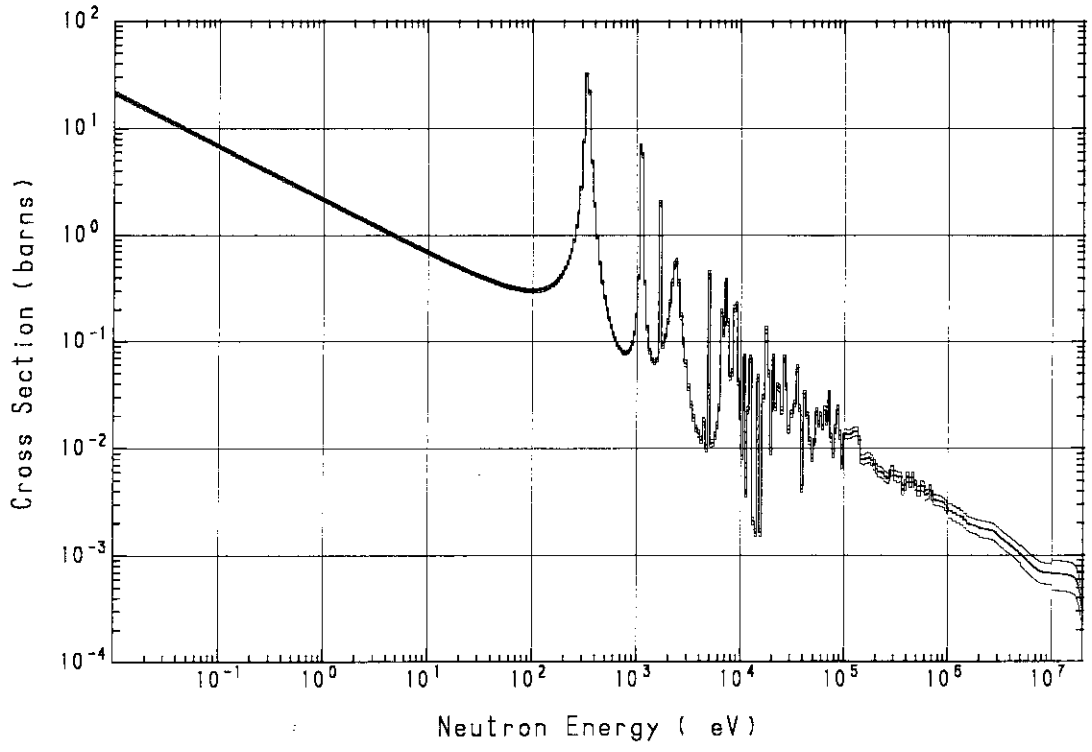

Fig. A.25 ^{55}Mn (n, γ) ^{56}Mn cross section

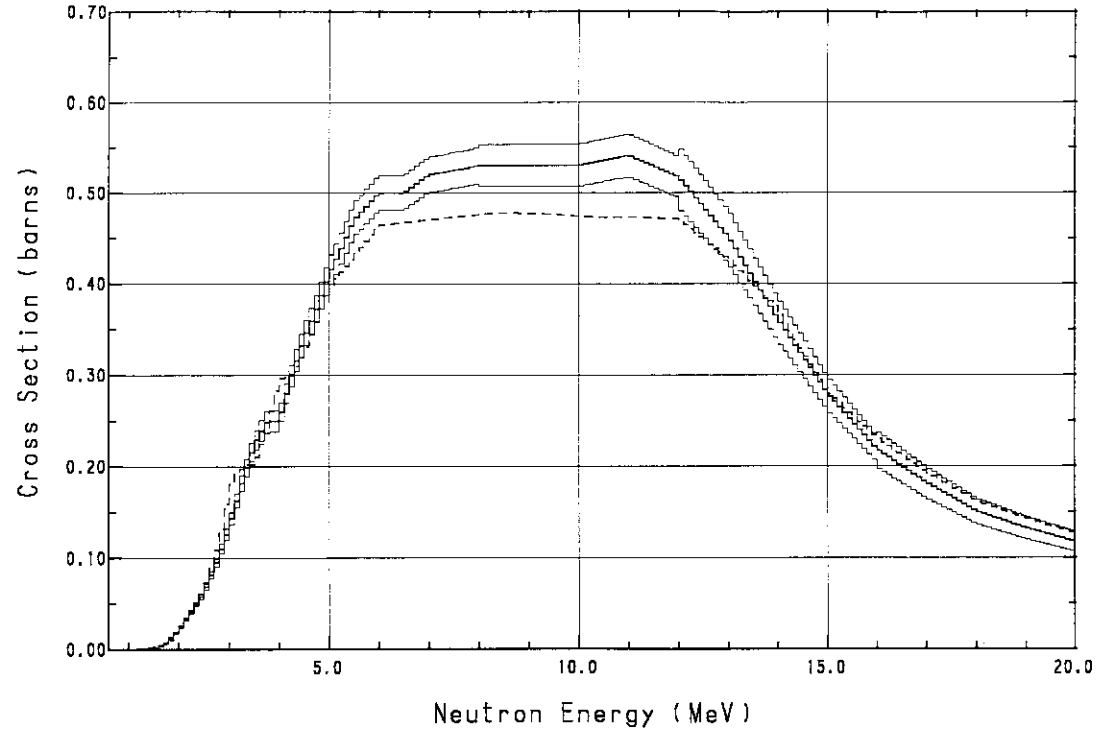

Fig. A.26 ^{54}Fe (n, p) ^{54}Mn cross section

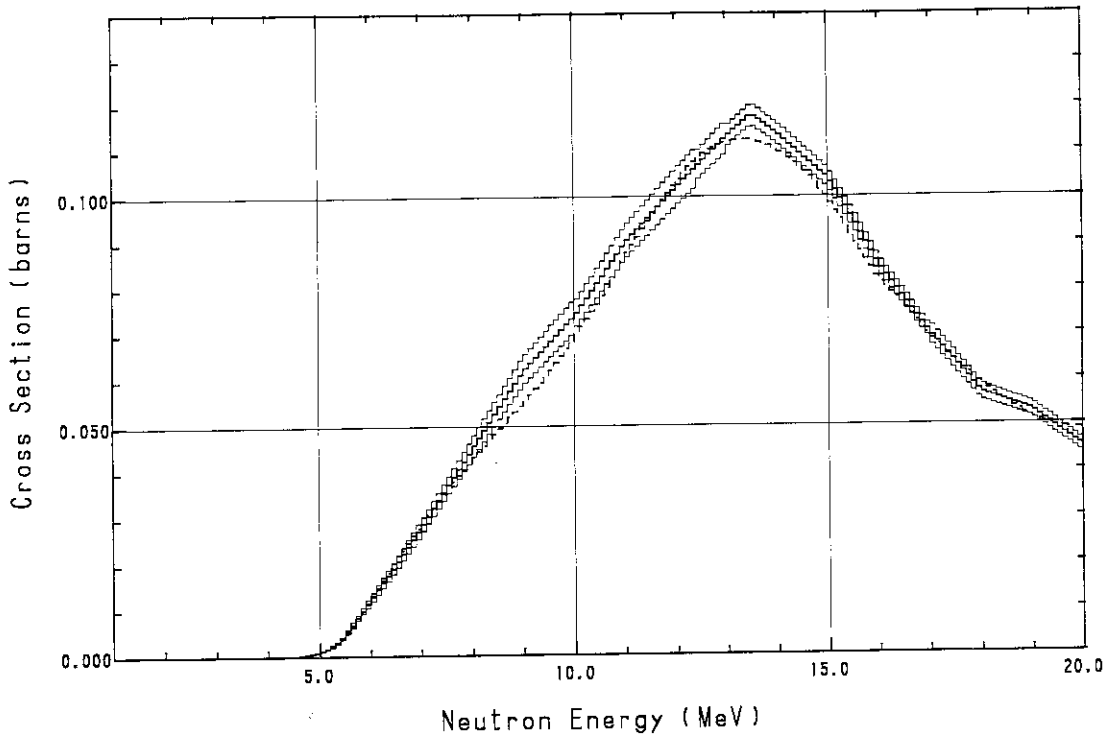

Fig. A.27 ^{56}Fe (n, p) ^{56}Mn cross section

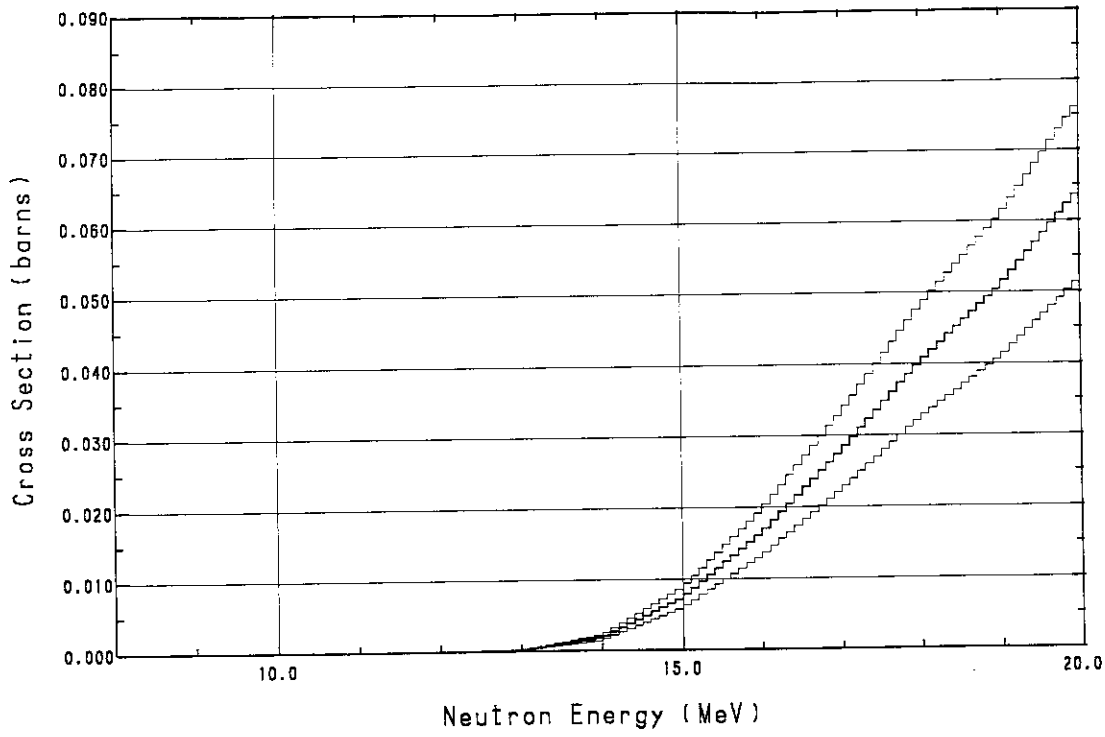

Fig. A.28 ^{57}Fe (n, np) ^{56}Mn cross section

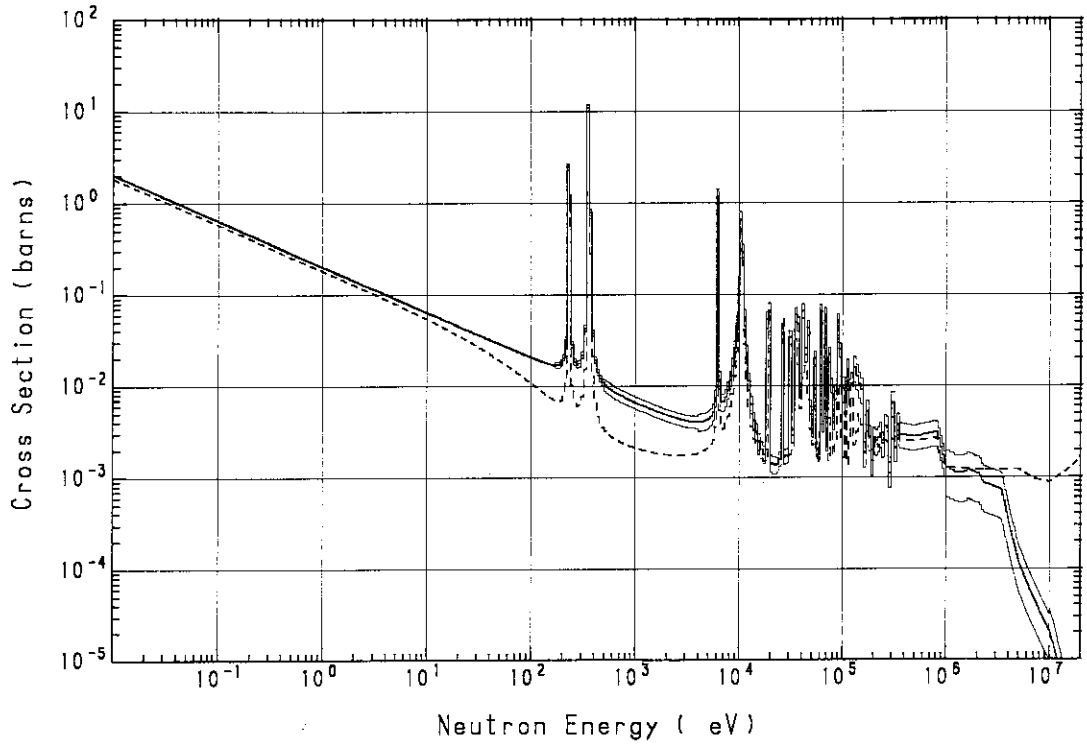

Fig. A.29 ^{58}Fe (n, γ) ^{59}Fe cross section

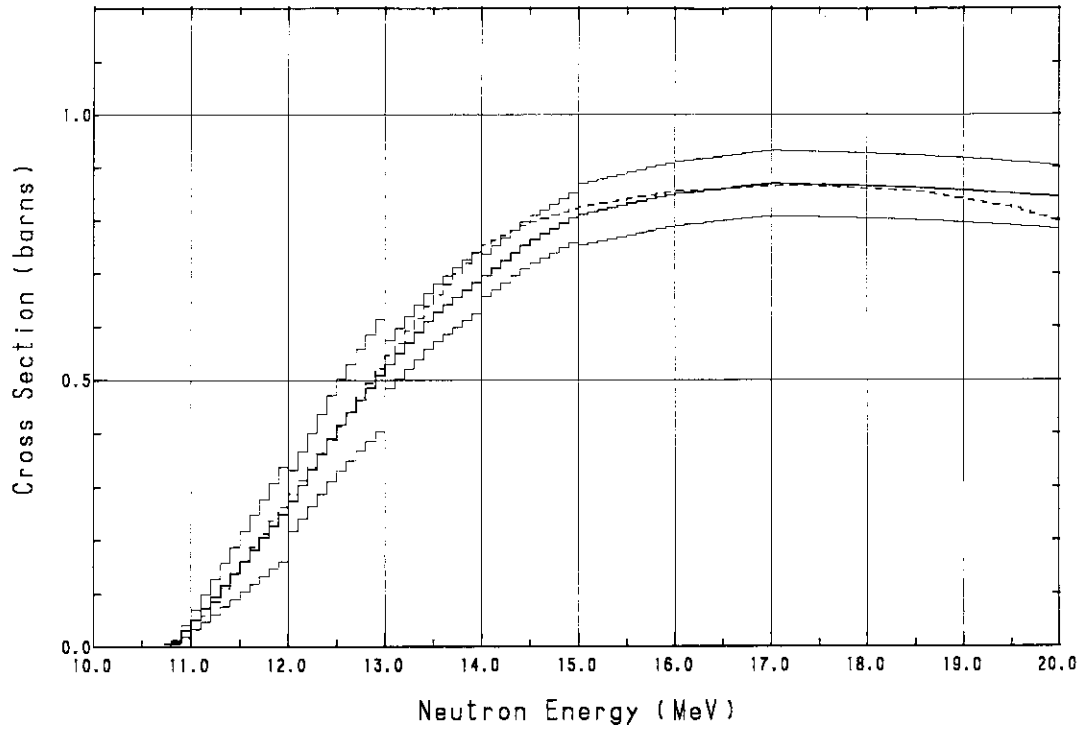

Fig. A.30 ^{59}Co (n, 2n) ^{58}Co cross section

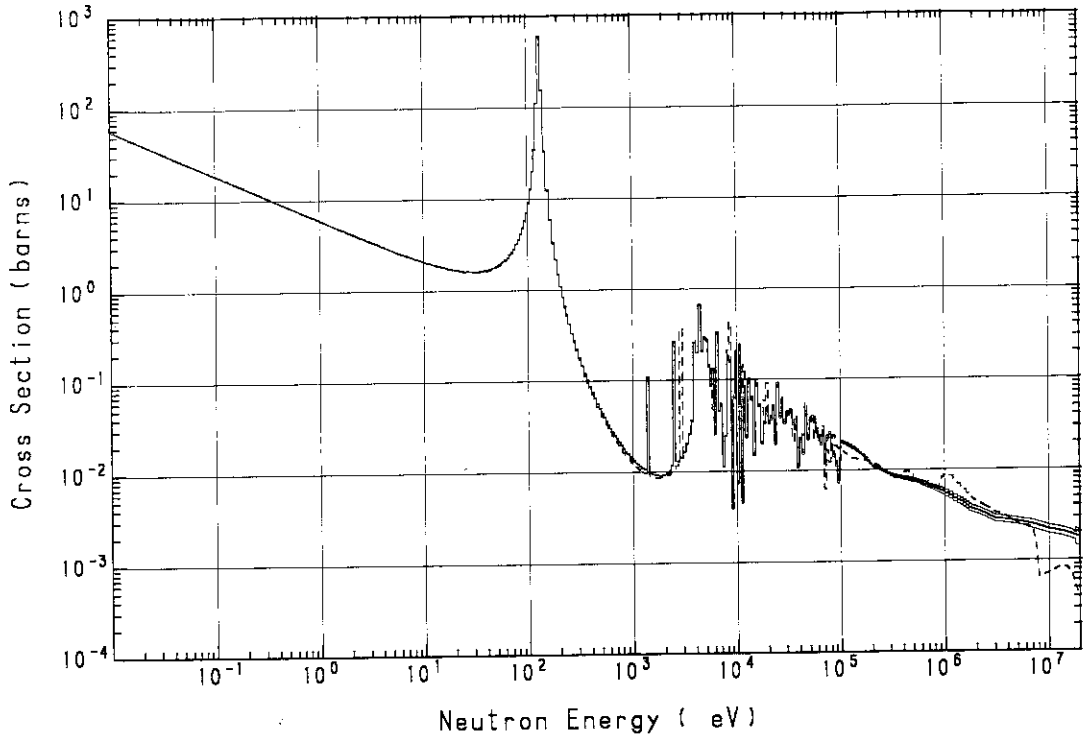

Fig. A.31 ^{59}Co (n, γ) ^{60}Co cross section

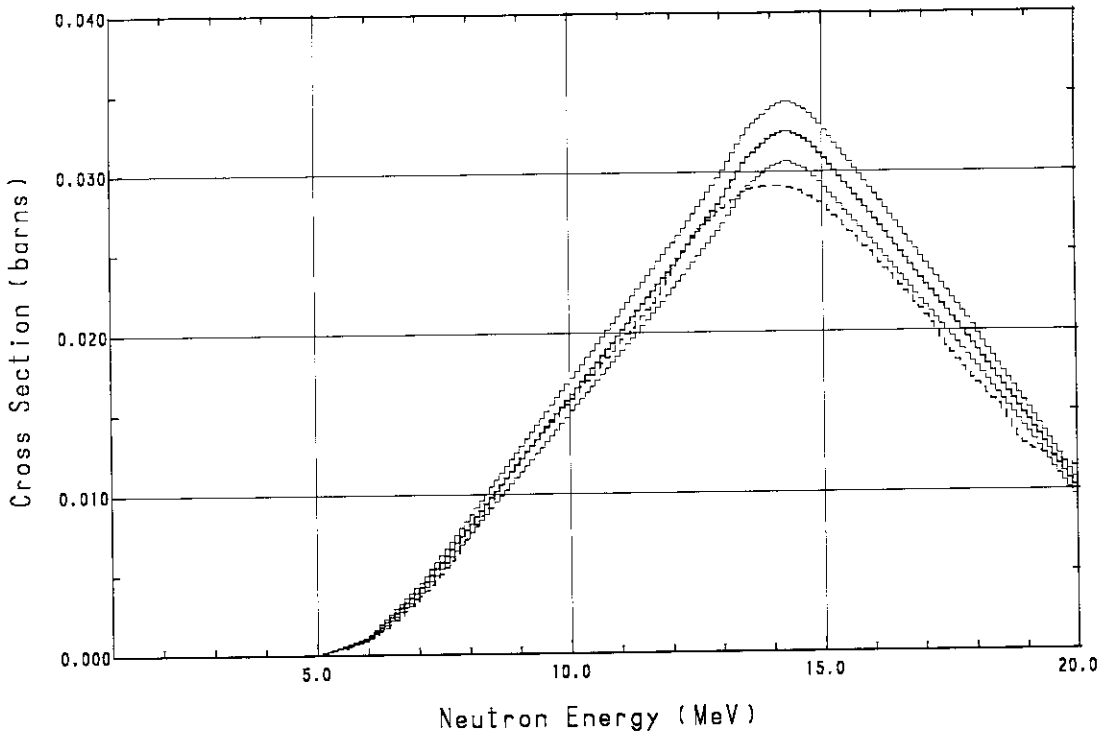

Fig. A.32 ^{59}Co (n, α) ^{56}Mn cross section

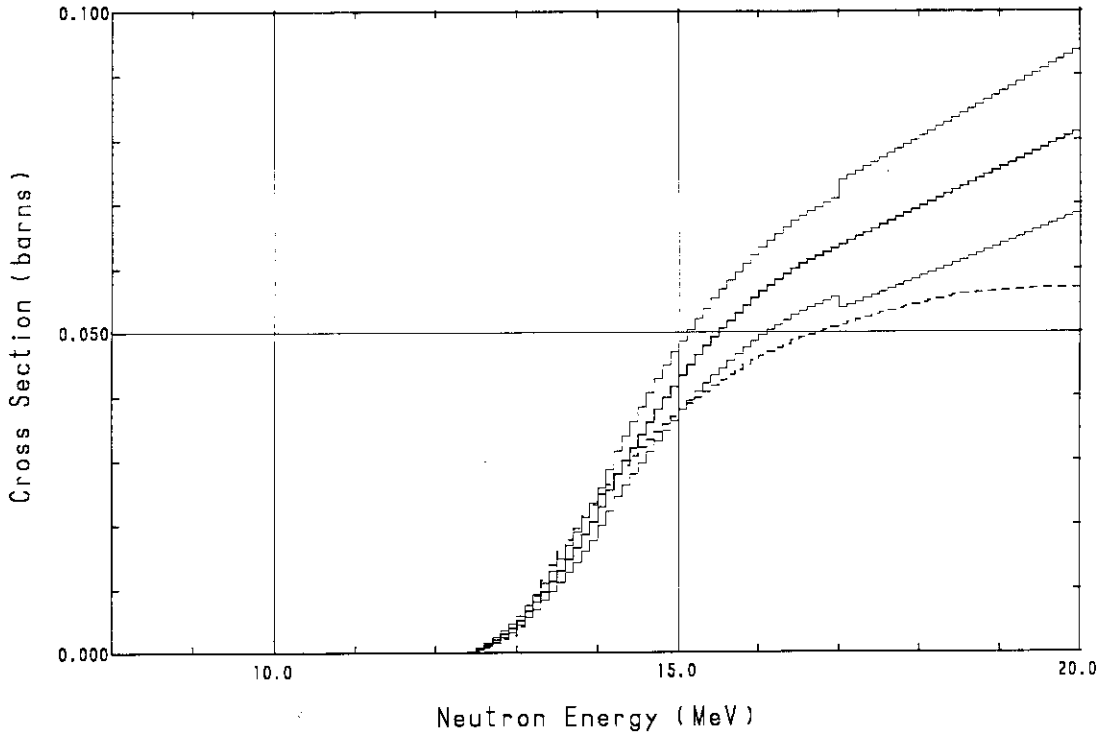

Fig. A.33 ^{58}Ni (n, 2n) ^{57}Ni cross section

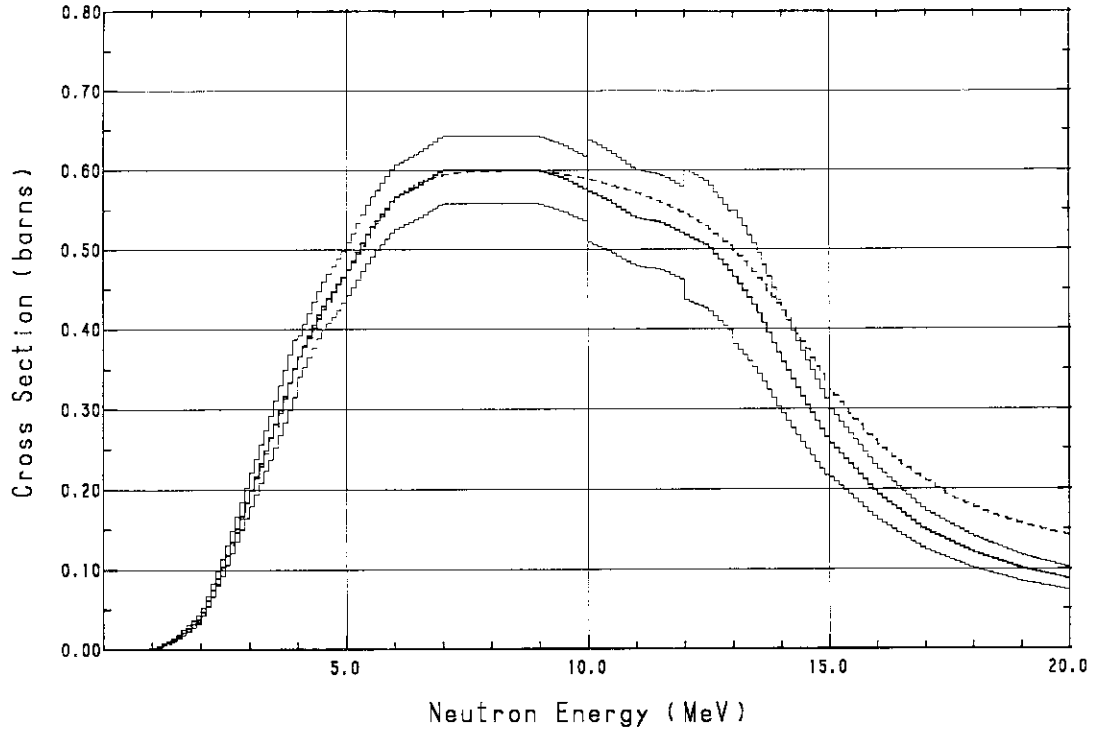

Fig. A.34 ^{58}Ni (n, p) ^{58}Co cross section

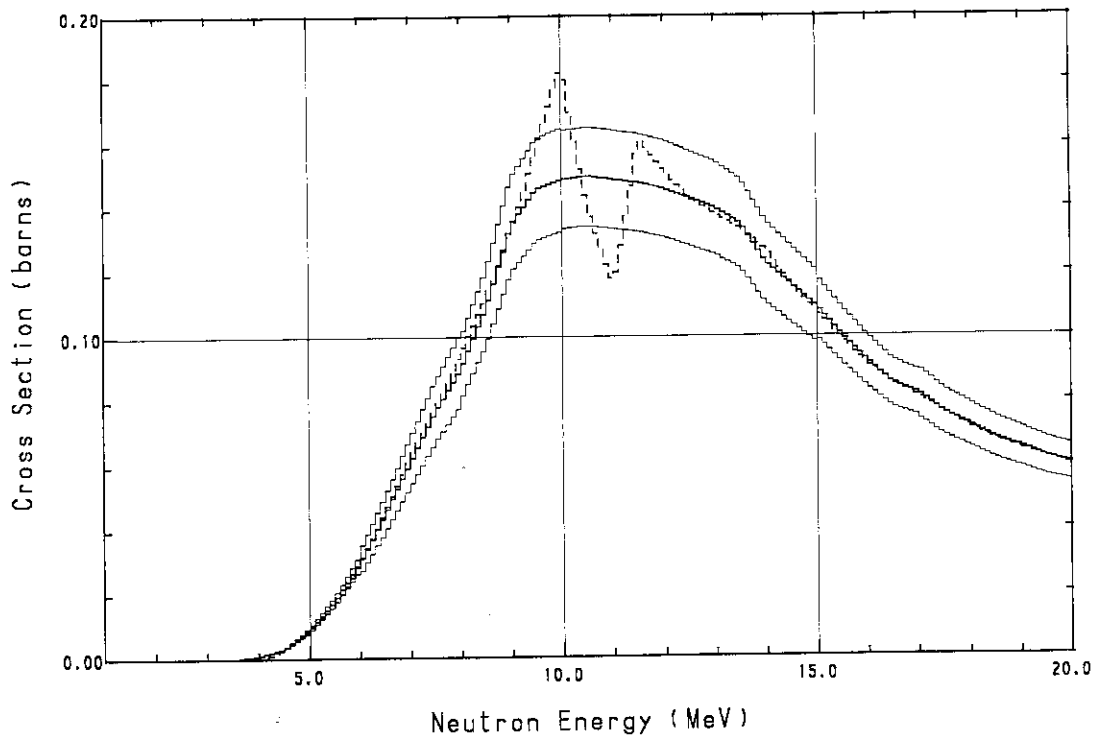

Fig. A.35 ^{60}Ni (n, p) ^{60}Co cross section

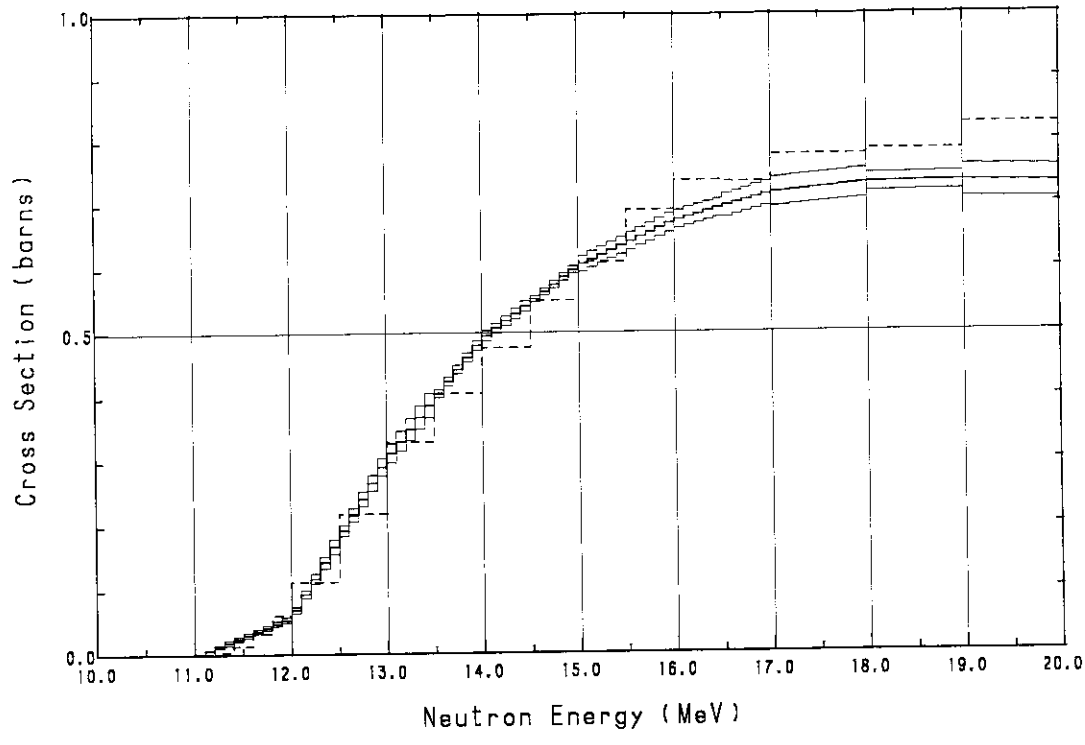

Fig. A.36 ^{63}Cu (n, 2n) ^{62}Cu cross section

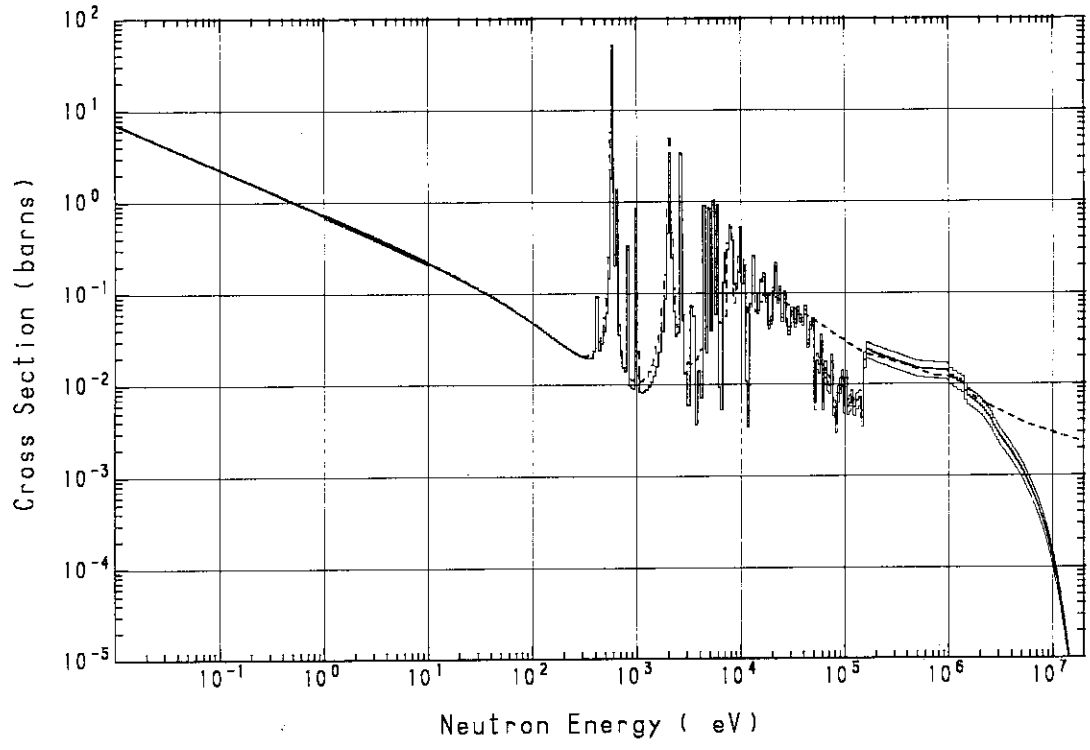

Fig. A.37 ^{63}Cu (n, γ) ^{64}Cu cross section

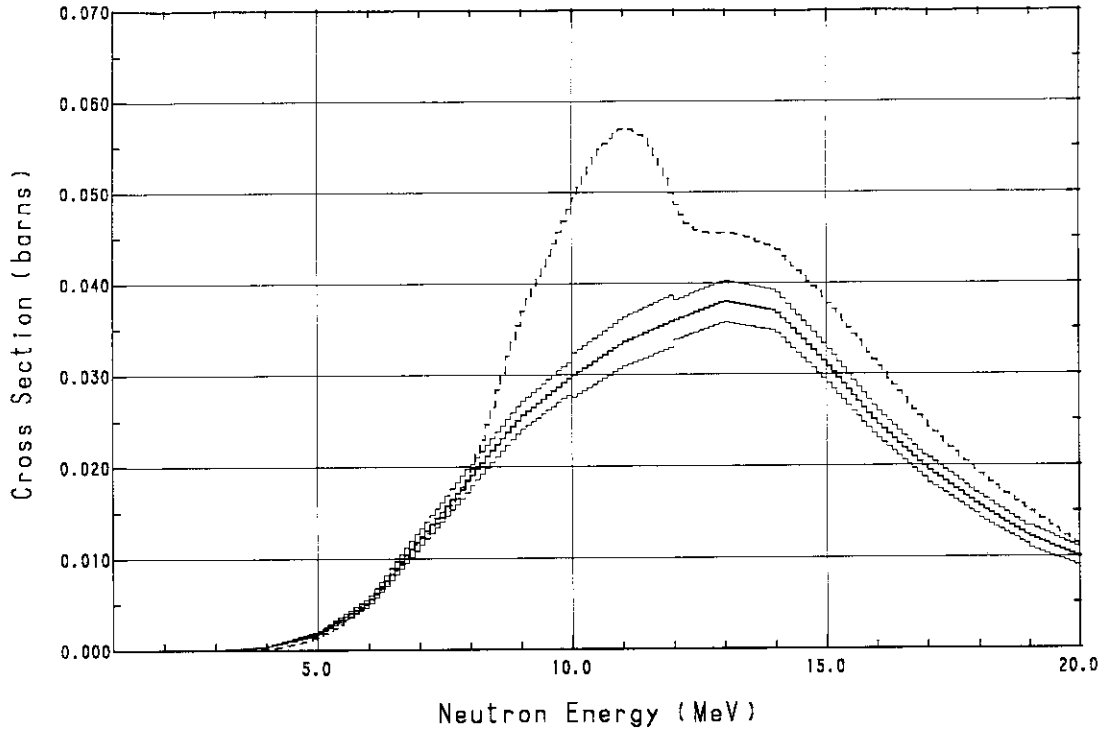

Fig. A.38 ^{63}Cu (n, α) ^{60}Co cross section

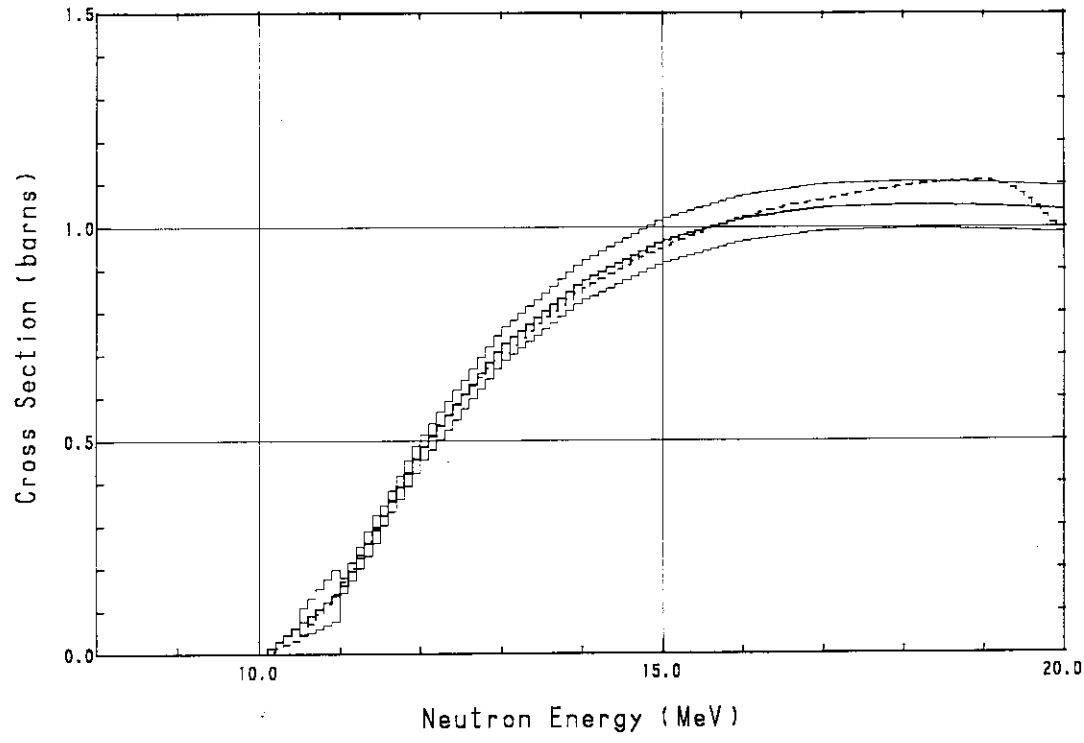

Fig. A.39 ^{65}Cu (n, 2n) ^{64}Cu cross section

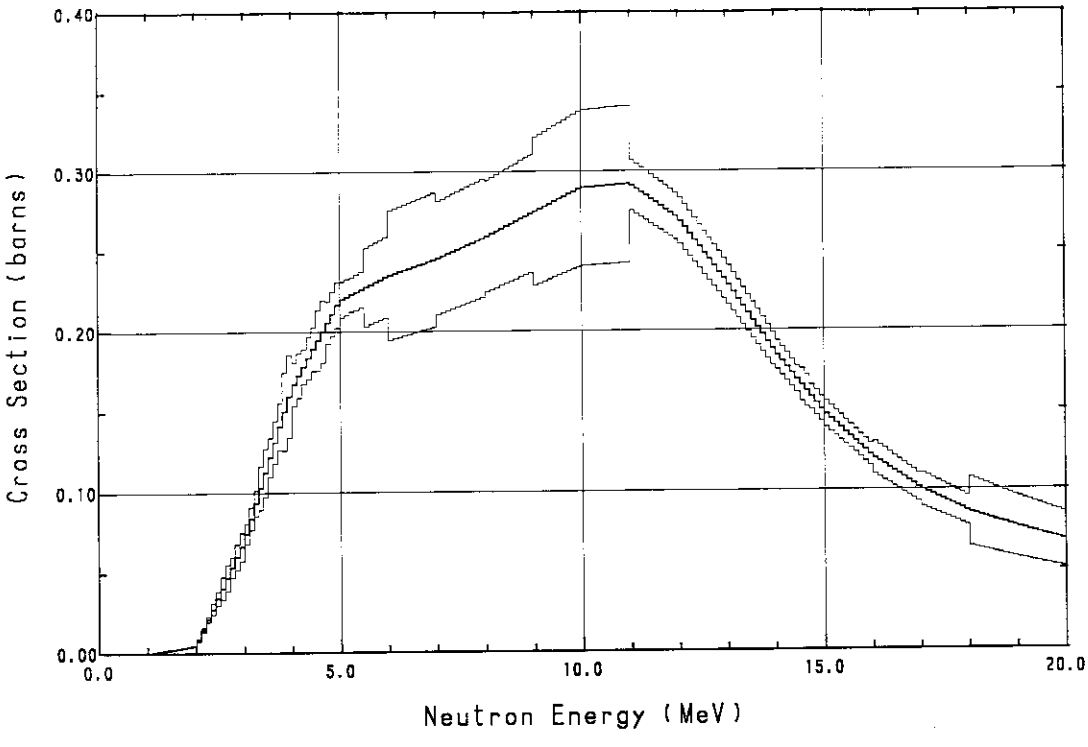

Fig. A.40 ^{64}Zn (n, p) ^{64}Cu cross section

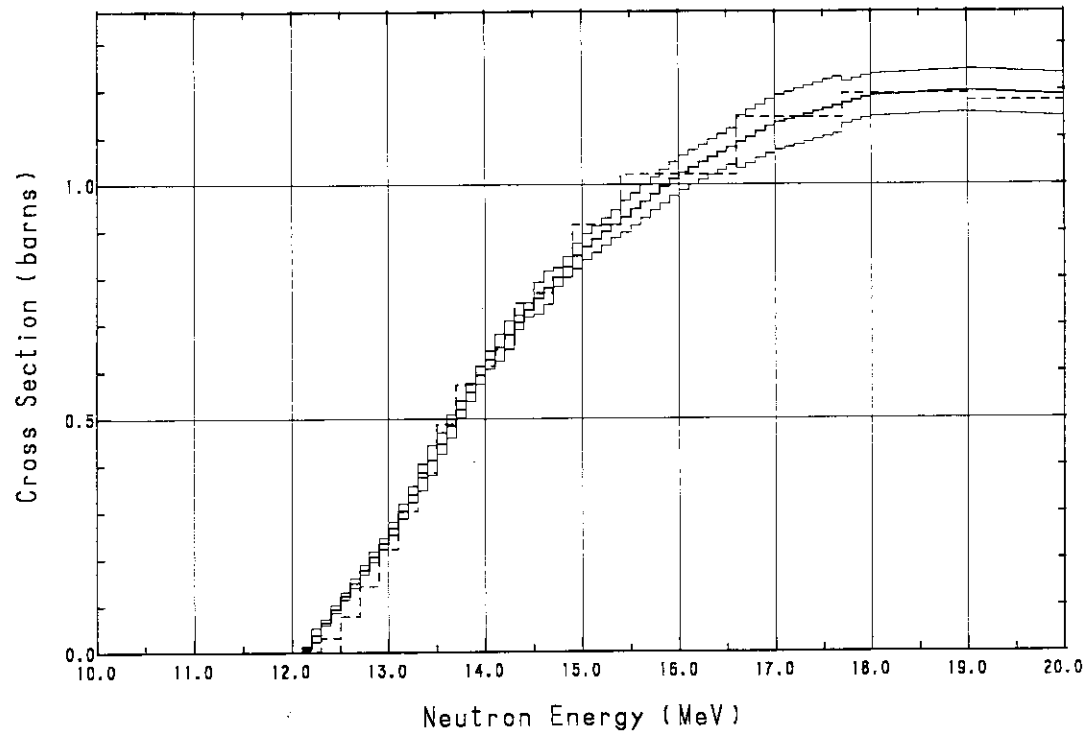

Fig. A.41 ^{90}Zr (n, 2n) ^{89}Zr cross section

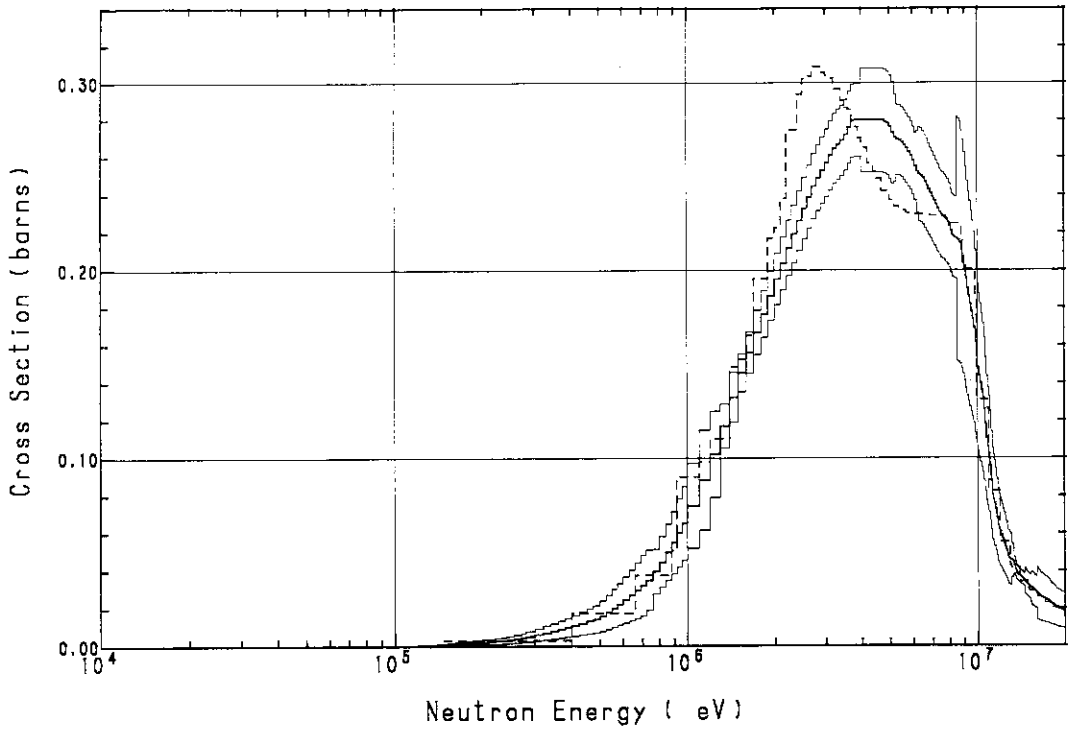

Fig. A.42 ^{93}Nb (n, n') ^{93m}Nb cross section

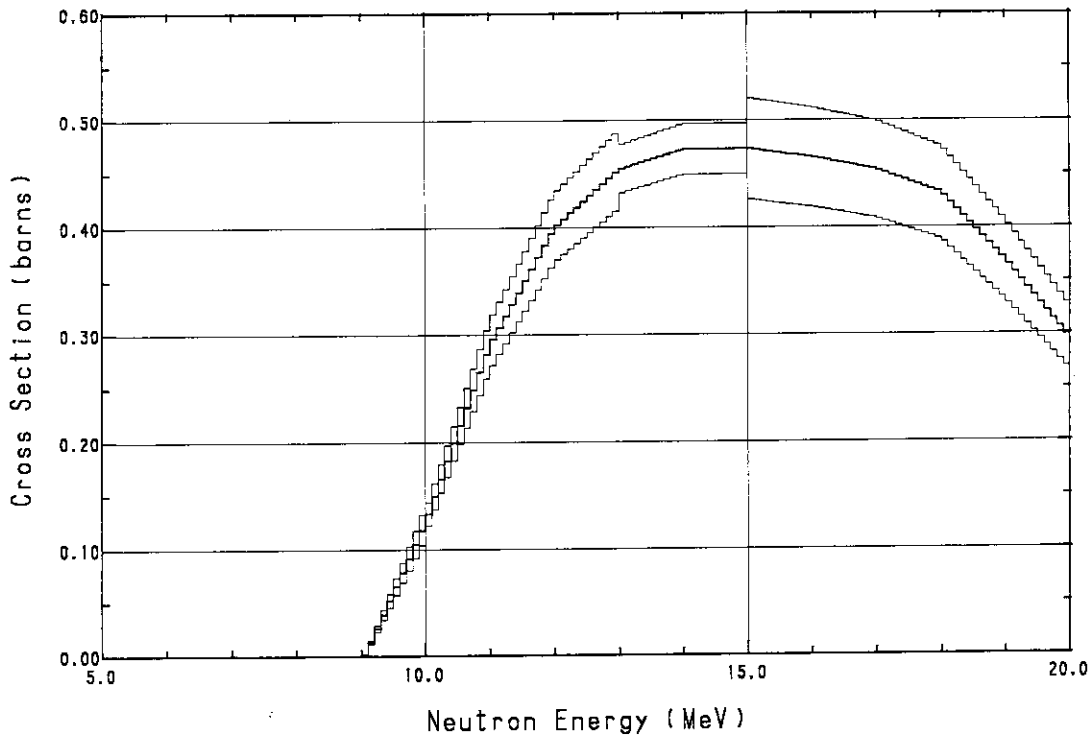

Fig. A.43 ^{93}Nb (n, 2n) ^{92m}Nb cross section

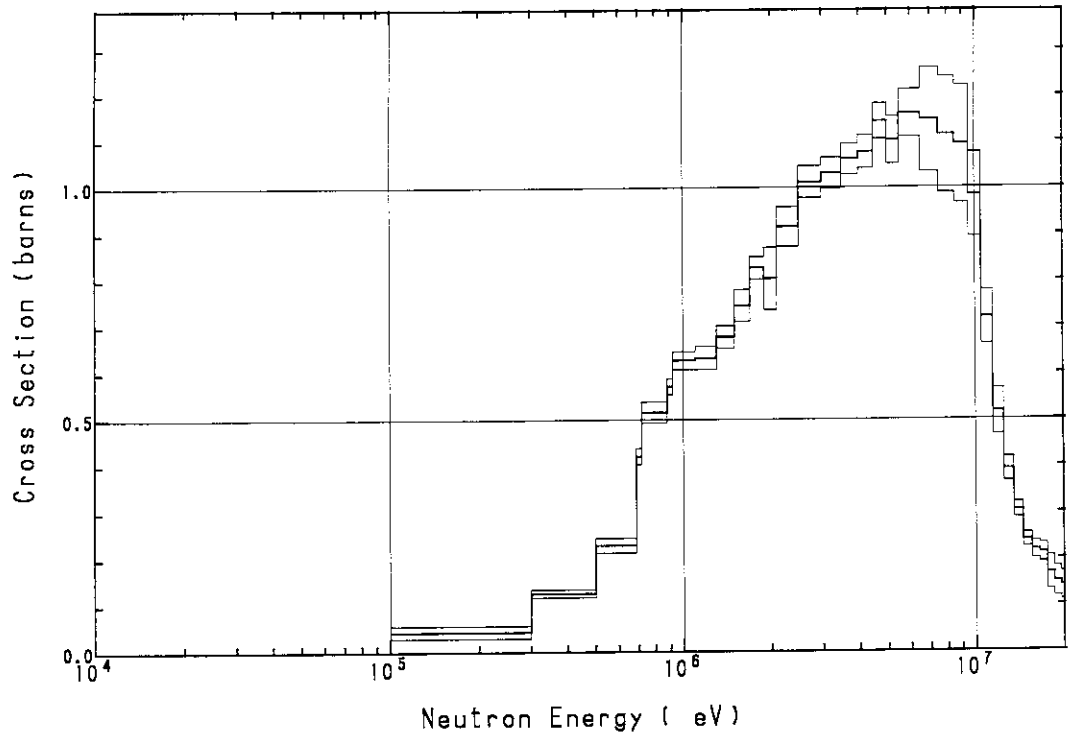

Fig. A.44 ^{103}Rh (n,n') ^{103m}Rh cross section

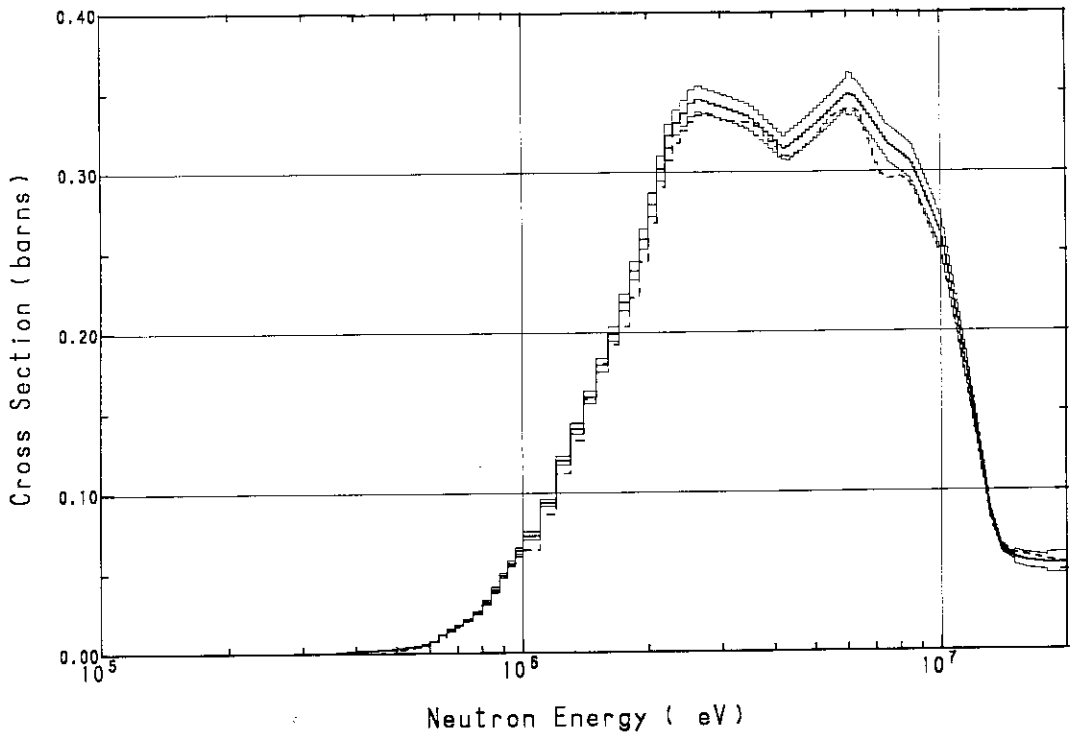

Fig. A.45 $^{115}In(n,n')^{115m}In$ cross section

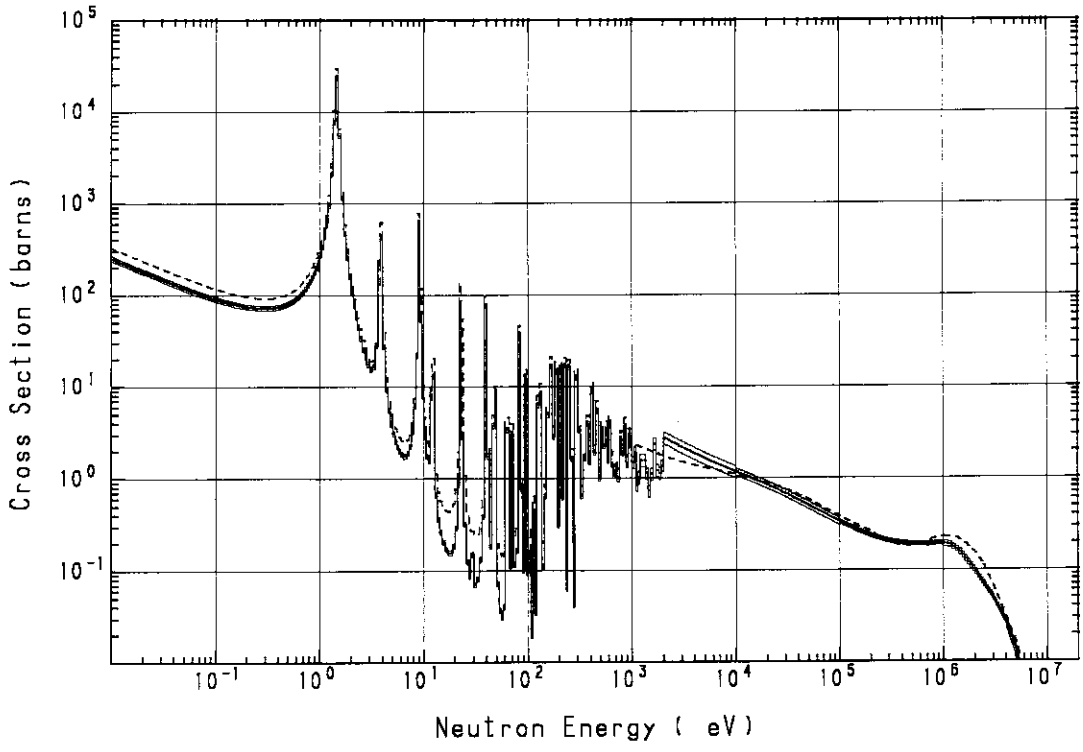

Fig. A.46 $^{115}In\ (n,\gamma)\ ^{116m}In$ cross section

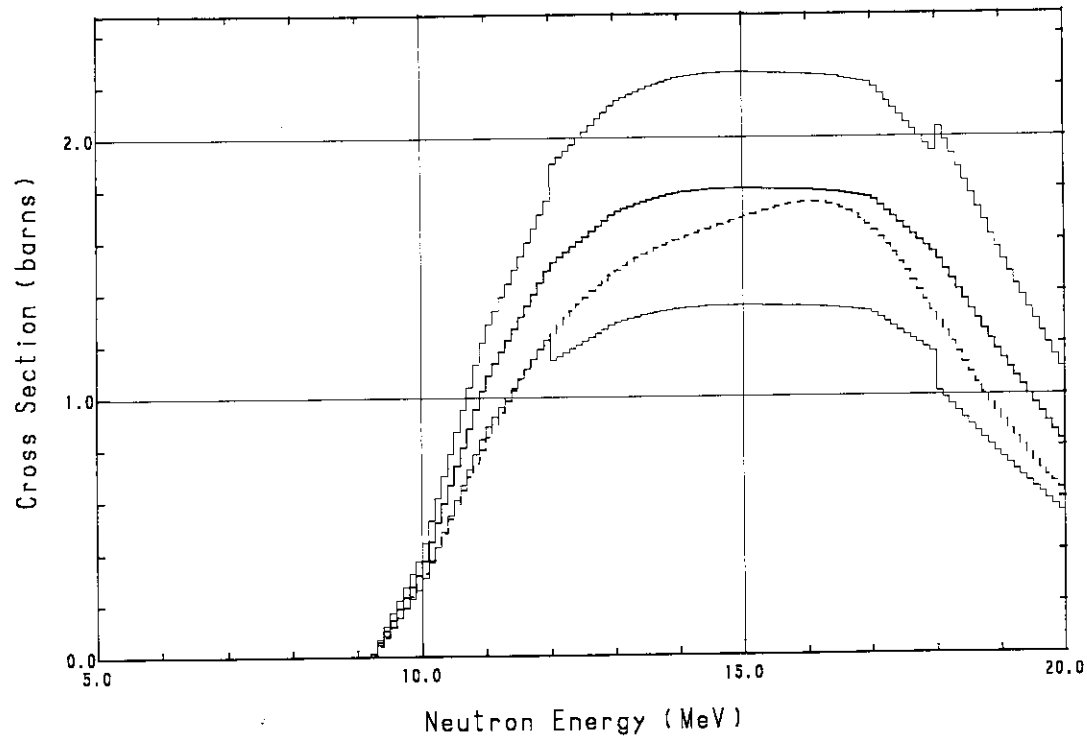

Fig. A.47 ^{127}I (n, 2n) ^{126}I cross section

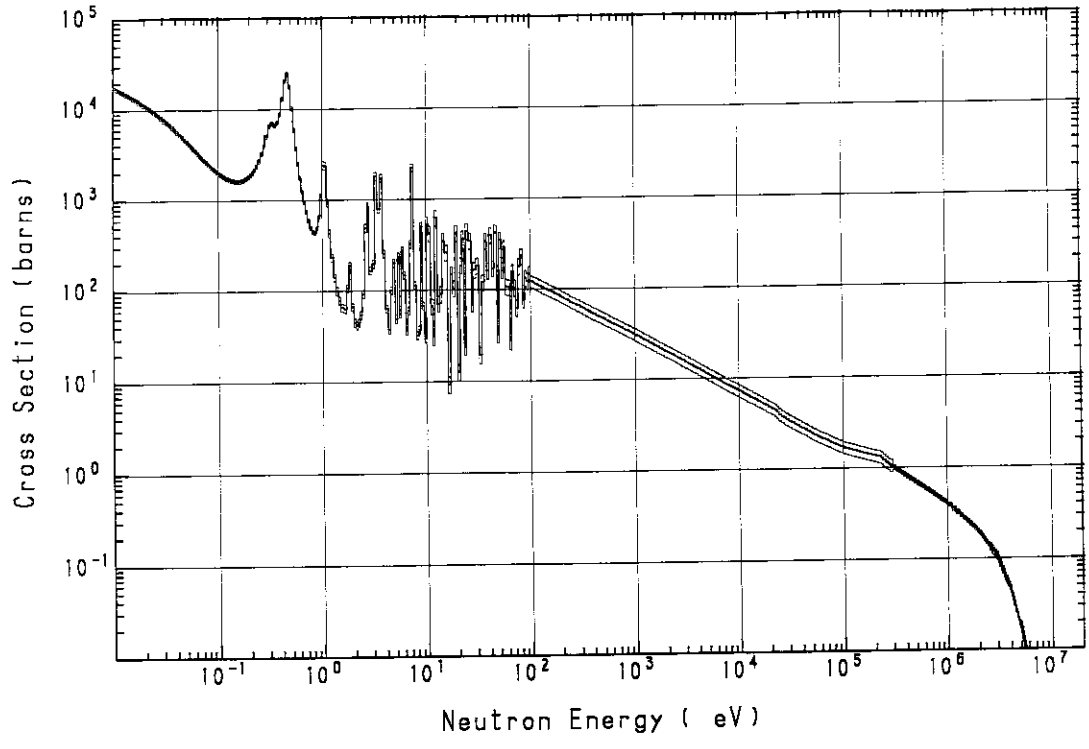

Fig. A.48 ^{151}Eu (n, γ) ^{152}Eu cross section

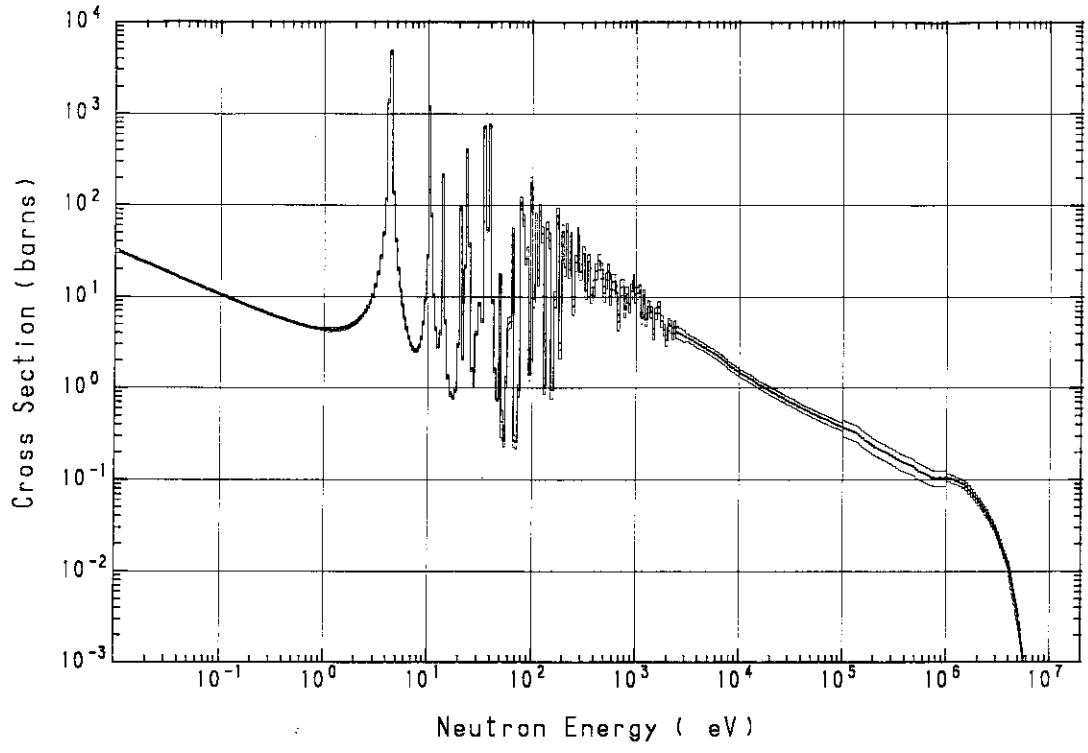

Fig. A.49 ^{181}Ta (n, γ) ^{182}Ta cross section

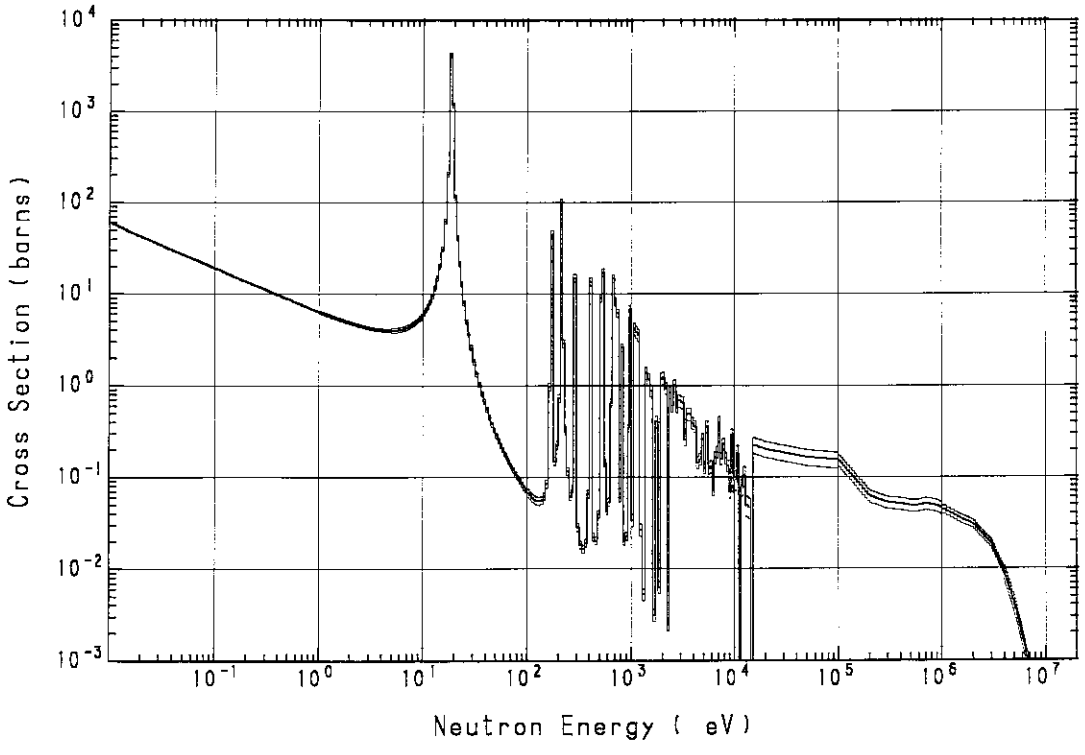

Fig. A.50 ^{186}W (n, γ) ^{187}W cross section

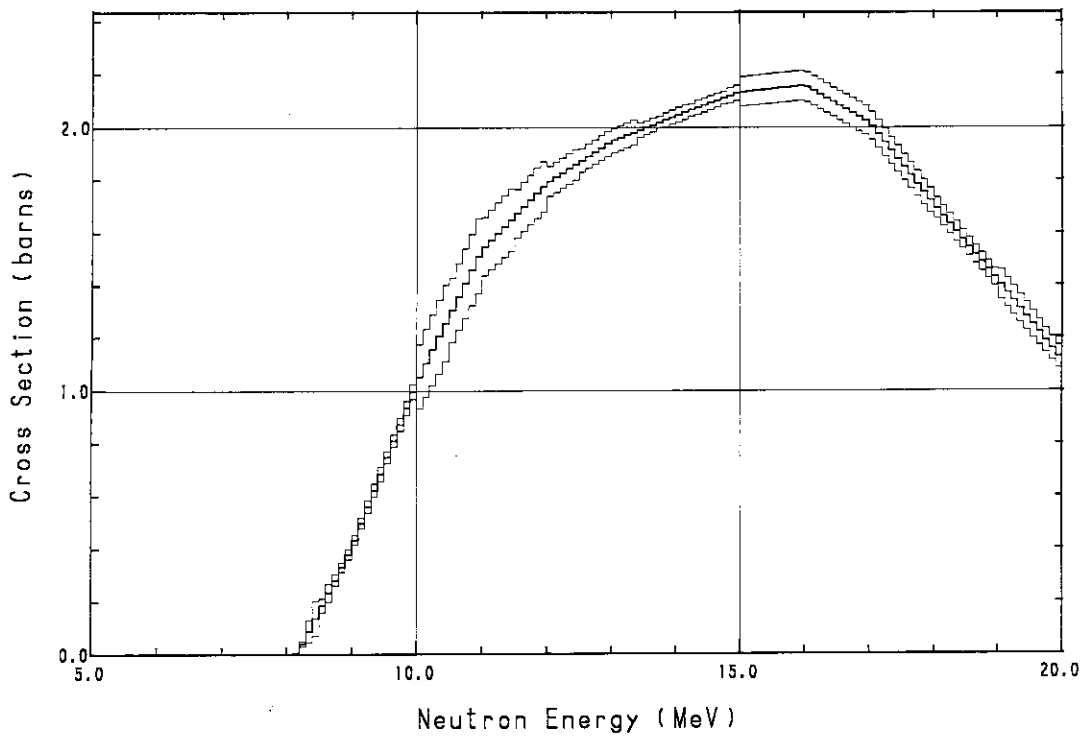

Fig. A.51 ^{197}Au (n, 2n) ^{196}Au cross section

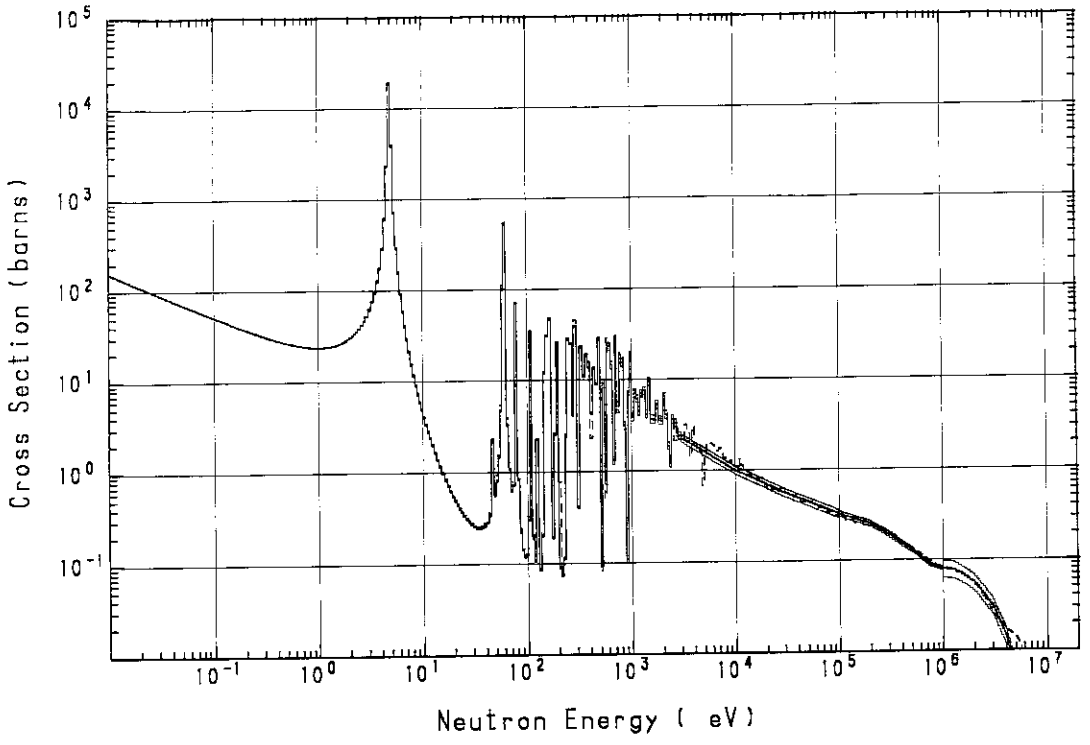

Fig. A.52 ^{197}Au (n, γ) ^{198}Au cross section

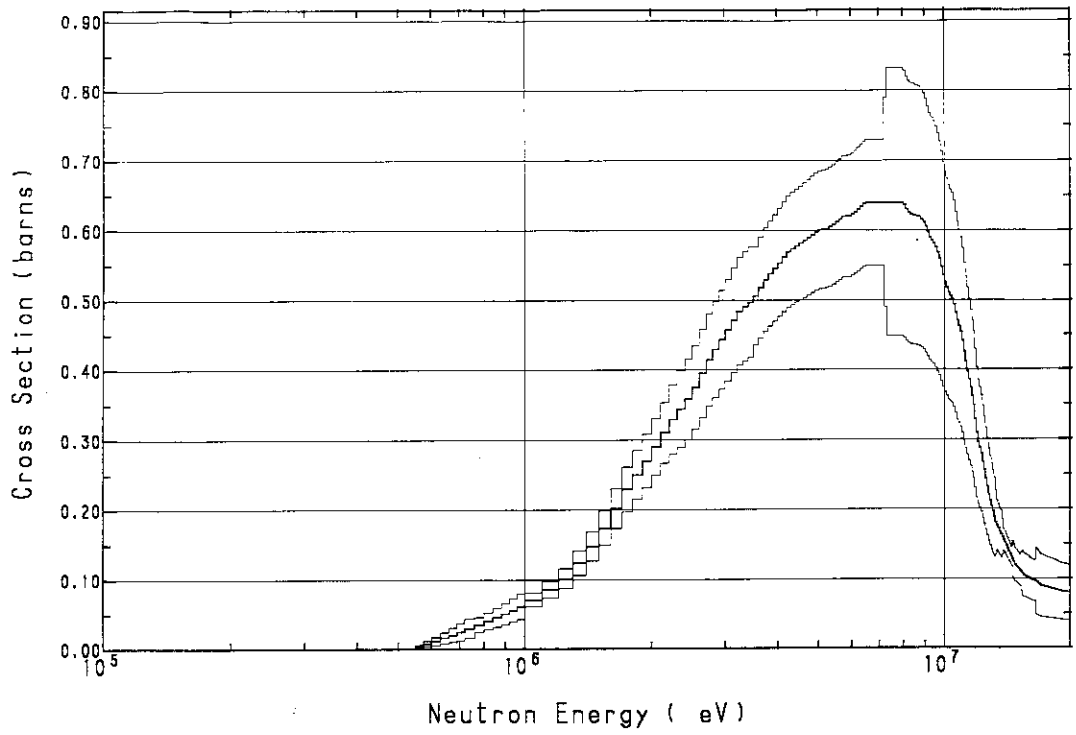

Fig. A.53 ^{199}Hg (n, n') ^{199m}Hg cross section

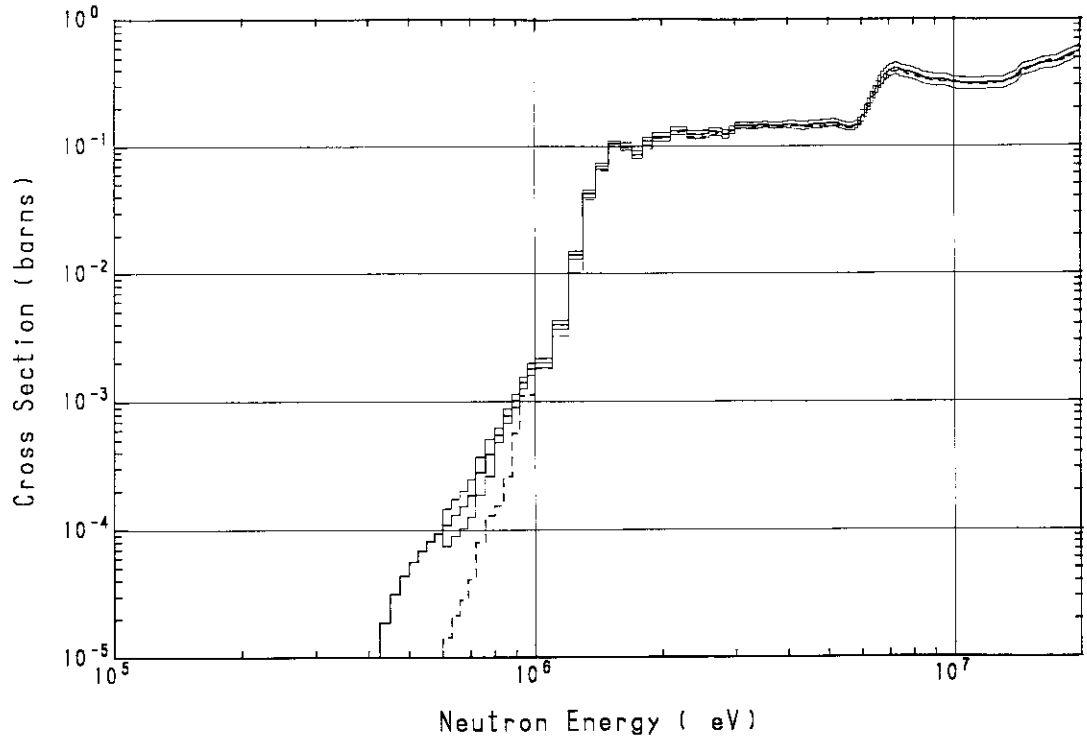

Fig. A.54 ^{232}Th fission cross section

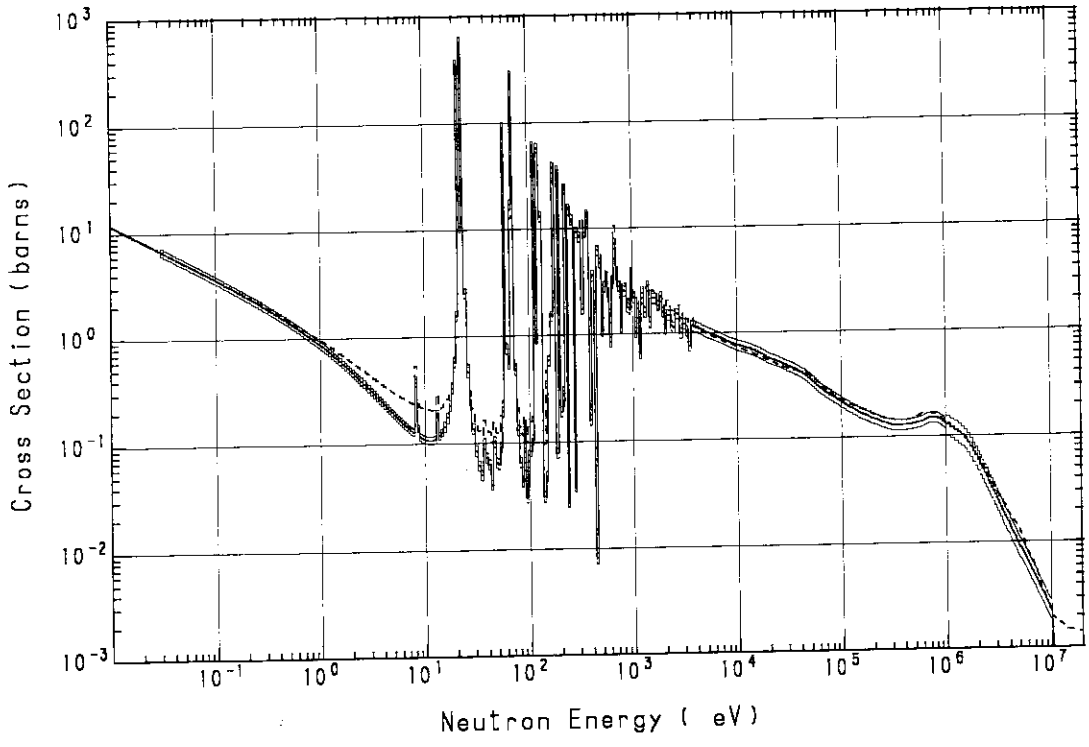

Fig. A.55 ^{232}Th (n, γ) ^{233}Th cross section

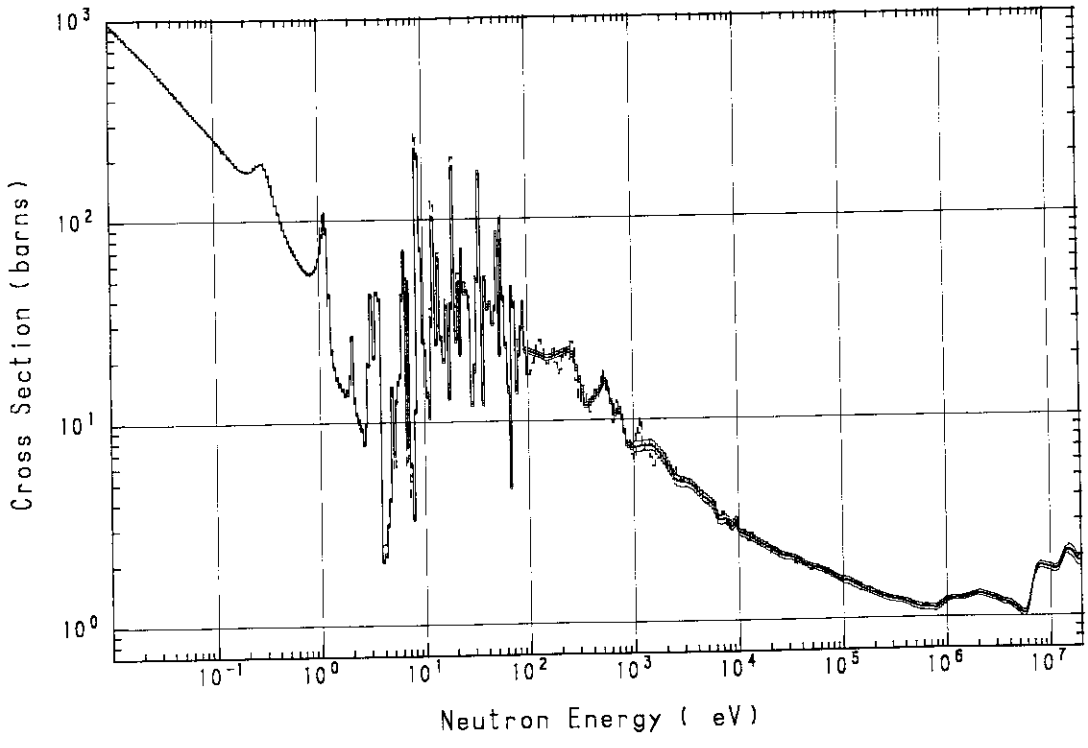

Fig. A.56 ^{235}U fission cross section

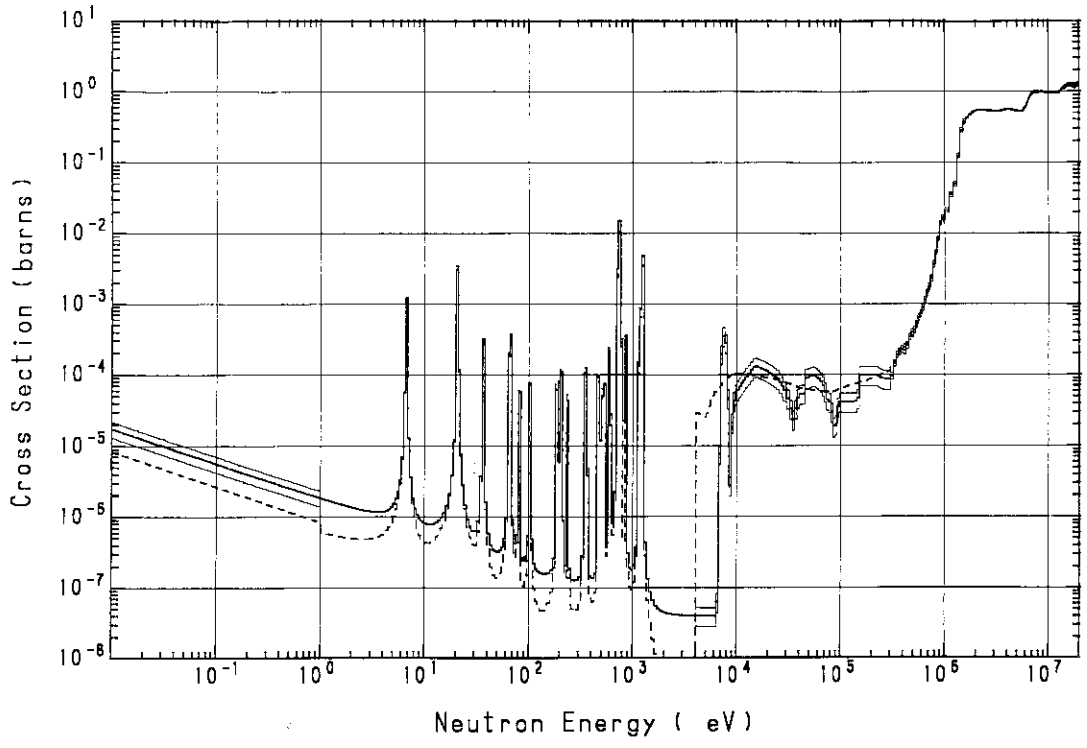

Fig. A.57 ^{238}U fission cross section

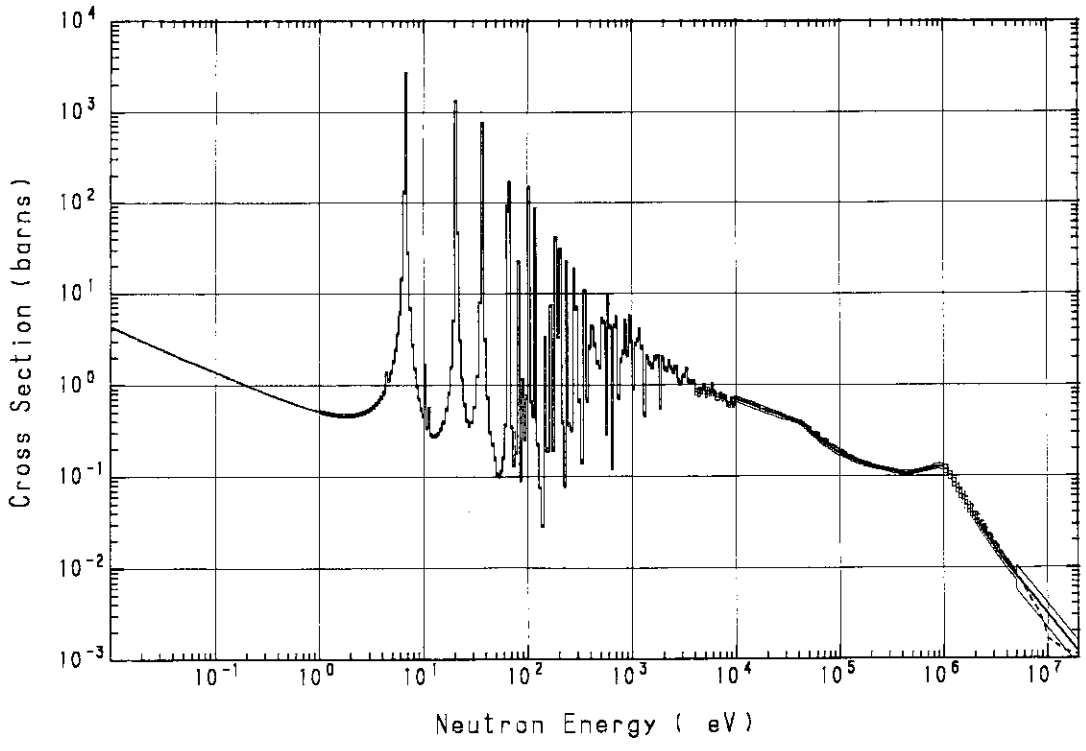

Fig. A.58 ^{238}U (n, γ) ^{239}U cross section

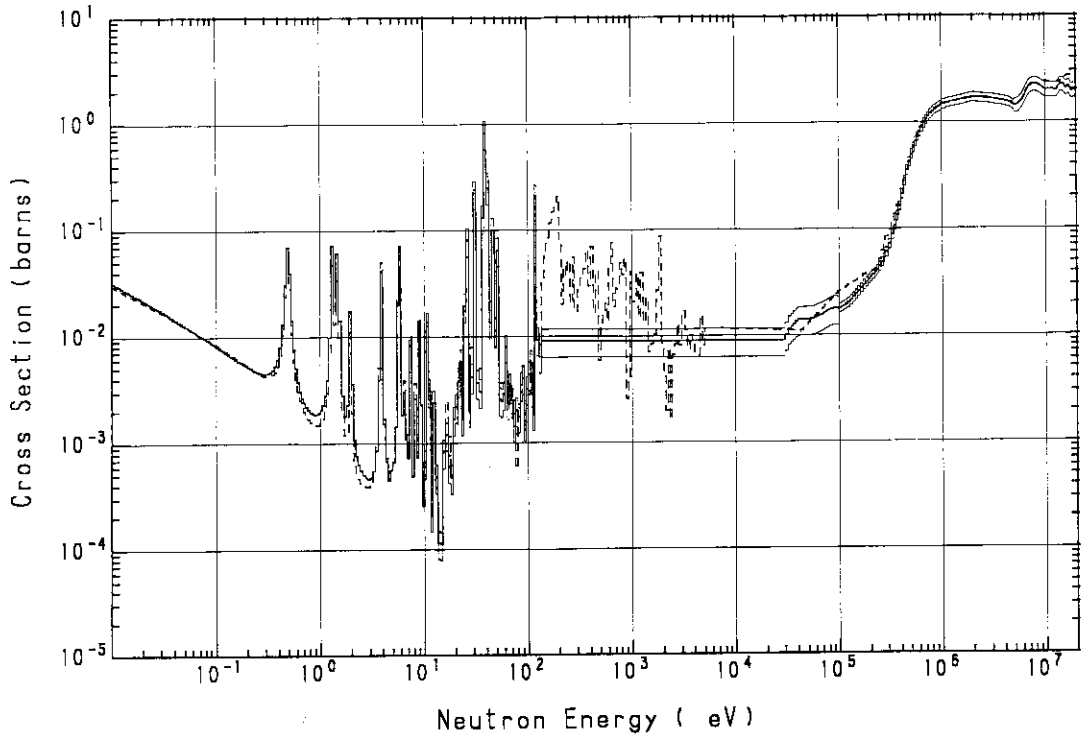

Fig. A.59 ^{237}Np fission cross section

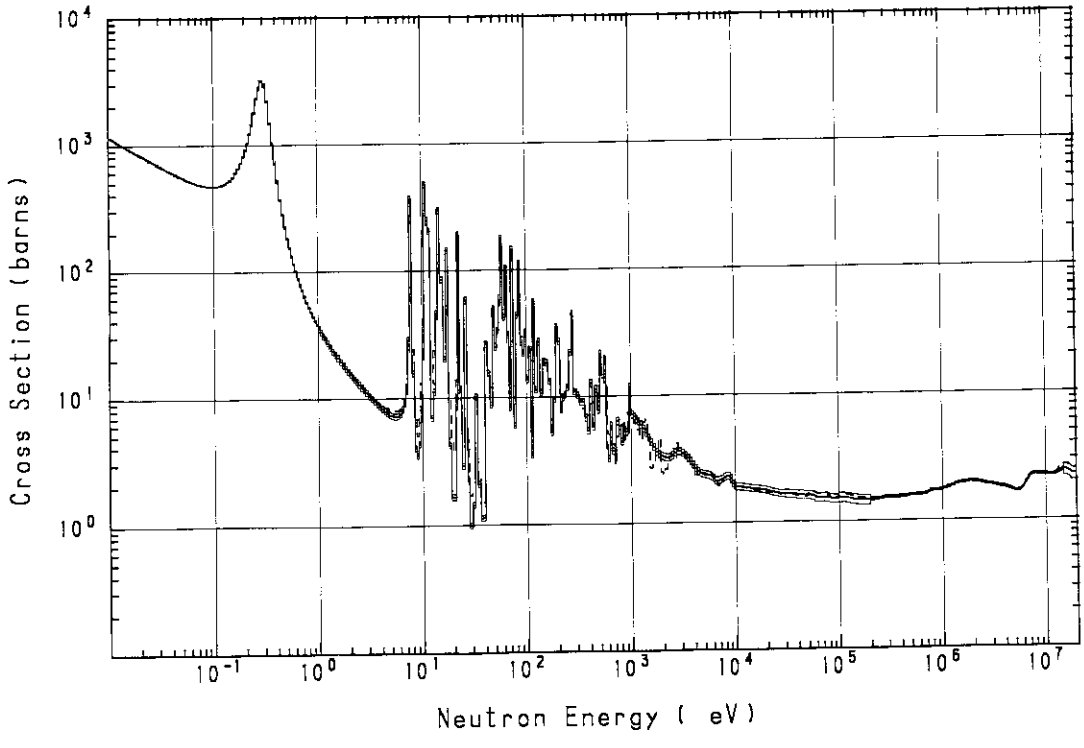

Fig. A.60 ^{239}Pu fission cross section

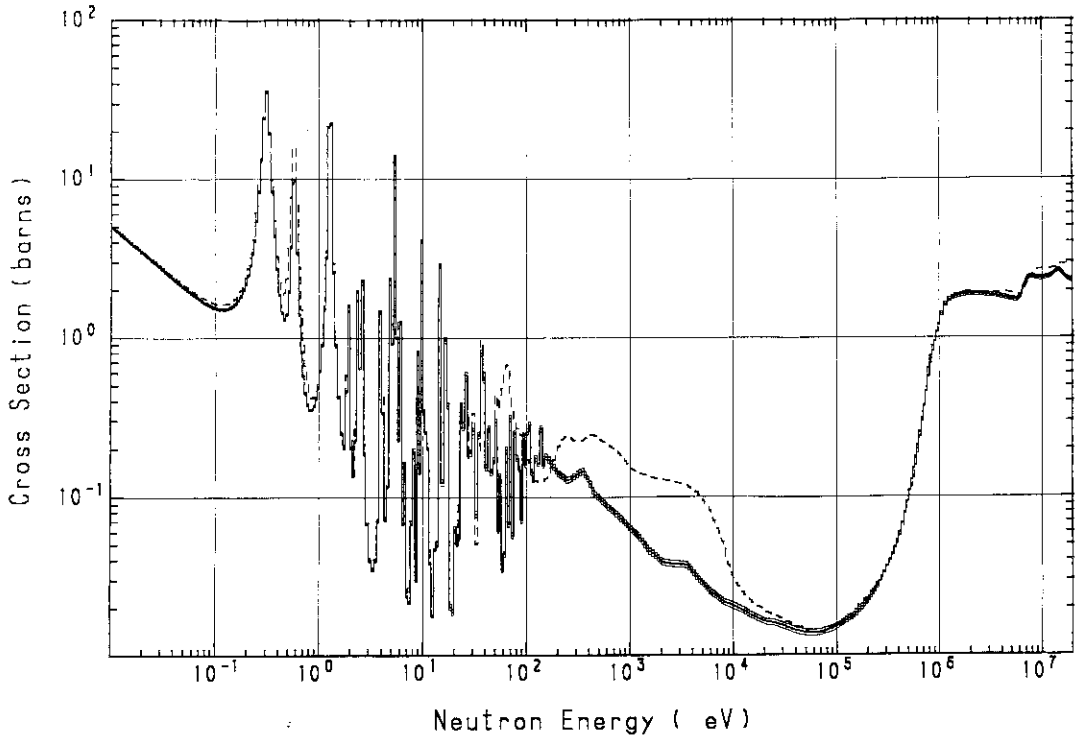

Fig. A.61 ^{241}Am fission cross section